UNIVERSITEIT GENT

FACULTY OF SCIENCES

Department of Organic and Macromolecular Chemistry

Separation Science Group

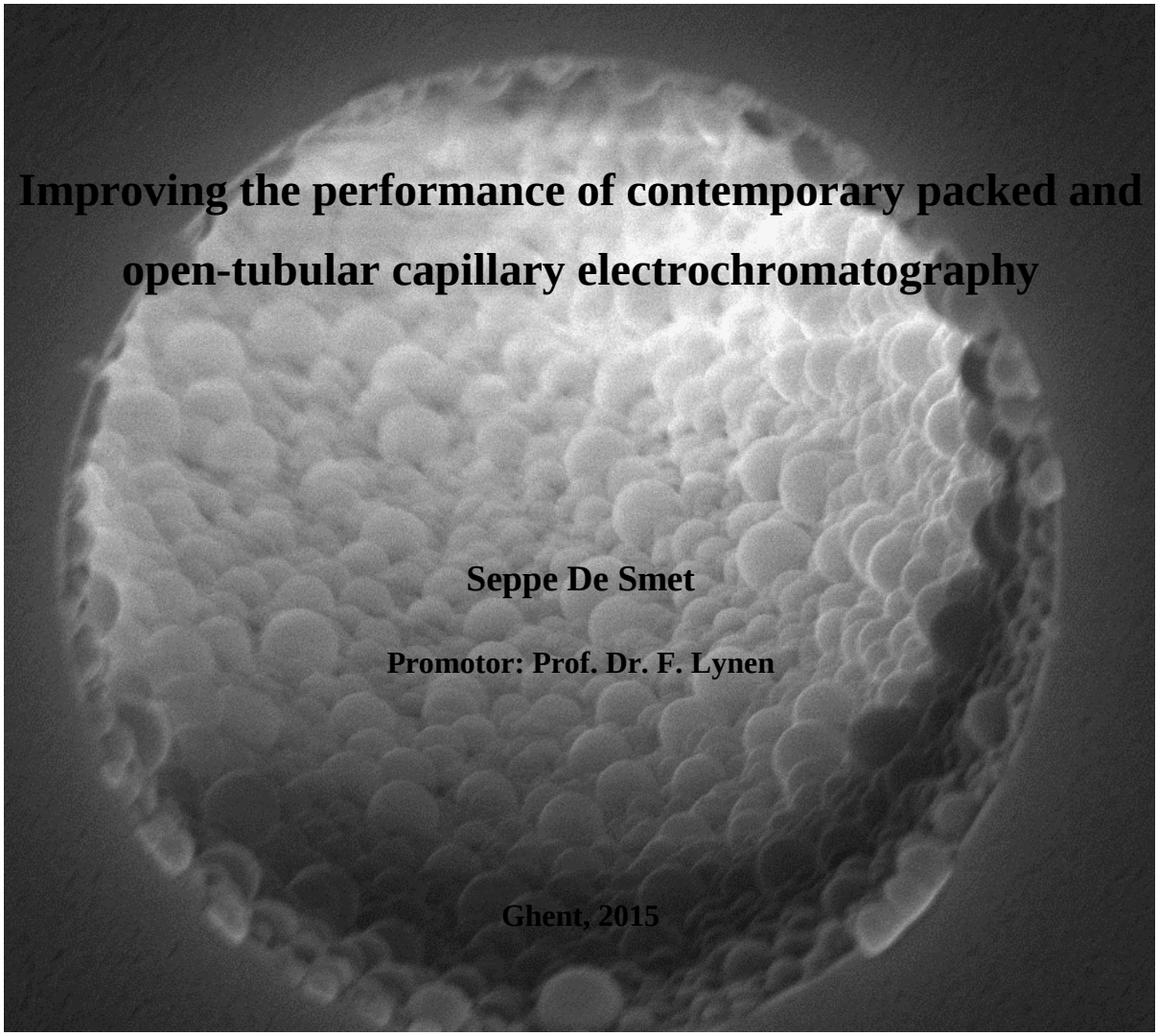

Improving the performance of contemporary packed and open-tubular capillary electrochromatography

Seppe De Smet

Promotor: Prof. Dr. F. Lynen

Ghent, 2015

Thesis submitted to obtain the degree of Doctor of Science: Chemistry

This research was funded by the Agency for Innovation by Science and Technology in Flanders (IWT)

Table Of Contents

List of abbreviations

A

ACN	Acetonitrile
AIBN	Azobisisobutyronitrile
API	Active pharmaceutical ingredient

B

BET	Brunuaer-Emett-Teller

C

CE	Capillary electrophoresis
CEC	Capillary electrochromatography
CF-FAB	Continuous flow fast atom bombardment
CSP	Chiral stationary phase
CZE	Capillary zone electrophoresis

D

DVB	Divinylbenzene

E

EOF	Electroosmotic flow
ESI	Electrospray ionization
EtOH	Ethanol

F

FTIR	Fourier transform infrared spectroscopy

G

GC	Gas chromatography

H

HILIC	Hydrophilic interaction liquid chromatography
HI-CEC	Hydrophilic interaction capillary electrochromatography
HPLC	High-performance liquid chromatography

I

ICD	In-column detection
IEC	Ion-exchange chromatography
IE-CEC	Ion-exchange capillary electrochromatography
ID	Internal diameter

K

KP	Kinetic plot
KPL	Kinetic plot limit

L

LC	Liquid chromatography
LIF	Laser induced fluorescence

M

MeOH	Methanol
MES	2-(N-morpholino)ethanesulfonic acid
MS	Mass spectrometry

N

NaOH	Sodium hydroxide
NP	Normal-phase

O

OCD	On-column detection
ODS	Octadecyl silane
OD	Outer diameter
OT	Open tubular

P

PAH	Polyaromatic hydrocarbons
PLOT	Porous layer open tubular
PS	Polystyrene

R

RP	Reversed-phase
RSD	Relative standard deviation
RPLC	Reversed-phase liquid chromatography

S

SEC	Size-exclusion chromatography
SEEC	Size-exclusion electrochromatography
SEM	Scanning electron microscope
SFC	Supercritical fluid chromatography

T

TES	Triethylsilane
TEOS	Tetraethyl orthosilicate
TRIS	Tris(hydroxymethyl)aminomethane

U

UPLC	Ultra performance liquid chromatography
UV-VIS	Ultraviolet-visible

V

VBSA	Vinyl benzyl sulfonic acid
VSA	Vinyl sulfonic acid
VWD	Variable wavelength detector

General introduction and scope

Since the introduction of chromatography in the beginning of the 20th century, many variants and alternative separation techniques have been developed. The quest for ever higher separation efficiencies has led to an impressive incremental series of innovations and improvements, particularly for liquid chromatography (LC). During the last two decades ultra-high pressure liquid chromatography has been developed, leading to a substantial gain in efficiency and speed of analysis. Simultaneously, super-critical fluid chromatography has become an increasingly interesting fast and viable alternative to LC. Nowadays, however, it can be argued that high-performance liquid chromatography (HPLC) reached its limit in terms of achievable performance. Although it outperforms gas chromatography (GC) in terms of selectivity, the maximum performance reached with LC cannot compare to GC. Parallel to the development of pressure-driven liquid chromatography, a number of powerful electrodriven techniques have also emerged. In the electrodriven modes the separation occurs by the movement of solutes under influence of an externally applied electrical field. In capillary zone electrophoresis (CZE) the separation will be solely the result of electrophoresis, which is the differential movement of charged solutes under influence of an external applied electrical field. Electrophoresis can be superimposed by other separation techniques, such as gel electrophoresis, where solutes are also separated by their size as they move through a gel with defined pores. The separation of neutral molecules can be obtained by micellar electrokinetic chromatography, where separation is obtained by the differences in partitioning of the solutes into micelles. Very high efficiencies (> 500,000 N) can typically be obtained with these methods.

The development of a hybrid technique combining the high efficiencies achievable in CE (capillary electrophoresis) and the selectivity of HPLC, was therefore the next logical step to achieve an even better performing separation technique. Capillary electrochromatography (CEC) is typically performed on fused-silica capillaries filled with LC types of stationary phases. The mobile phase which percolates through the stationary phase in the capillary

column is driven by an electrical field. Solutes are separated by differences in their degree of partitioning between the mobile phase and the stationary phase and additionally according to their charge over size ratios in the case of charged solutes. The use of electroosmosis as the driving force induces a plug-like profile which reduces the solute dispersion compared to a parabolic flow profile. Moreover, the electrodriven flow is independent of the particle size and the length of the column. This theoretically enables the application of long columns packed with sub-µm particles. As a consequence, very high efficiencies can be obtained with CEC.

The theoretical framework of CEC was established in the late eighties and initially this new separation technique gained a lot of academic interest, leading to the development of CEC analyses on different column formats, such as packed, monolithic and open-tubular columns. However, after three decades of CEC development, industrial implementation remains largely unreported, which is a telltale sign of an immature or flawed technique. After establishing the theoretical framework, most research focused on the development of new varieties of stationary phases with little attention for the investigation and elimination of the practical limitations of CEC, such as the challenging hyphenation to mass spectrometry, the lack of robustness and the lower than expected column performance in comparison with HPLC. A major issue in CEC is also the fact that the generation of flow is coupled to the properties of the particle and that therefore selectivity and flow generation are hard to optimize in an independent way.

Compared to gas chromatography, the performance of fluid-driven separation techniques remains much lower, resulting in an continuing drive and need for the development of highly efficient electrodriven separation approaches. Consequently, CEC still seems to be the best technique for these analyses as it combines chromatographic and electrodriven separation features.

However, to investigate and overcome the current limitations of CEC, the column performance of contemporary CEC should be evaluated in a more unbiased way. For example, in most of the available literature, the column performance in CEC has been evaluated by constructing van Deemter curves of slightly retained and/or ionized solutes. In this way high efficiencies are often obtained on packed columns. However, these are often

due to a variety of electrostatic peak focusing phenomena and are completely unrelated to the actual performance of the packed phase. Therefore, implementation of an independent tool, allowing the evaluation of CEC column performance, seems a necessary development.

The general objective of this thesis is the evaluation and critical appraisal of CEC as highly efficient separation technique. As a consequence, the first goal is the development of more universal ways to assess column performance in CEC, allowing less biased comparison of the performance of CEC columns with different dimensions of varying formats and containing different stationary phases. A related goal is the evaluation hydrophilic interaction CEC (HI-CEC) on packed capillaries. HI-CEC is not largely reported, but seems however promising to separate polar and basic solutes. More specifically, the application of packed bed HI-CEC is attractive as the packing procedure is less complex compared to the packing of reversed-phase type CEC columns.

As the use of open-tubular columns in CEC seems promising as very long columns can be made in an more facile way compared to the manufacturing of packed columns, an additional goal of this study has been the development efficient and performant open-tubular columns and consequently the evaluation of their performance by the kinetic plot method. Finally, one important goal of the thesis has also been the investigation of the influence and possibilities of temperature control and temperature gradients in CEC.

The first part of this work comprises of the theoretical framework, the instrumentation and the literature study. **Chapter I** introduces the theory of chromatography and electrodriven methods. **Chapter II** describes the instrumentation of capillary electrodriven methods and focuses particularly on the specific instrumentation for CEC and hyphenation to several detectors. In **Chapter III** a literature survey is performed on the different modes and the column technology applied in CEC.

The second part of this thesis comprises the development and evaluation of the packed and open-tubular capillaries. In **Chapter IV** the kinetic plot method is adapted to CEC as an universal comparative tool of the column formats in CEC versus HPLC. The kinetic performance limits of commercial capillaries are calculated and demonstrated. Furthermore, an in depth study of analysis temperature effects demonstrates that joule heating is still occurring in commercial packed capillaries with relatively large capillary diameters (ID 75

µm). Therefore, simulations are made to reveal the optimal performance of packed CEC, in the absence of joule heating, with smaller particles and when using ultra-high voltages. The application of hydrophilic interaction capillary electrochromatography is established in **Chapter V**. The packing strategy of native silica particles into a capillary column is described. Subsequently, the performance of the in-house packed capillaries is investigated by means of the kinetic plot method. Furthermore, the influence of the modifier concentration and the buffer concentration are described. Finally, the relevance of the hydrophilic interaction mode in CEC is demonstrated via the analysis of several test mixtures.

The application of a polystyrene-based open-tubular capillary in CEC for the separation of aromatic compounds is demonstrated in **Chapter VI**. The approach is promising as the length of the capillary is not limited by packing pressure. Less heat (Joule heat) will be generated in these capillaries as the generated current will also be limited due to the small internal diameters (10 µm) of these capillaries. Coupling to MS can be achieved more easily which overcomes the limited sensitivity of UV detection when using these narrow capillaries. Moreover, faster heat dissipation occurs due to the open-tubular nature of such columns. In this work, the polystyrene layer is copolymerized with sulfonic acid groups, which enhances EOF generation significantly. The procedure to prepare these columns is optimized and characterized. Furthermore, the influence of modifier and buffer concentration is investigated. Finally, the application of temperature gradients in open-tubular CEC is introduced.

Another open-tubular approach, based on the synthesis of a meso-porous layer of SBA-16, is reported in **Chapter VII.** This preliminary research focuses on the synthesis and coating of a finite layer of SBA-16 on the capillary wall, combined with the measurement of the retentive characteristics after grafting functional groups onto the modified column walls.

Chapter 1

Principles and theoretical considerations of CEC

This chapter describes the principles and theoretical considerations of capillary electrochromatography. Capillary electrochromatography is considered as a hybrid technique, combining features of capillary electrophoresis and liquid chromatography. Therefore, the characteristics of a chromatographic separation are first described, followed by a discussion of the retention mechanisms and achievable performance in liquid partitioning chromatography. Subsequently, the principle of electrophoresis is explained. Finally, the fundamental aspects of capillary electrochromatography are introduced by combining the principles of the two approaches.

1 Introduction

Capillary electrochromatography can be considered as a hybrid technique, combining the principles from electrophoresis and liquid chromatography. The mobile phase of this electrodriven technique percolates through the capillary and over the stationary phase under influence of an electrical field. Therefore, the technique is comparable to electrophoresis. However, the separation of neutral solutes rely on the partitioning of the solutes between the mobile and a stationary phase, which is characteristic for liquid chromatography. Furthermore, ionized solutes will be separated by both the process of partitioning chromatography and by electrophoresis. As a consequence, the theory describing capillary electrochromatography refers to the concepts of electrophoresis and partitioning chromatography. Therefore, the fundamentals of partition chromatography and electrophoresis will be discussed separately. Finally, the underlying theory of capillary electrochromatography will be explained. Hereby will be particular focus will be set on the unique features of CEC that will influence the flow generation mechanism and/or the separation process.

2. Theoretical aspects of chromatographic separations

In a chromatographic separation a mixture of solutes is introduced in a two-phase system. One phase is stationary while the other phase is mobile (liquid or gas) and flows through the column. Solutes in the mobile phase will move with the mobile-phase velocity, while solutes partitioned into the stationary phase will stay stationary. Therefore, separation can occur based on differences in the partitioning of the solutes.

2.1 Resolution as a measurement for the quality of the separation

The concentration distribution of a solute along the axis of a column displays in an ideal case a Gaussian distribution (bell shaped peak). The peak is characterized by the retention time t_r and its width w, as depicted in Figure I.1. The latter is the result of the peak broadening, occurring during the movement of the solute through the column. In ideal cases, only chromatographic processes contribute to the band broadening of the solute. However, extra peak broadening effects, contributing to the band width of the solute, can be caused by injection, detection, radial temperature gradients, etc.

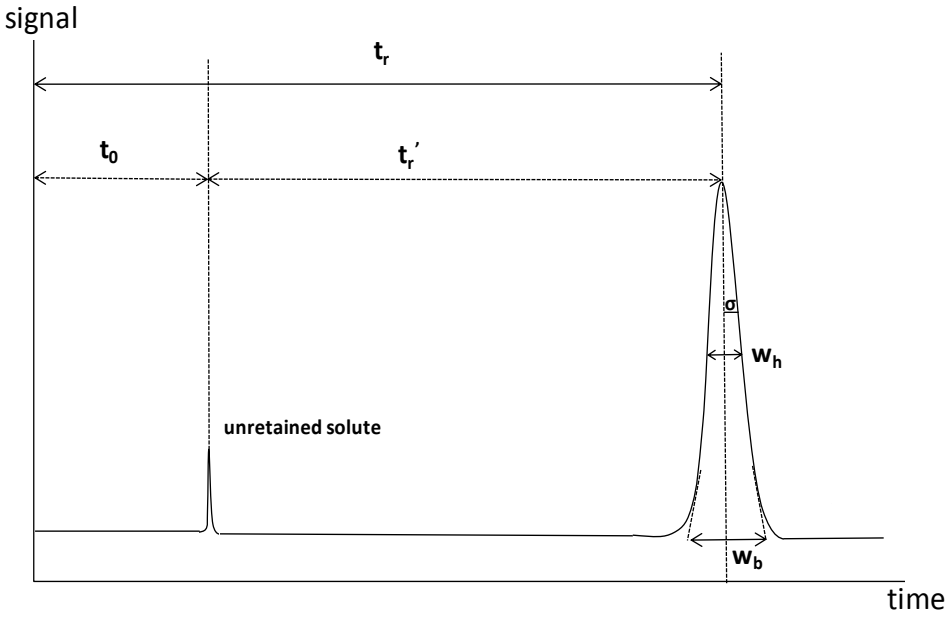

Figure I.1. Characterization of a chromatographic peak.

Band broadening in the column is traditionally expressed in units of dimensionless plate numbers (*N*) or plate heights (*H*). The former expresses the peak variance (or the efficiency of the column) while the latter expresses the variance per unit length [1].

The efficiency of the column can be derived from the peak characteristics:

$$\mathrm{N}=16\left(\frac{\mathrm{t_r}}{\mathrm{w_b}}\right)^2=5.54\left(\frac{\mathrm{t_r}}{\mathrm{w_h}}\right)^2=\left(\frac{t_r}{\sigma}\right)^2 \qquad \text{Eq. I.1}$$

where w_b represents the base width of the peak and w_h the peak width at half height. The plate height of a column is calculated by the ratio the column length, *L* and the plate number

$$H=\frac{L}{N} \qquad \text{Eq. I.2}$$

In chromatographic systems, the amount of retention of a component is by preference described by the dimensionless retention factor *k*. The retention factor describes the distribution of the component between the stationary phase and the mobile phase and can be defined as the dwell time in the stationary phase over the dwell time in the mobile phase. Therefore, the retention factor will specify the location of the peak in the chromatogram and give more insight in the interactions of the components with the stationary and mobile

phase. Prior to elution, the component will stay a certain time (the net retention time) in the stationary phase , t_r', and a certain time (the void time) in the mobile phase, t_0. The velocity of the mobile phase is the same for every component and therefore can be determined by monitoring the elution time of an unretained component.

Therefore the total elution time, t_r, of the component is described by the sum of the void and the net retention time (Eq I.3).

$$t_r = t_0 + t_r' = t_0 + kt_0 \qquad \text{Eq. I.3}$$

Consequently, the retention factor (k) corresponds to

$$k = \frac{t_r - t_0}{t_0} \qquad \text{Eq. I.4}$$

The relative difference in retention behavior between the stationary phase and two selected components can be expressed by the selectivity α_{21}

$$\alpha_{21} = \frac{k_2}{k_1} \qquad \text{Eq. I.5}$$

The overall separation for two solutes on a specific column (and under well defined conditions) is expressed by the resolution. The latter is dependent on the column efficiency, the selectivity and on the retention factor as shown in Eq. I.6.

$$R_s = \frac{\sqrt{N}}{4}\,\frac{\alpha - 1}{\alpha}\,\frac{k_2}{1 + k_2} \qquad \text{Eq. I.6}$$

The resolution is graphically expressed by the difference between the retention times of two adjacent peaks, divided by their averaged peak widths.

$$R_s = \frac{2(t_{r,2} - t_{r,1})}{w_{b,2} + w_{b,1}} \qquad \text{Eq. I.7}$$

Finally, the performance of acolumn can also be expressed in terms of peak capacity. The peak capacity of a column defines the number of peaks that can be separated with a

resolution of unity in a certain time interval. The peak capacity is often used to measure the performance of analyses with a mobile-phase gradient but can also be used for isocratic analyses [2,3].

2.2 Band broadening models and separation performance in liquid chromatography

As mentioned above, the plate height is a measurement of the degree of peak broadening a solute zone undergoes during an analysis. In an ideal case, this broadening effect is only caused by chromatographic processes, occurring in the column. The total band broadening, which can be described by several models, is then only dependent on the mobile-phase velocity and on the stationary phase characteristics.

2.2.1 The van Deemter model

The first model was proposed by J. J. van Deemter in 1956 and it is still the most used description of intra column peak broadening phenomena mainly due to its deductive clarity. The model states that the total plate height is dependent on the mobile-phase velocity and is constituted of the eddy diffusion (A), the influence of the longitudinal diffusion (B) and on the resistance to mass transfer between the mobile phase and the stationary phase (C). In the resulting van Deemter equation, it is assumed that these three parameters act independently of each other [4].

$$H = A + \frac{B}{u} + C_{s,m}.u \qquad \text{Eq. I.8}$$

The constant A represents the tortuosity of the flow path in packed columns and is better known as the eddy diffusion term. In packed beds, the flow paths are not straight lines but are formed by the interstitial channels between the particles. Consequently, two molecules of the same type will follow different paths with a different length, resulting in different elution times for both solvents. The eddy diffusion is related to the product of a constant, λ, and the particle diameter, *dp* (A=2.λ.*dp*). λ is hereby a measurement of the packing efficiency and consequently, the eddy diffusion term will be low when using homogeneously packed beds whereby preferably small spherical particles are used. Note that the eddy diffusion term is independent of the mobile-phase velocity.

The B-term corresponds to the axial molecular diffusion of a solute band during an analysis. During this process, the molecules in the band will naturally diffuse to areas of lower concentration, and therefore cause an additional broadening effect. The diffusion is a natural random process and therefore a Gaussian concentration band will be formed. this longitudinal diffusion effect will be larger if the solute band remains longer in the column and hence, at lower mobile-phase velocities. The B-term is also dependent on the diffusion constant, D_m, of the solute in the mobile phase.

Finally, the-*C*-term represents the slowness of mass transfer between the mobile phase and the stationary phase. During the analysis, the solute molecules will constantly transfer from the mobile phase to the stationary phase in a reversible way. The peak broadening process is induced by the time it requires for the diffusion of a solute in the mobile phase until it reaches the stationary phase (C_m) and the subsequent diffusion in the stationary phase (C_s). As molecules in the mobile phase are not located at the same distance to the stationary phase, differences in diffusion times will occur. Again these effects also occurs in the stationary phase. Furthermore, molecules in the mobile phase will move through the column with the mobile-phase velocity and therefore move away from molecules present in the stationary phase. As a consequence, a band broadening effect, related to both the diffusion velocity of the solute in the mobile phase (D_m) and in the stationary phase (D_s), is induced. Furthermore, the particle size (d_p), the film thickness (d_f) of the particle and the flow velocity all determine the degree of zone broadening due to mass transfer effects. As in LC and CEC, the particle size is much larger than the thickness of the stationary phase, only the former should be considered to contribute significantly to the C-term.

The A, B en C constants from the simplified van Deemter equation (Eq. I.9) can be interchanged by their proper terms to reveal the full van Deemter equation for a packed column [4].

$$H = 2\lambda d_p + \frac{2\gamma D_m}{u} + \frac{(1 + 6k + 11k^2)d_p^2}{24(1+k)^2 D_m} u + \frac{8k\, d_f^2}{\pi^2 (1+k)^2 D_s} u \qquad \text{Eq. I.9}$$

where γ represents the tortuosity and k represents the retention factor. Figure I.2 depicts the total van Deemter curve for a column packed with 5 µm particles. The A-, B- and C-terms were 4.5, 1.2 and 8, respectively [1,5].

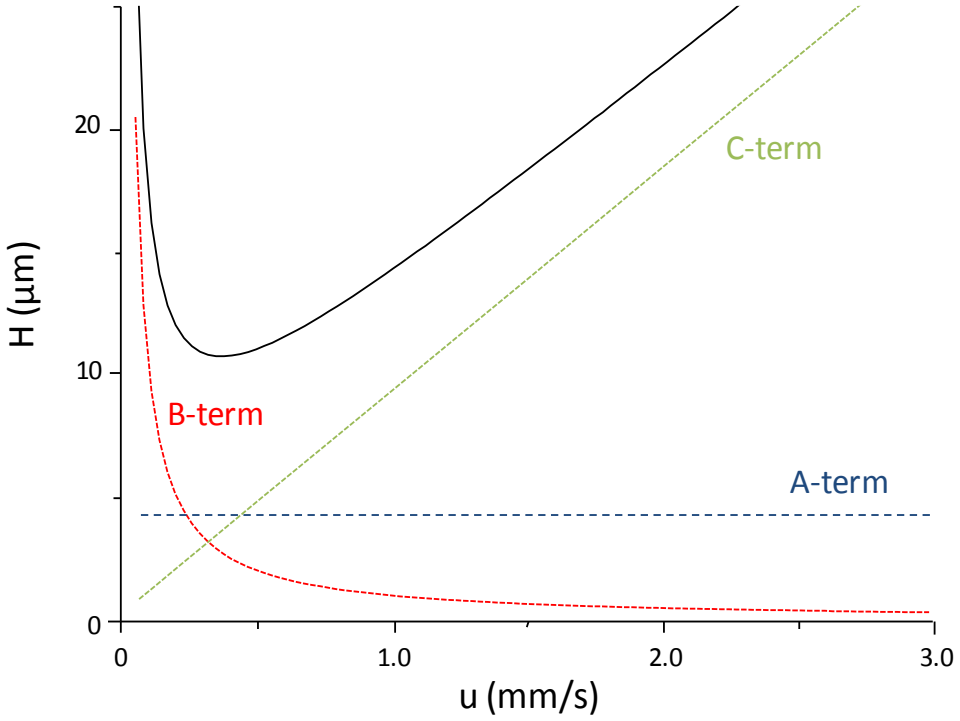

Figure I.2. Simulated plate height contributions for a column packed with 5 µm particles using the van Deemter equation.

A minimum of 10.5 µm is reached around an optimal mobile-phase velocity of 0.35 mm/s. Nowadays, it is generally assumed that a minimum plate height of $H \approx 2d_p$ can be achieved for well packed columns at their optimum mobile-phase velocity in HPLC when fully porous material is used as packing material. Note that the more recently introduced core shell particles allows reaching plate heights below 2*dp*

2.2.2 The Giddings approach

The van Deemter equation is a simple and easily applicable approach to describe the band broadening as a function of the mobile-phase velocity. However, the A-term in this equation is thereby not entirely theoretically founded. In the van Deemter equation the total variance σ (or band broadening) is the sum of the different variances.

$$\sigma_{tot}{}^2 = \sum_i \sigma_i{}^2 \qquad \text{Eq. I.10.}$$

However, Giddings argued that the random walk of the solutes is caused by the tortuosity of the flow paths (the A-term) but also by the diffusion of the solutes in the mobile phase (the C_m-term). Two dependent variances should therefore be added up harmonically:

$$\sigma_{tot}{}^2 = \frac{1}{\frac{1}{\sigma_1{}^2} + \frac{1}{\sigma_2{}^2}} \quad \text{Eq. I.11.}$$

Therefore, the combined contribution (H_c) to the plate height of the coupled mass transfer in the mobile phase and the eddy diffusion can be described as:

$$H_c = \frac{1}{\frac{1}{A} + \frac{1}{C_m u}} \quad \text{Eq. I.12.}$$

resulting in the Giddings equation for the total plate height *H*:

$$H = \frac{B}{u} + C_s u + \frac{1}{\frac{1}{A} + \frac{1}{C_m u}} \quad \text{Eq. I.13.}$$

2.2.3 The Knox equation

However, Giddings' theoretical approach is far from practical to describe the properties of the packed bed in a column. Therefore an empirical approach to describe the dispersion of the solute zone was introduced by Knox and Bristow in 1977 [6]. Knox introduced the use of the reduced plate height, *h*, and reduced velocity, *v*, which are independent of the particle size.

$$h = \frac{H}{d_p} \quad \text{Eq. I.14.}$$

and

$$v = \frac{u.d_p}{D_m} \quad \text{Eq. I.15.}$$

The resulting Knox equation is quite similar to the van Deemter expression, however the A-term depends on the 1/3 power of the reduced velocity [7].

$$h = A.v^{1/3} + \frac{B}{v} + C.v \qquad \text{Eq. I.16}$$

Although the Knox approach is often used, it should be noted that the proposed dependency of the A-term as a function of the linear velocity has only been tested for a limited number of particle sizes, shapes and column morphologies. There is only limited evidence about the validity of the model on the most recently developed particle sizes and types.

2.2.4 The Golay equation for open-tubular columns

In accordance with the van Deemter model, Golay developed the expression for the height of a theoretical plate for open-tubular columns in gas and liquid chromatography [8-11]. Due to the open channel character of the column, the contribution of the eddy diffusion will be zero. Therefore, only a longitudinal diffusion term and two mass transfer terms describe the total broadening in the column. Note that the particle diameter is replaced by the radius, r_c, of the column and that diffusion constants in the C_m-term will differ greatly between gas and liquid mobile phase. The Golay equation is given by

$$H = \frac{2D_m}{u} + \frac{(1+6k+11k^2)r_c^2}{24(1+k)^2 D_m}u + \frac{2}{3}\frac{k{d_f}^2}{(1+k)^2 D_s}u \qquad \text{Eq. I.17}$$

where K represents the distribution coefficient of the solute between the two phases.

2.2.5 The kinetic performance limit

Nowadays, a significant part of the research in chromatography is focused on the study of monolithic and open-tubular columns [12-17]. The greatest advantage of these stationary phase supports is their low resistance to flow (compared to packed beds). Therefore, a comparison of the separation performance of stationary phase supports should also incorporate the possible application of longer (and hence more efficient) columns or the possibility to apply very high flow rates (allowing to expedite the separation). Furthermore, the great variety of stationary phase formats, particle diameters and column dimensions that are available nowadays, increases the complexity of column choice for the chromatographic users. One of the contemporary trends is to obtain highly efficient separations in short analysis times. Therefore a plot yielding the kinetic performance of the

system, which can be defined as the efficiency (or peak capacity) a system can generate in a certain time, would give the most unbiased guideline to choose the right column with the right support. Generally, these kinds of plots are referred to as "kinetic plots".

Poppe described in 1997 a t_0/N plot versus N plot to gain more insight into the C-term dominated area. However, the first kinetic plots were already described in 1965 by Giddings and also used by Knox and Guiochon [18-21]. These plots are based on numerous iterations executed by computer programs.

Desmet et al. proposed a new and more practical approach, where the measured H versus u data were converted to a kinetic plot by implementing simple derived equations [22].

The kinetic performance of a pressure driven method is determined by the efficiency N obtained in certain time, t_0. However, the analysis time (and hence the mobile-phase velocity) is limited by the maximum pressure drop, ΔP, the system can apply. These three parameters are defined by:

$$N = \frac{L}{H} \qquad \text{Eq. I.18}$$

$$t_0 = \frac{L}{u} \qquad \text{Eq. I.19}$$

$$\Delta P = \frac{u\,\eta\,L}{K_v} \qquad \text{Eq. I.20}$$

where K_v represents the column permeability.

Combining Eqs. I.18-I.20 to eliminate the column length allows to define efficiency and the mobile-phase dwell time in terms of the pressure drop:

$$N = \frac{\Delta P.K_v}{\eta.u.H} \qquad \text{Eq. I.21}$$

$$t_0 = \frac{\Delta P.K_v}{\eta.u^2} \qquad \text{Eq. I.22}$$

Changing ΔP to the maximum pressure drop, ΔP_{max}, results in the maximum efficiency of a column with a maximum length at the maximum pressure drop for the same mobile-phase velocity [23]. By applying these calculations to each measured data point, the H versus u

curve is transferred to a series of $t_{0,max}$ versus N_{max} points, describing the kinetic performance limit (KPL) of a system with a certain stationary phase support.
This approach is straightforward for isocratic analyses, however for gradient runs a gradient plate height should be calculated, complicating the approach.

Therefore, a set of implicit expressions was developed, applicable for gradient and isocratic analyses. These expressions only require the calculation of a length rescaling factor λ [24].

$$\lambda = \frac{\Delta P_{max}}{\Delta P_{exp}} \quad \text{Eq. I.23}$$

where ΔP_{exp} represents the pressure drop of an isocratic run or the maximum encountered pressure drop during the gradient run. To calculate the data points of the KPL, it suffices to multiply the obtained parameters during the run with the length rescaling factor.

$$N_{KPL} = \lambda . N_{exp} \quad \text{Eq. I.24}$$

$$t_{0,KPL} = \lambda . t_{0,exp} \quad \text{Eq. I.25}$$

$$L_{KPL} = \lambda . L_o \quad \text{Eq. I.26}$$

Note that this approach can be expanded to the peak capacity, n_p, the total retention time, t_r or the resolution R_s.

As a consequence, the resulting kinetic plot (KP) thereby converts the plate height versus linear velocity curve to a speed versus efficiency curve and incorporates column permeability information, as the maximum efficiency is limited by the maximum applicable pressure drop. Consequently the KPL method represents the shortest possible separation time for a given efficiency (measured in plate number *N*) or the highest possible efficiency for a given separation time for each column. However, the method assumes a constant plate height at the same mobile-phase linear velocity, regardless of the column length. Therefore, one of the prerequisites is an invariable column permeability irrespectively of the length of the column.

Simulated kinetic plots for packed bed columns with 5 and 3 µm are depicted in Figure I.3. The plot was simulated for a system with a maximum pressure drop of 400 bar.

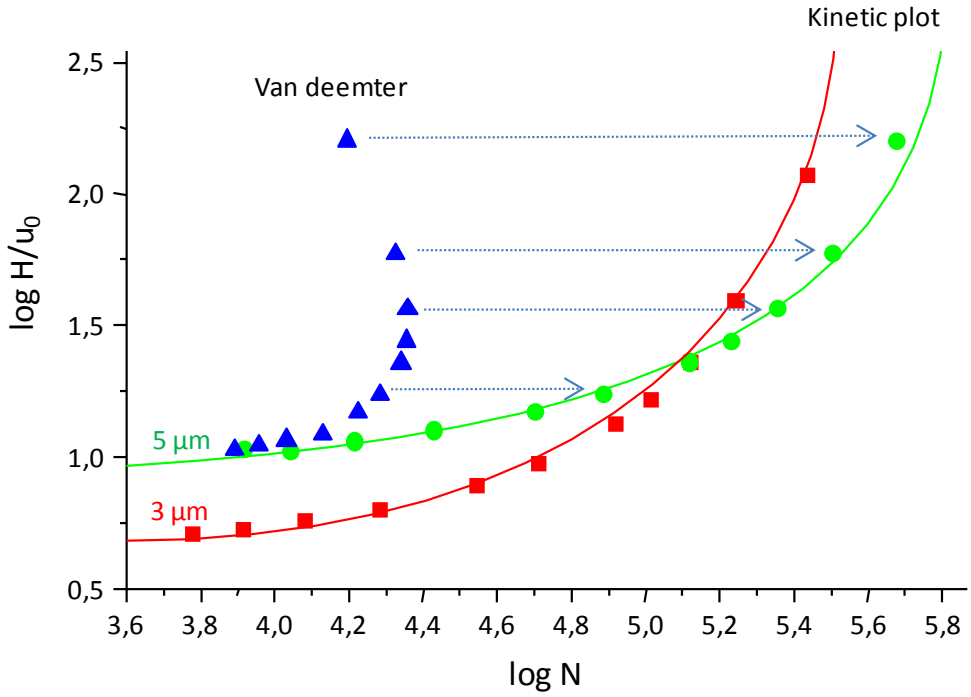

Figure I.3. The simulated kinetic plot of packed columns with 5 (green circles) and 3 (red squares) µm particles. The original values for a 25 cm packed column with 5 µm particles are depicted with blue triangles.

The y-axis of Figure I.3 represents the speed of the analysis, while the x-axis represents the efficiency. The kinetic plot reveals that for short analysis times, the 3 µm particles are more efficient than 5 µm particles. However, the highest efficiency is reached (when using high analysis times and long columns) by the column packed with the 5 µm particles. This can be explained by the higher pressure drop created by the 3 µm particles which ultimately constrains the length of the column.

Although the kinetic plot was originally developed and tested with isocratic analyses on packed columns, the methodology can be also applied for gradient analyses [24]. This technique is applied to compare the performance of pressure dependent column characteristics, like morphology, particle size, temperature, ultra-high pressure analyses and packing efficiencies in packed capillary columns [25-30].

The KPL method is not limited to conventional liquid chromatography but has already been described for the study of supercritical fluid chromatography and of shear driven separation techniques [31].

3 Separation by capillary electrophoresis

The separation of solutes in electrodriven technique is based on electrophoretic phenomena, which can be superimposed with other separation modes, dependent on the technique. The mobile-phase flow is generated by applying an electrical field over the capillary. The mobile-phase velocity is thereby dependent on the capillary dimensions, the mobile-phase composition and on the applied field strength amongst other parameters.

3.1 Separation of ions by electrophoresis

The ions in an electrolyte subjected to an electrical field will be accelerated to the electrode of the opposite sign. After a short time the ions will reach a constant velocity which is the product of the electrophoretic mobility of the solute and the electric field strength:

$$v = \mu_e E \qquad \text{Eq. I.27}$$

where the electrophoretic mobility is given by μ_e and E stands for the applied electric field. The mobility of the solute is for a given ion and medium a characteristic constant. The movement of the ion will be balanced by the electromotive force experienced by the ion in the electrical field and the frictional force, created by the drag of the solute in the medium (Stoke's law):

$$qE = 6\,\pi\,\eta\,r\,v \qquad \text{Eq. I.28}$$

Combining Equation I.27 and I.28 leads to the equation describing the electrophoretic mobility:

$$\mu_E = \frac{q}{6\,\pi\,\eta\,r\,v} \qquad \text{Eq. I.29}$$

Therefore, the mobility is dependent on the size and the charge of the ion. Increasing the size of the ion will result in a lower mobility. For similarly charged ions, the mobility will

therefore decrease with molecular size. For similarly sized ions, the mobility will increase with increasing charge. These rules of thumb are straightforward. However, the solvation of the ion influences the effective ion radius and should also be considered. As a consequence, the mobility of small inorganic ions increases with an increase in the molecular weight due to the differences in solvation (smallest ion is the strongest solvated). Solvation is, however, less important for organic ions.

However, Stoke's law is only valid for spherical ions and consequently, Eq I.29 cannot be used for more complex ions. Therefore, the electrophoretic mobility is generally expressed as a function of the zeta-potential, ζ.

$$\mu_E = \frac{\varepsilon\,\zeta}{6\,\pi\,\eta} = \frac{2\,\varepsilon_0\,\varepsilon_r\,\zeta}{3\,\pi\,\eta} \qquad \text{Eq. I.30}$$

where ε_0 represents the permittivity of vacuum and ε_r stand for the permittivity of the buffer.

The mobility of the solute is for a given ion and medium a characteristic constant and can be found in tables. However these constants are merely theoretical ones as they often differ from experimentally determined values. The latter is called the effective electrophoretic mobility and is mainly dependent on the pH of the medium. Weak electrolytes are partly charged when the pH of the solution is close to the pK_a-value of the electrolyte. In this case, the effective electrophoretic mobility, μ_{eff}, will only be a fraction of the absolute electrophoretic mobility, μ_{abs}, defined as the mobility noted when all ionic groups on these molecules are fully charged.

$$\mu_{eff} = \alpha.\,\mu_{abs} \qquad \text{Eq. I.31}$$

where α represents the dissociation coefficient. Different ions will exhibit different mobility's and can therefore be separated from each other. It has been demonstrated that for analytes with very similar absolute mobilities and with subtle differences in pK_a values, differences in effective mobilities can be induced by selecting an optimal pH value.

In CZE, the electrophoretic velocity factor, k_e describes the amount of migration of the component. This migration parameter is defined in analogy with HPLC, but the dead time is hereby replaced by the EOF time, t_{eof} and retention times by the migration times, t_m [32].

$$k_e = \frac{t_{eof} - t_m}{t_m} \qquad \text{Eq. I.32}$$

The selectivity in CZE is defined by the ratio of the electrophoretic mobility's (μ_{ep}) of the two selected components.

$$\alpha_{21} = \frac{\mu_{ep,2}}{\mu_{ep,1}} \qquad \text{Eq. I.33}$$

3.1 The origin of Electroosmosis

Electroosmosis is the bulk flow of the electrolyte in the capillary under influence of an electrical field. The wall of the fused-silica capillary will be negatively charged and adjacent to the wall a double layer of counter-ions in the solution will be formed. These positive charged ions will be attracted to the positive electrode, resulting in the bulk flow of the liquid.

3.1.1 The double layer theory and the zeta-potential

A charged surface, whether it is a solid (metal under potential) or a dissolved ion, suspended in an electrolyte will be counter-balanced by ions of the opposite sign to such an extent that the net charge is zero. These counter-ions form a double layer around the charged surface. According to the Stern theory, which is the most used theory to describe this phenomenon, ions have a finite size and therefore they cannot approach the surface closer than a few nm, which is basically the radius of the ion. The theory divides the double layer in two regions. In the inner region, also called the Stern layer, the counter-ions will be adsorbed and rigid. In the Stern layer there is an excess of counter ions. In the other region the ions will be diffused and distributed according to the influences of the electrical forces and the random thermal motions. Due to the interactions of the adsorbed counter-ions, there will be a stagnant layer of liquid surrounding the surface. The border between this stagnant layer and the bulk liquid is called the slip or shear-plane. The double layer causes an electrokinetic potential between the surface and any point in the bulk liquid. This potential drops linearly in the Stern layer

and exponentially in the diffuse layer until it reaches zero at the end of the diffuse layer, as depicted in Figure I.4. The potential at the slip plane is called the zeta-potential (ζ) and characterize the double-layer properties [33]. Note that the double layer theory is not only applicable to spherical ions but also to charged solids in different shapes.

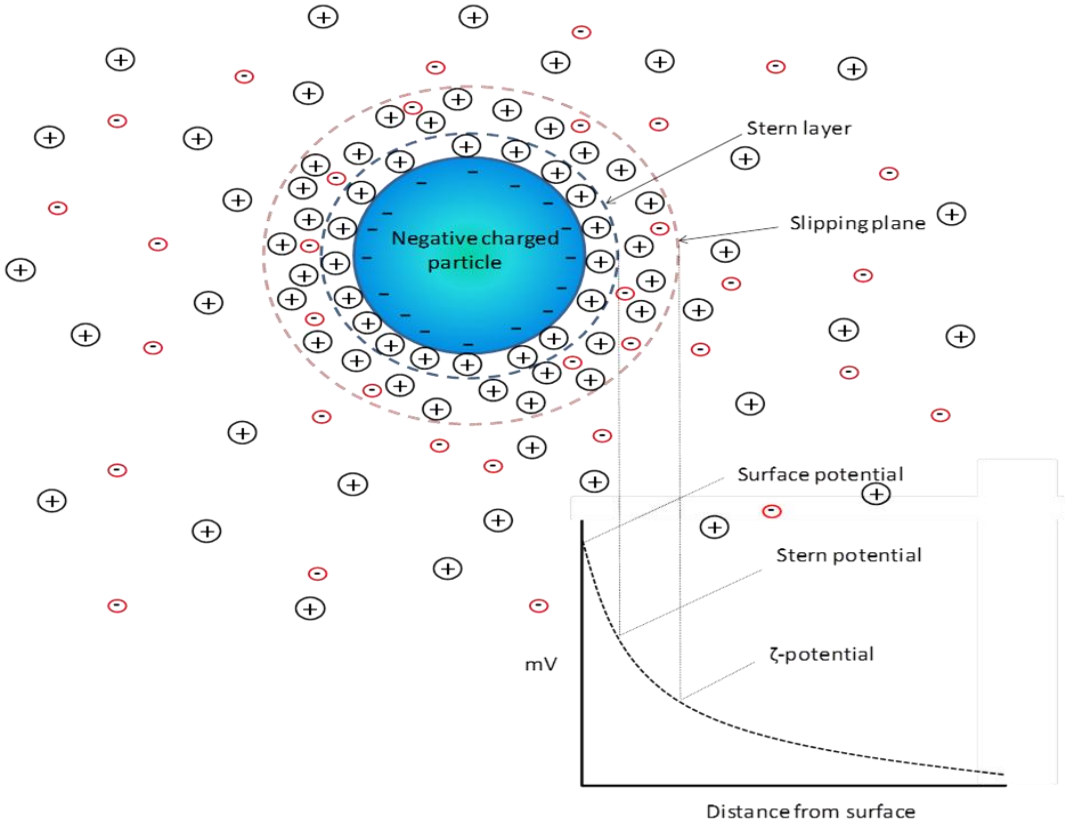

Figure I.4. Graphical representation of the Stern model. A negatively charged particle suspended in an electrolyte builds up a stagnant double layer of counter-ions.

3.1.2 Electroosmosis applied in electrodriven separation techniques

In fused-silica capillaries, the silanol groups on the inner wall will be ionized when in contact with an electrolyte solution at a certain pH. This dissociation process creates an excessive negative charge at the wall, which will be counter balanced by a double layer of positive ions. The wall acts as a charged surface, therefore the counter ions in the stern layer will be rigid while the (positive) ions in the diffuse layer will move towards the cathode, when an electrical field is applied. The counter ions are solvated and therefore a net bulk flow towards the cathode is generated, as depicted in Figure I.5.

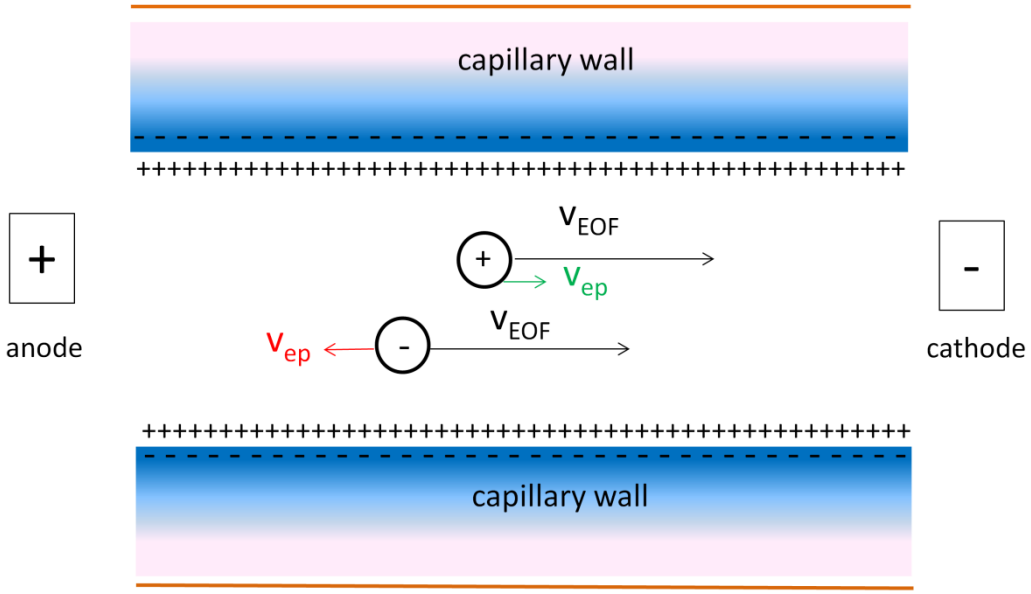

Figure I.5. Schematic representation of the net bulk flow in CZE and the differences in electrophoretic mobility.

The magnitude of the generated EOF is the product of the electrical field and the electrophoretic mobility of the EOF (μ_{EOF}) and is given by

$$v_{EOF} = \mu_{EOF} E \qquad \text{Eq I.34}$$

where v_{EOF} is the velocity. The mobility of the EOF is dependent of the viscosity of the medium (η) and the zeta-potential (ζ) and can therefore be expressed by

$$\mu_{EOF} = \frac{(\varepsilon_0 \varepsilon_r \zeta)}{\eta} \qquad \text{Eq I.35}$$

where ε_0 represents the permittivity of vacuum and ε_r is the dielectric constant of the electrolyte solution [34].

Substituting Eq I.35 in Eq I.34 results in the general used expression for the EOF velocity, named the von Smoluchowski equation:

$$v_{EOF} = \frac{(\varepsilon_0 \varepsilon_r \zeta)}{\eta} E = \frac{(\varepsilon_0 \varepsilon_r \zeta) V}{\eta L} \qquad \text{Eq I.36}$$

A theoretical approach of Rice and Whitehead stated that the EOF profile is flat and independent of the tube radius when the tube radius, *r*, is at least ten times thicker than the double layer, *δ* (*r*/*δ*> 10) [35]. The flat EOF profile is contrary to the parabolic laminar flow in pressure driven techniques, as illustrated in Figure I.6.

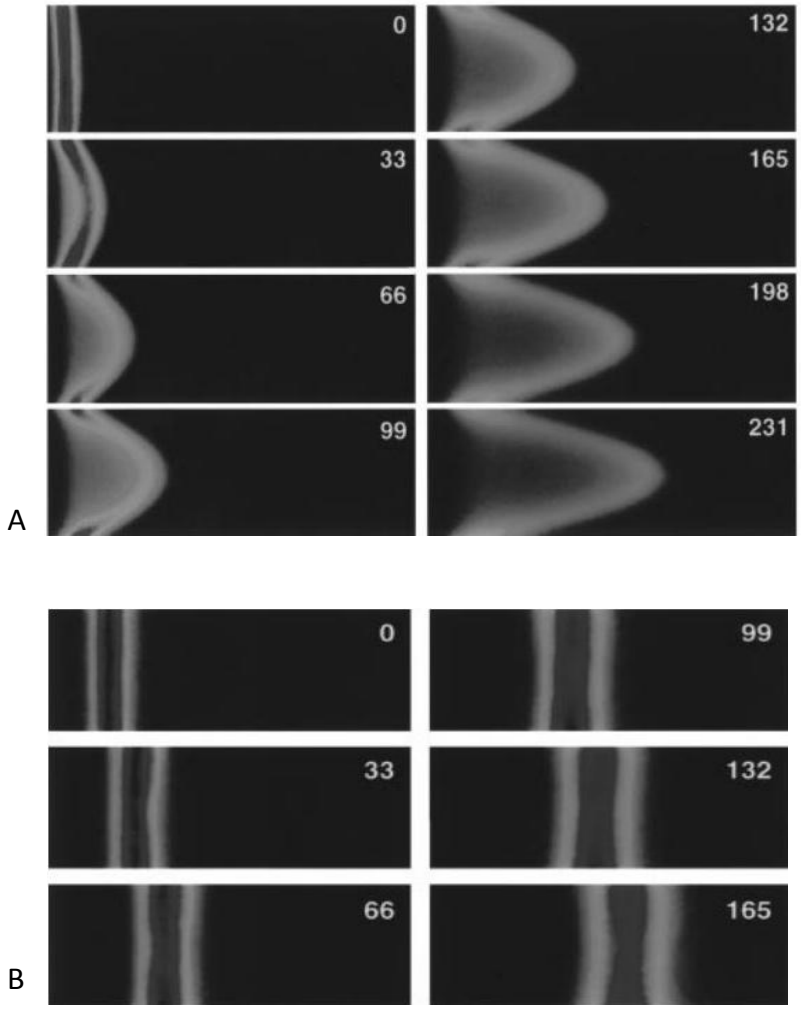

Figure I.6. Image of pressure driven flow (A) and electrodriven flow (B). Conditions: (A) flow through an open 100 µm i.d. fused-silica capillary using a caged fluorescein dextran dye and pressure differential of 5 cm of H_2O per 60 cm of column length; (B) flow through an open 75 µm ID fused-silica capillary using a caged rhodamine dye with an applied field of 200 V/cm. The frames are numbered in millisecond from the uncaging event [36].

Figure I.6 demonstrates that the resulting band of solutes, carried by an electrodriven flow, will be narrower compared to the band driven by a parabolic flow due to the flat profile of the EOF.

The EOF direction can be controlled by dynamic or static coating of the capillary wall. These coatings can increase, decrease or reverse the excess surface charge and hence the EOF.

3.2 Practical parameters influencing the velocity of the EOF

In electrodriven methods, the electroosmotic flow velocity is influenced by several parameters. However, the velocity is an important chromatographic characteristic which can influence the efficiency and separation. Therefore, the velocity is monitored for most analyses in CE. In practice, an EOF marker is added to the solute. This EOF marker is an easily detected neutral small molecule. By measurement of the elution time and the traveled length through the capillary, the EOF velocity can be subsequently calculated.

3.2.1 The effect of the pH on the EOF velocity

The pH of the electrolyte is the most important parameter influencing the EOF velocity. The surface charge, and hence the zeta-potential, on the wall and/or the stationary phase is directly linked to the pH. Acidic surface groups, like silanol and carboxylic groups, will be more ionized at high pH values and therefore exhibit the highest EOF velocity at high pH values, as depicted in Figure I.7. On the other hand, basic surface groups will be more ionized at low pH's and therefore show the highest EOF velocities in acidic environments. Silanol groups exhibit pKa's of 5-6 and therefore a significant EOF can be generated from pH 3 and upwards.

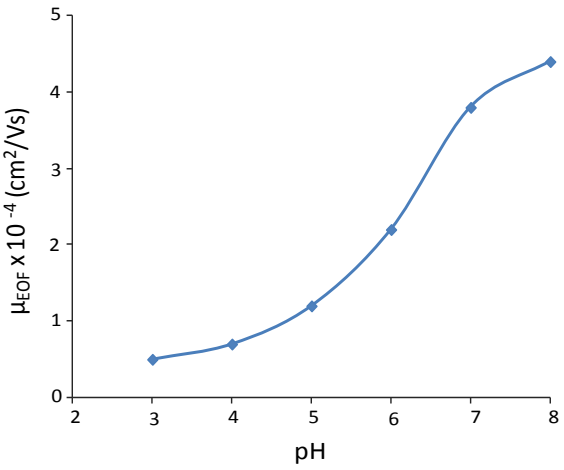

Figure I.7. Effect of the pH of the mobile phase on the electroosmotic mobility in fused-silica capillaries.

Consequently, varying the pH is an easy tool to change the EOF velocity. Furthermore, the pH influences the charged state of the solutes of interest and therefore the pH (and buffer) should be carefully selected in function of the analysis.

3.2.2 The influence of the ionic concentration on the mobility

The addition of ionic species or increasing the electrolyte concentration in CE(C) results in a decrease of mobility. The higher ionic concentration leads to a faster decay in potential and thus, to a smaller double layer, as can be derived from the (simplified) equation of the Debye length, δ:

$$\delta^{-1} = \frac{0.3}{\sqrt{I}} \qquad \text{Eq I.37}$$

Subsequently, the ionic strength is given by

$$I = \frac{1}{2}\sum_{i} c_i \, z_i^2 \qquad \text{Eq I.38}$$

where *c* stands for the concentration of the ion with charge *z* [37,38].

In practice, buffer concentrations ranging between 1 and 50 mM are commonly used. Note that high buffer concentrations will cause a rise in Joule heating phenomena.

3.2.3 The dependency of the EOF as a function of the temperature

Temperature influences the pH, the viscosity, the dielectric constant and hence the zeta-potential. In general, an increase in temperature results in a corresponding increase in the electroosmotic mobility and electrophoretic mobility [39,40].

3.2.4 The importance of the solvent composition of the mobile phase

In CZE, most analyses are executed with a pure aqueous buffer. However, it has been shown that the mobile-phase velocity and the solute selectivity can be enhanced by addition of organic solvents, such as methanol and acetonitrile. The organic modifiers will alter the viscosity, the dielectric constant and the zeta-potential, resulting in a maximum increase in velocity at a mobile composition with 50-70% organic solvent [41]. Furthermore, the organic

solvent will change the effective mobility of the solutes and the pKa values of weak electrolytes and can therefore induce a change in the selectivity of a separation [42].

3.4 Self heating effects in electrophoresis

The heat, generated by the electric current passing through conductor, is called Joule heat. The temperature increase depends on the power (which is the product of the voltage ,*V*, and the current ,*i*). The Joule heat can be calculated by following expression:

$$J\,(t) = iVt = i^2Rt = \frac{V^2t}{R} = \frac{V^2\sigma AT}{L} \qquad \text{Eq I.39}$$

where, *J* is the generated heat as a function of time (*t*), in a capillary with resistance, *R*, and length, *L* and a cross section, *A*, while a current (*i*) is flowing through the background electrolyte with electrical conductivity, *σ*, under the influence of an applied potential, *V*. The built-up heat will dissipate across the capillary wall by natural cooling or forced (air, liquid) cooling [43]. As expressed by Eq. I.39, the effect of Joule heating will increase with increasing time, voltage and capillary diameter. Internal diameters larger than 100 µm lead to temperature rises in excess of 50 to 100°C, resulting in the degassing, boiling and the evaporation of the electrolyte. Therefore, the application of capillaries with small internal diameters in electrophoretic driven separation methods is apparent. In capillaries with diameters of 100 µm and below, the rise in temperature itself, is generally not detrimental but thermal dissipation will occur more near the capillary wall then at the center, resulting in thermal gradients across the capillary, as depicted in Figure I.8.

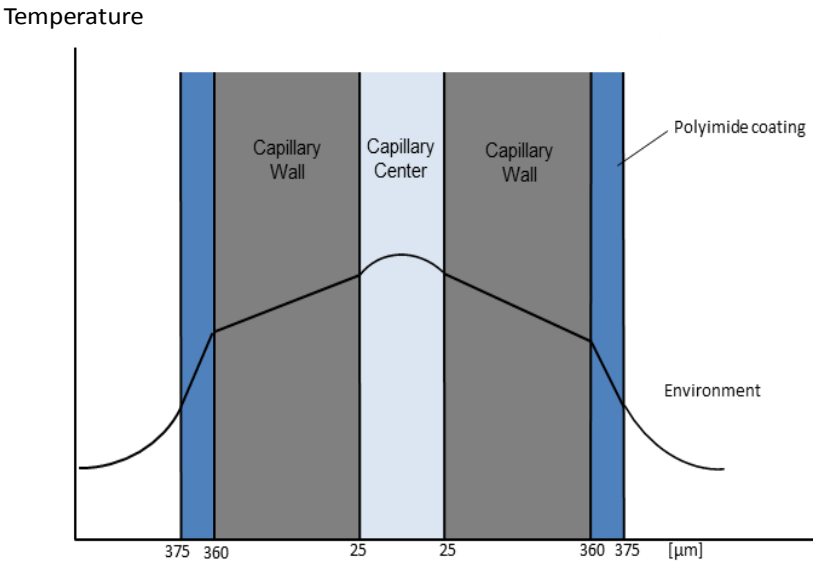

Figure I.8. The thermal gradient across a fused-silica capillary. Reproduction from [44].

These temperature gradients lead to differences in local viscosities and therefore in local differences in EOF velocity (Eq. I.36) [45]. The latter distort the flat velocity profile to a parabolic velocity profile, which leads to extra band broadening, and therefore have a negative effect on the efficiency. Furthermore, the reproducibility of the analysis will be limited when Joule heating is occurring. Independent from Joule heating, an increase in temperature of 1°C results in a 2 to 3% change in viscosity and hence in mobility [46]. Therefore, the control of temperature during the analysis is of utmost importance, which can be done by "thermostating" (air-or liquid cooling) the surrounding environment of the capillary. Berezovski et al. proved that at very high electrical field strengths the temperature in the capillary still rises, notwithstanding the cooling procedure. However, the rise in temperature is only noticeable from 500 V/cm on, as depicted in Figure I.9.

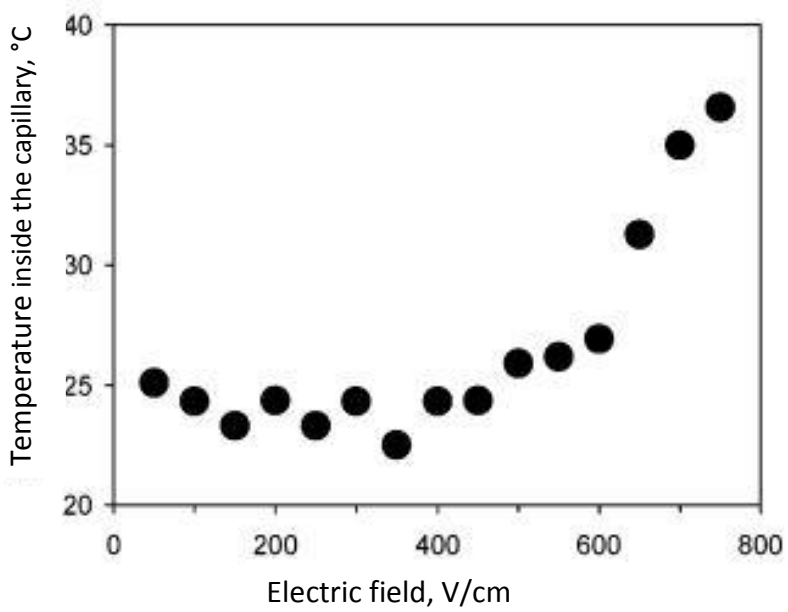

Figure I.9. The dependence of the temperature with the electric field in a 40 cm capillary with an ID of 20 µm. Surrounding temperature was set at 25°C. Data is retrieved from reference [47].

4 Fundamental aspects of capillary electrochromatography

Capillary electrochromatography is a hybrid technique combining the advantages of electrophoresis and chromatography. Hereby, a stationary phase is immobilized in a fused-silica capillary while a flow of the mobile phase (buffer) will be generated by applying an voltage difference over the capillary. Consequently, solutes can be separated in CEC as ions which will undergo both electrophoretic and partitioning separation processes. Neutral molecules will be separated according to only the latter.

Electrodriven chromatographic separations were already described for the first time in 1939 by Strain, who combined electrophoretic and chromatographic forces to achieve higher selectivity on an adsorption column [48]. The concept of the use of electro(endo)osmosis to mobilize an electrodriven flow through a capillary column was effectively demonstrated for the first time by Pretorius in 1974 [49]. The idea to apply the EOF as pumping mechanism for packed glass capillaries was further developed by Jorgenson in 1981 and theoretically described by Knox and Grant in 1987 [50,51].

To exploit the potential of CEC as a highly efficient separation mechanism the control and understanding of the EOF generation is of utmost importance. Furthermore, the application of an electrical field over the columns will also lead to the electrophoretic separation of ions.

Journal of Chromatography, 99 (1974) 23–30

CHROM. 7638

ELECTRO-OSMOSIS

A NEW CONCEPT FOR HIGH-SPEED LIQUID CHROMATOGRAPHY

VICTOR PRETORIUS, B. J. HOPKINS and J. D. SCHIEKE
Department of Physical, Organic and Theoretical Chemistry, University of Pretoria, Pretoria (Republic of South Africa)

SUMMARY

Electro-osmosis has been used to pump solvents in both thin-layer and high-speed liquid chromatography. The advantages of this technique over conventional methods of driving solvent are discussed.

INTRODUCTION

Possibly the two most successful descendants of classical column liquid chromatography are thin-layer chromatography (TLC) and what has come to be known as high-speed liquid chromatography (HSLC). Both have been extensively described (see, *e.g.*, refs. 1 and 2). For our purpose, it suffices to draw attention to only those aspects where, as is described below, electro-osmosis may be usefully employed.

HSLC requires, for its successful operation, columns packed with small (1–20 μm) support particles, covered with a thin layer (pellicular) of chromatographic material, through which solvent is driven at relative high linear flow-rates (*ca.* 0.1–1 cm·sec^{-1}). Most commonly, the solvent is driven through the column by applying sufficient pressure (up to 10,000 p.s.i.) and this introduces several disadvantages:

(i) special pumps and inlet devices must be used;

(ii) columns must be constructed from mechanically strong materials; glass columns, which are useful for handling many biological samples, are not easily constructed,

(iii) columns are, perforce, narrow-bore and preparative chromatography becomes technically formidable;

(iv) detector dead volumes must be kept extremely small (several microlitres) in order to avoid additional band spreading.

Less commonly, the solvent is driven by placing the entire column in a strong centrifugal field[3]. Among the disadvantages of this technique are:

(i) columns are short (*ca.* 10 cm);

(ii) detection must be carried out, after separation has taken place, by extruding the packing from the column;

(iv) the entire available column length can seldom be effectively used.

Figure I.10. Title page of the pioneering article of Pretorius et al. which appeared in 1974 in Journal of Chromatography [49].

CEC is generally depicted as a hybrid between capillary electrophoresis and liquid chromatography. However, to asses CEC in a more fundamental way some extra considerations have to be made. For example, the generation of EOF and the retention mechanism will be different due to the presence of a stationary phase and an electrical field. Moreover, the assessment of band broadening in CEC should be reinvestigated. Finally, the

importance of the analysis temperature should be re-examined as temperature influences both the flow profile and the retention mechanism.

4.1 Separation mechanisms occurring in CEC

In CEC a separation can occur by electrophoretic migration and chromatographic retention but the mobile phase will move due to electroosmosis. Combination of Eq. I.4 and Eq. I.32 gives a general expression for the retention factor in CEC, k_c, taken into account that the total separation time constitutes out the retention and electromigration time.

$$k_c = k + kk_e + k_e \qquad \text{Eq I.40}$$

In CEC four different possibilities can occur. If the analyte is neutral (k_e=0) and not retained by the stationary phase (k=0), it will elute with the EOF time. If the analyte is charged but exhibit no retention, only electrophoretic migration will occur (k_c= k_e). A neutral but retained analyte will be only chromatographically retained (k_c= k). Finally, a charged and retained solute will exhibit a retention factor as described in Eq. I.40. Note that in the last case retention and electrophoretic migration can influence the retention factor in opposite ways.

The selectivity in CEC is, accordingly to HPLC and CZE, described by:

$$\alpha_{21} = \frac{k_{c,2}}{k_{c,1}} \qquad \text{Eq I.41}$$

4.2 Some considerations for the EOF generation in CEC

The generation of an EOF in CEC is not as straightforward as in other electrodriven techniques. Comparable to CZE, the EOF generation is dependent on the pH, ionic strength and zeta-potential of the buffer. Furthermore, the analysis temperature and the applied voltage will influence the mobile-phase velocity. Next to these parameters, the organic modifier, necessary to achieve successful chromatographic separation in a timely manner, will also influence the EOF but more important charges on the stationary phases will also contribute to the EOF generation.

4.2.1 The influence of the stationary phase on the EOF

In CEC, the EOF will be generated by the free charge bearing moieties at the surface of the stationary phase and the wall. The EOF in CEC capillaries can also be described by the approach of Rice and Whitehead whereby the packed capillary is considered as a bundle of combined capillaries in which the particles constitute the walls of the channels. therefore, the magnitude of the EOF would be independent of the particle diameter (channel separator) as long the double layers do not overlap, as illustrated in Figure I.11 [52]. Subsequently, Knox and Grant calculated that the EOF velocity does not depend on the size of the particles as long their radii is larger than 0.4 µm [51,53]. This was attested by Lüdtke et al., who packed capillaries with 0.5 µm C8 particles and measured an EOF up to 3 mm/s [54]. Tallarek et al. used NMR displacement imaging to demonstrate the flat electroosmotic flow profile in porous media [55].

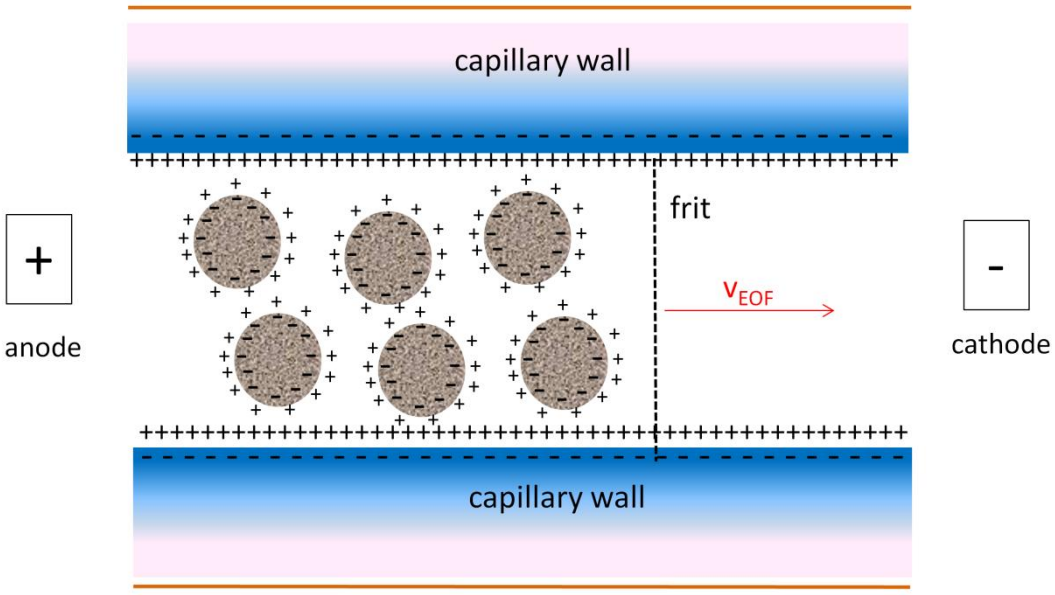

Figure I.11. Generation of the EOF in packed capillaries.

In CEC both the stationary phase as the capillary wall can exhibit charges, capable of supporting the EOF generation. To assess the contribution of the stationary phase, Dittmann and Rozing inhibited the EOF generation originating from the free silanol functions on the wall by coating the capillary with polyvinylalcohol [56]. Consequently, the capillary was packed and an EOF of 1.6 mm/s was measured. Comparison with packed, uncoated capillaries revealed that there was no difference in EOF velocity and hence, that the EOF was

mainly generated by the free silanol function of the particles. Note that more recent introduced packing materials are generally endcapped and are therefore not always able to generate an EOF.

Open-tubular capillaries and monolithic capillaries with a non-siloxane based backbone, on the other hand, will not generate any EOF unless charge bearing groups are implemented on the surface of the stationary phase. The generated EOF will increase with increasing charge surface density and surface area.

Alternatively, Lelièvre et al. noticed a reduction of 40 to 50% of the EOF in packed capillaries compared to open channel capillaries [57]. This effect was attributed to modifications on the silica particles (endcapping, functional groups), resulting in a lower free silanol surface density and hence a lower zeta-potential. Furthermore, the channels formed by the particles are not all aligned with the capillary which can therefore also explain the decrease in EOF velocity [57].

4.2.2 The influence of the organic modifier on the EOF and retention in CEC

Just as in HPLC, organic modifiers in CEC will influence the retention behavior of the solutes, as the retention factor k is roughly related to the organic modifier fraction in the mobile phase by

$$\ln k = \ln k_0 - a.p \qquad \text{Eq I.42}$$

where k_0 represents the retention factor in pure aqueous environment, "a" is a constant and p is the percentage organic modifier in the buffer [39].

In most cases acetonitrile is applied as organic modifier, however others has occasionally been used as well [58]. The reasoning for the choice of acetonitrile can be seen in Table I.1, which compares the ratio of the dielectric value over the viscosity of binary mixtures of several organic solvents and water. This ratio is directly related with the electroosmotic velocity, as described in Eq. I.36.

Table I.1. ε_r/η ratios for binary mixtures with water at 25°C

Solvent	ε_r/η (cP^{-1}) for varying organic ratio's		
	0%	50%	75%
Acetone	88	23	68
Acetonitrile	88	75	105
Methanol	88	37	60
2-propanol	88	15	7

data retrieved from reference[39]

Acetonitrile (ACN) shows the best ε_r/η ratio at 50% for all organic solvents and even an improved ratio at 75%, which means that the EOF velocity will be higher under these conditions compared to the pure buffer. Furthermore, the eluotropic strength of ACN is higher compared to methanol.

4.3 Band broadening processes occurring in CEC

4.3.1 The van Deemter model applied to CEC

As explained before, despite the theoretical shortcomings and the existence of several other zone dispersion models, the van Deemter theory is still the most applied model to describe the band broadening (and the efficiency) of columns [59]. However, some significant distinctions between CEC and HPLC have to be made to describe the eddy diffusion and the resistance to mass transfer.

In pressure-driven methods (as LC) the tortuosity of the flow paths is enhanced by the difference in speed of the laminar flow at the center of the flow channel as compared to the speed of the mobile phase near the particle wall. In CEC, the flow velocity is largely independent on the channel width, as discussed in section I.3.2, resulting in a much lower zone dispersion and therefore lower A-term (with a factor 4) [60]. As the EOF velocity is independent of particle diameters, this allows the use of smaller particles than in LC, in this way further reducing the A-term.

Moreover, a lower C-term is occurring in CEC compared to in HPLC. This is especially the case when the packed bed contains particles depicting pore sizes of 300 A° and larger. This is

related to mass transfer in the particle pores, which is the sum of the diffusion and of additional EOF transport effect [61]. By contrast, for HPLC, the mobile phase in the particle pores is stagnant and therefore only diffusion creates the transfer of the solutes from mobile phase to the stationary phase. Note that the additional EOF transport only starts to occur when broad pores (> 100 A°) are present in the particle. Otherwise, double layer overlap will prevent the generation of the EOF [1].

A comparison of simulated van Deemter curves for CEC and HPLC is shown in Figure I.12. It can be concluded that CEC will have a lower minimum plate height at the optimum velocity, due to the beneficial lower contribution of the A- and of the C-term (λ is set as 0.1).

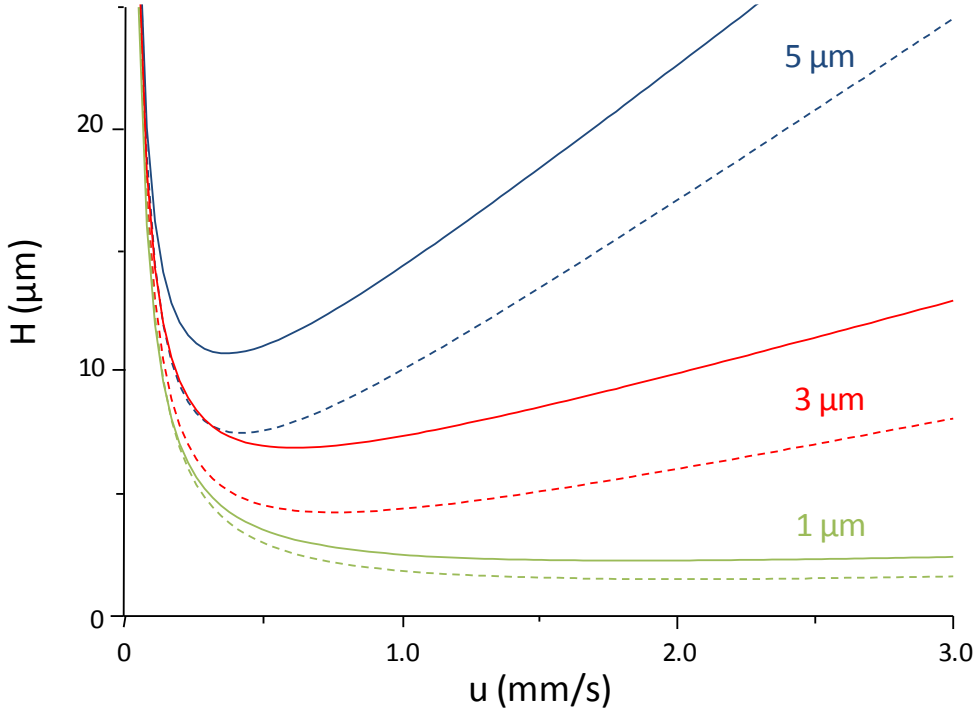

Figure I.12. Simulated van Deemter Curves for HPLC (full lines) and CEC (dashed lines) with varying particle diameters [5].

4.3.2 Kinetic plots for electrodriven techniques

Up to now, the comparison between CEC and HPLC has been performed by comparing the obtained minimum plate heights as a function of the mobile phase velocity. Also comparisons between formats have been focused on the H vs. u curves. However, as explained before, the minimum plate height does not demonstrate the potential of the

column. In particular, the comparison between HPLC and CEC is ambiguous since the maximum number of plates which can be obtained with a certain mobile-phase velocity is determined by the permeability of the column for pressure-driven techniques such as LC. Therefore the kinetic plot for CEC should be developed.

Fekete et al. developed several kinetic plot methods for liquid-phase separation techniques with different driving forces (shear-driven, electrodriven) [62]. As the mobile phase velocity in the capillary electrophoresis is only limited by the mobility of the electro-osmotic flow (EOF). The practical constraint in CE is therefore not the pressure drop but the potential drop according to Eq. I.43.

$$u_0 = \mu_{EOF} \frac{\Delta V}{L} \qquad \text{Eq. I.43}$$

However, the experimentally measured kinetic plot of CE differed from the theoretical expected values. This can be explained by the differences between separation based on chromatographic behavior and electromigration. After all, the kinetic plot method is constructed for chromatographic systems. More specific, the efficiency of the separations in capillary electrophoresis will only increase with higher applied voltages and hence higher velocities.
However, the construction of kinetic plots for CEC analyses of neutral molecules should be possible, if separation occurs in a purely chromatographic manner.

4.4 Influence of temperature in CEC on retention and performance

In packed CEC, control over the temperature is even more important. Several theoretical approaches revealed that packed columns generate less Joule heat but also dissipate heat less efficiently. The Joule heat will increase with increasing conductivity (ionic strength of the background electrolyte) and with the cross sectional area of the capillary. However, the particles in the packed bed segment of the capillary separate the electrical conductivity into small channels. Therefore, the cross section that plays a role in the total conductivity (particles are assumed not to be conductive) will be smaller compared to the open channel capillaries with the same internal diameter, resulting in a lower generated heat [43]. Nevertheless, heat dissipation through a liquid is more effective than through silica material.

Therefore the heat dissipation will be enhanced in open channel segment rather than in a packed segment. Overall, less Joule heating will be developed during the analysis but effective dissipation of the built-up heat has proved to be more difficult.

Djordjevic et al. performed CEC analyses of steroids with a temperature programmed separation and compared the result with isothermal and isocratic analyses [63]. The analysis time was reduced by 50%, while there was no significant change in the quality of the separation.

Like every chromatographic system, the relationship between retention and temperature in CEC can be described by the van 't Hoff equation, which states that a linear relationship exists between the logarithmic of the retention factor (*k*) and the multiplicative inverse of the absolute temperature (T) [64,65].

$$\log(k) = \frac{-\Delta H}{RT} + \frac{\Delta S}{R} + \log \Phi \qquad \text{Eq I.44}$$

where *R* is the universal gas constant, *Φ* is the phase ratio, *ΔH* is the enthalpy change and *ΔS* represents the entropy change. Consequently, the retention will lower and the stationary phase selectivity can change with increasing temperature [39].

The primary purpose of thermostatically controlling the capillary temperature is the efficient removal of Joule heat, but the control of temperature can also be used to optimize the CEC separation. This effect can only be achieved if the temperature is homogeneous over the capillary as local differences in retention will contribute to band broadening.

5. References

[1] E. Wen, R. Asiaie, C. Horvath, J. Chromatogr. A 855 (1999) 349.

[2] J.W. Dolan, L.R. Snyder, N.M. Djordjevic, D.W. Hill, T.J. Waeghe, J. Chromatogr. A 857 (1999) 1.

[3] U.D. Neue, J. Chromatogr. A 1079 (2005) 153.

[4] J.J. van Deemter, F.J. Zuiderweg, A. Klinkenberg, Chem. Eng. Sci. 5 (1956) 271.

[5] A. Dermaux, PhD dissertation, University of Ghent, Belgium, 1999.

[6] P.A. Bristow, J.H. Knox, Chromatographia 10 (1977) 279.

[7] J.H. Knox, J. Chromatogr. A 831 (1999) 3.

[8] M.J.E. Golay, Anal. Chem. 40 (1968) 382.

[9] M. Horka, V. Kahle, M. Krejci, K. Slais, J. Chromatogr. A 697 (1995) 45.

[10] J.H. Knox, M.T. Gilbert, J. Chromatogr. 186 (1979) 405.

[11] R. Swart, J.C. Kraak, H. Poppe, Chromatographia 40 (1995) 587.

[12] I. Gusev, X. Huang, C. Horvath, J. Chromatogr. A 855 (1999) 273.

[13] G. Guiochon, J. Chromatogr. A 1168 (2007) 101.

[14] C. Legido-Quigley, N.D. Marlin, V. Melin, A. Manz, N.W. Smith, Electrophoresis 24 (2003) 917.

[15] K.K. Unger, R. Skudas, M.M. Schulte, J. Chromatogr. A 1184 (2008) 393.

[16] Y. Guo, L.A. Colon, Chromatographia 43 (1996) 477.

[17] Y. Saito, K. Jinno, T. Greibrokk, J. Sep. Sci. 27 (2004) 1379.

[18] H. Poppe, J. Chromatogr. A 778 (1997) 3.

[19] J.C. Giddings, Anal. Chem. 37 (1965) 60.

[20] G. Guiochon, Anal. Chem. 53 (1981) 1318.

[21] J.H. Knox, M. Saleem, J. Chromatogr. Sci. 7 (1969) 614.

[22] G. Desmet, D. Clicq, P. Gzil, Anal. Chem. 77 (2005) 4058.

[23] G. Desmet, D. Clicq, D.T.T. Nguyen, D. Guillarme, S. Rudaz, J.L. Veuthey, N. Vervoort, G. Torok, D. Cabooter, P. Gzil, Anal. Chem. 78 (2006) 2150.

[24] K. Broeckhoven, D. Cabooter, F. Lynen, P. Sandra, G. Desmet, J. Chromatogr. A 1217 (2010) 2787.

[25] K. Broeckhoven, D. Cabooter, S. Eeltink, G. Desmet, J. Chromatogr. A 1228 (2012) 20.

[26] A. Vaast, K. Broeckhoven, S. Dolman, G. Desmet, S. Eeltink, J. Chromatogr. A 1228 (2012) 270.

[27] S. Eeltink, W.M.C. Decrop, F. Steiner, M. Ursem, D. Cabooter, G. Desmet, W.T. Kok, J. Sep. Sci. 33 (2010) 2629.

[28] D. Clicq, S. Heinisch, J.L. Rocca, D. Cabooter, P. Gzil, G. Desmet, J. Chromatogr. A 1146 (2007) 193.

[29] D. Cabooter, F. Lestremau, F. Lynen, P. Sandra, G. Desmet, J. Chromatogr. A 1212 (2008) 23.

[30] F. Lestremau, A. de Villiers, F. Lynen, A. Cooper, R. Szucs, P. Sandra, J. Chromatogr. A 1138 (2007) 120.

[31] S. Delahaye, K. Broeckhoven, G. Desmet, F. Lynen, Talanta 116 (2013) 1105.

[32] A.S. Rathore, C. Horvath, J. Chromatogr. A 743 (1996) 231.

[33] D. Henderson, D. Boda, PCCP 11 (2009) 3822.

[34] F. Robert, J.P. Bouilloux, L. Denoroy, Ann. Biol. Clin. 49 (1991) 137.

[35] C.L. Rice, R. Whitehead, J. Phys. Chem. 69 (1965) 4017.

[36] P.H. Paul, M.G. Garguilo, D.J. Rakestraw, Anal. Chem. 70 (1998) 2459.

[37] G.J.M. Bruin, J.P. Chang, R.H. Kuhlman, K. Zegers, J.C. Kraak, H. Poppe, J. Chromatogr. 471 (1989) 429.

[38] B.M. Michov, Electrophoresis 6 (1985) 471.

[39] K.D. Bartle, P. Myers, J. Chromatogr. A 916 (2001) 3.

[40] M.M. Dittmann, K. Wienand, F. Bek, G.P. Rozing, Lc Gc-Mag Sep Sci 13 (1995) 800.

[41] S. Kitagawa, T. Tsuda, J. Microcolumn Sep. 6 (1994) 91.

[42] K. Sarmini, E. Kenndler, J. Chromatogr. A 792 (1997) 3.

[43] A.S. Rathore, K.J. Reynolds, L.A. Colon, Electrophoresis 23 (2002) 2918.

[44] High Performance Capillary Electrophoresis: A primer, Agilent Technologies, 2009, 174.

[45] G.Y. Tang, C. Yang, J.C. Chai, H.Q. Gong, Int. J. Heat Mass Transfer 47 (2004) 215.

[46] C.J. Evenhuis, R.M. Guijt, M. Macka, P.J. Marriott, P.R. Haddad, Anal. Chem. 78 (2006) 2684.

[47] M. Berezovski, S.N. Krylov, Anal. Chem. 76 (2004) 7114.

[48] H. Strain, J. Am. Chem. Soc. 61 (1939) 1292.

[49] V. Pretorius, B.J. Hopkins, J.D. Schieke, J. Chromatogr. 99 (1974) 23.

[50] J.W. Jorgenson, K.D. Lukacs, J. Chromatogr. 218 (1981) 209.

[51] J.H. Knox, I.H. Grant, Chromatographia 24 (1987) 135.

[52] G. Choudhary, C. Horvath, J. Chromatogr. A 781 (1997) 161.

[53] J.H. Knox, I.H. Grant, Chromatographia 32 (1991) 317.

[54] S. Ludtke, T. Adam, K.K. Unger, J. Chromatogr. A 786 (1997) 229.

[55] U. Tallarek, T.W.J. Scheenen, P.A. de Jager, H. Van As, Magnetic Resonance Imaging 19 (2001) 453.

[56] M.M. Dittmann, G.P. Rozing, J. Microcolumn Sep. 9 (1997) 399.

[57] F. Lelievre, C. Yan, R.N. Zare, P. Gareil, J. Chromatogr. A 723 (1996) 145.

[58] A. Banholczer, U. Pyell, J. Chromatogr. A 869 (2000) 363.

[59] L. Kirkup, M. Foot, M. Mulholland, J. Chromatogr. A 1030 (2004) 25.

[60] M.M. Dittmann, G.P. Rozing, J. Chromatogr. A 744 (1996) 63.

[61] D.M. Li, V.T. Remcho, J. Microcolumn Sep. 9 (1997) 389.

[62] V. Fekete, A. Fekete, J. Fekete, A. Liekens, P. Schmitt-Kopplin, G. Desmet, Jpc-Journal of Planar Chromatography-Modern Tlc 23 (2010) 440.

[63] N.M. Djordjevic, F. Fitzpatrick, F. Houdiere, G. Lerch, G. Rozing, J. Chromatogr. A 887 (2000) 245.

[64] G.F. Chen, U. Tallarek, A. Seidel-Morgenstern, Y.K. Zhang, J. Chromatogr. A 1044 (2004) 287.

[65] N.M. Djordjevic, P.W.J. Fowler, F. Houdiere, G. Lerch, J. Liq. Chromatogr. Relat. Technol. 21 (1998) 2219.

Chapter 2

Practical aspects of capillary electrochromatography

The specific instrumentation necessary to perform CEC analyses is portrayed in this chapter. Four key components of the instrumentation are described in detail: the injection system, the power supply, the temperature control device and the hyphenation to the detector. The state-of-the-art-instrumentation is discussed and particular attention is focused on the detector as sensitive and/or universal detection is hard to acquire with capillary electrodriven techniques. Furthermore, the possible application of high voltages in CE and CEC analyses is discussed.

1 Introduction

CEC can be performed with a regular CE apparatus, which can be a commercial or an in-house constructed system. A CE instrument consists of several basic elements: an injection system, a high voltage power supply, a temperature control device and a detector. Furthermore, CEC analyses with packed capillaries requires the inclusion of pressurization (max 12 bar) at both the inlet and outlet buffer vials, to suppress the formation of gaseous bubbles in the packed bed and frits. Figure II.1 depicts a schematic overview of a capillary electrophoresis system.

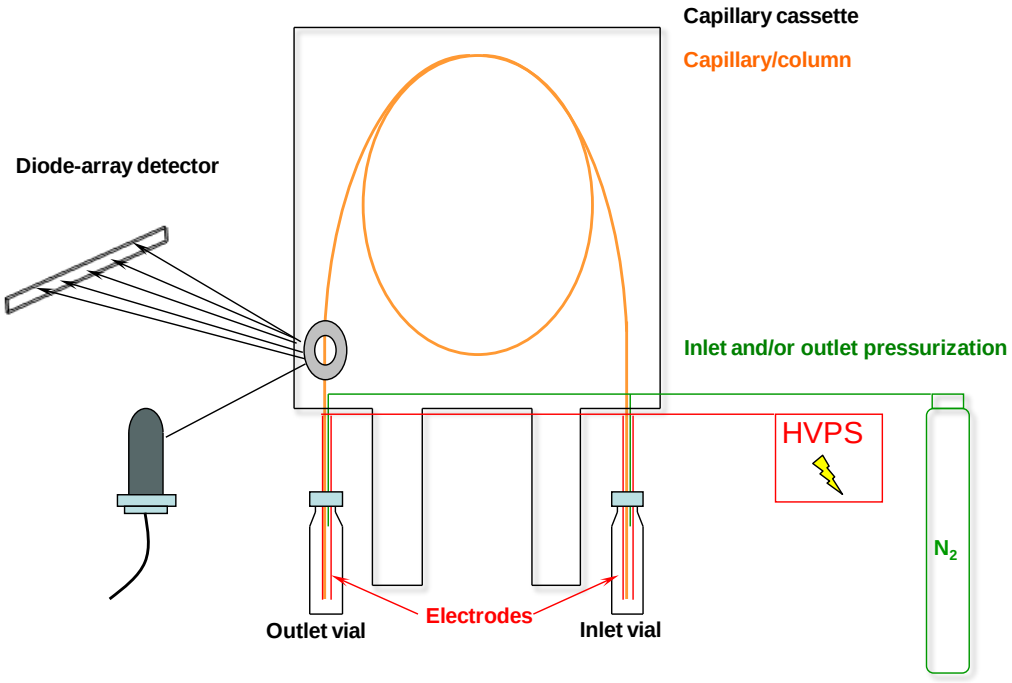

Figure II.1. Schematic representation of a commercial CEC apparatus with vial pressurization.

Contemporary capillary electrophoresis systems are almost completely automated, allowing full sequential analyses without an operator present. The system contains one or more vial trays for the buffer vials and state-of-the art systems even have a replenishing system where the buffer vials can be emptied and refilled with buffer.

Several detection methods can be used directly or hyphenated to a CE-system such as: UV detection, contactless conductivity detection, mass spectrometry (MS), laser induced

fluorescence detection (LIF) and many more. However, control over injection, temperature, voltage and other parameters is mandatory to achieve repeatable CE(C) analyses.

2 Instrumentation applied in this thesis

All electrodriven experiments were performed on an Agilent CE 7100 instrument equipped with a DAD detector, an auto sampler and an air-cooled thermostat. Pressurization of the inlet and outlet vial could be performed by an internal pump (max 1 bar) or an external pressure source (max 12 bar). All recorded data was processed with Chemstation B.04.03 software.

3 Sample introduction in CE(C)

During CE(C) injections, only a minute sample volume will be loaded into the capillary column. These small volumes are required to maintain the high efficiency and repeatability of the analyses. Overloading of the column will result in a proportional increase of band broadening and has a detrimental effect on the peak shape due to the mismatched conductivity between the electrolyte and the solute zone [1].
Like every miniaturized separation method, the small sample volumes are beneficial if the total sample volume is limited. The most common injection modes in CE(C) systems are hydrodynamic injection and electrokinetic injection. In contrast to HPLC and GC, the injection volume is not a known quantity but is expressed in "pressure x seconds" or "voltage x seconds". However, the volume can always theoretically be calculated.

3.1 Hydrodynamic injection

Hydrodynamic injection is achieved by applying pressure to the injection vial (at the beginning of the capillary) or to establish a vacuum at the outlet vial. The injected volume V_{inj} can be calculated by the Hagen-Poiseuille equation [2,3]

$$V_{inj} = \frac{\Delta P r^4 \pi \, t_{inj}}{128 \eta L} \qquad \text{Eq II.1}$$

where r is the radii of the capillary, η is the dynamic viscosity, L is the total length of the capillary, ΔP the pressure difference across the capillary and t_{inj} represents the injection

time. The total amount of injected analyte molecules, n_a, can be obtained by multiplying V_s with the analyte concentration, c_a.

$$n_a = V_{inj}.c_a = \frac{\Delta P r^4 \pi\, t_{inj}}{8\eta L}.c_a \qquad \text{Eq II.2}$$

Typically applied injection pressure and time ranges are 5 to 100 mbar and 1 to 10 seconds, respectively.

Hydrostatic injection is an alternative to hydrodynamic injection. The injection is then obtained by raising the injection vial 5 to 10 cm relative to the outlet vial for 5-20 seconds. A siphoning effect introduces a finite sample volume into the column. Typically, this kind of injection is performed on systems lacking an internal pressurization system.

3.2 Electrokinetic injection

Electrokinetic injection is obtained by applying an injection voltage *(V_{inj})* during a short time interval between the sample vial and the outlet buffer vial. The sample molecules will be dragged into the column by the generated EOF and the injection volume is therefore dependent on the electroosmotic mobility, μ_{EOF} [4].

$$Vol_{inj} = \frac{\mu_{EOF} V_{inj} r^2 \pi\, t_{inj}}{L} \qquad \text{Eq II.3}$$

The amount of the solutes loaded into to the column is dependent on their electrophoretic mobility. Ionic species with higher mobility will be introduced into the column to a greater extent than ionic species with lower mobility and depending on the polarity of the electrodes, ions with the opposite charge can be excluded from entering the column (at low generated EOF). The amount of solute loaded into the column can be expressed as:

$$n_a = \frac{(\mu_a + \mu_{EOF}) V_{inj} r^2 \pi\, t_{inj}}{L}.c_a \qquad \text{Eq II.4}$$

where μ_a represents the electrophoretic mobility of the molecule. Consequently, quantitative analysis is only achievable with neutral solutes. Typically voltages 3 to 5 times lower than used for the separation are applied with injection times ranging between 5 to 30

seconds.

Next to the discrimination of the charged ions, electrokinetic injection is depending on different parameters as temperature, pH, ionic strength... and is therefore less repeatable than hydrodynamic injection.

3.3 Injection in CEC

The Hagen-Poiseuille equation (Eq. II.1) states that the injected volume is correlated directly with the open channel. However, the stationary phase of packed and monolithic capillaries reduces the diameter of the open channel to the average interparticle distance and the average through pore size. Therefore, long injection times should be applied to obtain a large enough volume with pressure injections resulting in extensive band broadening. Therefore, in most CEC analyses electrokinetic injection is applied.

3.4 On-capillary sample preconcentration in CE and CEC

A unique feature of capillary electrodriven technique is the possibility to enhance the sensitivity by the preconcentration of the solute at the beginning of the capillary. A large volume of sample solution is thereby injected and refocused in a narrow band. Several preconcentration techniques, such as sample stacking, transient isotachophoresis, pH-mediated stacking, and dynamic pH junction, utilize the difference in the properties of the background electrolyte and the sample diluent (conductivity, pH, ...) to focus the sample bands [5-11]. Some other techniques (sweeping, self-focusing with monoliths and solvent gradient effects) rely on the chromatographic partitioning or complexation of the solute to focus the band [12-15].

Note that the use of preconcentration is limited as electro-osmotic pressure is developed between the boundaries of the sample solvent and the background electrolyte, which causes the generation of a laminar flow and creates broadening of the solute zone. Unwanted preconcentration (and band broadening) can occur easily in CEC, where the focusing can happen by differences in solvent properties (when the injection solvent is highly different from buffer composition) and by chromatographic partitioning.

4 Detection in CEC: challenges and limitations

Detection in CEC (and CE methods in general) remains challenging due to the miniaturized dimensions, very low flow rates (nL/min) and practical problems with hyphenation of detectors. The most common detection methods and their detection limits are described in Table II.1 alongside the advantages and disadvantages.

Table II.1. Detection methods applied in CEC

Method	Mass detection limit (moles)	Concentration detection limit (molar)*	Advantages/ disadvantages
UV-Vis adsorption	$10^{-13} – 10^{-16}$	$10^{-5} – 10^{-8}$	• universal • diode-array offers spectral information
Fluorescence	$10^{-15} – 10^{-17}$	$10^{-7} – 10^{-9}$	• sensitive • usually requires sample derivatization
LIF	$10^{-18} – 10^{-20}$	$10^{-14} – 10^{-16}$	• extremely sensitive • usually requires sample derivatization • expensive
Amperometry	$10^{-18} – 10^{-19}$	$10^{-10} – 10^{-11}$	• sensitive • selective, but only useful for electro-active analytes • requires special electronics and capillary modification
Conductivity	$10^{-15} – 10^{-16}$	$10^{-7} – 10^{-8}$	• universal • requires special electronics and capillary modification
MS	$10^{-16} – 10^{-17}$	$10^{-8} – 10^{-9}$	• sensitive and offers structural information • hyphenation can be a problem • expensive
Indirect UV, fluorescence, amperometry	10-100 times less than direct method		• universal • decreased sensitivity

4.1 UV-VIS detection in CEC

Just as in HPLC, UV-VIS detection is the principal detection method in CEC. Detection can occur at several places but generally, a detection window is formed on the capillary by removing the polyimide layer and transmissions occurs through the fused-silica wall of the capillary. Consequently, the sensitivity of UV-VIS detection is limited in CEC due to the very small radii of the capillaries an hence small path lengths.
A distinction has to be made between the variable wavelength detector (VWD) and the diode array detector (DAD). The former can only measure the absorbance at one or two different wavelengths where the latter can obtain the absorbance over a whole range of wavelengths and the UV-VIS spectrum. Therefore the DAD can be used to identify the solutes and asses the peak purity.

In packed bed CEC, the detection generally occurs in the unpacked section of the capillary, which is called on-column detection (OCD). However, Rebscher et al. and Robson et al. reported photometric detection in the packed bed of the column (in-column detection, ICD), resulting in low reduced plate heights [16-18]. A comparison between OCD and ICD was made by Banholczer et al. [19]. With in-column detection an increase in the base line noise (with a factor 2) was noticed, resulting in higher detection limits. This can be explained by the presence of the stationary phase, causing a diffuse scattering of the UV-beams at their irregular interfaces. In open-tubular and monolithic columns, in-column detection is the standard UV-VIS detection method.

4.2 Contactless conductivity detection in electrodriven techniques

Contactless conductivity detection (CCD) is an universal and very sensitive detection system and is therefore widely used in CE and in some extent in CE(C). With conductivity detection, an alternating current generated by applying an alternating voltage on one electrode is picked up by a second electrode and is transformed back to an alternating voltage by use of a modified amplifier. The conductivity of the measured solutions determines the frequency. Therefore, an analyte band, which influences the local conductivity of the background electrolyte, can be monitored and detected. The contactless conductivity detector was developed to prevent fouling, degradation and formation of gaseous bubbles. Hereby the alternating voltage of one electrode is capacitively coupled into the electrolyte and picked

up in a contactless way by the other electrode [20]. The fundamentals of the technique is described in depth by Brito-Neto et al; and some recent reviews described the latest applications and developments [21-28]. CCD is also implemented as detection technique in CEC, however is not yet widely used [29-31].

4.3 Fluorescence detection and laser induced fluorescence detection in CEC

Fluorometric detection methods are based on the measurement of the emission spectrum (emitted photons) when an excited molecule falls back to its lowest energy level. In practice, the fluorescence spectrum will resemble the absorption spectrum but shifted to higher wavelengths.

Generally, a laser is used as the excitation source in CE(C). The laser provides a high intensity light source and can be focused on the fused-silica capillary, which acts as the detection cell. This method is called laser induced fluorescence detection (LIF) [16]. LIF is the most sensitive detector for CE to date and can be performed on-column and post-column. The high sensitivity arises from the high photon flux created by the laser excitation source and from the very low (dark) background obtained with fluorescence detection. Note that only few compounds are suited for fluorometric detection, generally molecules with a planar rigid structure. However, several approaches to label the solutes (carbohydrates, peptides, DNA) with fluorometric groups have been described [32-35].

4.4 Indirect UV and LIF-detection: unique detection feature in CE(C)

Electrodriven separation methods exhibit a unique feature allowing the detection of molecules without a chromo-and/or fluorophore groups. The indirect method is often applied to detect inorganic alkali metals in capillary electrophoresis. Indirect UV detection is achieved by monitoring the absorbance of an ionized molecule, which is added to the buffer solution. The presence of a zone of non-absorbing analyte causes the displacement of the monitored ions. The decrease in concentration causes consequently a decrease in the absorbance and the analyte zone will now be depicted in the chromatogram as a valley or an inverted peak. The same technique can be applied for LIF detection when the monitored ion contains a strong fluorophore group. However the sensitivity of indirect detection is 10 to 100 times lower compared to the corresponding direct detection methods.

4.5 Hyphenation of mass spectrometry to CEC

The majority of CEC analyses have been performed with on-column photometric detection as this method is easily applied, not-expensive and universal. However, the small optical path lengths limits the sensitivity. The hyphenation of mass spectrometric detection (MS) eliminates the sensitivity problem (sensitivity does not depend on the detection cells size) and delivers molecular mass and structural information, allowing to detect and identify unknown solutes [36]. However, the combination of a liquid-phase separation mechanism with a vacuum detection technique is already challenging but in CEC some extra challenges have to be dealt with.

A first step towards successful MS detection is the proper and efficient ionization of the mobile phase and analytes in the ionization source. Consequently, compatible mobile phases should be volatile and not leading to the formation of ion-pairs. Electrospray ionization (ESI) is generally applied as ionization source in CEC-MS, especially since ESI obtains high ionization efficiencies (and hence improved sensitivities) at low flow rates. Moreover, the mobile phase is already ionized and therefore particularly suited for ESI ionization. However, in CEC often capillaries with small internal diameters (< 25 µm) are applied, resulting in very low flow rates (few nL/min), which are not compatible with normal ESI sources. Moreover, MS-detection occurs at the end of the column and therefore differs in set-up compared to CEC-UV. Due to the missing outlet vial, the electronic circuit has to be closed in an alternative way. However, both CEC and ESI are electrodriven but there is a mismatch between their applied voltage drops. Hence, the decoupling of the electronic system of the separation voltage and the MS-ionization source is beneficial but not straightforward.

The first reported hyphenation between CEC and MS was described in 1991 by Verheij et al [37]. A continuous-flow fast atom bombardment (CF-FAB) ionization source was thereby used. However, this ionization method had some major limitations and drawbacks. For example, at measurement of low mass molecules a high chemical background was obtained and an unstable current could be noticed during the run. However, CEC-MS has evolved over time and the most recent applied interfaces can be divided in coaxial sheath flow interfaces, liquid junction interfaces and sheathless interfaces, which have been thoroughly described in literature [36,38,39]. In sheath-flow and liquid-flow interfaces, ionization occurs with normal

ESI sources which have an optimal flow rate of 50-500 µL/min. However, CEC capillaries only generate a mobile phase flow of several nL/min. Therefore an extra flow is added to the end of the capillary to achieve a proper ionization. Nevertheless, the sensitivity will be hampered due to the dilution of the analyte by the sheath flow.
On the other hand, with the sheathless interface the eluent of the capillary is directly sprayed in to the ESI source and sensitivity will be higher. However, specialized nano-ESI sources have to be installed to achieve a proper ionization or CEC capillaries with wider radius and hence higher eluting volumes have to be used.

Dispersion of the solute band will occur between the outlet end of the column and the ionization source, decreasing the performance. Consequently, the set-up of the hyphenation is from utmost importance to keep the loss in performance as minimal as possible. Boughtflower et al. investigated the influence on the performance of the different interfaces and proposed the best set-up to minimize dispersion caused by the empty tube connection between capillary and MS [38,40]. It could be concluded that the end of the stationary phase should be as close to (or used as) the spray tip as possible to avoid significant dispersion effects. Therefore, the combination of on-column detection and MS is not advisable, however in-column detection and MS are still compatible.

5 Efficient temperature control in CEC

The generation of Joule heat during an electrophoretic run and the possible detrimental effect of local temperature differences in the capillary is thoroughly described in Chapter I. The effective dissipation of heat to the close environment of the capillary is therefore from utmost importance, certainly with relatively wide packed bed capillaries.

Generally, the dissipation of heat is maintained by cooling down the nearest environment. To keep the temperature differences under control in commercial CE instruments, the capillary is generally bathed in a fast cold air stream (e.g. Agilent CE systems) or in a cooling liquid (e.g. Beckman CE systems). To measure the amount of Joule heating, the current versus voltage plots are plotted. A non-linear increase in current with voltage (Ohm's law) indicates an increase in the buffer temperature, as depicted in Figure II.2 [1].

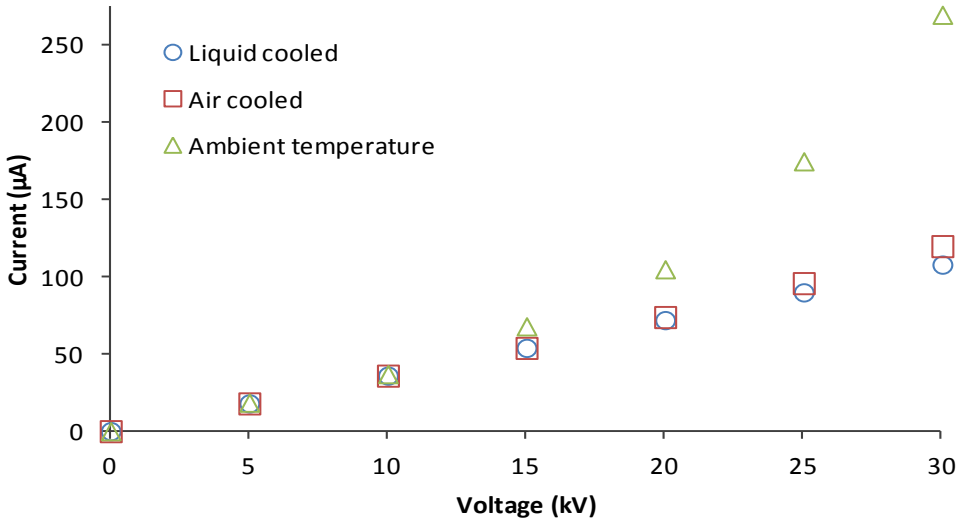

Figure II.2. Current versus Voltage plot for a 100 µm ID capillary. Data retrieved from [1].

6 High and ultra-high voltages applied in CEC

In CE systems the high voltage power supply apply potential differences up to 30 kV. The main requirement of the supply is the stable regulation of the voltage to obtain stable and repeatable analyses. In CEC with fused-silica capillaries and silica-based particles, the EOF will move towards the cathode. Therefore, detection will occur at the end of cathode. As a consequence, the anode will be positioned at the inlet side. Due to the fixed position of the detector in the CE system the electrodes remain also in a fixed position. However, in some cases a counter directional EOF will be created. That means that under influence of a coating, stationary phase or functional groups bounded on the stationary phase the EOF will move towards the anode. Nevertheless, as the detector is in a fixed position, the electrodes should switch polarity. As a consequence, a DC voltage power supply is typically used in combination with a ground electrode and a high voltage electrode. The latter will either be positively or negatively driven relative to the former.

Very high voltages are theoretically beneficial in terms of analysis speed and efficiency. In CEC, ultra-high voltages would allow the use of longer columns and hence improved efficiencies. However, ultra-high voltages (>30kV) will cause the dielectric breakdown of the fused-silica wall due to the high radial electrical field, resulting in broken capillaries. The high radial electrical field originates from the potential drop between the grounded electrode and the high-voltage electrode. The current will drop to zero across the capillary and will not

recover, resulting in stress at the capillary wall. Furthermore, an increased risk for corona discharge, arcing and electrical sparks is associated with the use of ultra-high voltages. Therefore, the maximum potential drop of commercial instruments is limited to 30 kV.

Hutterer and Jorgenson developed in 1999 a CE system, capable of applying 120 kV without dielectric breakdown [41]. The capillary was protected with a series of metal conductors. The whole set-up was immersed in transformator oil to prevent arcing and corona discharges. A four times faster separation of a tryptic digest was obtained with efficiencies up to 2.6 million plates, as illustrated in Figure II.3.

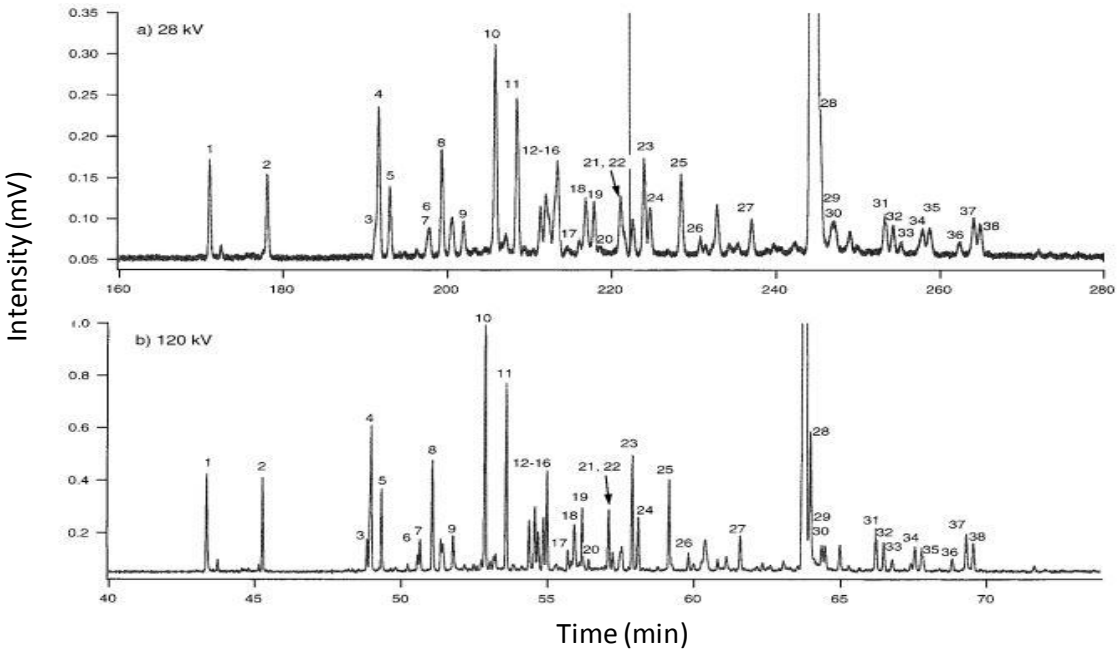

Fig. II.3. Electropherogram of a myoglobin digest, analyzed at 28 kV (a) and 120 kV (b). Data reproduced from [41].

The ultra-high-voltage analyses were successfully expanded to gel electrophoresis and micellar electrokinetic chromatography [42,43]. More recently, the ultra-high voltage set-up was adjusted by changing the transformator oil to plastic insulators. The insulator prevents more adequately the possible corona discharges and sparking between the capillary and the metal shields. Consequently, even higher voltages (up to 300 kV) could be successfully applied resulting in ultra-high efficiently analyses in the same or in shorter analysis times [44].

However, the majority of CE(C) instruments and analyses are still equipped with 30 kV DC power supply's as this instrumental set-up is less complex and as the thereby obtained efficiencies are already high (>500,000 plates/meter).

7 References

[1] High Performance Capillary Electrophoresis: A primer, Agilent Technologies, 2009, 174.

[2] D.J. Rose, J.W. Jorgenson, Anal. Chem. 60 (1988) 642.

[3] J.D. Olechno, J.M.Y. Tso, J. Thayer, A. Wainright, Am. Lab. 22 (1990) 30.

[4] Z. Krivacsy, A. Gelencser, J. Hlavay, G. Kiss, Z. Sarvari, J. Chromatogr. A 834 (1999) 21.

[5] D.S. Burgi, R.L. Chien, Anal. Biochem. 202 (1992) 306.

[6] R.L. Chien, D.S. Burgi, Anal. Chem. 64 (1992) 1046.

[7] R.L. Chien, D.S. Burgi, Anal. Chem. 64 (1992) A489.

[8] Z. Mala, A. Slampova, L. Krivankova, P. Gebauer, P. Bocek, Electrophoresis 36 (2015) 15.

[9] P. Gebauer, W. Thormann, P. Bocek, J. Chromatogr. 608 (1992) 47.

[10] Z.K. Shihabi, J. Chromatogr. A 744 (1996) 231.

[11] J.P. Quirino, N. Inoue, S. Terabe, J. Chromatogr. A 892 (2000) 187.

[12] J.P. Quirino, S. Terabe, Chromatographia 53 (2001) 285.

[13] J.P. Quirino, S. Terabe, J. Chromatogr. A 902 (2000) 119.

[14] J.P. Quirino, S. Terabe, P. Bocek, Anal. Chem. 72 (2000) 1934.

[15] P. Britz-McKibbin, K. Otsuka, S. Terabe, Anal. Chem. 74 (2002) 3736.

[16] H. Rebscher, U. Pyell, J. Chromatogr. A 737 (1996) 171.

[17] M.M. Robson, S. Roulin, S.M. Shariff, M.W. Raynor, K.D. Bartle, A.A. Clifford, P. Meyers, M.R. Euerby, C.M. Johnson, Chromatographia 43 (1996) 313.

[18] H. Rebscher, U. Pyell, Chromatographia 38 (1994) 737.

[19] A. Banholczer, U. Pyell, J. Chromatogr. A 869 (2000) 363.

[20] A.J. Zemann, E. Schnell, D. Volgger, G.K. Bonn, Anal. Chem. 70 (1998) 563.

[21] J.G.A. Brito-Neto, J.A.F. da Silva, L. Blanes, C.L. do Lago, Electroanal. 17 (2005) 1198.

[22] J.G.A. Brito-Neto, J.A.F. da Silva, L. Blanes, C.L. do Lago, Electroanal. 17 (2005) 1207.

[23] M. Pumera, Talanta 74 (2007) 358.

[24] F.-M. Matysik, Microchim. Acta 160 (2008) 1.

[25] P. Kuban, P.C. Hauser, Electrophoresis 36 (2015) 195.

[26] P. Kuban, P.C. Hauser, Electrophoresis 34 (2013) 55.

[27] P. Kuban, P.C. Hauser, Electrophoresis 32 (2011) 30.

[28] P. Kuban, P.C. Hauser, Electrophoresis 30 (2009) 3305.

[29] T.D. Mai, H.V. Pham, P.C. Hauser, Anal. Chim. Acta 653 (2009) 228.

[30] X.-j. Chen, J. Zhao, Y.-t. Wang, L.-q. Huang, S.-p. Li, Electrophoresis 33 (2012) 168.

[31] E. Dabek-Zlotorzynska, V. Celo, M.M. Yassine, Electrophoresis 29 (2008) 310.

[32] A.H. Que, A. Palm, A.G. Baker, M.V. Novotny, J. Chromatogr. A 887 (2000) 379.

[33] V. Kasicka, Electrophoresis 31 (2010) 122.

[34] M.C. Ruizmartinez, J. Berka, A. Belenkii, F. Foret, A.W. Miller, B.L. Karger, Anal. Chem. 65 (1993) 2851.

[35] C. Colyer, Cell Biochem. Biophys. 33 (2000) 323.

[36] C.W. Klampfl, J. Chromatogr. A 1044 (2004) 131.

[37] E.R. Verheij, U.R. Tjaden, W.M.A. Niessen, J. Vandergreef, J. Chromatogr. 554 (1991) 339.

[38] G. Choudhary, A. Apffel, H.F. Yin, W. Hancock, J. Chromatogr. A 887 (2000) 85.

[39] E. Barcelo-Barrachina, E. Moyano, M.T. Galceran, Electrophoresis 25 (2004) 1927.

[40] R.J. Boughtflower, C.J. Paterson, J.H. Knox, J. Chromatogr. A 887 (2000) 409.

[41] K.M. Hutterer, J.W. Jorgenson, Anal. Chem. 71 (1999) 1293.

[42] K.M. Hutterer, J.W. Jorgenson, Electrophoresis 26 (2005) 2027.

[43] K.M. Hutterer, H. Birrell, P. Camilleri, J.W. Jorgenson, J. Chromatogr. B 745 (2000) 365.

[44] W.H. Henley, J.W. Jorgenson, J. Chromatogr. A 1261 (2012) 171.

Chapter 3

Column technology, stationary phases and the different modes applied in capillary electrochromatography

This chapter provides a literature study of the different stationary-phase supports applied in CEC. These supports can be divided in three main groups: packed bed capillaries, open-tubular capillaries and monolithic capillary columns. The different manufacturing procedures of the first two types are discussed in depth in this Chapter. Furthermore, a focus is set on the necessity and drawbacks of frits in packed capillaries and on the sensitivity problems of open-tubular capillaries. Finally, all the applicable CEC separation modes are described and a comparison with the corresponding modes in liquid chromatography is given.

1 Introduction

In every chromatographic set-up the column is the "heart" of the separation method as it defines the overall separation characteristics. In CEC, the column plays a dual role and it is also responsible for the generation of the EOF. Therefore, varying the physical characteristics (length and inner diameter) and the stationary phase characteristics (support, type, thickness) will not only influence the separation but also the mobile-phase velocity.

The stationary-phase supports applied in CEC can be mainly divided in three categories: packed capillaries, monolithic capillaries and open-tubular particles. These CEC capillaries are generally fabricated in-house, however, several commercial capillary manufacturers exist.

This chapter will elaborate on the different techniques used to manufacture capillaries with these supports and will discuss the encountered advantages and drawbacks of each stationary-phase format.

2 Technology, particles and frits applied in packed CEC

The most utilized and researched format in CEC is the particle packed capillary. Thereby particles are introduced into a fused-silica column with a typical internal diameter ranging between 25 and 100 µm. The packed capillaries have a typical length between 200 and 1000 mm and consists of a packed segment, where the particles are immobilized by an inlet and outlet frit, and an open segment. UV-detection occurs in the open segment, as close as possible to the packed segment. However, successful UV-detection requires the local removal of polyimide coating, which weakens the capillary locally.

The packing of the capillary is considered to be a "skill" rather than a science as experience of the manufacturer is mainly the key parameter to obtain a satisfactory packed column. The integrity and performance of the packed bed is determined by a variety of parameters, such as the slurry solvent, the impact velocity (particle velocity), the type of packing material and the packing procedure. Poorly packed columns can lead to lowered efficiencies, worse resolutions, asymmetric peak shapes and splitted peaks.

2.1 Packing procedures applied in CEC

The packing procedures for capillaries can be divided in 5 categories: slurry packing by pressure, packing with supercritical CO_2, packing by electrokinetical forces, packing by centripetal forces and packing by gravity [1]. However, the vast majority of packed particles are manufactured with a slurry packing method (including the pressure packing and supercritical fluid packing strategies), while the use of the other packing methods is seldom reported.

2.1.1 Slurry packed capillaries with pressure

The slurry-packing procedure involves a series of steps, including the rinsing of the capillary, preparation of frits, the packing of the capillary and finally, the conditioning of the packed capillary [2]. First, a temporary frit was manufactured by tipping the fused-silica capillary into a mixture of sodium silicate and silica particles. The introduced small plug of wetted particles is then subsequently sintered, resulting in a mechanically stable frit. The packing reservoir, an adapted emptied HPLC column is placed in a ultrasonic bath. The packing slurry is sonicated for 30 minutes and introduced in the packing reservoir. Subsequently, the capillary is packed by applying a MeOH flow at a constant pressure of 600 bar. The packing reservoir and slurry is sonicated during the packing procedure. The packed capillary is flushed for 16 hours with water. Subsequently, the final outlet frit is sintered and the temporary frit is removed. After inversing the flow direction, the final inlet frit is formed in the same manner. Using this method overall efficiencies of 300,000 plates/meter could be obtained for 50 µm ID capillaries packed with 3 µm HyperSil particles [2].

Several other pressure packing procedures are described in literature, utilizing different methods to fabricate frits, using different packing solvents, pressures or different set-ups [3-7]. However, the main factor influencing the packing efficiency and the final performance of the packed capillary is the velocity of the particles during the packing. To obtain a homogeneous and dense beds, a constant and low packing speed is necessary. The variation in packing speed leads to inconsistencies and loose packed segments, lowering the column performance. furthermore, the sedimentation of particles in the slurry restricts the maximal packing time. To maintain the slurry in solution, the slurry reservoir is in some cases

sonicated and a suitable solvent or solvent mixture with an optimal density can be selected [8].

2.1.2 Packing with supercritical CO_2

Supercritical CO_2 has been used as carrier to pack HPLC and SFC columns in an efficient and repeatable way [9,10]. This approach was adapted by Robson et al. to produce highly performant CEC capillaries [11,12]. One end of the capillary was thereby connected to a packing reservoir, containing the dry packing material. The outlet end of the capillary, with the retaining frit, was connected by an union to a second capillary, with smaller internal diameter (10 µm ID). The second capillary acts as a restrictor and is necessary to maintain supercritical conditions while packing. The whole set-up is submerged in an ultrasonic bath and sonicated during packing with supercritical CO_2 as carrier. Typically, the columns are packed at 60-70°C at a pressure of 250-350 bar (above supercritical conditions). Subsequently, pressure is released very slowly to avoid disturbances in the packed bed. Finally, the packed capillary is carefully rinsed with water and frits are sintered.

2.1.3 Packing by electrokinetical forces

The electrokinetic packing of capillaries was developed and patented by Yan et al. in 1996 [13]. In this method, a slurry is sonicated in a buffer-methanol mixture and added in vial. Into this vial the empty capillary is inserted by means of a septum cap, together with the anode. The outlet end (with frit) of the capillary is then introduced in a second vial. This second vial also contains an electrode and the buffer-methanol mixture, which will function as cathode and is placed on a lower level than the first vial. During packing both the vials and the capillary are vibrated by ultrasonication. To start the packing procedure, a voltage ramp between 2 and 30 kV is gradually applied and kept constant at the maximum (30kV). The generation of an EOF will drag the particles into the capillary. After packing of the column, the capillary is removed from the vials and consequently pressurized with H_2O. In the final step, the final retaining frits are formed by sintering and an UV-window is formed.

Dadoo et al. utilized this packing method to pack a 1.5 µm particles over a length of 6.5 cm. A highly-efficient separation of low retained PAH's was obtained with a maximum efficiency of 45,000 plates in less than 5 minutes [14].

To speed-up the rather slow process of electrokinetic packing, Stol et al. introduced the slurry into the capillary by applying a very low (2.5 bar) hydrodynamic pressure. Subsequently, the final packing is established by applying an electrical field over the column, as described previously. With this pseudo-electrokinetical packing method, separations of 5 PAH's were obtained with an efficiency of 45,000 plates on a 16 cm packed bed (3 µm particles) [15].

2.1.4 Packing by centripetal forces

Colon et al. utilized centripetal forces to pack columns in a short time window (< 10 min). Capillaries with an outlet frit are thereby connected by stainless steel arms to a central reservoir, containing the slurry of the particles. The set-up is rotated with high frequency (≈ 2,000 rpm) and the particles are introduced into the column by a sedimentation process [16,17].

2.1.5 Packing by gravity

In this method, the particles are transported into the capillary by gravity. Thereby a 1 mL syringe, filled with a particle slurry in acetone, acts as the packing reservoir. The syringe is connected to a capillary with an outlet frit, which has been filled with acetone. Sedimentation of the particles takes place during minimum 10-12 hours but can take up to 48 hours, while the slurries are replaced every 4 hours. Subsequently, the packed capillaries are rinsed with water and frits are sintered [18]. A reduced plate height of 1.7 µm for a 20 cm packed bed capillary with 3 µm particles was obtained in this way. However, only one (preliminary) research (to the best of the authors knowledge) is reported with this method. This is probably due to the very long preparation time, while efficiencies and plate heights are comparable or worse compared to faster packing methods.

2.1.6 Comparison of the applied packing procedures

The different packing methods were developed, investigated and evaluated by different research groups and therefore evalueted with different sample mixtures and different methods. Consequently, an unambiguous comparison is difficult. Colon et al. made a comparison by packing the capillaries with the five described methods (and utilizing the same particles) and evaluating the packing efficiency with the same sample mixture and method [19]. Surprisingly, the evaluation revealed no large differences between the

methods in terms of efficiency and resolution. It can be concluded that all methods are suitable to pack CEC capillaries, however the set-up of the slurry packed capillaries with pressure is by far the least complex one. Consequently, the slurry packed capillaries (with pressure) is also the most reported method.

2.2 Sintered frits and alternatives in packed CEC

The two porous plugs at the beginning and the end of the packed bed are called "frits". These frits retain and immobilize the packing material but are often considered as the "Achilles heel" of packed bed electrochromatography. The frits should be mechanically stable enough to endure the applied high packing and flushing pressures and simultaneously exhibiting a high permeability to enable an efficient solvent flow. The frit material is generally foreign to the packed bed material and presents therefore an inhomogeneity in the packed bed. Consequently, the frit should be produced in a repeatable manner while minimizing the frit length [12,20].

Sintering of silica-based frits is the most straightforward and commonly used method. Lynen et al. for example, described a method where parts of the packed bed itself was sintered as frits [2]. During the sintering (>550°C) polysilicates are formed, resulting in a porous frit. However, the altering of the silica material creates an inhomogeneity in the packed bed. The mis-match in zeta potential between the frit and the packed bed induces the formation of gaseous bubbles during the run, hampering baseline and current stability [4,21]. To prevent this formation, the buffer vials should be degassed prior to the analysis and pressurized during the run. Additionally, gaseous bubbles are less prone to form at higher organic modifier contents in the mobile phase.

Besides the formation of gaseous bubbles, the inhomogeneity in the flow velocity causes a poorer peak shape. According to Lelièvre et al., 34% percent of the band broadening is caused by the frit in a packed bed capillary with sintered frits [22]. Moreover, during the sintering the protective polyimide layer is removed by the high temperature. Hence, the capillary is more fragile.

To address these problems, several other methods to fabricate frits or to immobilize the packed bed have been developed during the last years, and have recently been extensively

reviewed by Cheong [23]. Figure III.1 depicts the most common methods to immobilize the packed bed.

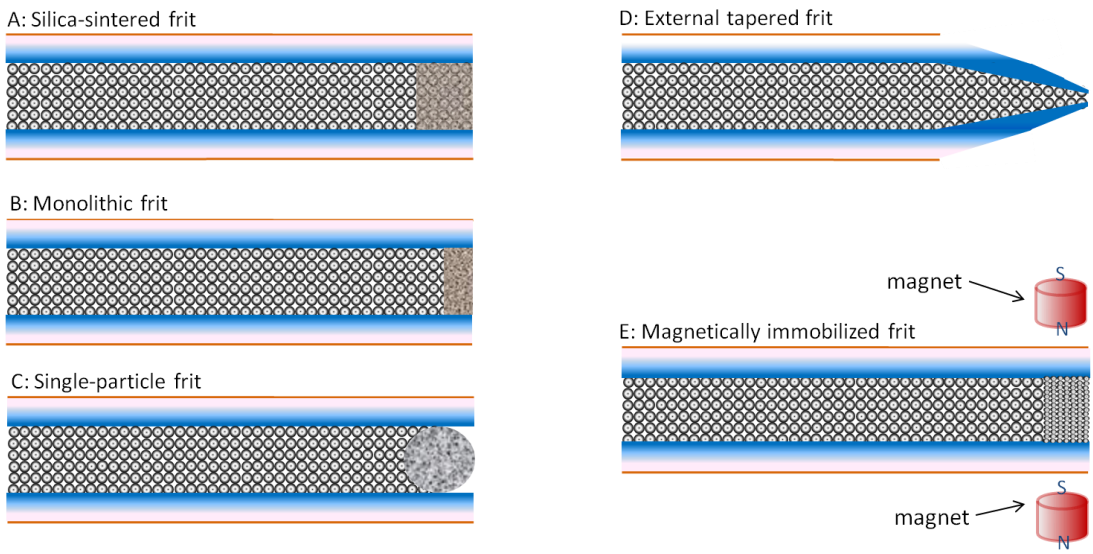

Figure III.1. A schematic overview of the frit types developed for packed column CEC. Silica based sintered frit (A), monolithic frit (B), single-particle frit (C), external tapered frit (D), magnetically immobilized frit (E).

Chen et al. prepared a monolithic frit by the free radical polymerization of two methacrylates in the presence of a porogen, resulting in a monolithic porous plug. The frits were mechanically stable and the method was repeatable [24,25]. The potential of monolithic frits has widely been investigated. Polymerization thereby occurred via photo initiation and thermal initiation (at low temperatures) [26-28]. As a consequence, the polyimide layer has not to be removed, resulting in a more robust capillary. Moreover, no bubble formation occurrs with the use of monolithic frits [29,30].

Oguri et al. and Wang et al. explored the possibility to immobilize magnetically responsive particles in fused-silica capillary by applying a local magnetic field. The performance of an ODS packed capillary in such a way was comparable to a packed capillary with sintered frits. The magnetic frits are easy to prepare, reliable under a variety of conditions, compatible with almost every packing material and repeatable [31,32].

Zhang et al. introduced the single particle bead frit. A single particle of 110 µm was thereby forced into the end of a 100 µm ID capillary column (and placed in the right position by a 90 µm OD capillary). The edge of the large particle has particle fines attached due to

electrostatic interactions. These particulate fines originated from the scratched surface or consisted of smaller added packing material. Upon applying hydraulic pressure, a keystone effects takes place between the particle bead, the particulate fines and the wall, locking the single bead frit in its place. The short length of the frit (=100 µm) results in smaller frit-induced inhomogeneities in the packed bed and therefore the band broadening caused by the frit is minimal [33,34].

Lord et al. introduced a fritless packed column with tapered ends, suitable for hyphenation with MS. The capillaries are tapered by applying heat and tension simultaneously. The particles (3 µm) were immobilized by the keystone effect if the capillary was tapered to a 10 µm tip. These external tapered columns were utilized for sheath-liquid and sheathless MS-interfaces without any bubble formation [35,36]. However, the external tapered tip is not robust and breaks down after a few runs. An alternative was introduced by Zheng et al. who produced internal tapers in an easy and repeatable manner. Compared to the external taper, the internal taper showed an improved durability, repeatability and electrospray stability [20,37].

2.3 Packing materials utilized in CEC

Generally, CEC capillaries are packed with commercially available particles, which have been developed for HPLC. The first reports primarily investigated the use of reversed phase particles with a 3-5 µm diameter. Nowadays, the 3 µm particles are still the most reported size but sizes between 0.5-10 µm have been investigated. The stationary phase in CEC generates the EOF and should therefore exhibit a high enough zeta-potential in a buffer medium. However, modern LC reversed phase packing materials are endcapped and none or only a little amount of free silanol groups are available to enable the EOF generation [38]. Besides the classical ODS particles, the performance of a wide range of packing materials has been investigated. For example, the application of mixed mode particles has been investigated in CEC. These particles are functionalized with alkyl (C18) chains ending in ion-exchange groups, resulting in a mixed retention mechanism. However, the ion-exchange groups are mainly used to enhance the EOF generation during the analysis of neutral solutes [39-41].

Next to the classical ODS particles, a wide range of silica and polymer particles have been used in packed CEC, such as bare silica particles, aminopropyl silica particles, polymer based particles and octadecyl sulfonated particles [42-47]. Furthermore, Fanali et al. compared the performance of porous and superficial porous particles coated with a polysaccharide chiral selector [48].

2.4 The limitations of packed capillary CEC

Capillary electrochromatography is often associated with numerous advantages, such as the high efficiencies of this miniaturized technique compared to micro-LC and the introduction of a new separation mechanism for ionized solutes. However, a few drawbacks, in particular associated with packed CEC capillaries, limits the useful CEC applications in industry. In particular, the formation of gaseous bubbles and the band broadening induced by the frits limit the robustness and the gain in efficiency. Moreover, rinsing the fused-silica capillaries with a basic solution (1 M NaOH), prior to conditioning the capillary with the background electrolyte, has proven to be essential to obtain repeatable analyses. However, capillaries packed with (functionalized) silica particles will dissolve at high and low pH conditions (2<pH<8), limiting the repeatability of packed CEC. In addition, basic solutes will tend to form ion pairs with the negatively ionized silanol groups, which causes elongated elution times and tailed and broadened peaks, limiting once again the obtainable efficiency.

3 The application of open-tubular capillaries in CEC

Open-tubular capillaries are fused-silica capillaries where the stationary phase is attached to the capillary wall in the form of a thin layer. These capillaries have numerous advantages compared to the traditional applied packed bed capillaries including the fritless formation of the stationary phase, the simplicity of the preparation procedure and the easy stationary phase modification. More importantly, open-tubular CEC would offer significant practical benefits such as the possibility to cut off parts of the capillary, easier rinsing, less clogging issues and the facile hyphenation with ESI-MS.

Unlike the packed and monolithic column formats, the performance of open-tubular capillaries is directly linked to the internal diameter of the capillary. Small internal diameters are required to facilitate efficient solute diffusion into the stationary phase [49]. Narrower capillaries provide higher efficiencies and a higher concentration of an on-column loaded

sample [50]. Furthermore, the Joule heating in open-tubular columns will be non-existing or limited due to the small internal diameters (5-20 µm). However, the loading capacity and retention of many OT-LC (and CEC) capillaries is limited due to the high phase ratio ($\beta = V_m/V_s$, whereby V_m and V_s correspond to the volume of mobile and stationary phase, respectively).

The stationary phases in open-tubular capillary chromatography can be either covalently bonded to the wall or applied as a physical coating to the wall. Next to open-tubular capillaries, microchips with open channels can also be utilized in electrochromatography. The stationary phases applied in open-tubular electrochromatography have been extensively described in several reviews [50-54]. Only a general overview of the different stationary-phase structures in open-tubular CEC will therefore be given.

3.1 Chemically bonded stationary phases

Chemically bonded stationary phases are more stable and have longer lifetimes compared to physically absorbed stationary phases. However, the preparation is more time consuming and complex [51]. The chemically bonded stationary phases can be divided according their preparation method and chemical structure.

3.1.1 Directly covalent bonded stationary phases

Open-tubular electrochromatography has already been reported in 1982 by Tsuda et al. who bonded chemically octadecylsilane (ODS) on the inner surface of glass capillaries [55]. A separation of a PAH mixture was obtained.

Next to ODS, several other synthetic ligands have been bonded as stationary phases in OT-CEC. Initially, most research focused on the immobilization of some host ligands, such as crown ethers, aptamers, cyclodextrins and calixarenes [56-62]. However, the utility of these molecular recognition ligands as stationary phase is limited due to their specific interaction. Brush synthetic ligands, such as ODS variants, amino acids, triamine ligands and phenylaminopropyl ligands are more universal retaining stationary phases and can be coupled to the wall via a single step silanization or via coupling reagents [63]. OT-CEC with synthetic ligands as stationary phase often display high separation efficiencies as the thin layer thickness enhances the mass-transfer kinetics and the separation efficiencies.

However, the small carbon load and the small surface area of the ligands limit the retention and the loading capacity of the solutes in the sample.

Some attempts to bind single polymer strands to a silanized capillary wall have been reported. Qiao et al. produced several types of block copolymers based on styrene and acrylates [64,65]. A separation with improved selectivity but worse efficiencies was obtained in this way, even with very thin applied coatings. The authors claimed that the block copolymer coatings eliminated the necessity of sodium dodecyl sulfate as micelle forming additive in CE runs for the separation of steroids and aromatic amines and hence hyphenation of the coated capillaries with MS should been possible. However the significant loss in efficiency and the poor peak shape limits the use of these copolymers [51].
To increase the phase ratio, Xu et al. introduced a new tentacle-type metal-chelating polymer chains as stationary phase in OT-CEC. Compared to a monolayer of the polymer, the tentacle metal chelating polymer exhibit an enhanced retention and better selectivity for the separation of amino acids and purine derivates [66]. Moreover, other tentacle-type polymer stationary phase were developed for the successful separation of proteins and peptides. Separations were obtained in a pH range of 2.5-7 with efficiencies up to 180,000 plates/meter [67-69].

Various other forms of covalently bonded stationary phases haven been explored such as coatings of proteins, polysaccharides, carbon nanotubes and nanoparticles [20,51,70-72]. However, one significant drawback of this approach remains the low surface area of the stationary phases, resulting in low retention and limited loading capacities. Thicker coatings results in a slower mass-transfers kinetics and therefore lower efficiencies. Some methods to enlarge the surface area (with fast mass-transfer kinetics) have been investigated, such as the etching of the surface of the capillary wall and the preparation of porous polymer layers as stationary phase.

3.1.2 Etched modified stationary phases

The capillary wall can be etched to increase the surface area up to 1000 fold. The capillary walls are etched at high temperatures (300-400°C) in the presence of an etching reagent, $(NH_4)HF_2$. Consequently, the density of the free silanol groups on the surface is increased and the etched capillaries are coated with triethoxysilane (TES) via a silanization step. Finally, the etched silica-hydride wall can now be functionalized via hydrosilanization with the proper functional groups [73]. The silanization of the silanol groups is advantageous for the analysis of basic solutes, which interacts strongly with free silanol groups. Etched silica capillaries have been functionalized with octadecyl, diol and cholestrol groups and several chiral recognition groups [74-76]. Compared to bare fused-silica capillaries and coated fused-silica capillaries, the etched capillaries exhibit an improved retention for the solutes of interest. Chen et al. prepared etched capillaries for OT-CEC by immobilizing ionizable succinate and phtalate-monomers on the surface [77,78]. The functionalized capillaries generated a significant higher EOF then an etched (not functionalized) capillary. Moreover, the phtalate functionalized capillary demonstrated an enhanced retention for aromatic compounds compared to the succinate functionalized capillary, due to additional π-π interactions of the stationary phase with the solutes.

Overall, the reports of application for etched capillaries in OT-CEC are still limited. This is probably due to the high number of anchoring sites (Si-OH groups) for ligands, resulting in a dense layer of functional groups. Ligands with a big molecular size (proteins, polysaccharides...) will form a too dense stationary phase with low mass-transfer kinetics. On the other hand, small ligands, such as C5-C18 chains, are not retentive enough to induce a separation of small organic molecules with sufficient resolution [51].

3.1.3 Porous layer open-tubular columns by polymerization

Another approach to enhance the surface area is the preparation of a porous polymer layer on the surface wall of the capillary. Thereby will the dramatically increased surface area result in an increased retention of the solutes while the mass-transfer kinetics will remain fast due to the porosity (if there is no double layer overlap) of the polymer. In general, the fused-silica wall is first derivatized by a double bond ligand, which can be used as anchoring point for the polymerization chains.

Huang et al. introduced in 1999 the first porous layer open-tubular (PLOT) capillary suited for CEC analyses. The silica capillary was pretreated with 3-(trimethoxysilyl) propyl methacrylate prior to the in-situ polymerization of vinylbenzylchloride and divinylbenzene in the presence of 2-octanol as porogen. The PLOT capillary was characterized by SEM pictures, as depicted in Figure III.2 and optimized on a trial and error base.

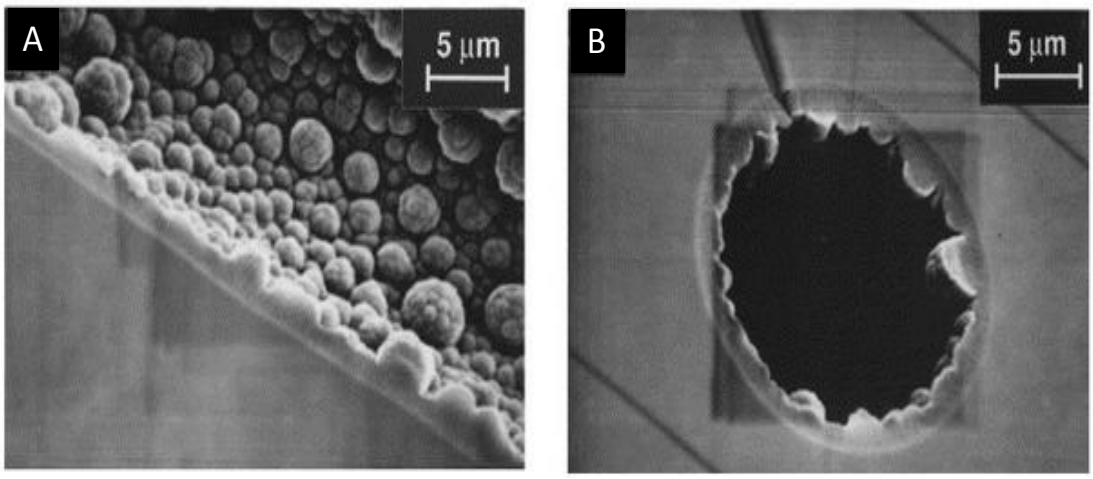

Figure III.2. Scanning electron micrographs of the porous layer of a polydivinylbenzene based polymer layer (A) and the cross section of the same capillary (B).

This PLOT capillary exhibited a high chemical stability with anodic EOF flow and was attested by the separation of basic proteins [79]. Various other PLOT columns, based on acrylamides and methacrylates, have been prepared by in-situ polymerizations [80,81]. The amount of accessible free silanol groups after the silanization and formation of the porous polymer layer is finite and therefore an ionizable group, responsible for the EOF generation, has to be grafted or copolymerized in the process.

PLOT columns can also be produced by a sol-gel technique, which provides a tool to synthesize a wide variety of hybrid organic-inorganic porous layers. The procedures for the sol-gel prepared CEC PLOT columns have extensively been reviewed by Malik et al. [82,83]. This technique produces a stable, thick, monolith like layer on the inner lining of the capillary wall, resulting in stationary phase with high loading capacity, fast mass-transfer kinetics and high retentive characteristics. The selectivity and the EOF control can be easily adapted by adjusting the sol-gel composition (concentration and precursors). Sol-gel prepared PLOT

columns have been utilized in the RP mode, hydrophilic interaction mode and for the separation of enantiomers [84-86].

Overall, PLOT columns exhibit some advantages. However, the characterization of the polymer layers can only be performed by SEM pictures and optimization should be executed on a trial and error basis. Other characterization is more complicated as the removal of the polymer layer from the capillary implicits the destruction of the morphology. However, it can be stated that the loading capacity of the porous layer is advantageous compared to the (previously described) thin coatings.

3.2 Physical and dynamically coating of stationary phases to the fused-silica wall

In CE(C), adsorption of analytes to the capillary wall is deleterious for the separation efficiency. However, this adsorption effect can be used as driving force to prepare a stationary phase layer in a controlled and structured manner. The preparation of such coatings is more facile and inexpensive compared to chemically bonded stationary phases. However, the lifetime and the stability of such adsorbed layers is limited.

The adsorbed coatings are categorized in physical and dynamic coatings, according to the strength of adsorption. Physical coatings are strongly adsorbed on the capillary wall and will shield the negatively charged silanol groups. Dynamic coatings are only weakly attached to the wall and the adsorbed modifier is actually added to the mobile phase [50].

The first applications of adsorbed stationary phases have already been reported in CE analyses, where the coating suppressed or inverted the EOF [87-92]. In electrochromatography, however, the coated stationary phase should introduce a chromatographic mode, while avoiding the time consuming steps to anchor the coating chemically to the wall.

Liu and co-workers investigated and reviewed in 1999 the adsorption effects and the chromatographic behavior of several cationic surfactants, basic proteins, peptides and amino acids [93-95]. More recently, new developments in physically and dynamically adsorbed coatings have extensively been reviewed by Doherty et al., Guihen et al., Cheong et al. and Xu et al. [20,50,51,53].

More recently, the application of graphene coated capillaries attracted some interest for the separation in RP-CEC mode [96-100]. In a first step the capillary wall is functionalized with amino-groups. Consequently, the epoxy groups of the graphene-oxide nano sheets will react with the amino-moieties via a SN_2 nucleophilic displacement. The successful separation of some non steroidal anti-inflammatory drugs and a mixture of endocrine-disrupting chemicals has been reported on this type of column. However, the separations are characterized by low retentions due to the finite thickness of the coating. Therefore, the thickness of the layers should be optimized without any loss of efficiency.

4 Monolithic columns in capillary electrochromatography

Initially, monolithic columns were developed as an alternative for the packed bed columns in HPLC. The application of monolithic columns in liquid chromatography gained a lot of interest as the permeability of these columns are higher compared to packed columns. The higher permeability results in longer columns as column lengths are restricted by the generated back pressure. Furthermore, monolithic columns demonstrate a slow decrease of efficiency with high mobile-phase velocities and are therefore applicable for fast, efficient analyses [101-104]. Monolithic columns for CEC were already developed in the early stages of electrochromatography as they exhibit some specific advantages such as the easiness of preparation, the easy modification of the functional groups and the compatibility with small inner diameter capillaries (20-100 µm) [105-108]. Moreover, the absence of retaining frits combined with the high sample capacity explains the high interest in monolithic CEC.

Monolithic CEC will not be a subject in this work and therefore the further literature study will be concise. However, CEC with monoliths and all their aspects have been extensively researched during the last 15 years and numerous reviews have been published [83,109-118].

Monolithic CEC can be divided in two main categories: silica-based monoliths and organic polymer monoliths.

The organic monoliths are synthesized in the capillary by the in-situ polymerization of various copolymers. The reaction is instigated by free radical, thermal or UV-initiation. The organic porous monoliths in CEC are typically based on acrylamide, methacrylate and

styrene polymers and the pore size can be controlled by selecting the monomer concentration, the type of crosslinker and by adjusting the porogen solvent. Generally, the hydroxyl functions of the silica wall are no longer accessible, therefore an EOF generating moiety has to be copolymerized or grafted on the monolith to instigate the mobile-phase flow in CEC. However, the organic polymers are prone to swelling and shrinkage effects in organic solvents, limiting their repeatability and life time [119-121].

Silica based monoliths can be prepared by three different approaches: the fusion of silica particles by sintering, the entrapping of silica particles by a sol-gel process and the polymerization of silicon alkoxide precursors by sol-gel processes. Actually, the last approach is the most genuine one and therefore the most popular one to create a monolithic column. The two other approaches are developed to immobilize a packed bed without the necessity of frits. Silica monoliths do not exhibit the swelling process during analyses but are more complicated to synthesize as they need post-modification [102,115]. Moreover, the silica monoliths are only applicable in a limited pH range (3-9). Furthermore, silica monoliths are prone to shrinkage during the curing step of their preparation. As a consequence, a small gap will exist between the wall and the monolith, inducing wall effects and band broadening effects [103,122].

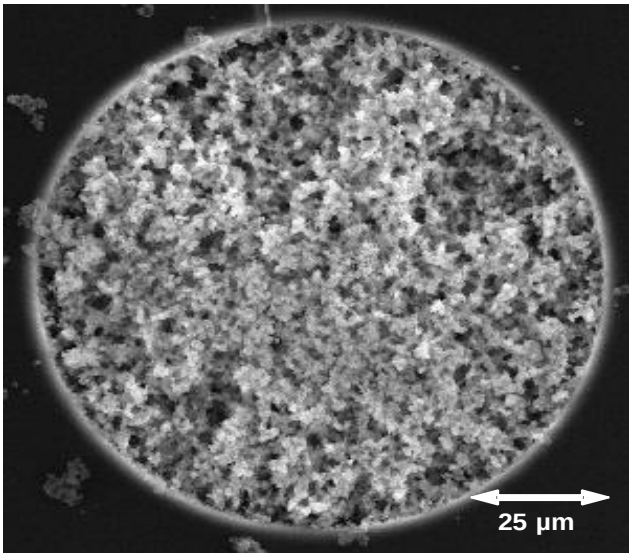

Figure III.3. SEM image of a silica-based monolith with through pore sizes of 1-2 µm [122].

5 Separation modes applied in CEC

The described column formats and their varieties can be applied in different separation modes. Comparable to HPLC, CEC separations can be divided into four major categories. The majority of the separations performed in CEC are based on the differences in polarity or hydrophobicity of the solute molecules. Also, a significant amount of research in CEC is focused at the separation of enantiomers. To a lesser extent the selective separations of charged ions via an ion-exchange type of method and the separations of solutes based on their sizes is also described in literature.

5.1 Separations based on polarity of the solute

The vast majority of CEC separation are based on differences in polarity and hydrophobicity of the solutes. Three different modes, based on the stationary phase and mobile-phase conditions, can thereby be distinguished: reversed phase chromatography, normal-phase chromatography and hydrophilic interaction chromatography.

5.1.1 Separation of non- to mildly polar compounds in the reversed phase mode

Approximately 85% of all CEC analyses are performed in the reversed phase (RP) mode. RP-CEC employs a non-polar stationary phase combined with a more polar eluent. Separation occurs by partitioning of the solutes between the stationary phase and the mobile phase. The more hydrophobic solutes will be retained longer by the stationary phase compared to the less hydrophobic and hence more polar solutes, resulting in a separation based on polarity. In RP-CEC non-polar to mildly polar solutes can be separated in this way. However, highly polar compounds are more difficult to retain and therefore to separate in this mode. Traditionally, capillaries are packed with LC types of silica particles, which are in the RP mode functionalized by long non-polar carbon chains. The EOF is thereby generated by the free silanol groups on the particles which indicates that the use of endcapped particles is not advantageous. There are numerous reports of highly efficient RP-CEC separations on packed capillaries. For example, Dadoo et al. reported efficiencies up to 750,000 plates for a 25 cm column packed with 1.5 µm particles [14]. Next to the classical packed beds, RP-CEC can also be performed on monolithic or open-tubular columns. Thereby the non-polar support is formed via organic or functionalized inorganic polymers [3,105,107,123,124].

The mobile phase is generally composed of an aqueous buffer with an organic modifier

added to it. The amount of the organic modifier regulates the retention and hence, the analysis time. In RP-CEC, the organic modifier is usually acetonitrile due to the beneficial dielectric value over the viscosity ratio of water/acetonitrile (see Chapter I) [125,126]. The elution of highly non-polar solutes can be difficult or impossible due to the limited eluotropic strength of the buffer/ACN binary mixture (even at high organic modifier concentrations). To achieve successful separation in an timely manner, non-aqueous mobile phases can be employed, increasing the eluotropic strength significantly. Dermaux et al. applied a ternary mixture of isopropanol/hexane/acetonitrile to separate successfully triglycerides in fish oil [127,128]. The separation of retinyl esters on a C30 column with a mobile phase consisting of lithium acetate dissolved in N,N-dimethylformamide/acetonitrile/methanol was reported by Roed et al. [129,130].

5.1.2 Separation of polar compounds: non-aqueous and hydrophilic-interaction mode

To separate very polar compounds in an effective way, a polar stationary phase should be used combined with a relatively non-polar solvent. However, two different separation modes can thereby be distinguished, a non-aqueous (normal phase) mode and hydrophilic interaction (HI) mode. The former method utilizes a non-aqueous mobile phase, composed of organic solvents, while the latter utilizes an organic solvent (usually acetonitrile) with a small amount(2-40%) of water or aqueous buffer added.

The polar stationary phases consists generally of silica particles functionalized with polar functional groups such as aminopropyl, diol functions or cyanopropyl functions. Accordingly to the RP-mode, the solutes will be separated by their partitioning between the stationary and the mobile phase. The retention of the solutes will thereby increase with their polarity. However, the separation of polar solutes with non-aqueous CEC is rarely reported as the use of non-aqueous mobile phase causes some practical difficulties. For example, polar compounds exhibit a low solubility in the non-polar solvents, hampering the already limited sensitivity in CEC. Furthermore, pH control in non-aqueous environments is fairly difficult and most buffer salts are difficult to dissolve in non-aqueous media. The few reported non-aqueous CEC analyses with polar stationary phases revealed that only low efficiencies were encountered combined with a poor EOF control [42,43]. Nevertheless, some efforts to

obtain non-aqueous CEC separation with polar monolithic columns have been reported [131-133].

The aqueous rich mobile phase of hydrophilic interaction chromatography on the other hand will be more suitable for CEC. This separation mode is already extensively researched in liquid chromatography (HILIC, hydrophilic interaction liquid chromatography). HILIC utilizes a polar stationary phase with a less polar mobile phase, usually a mixture of acetonitrile and an aqueous buffer. Retention in hydrophilic interaction chromatography is the result of the partitioning of the polar compounds between a more or less stagnant water enriched layer on top of the stationary phase and the less polar mobile-phase bulk. The water layer is partially immobilized by adsorption to the stationary phase. In addition to the better EOF control, HI-CEC exhibits the same advantages as HILIC compared to non-aqueous chromatography. The coupling to ESI–MS will be more efficient in HI-CEC as total non-polar solvents are difficult to ionize. Furthermore, the elution order in HI-CEC and HILIC will be the opposite as expected in RP separations, implying that HI-CEC will work the best on the lowest retained and therefore problematic solutes in RP separations.
Hydrophilic interaction chromatography has already been proven to be a strong and efficient tool for the separation of polar and basic solutes in liquid chromatography but there has only little research been done to implement the technique in CEC [3,134-138].

5.2 Enantioseparation by CEC

Nowadays, half of all drugs are synthesized as chiral compounds, and nearly 90% of these last ones are racemic mixtures. Although there is no difference in chemical structure , these enantiomers can influence biological pathways in a different manner. The separation and purification of the targeted chiral drug molecule is therefore critical. Currently, chiral separations occurs mostly by LC, SFC and CE techniques [139-143]. The separation can thereby be performed via a direct or an indirect approach. The indirect method relies on the derivatization of the enantiomeric solutes with a stereochemically pure agent in order to form diastereomers, which are subsequently separated in a achiral system. Separation of enantiomers in LC and SFC is based on the their interaction with a chiral selector, embedded in the stationary phase. Direct separation in CE is obtained by adding a chiral selector to the

BGE. As a consequence, diastereomers will be formed and separation will be based on the differences between the migration velocities of the formed diastereomers.

The first enantioseparation in CEC was reported by Schurig et al. in 1992 [144]. Due to the high efficiency ascribed to CEC, enantiomeric separations in CEC attained a lot of attention. Furthermore, direct chiral CEC could be obtained by adding a chiral selector to the mobile phase or by the use of a chiral stationary phase. Therefore, the advantages of chiral CEC has been explored in open-tubular, packed and monolithic formats. The power of chiral CEC resides in the high selectivity delivered by the stationary phase and the high peak capacities empowered by the electrodriven flow [145-148]. As a consequence, fast separations can be obtained as efficient separation can be obtained on shorter capillaries.

Comparable to HPLC, the chiral stationary phase (CSP) in CEC consists of two basic components: the chiral selector and an "inert" support. While the influence of the latter is unequivocally important for the separation characteristics, such as efficiency and mobile-phase velocity, it is the chiral selector which defines the separation. The chiral selector must exhibit the same properties as in chiral HPLC. For example, the selector must be universal but as powerful (in selectivity) as possible. Furthermore, the selector should be easily immobilized on the stationary phase by grafting, copolymerization or via other immobilization procedures. However, the application in CEC requires a stable and insoluble selector in aqueous and non-aqueous solvents at different pH's values. Furthermore, in the ideal case the EOF generation should be supported or at least not be hampered by the chiral selector [145]. The most common CSP's in CEC consist of cyclodextrin derivatives or polysaccharides derivatives as chiral selectors [22,139,149-156]. However, numerous other (macro)-molecules have been reported as successful chiral selector in CEC, such as Pirkle type selectors ,proteins and macrocyclic antibiotics [133,147,148,157-159].

5.3 Ion-exchange electrochromatography

Generally, the separation of ions is obtained by ion-exchange chromatography (IEC) or by capillary electrophoresis. The former method is based on differences in the electrostatic interactions between solutes and ion-exchange(charged functional) groups present in the stationary phase, as where the latter separates ions based on their charge to size ratio.

These methods are distinctive in sensitivity, selectivity and analysis time. In ion-exchange electrochromatography (IE-CEC), stationary phases also applied in IEC are packed or introduced in fused-silica capillaries. Therefore, a new separation selectivity will be provided, combining the characteristic of both methods. selectivity can be fine tuned by controlling the relative contributions of IE and CE [160]. Furthermore, the EOF will be generated by the charged functional groups present in the IEC stationary phase. Several successful IE-CEC separations of inorganic ions with packed, monolithic and open-tubular capillaries have been reported [114,161-165].

However, IE-CEC is mostly applied to separate successfully ionic organic solutes. In classic reversed (or normal) phase CEC, the EOF is generated by the acidic ionized silanol groups. IEC-CEC is mostly performed with a mixed mode stationary phases. These stationary phases exhibit ion-exchange groups as well as (non-)polar functional groups, and the EOF is generated by the ion-exchange groups rather than by the ionized silanol groups. In 1997, Dittmann and Rozing separated a series of PAH's with a mixed mode stationary phase containing C18 chains as retentive sites, while cation-exchange groups, propane sulfonic acid, generated an stable and constant EOF over a wide pH range [166]. Moreover, these stationary phases are often beneficial for the separation of basic or acidic organic compounds, which have been proven difficult to separate in the normal or reversed phase mode, due to electrostatic interaction with the ionized silanol groups (basic solutes) and long analysis times (acidic solutes). Wu et al. reported a highly efficient separation of peptides with a mixed mode monolithic column. Separation was based on hydrophobic interaction, electrostatic interactions and electrophoretic migration resulting in efficiencies of 280,000 plates. Up to today, several applications of mixed-mode electrochromatography are reported including the separations of peptides, proteins, organic acids and bases, amino acids and pesticides [39-41,110,163,167-176].

5.4 Molecular size-based separations in CEC

In size-exclusion chromatography (SEC), separation occurs by the differences in velocities of molecules with different hydrodynamic volumes. In pressure driven techniques, the mobile phase will move with a certain interstitial velocity but form stagnant pools in the pores (pore flow≈0). Smaller molecules will enter a bigger fraction of the total pore volume, therefore their average velocity will be lower compared to bigger molecules. Hence, a separation

based on molecular size can be obtained in this way. As a consequence, a broad pore distribution is beneficial for the separation in SEC mode, as it broadens the retention window.

Only few reports investigated the possibilities of size-exclusion electrochromatography (SEEC) [106,177-179]. As SEEC is electrodriven, higher efficiencies will be obtained by the flat flow velocity profile compared to pressure driven techniques. Furthermore, the use of particles with large pores (250 A°) will result in a perfusive electrokinetic flow through the pores and therefore a beneficial effect in the mass-transfer of the solutes (C-term) should be observed. This mass-transfer improvement is particularly interesting as most SE(E)C analyses are performed on synthetic and natural macromolecules, which have slow diffusion coefficients [180]. However, this extra pore flow causes a decrease in the difference of the interstitial mobile phase velocity and the pore flow velocity, leading to a smaller retention window and decreased selectivity. Even more important is the inferior precision of SEEC compared to SEC. A study on the calibration curves of SEC and SEEC by Vander Heyden et al. demonstrated that the prediction errors of SEEC are two to three times larger compared to conventional pressure driven SEC, which explains the limited interest in SEEC [181].

6 References

[1] L.A. Colon, T.D. Maloney, A.M. Fermier, J. Chromatogr. A 887 (2000) 43.

[2] F. Lynen, A. Buica, A. de Villiers, A. Crouch, P. Sandra, J. Sep. Sci. 28 (2005) 1539.

[3] N.W. Smith, M.B. Evans, Chromatographia 38 (1994) 649.

[4] H. Rebscher, U. Pyell, Chromatographia 38 (1994) 737.

[5] S.E. vandenBosch, S. Heemstra, J.C. Kraak, H. Poppe, J. Chromatogr. A 755 (1996) 165.

[6] R.T. Kennedy, J.W. Jorgenson, Anal. Chem. 61 (1989) 1128.

[7] H. Yamamoto, J. Baumann, F. Erni, J. Chromatogr. 593 (1992) 313.

[8] R.J. Boughtflower, T. Underwood, C.J. Paterson, Chromatographia 40 (1995) 329.

[9] K.D. Bartle, A.A. Clifford, P. Myers, M.M. Robson, K. Seale, D. Tong, D.N. Batchelder, S. Cooper, in: J.F. Parcher, T.L. Chester (Eds.), Unified Chromatography, 2000, p. 142.

[10] A. Malik, W.B. Li, M.L. Lee, J. Microcolumn Sep. 5 (1993) 361.

[11] M.M. Robson, S. Roulin, S.M. Shariff, M.W. Raynor, K.D. Bartle, A.A. Clifford, P. Meyers, M.R. Euerby, C.M. Johnson, Chromatographia 43 (1996) 313.

[12] M.M. Robson, M.G. Cikalo, P. Myers, M.R. Euerby, K.D. Bartle, J. Microcolumn Sep. 9 (1997) 357.

[13] M.T. Dulay, C. Yan, D.J. Rakestraw, R.N. Zare, J. Chromatogr. A 725 (1996) 361.

[14] R. Dadoo, R.N. Zare, C. Yan, D.S. Anex, Anal. Chem. 70 (1998) 4787.

[15] R. Stol, M. Mazereeuw, U.R. Tjaden, J. van der Greef, J. Chromatogr. A 873 (2000) 293.

[16] A.M. Fermier, L.A. Colon, J. Microcolumn Sep. 10 (1998) 439.

[17] T.D. Maloney, L.A. Colon, Electrophoresis 20 (1999) 2360.

[18] K.J. Reynolds, T.D. Maloney, A.M. Fermier, L.A. Colon, Analyst 123 (1998) 1493.

[19] T.D. Maloney, L.A. Colon, J. Sep. Sci. 25 (2002) 1215.

[20] Y. Xue, X. Gu, Y. Wang, C. Yan, Electrophoresis 36 (2015) 124.

[21] M. Hugener, A.P. Tinke, W.M.A. Niessen, U.R. Tjaden, J. Vandergreef, J. Chromatogr. 647 (1993) 375.

[22] F. Lelievre, C. Yan, R.N. Zare, P. Gareil, J. Chromatogr. A 723 (1996) 145.

[23] W.J. Cheong, J. Sep. Sci. 37 (2014) 603.

[24] S.L. Zeng, C.H. Chen, J.G. Santiago, J.R. Chen, R.N. Zare, J.A. Tripp, F. Svec, J.M.J. Frechet, Sensors and Actuators B-Chemical 82 (2002) 209.

[25] J.R. Chen, M.T. Dulay, R.N. Zare, F. Svec, E. Peters, Anal. Chem. 72 (2000) 1224.

[26] L.S. Li, Y. Wang, D.J. Young, S.C. Ng, T.T.Y. Tan, Electrophoresis 31 (2010) 378.

[27] D. Chen, J. Wang, Y. Jiang, T. Zhou, G. Fan, Y. Wu, J. Pharm. Biomed. Anal. 50 (2009) 695.

[28] A. Rocco, S. Fanali, J. Chromatogr. A 1191 (2008) 263.

[29] G. D'Orazio, A. Rocco, S. Fanali, J. Chromatogr. A 1228 (2012) 213.

[30] M. Franc, J. Sobotnikova, P. Coufal, Z. Bosakova, J. Sep. Sci. 37 (2014) 2278.

[31] H. Wang, J. Cao, Y. Bi, L. Chen, Q.-H. Wan, J. Chromatogr. A 1216 (2009) 5882.

[32] S. Oguri, C. Oga, H. Takeda, J. Chromatogr. A 1157 (2007) 304.

[33] B. Zhang, Q. Liu, L. Yang, Q. Wang, J. Chromatogr. A 1272 (2013) 136.

[34] B. Zhang, E.T. Bergstrom, D.M. Goodall, P. Myers, Anal. Chem. 79 (2007) 9229.

[35] J. Zheng, S.A. Shamsi, Anal. Chem. 75 (2003) 6295.

[36] G. Choudhary, A. Apffel, H.F. Yin, W. Hancock, J. Chromatogr. A 887 (2000) 85.

[37] J. Zheng, D. Norton, S.A. Shamsi, Anal. Chem. 78 (2006) 1323.

[38] T.M. Zimina, R.M. Smith, P. Myers, J. Chromatogr. A 758 (1997) 191.

[39] K. Ohyama, N. Kuroda, J. Liq. Chromatogr. Relat. Technol. 30 (2007) 833.

[40] K. Ohyama, Y. Shirasawa, M. Wada, N. Kishikawa, Y. Ohba, K. Nakashima, N. Kuroda, J. Chromatogr. A 1042 (2004) 189.

[41] K. Walhagen, K.K. Unger, A.M. Olsson, M.T.W. Hearn, J. Chromatogr. A 853 (1999) 263.

[42] A. Maruska, U. Pyell, J. Chromatogr. A 782 (1997) 167.

[43] E.P.C. Lai, E. Dabek-Zlotorzynska, Electrophoresis 20 (1999) 2366.

[44] R. Alicea-Maldonado, L.A. Colon, Electrophoresis 20 (1999) 37.

[45] M.Q. Zhang, Z. El Rassi, Electrophoresis 20 (1999) 31.

[46] M.Q. Zhang, G.K. Ostrander, Z. El Rassi, J. Chromatogr. A 887 (2000) 287.

[47] M.Q. Zhang, C.M. Yang, Z. El Rassi, Anal. Chem. 71 (1999) 3277.

[48] S. Fanali, G. D'Orazio, T. Farkas, B. Chankvetadze, J. Chromatogr. A 1269 (2012) 136.

[49] J.W. Jorgenson, E.J. Guthrie, J. Chromatogr. 255 (1983) 335.

[50] E. Guihen, J.D. Glennon, J. Chromatogr. A 1044 (2004) 67.

[51] W.J. Cheong, F. Ali, Y.S. Kim, J.W. Lee, J. Chromatogr. A 1308 (2013) 1.

[52] K. Jinno, H. Sawada, Trac-Trend. Anal. Chem. 19 (2000) 664.

[53] E.A.S. Doherty, R.J. Meagher, M.N. Albarghouthi, A.E. Barron, Electrophoresis 24 (2003) 34.

[54] C.P. Kapnissi-Christodoulou, X.F. Zhu, I.M. Warner, Electrophoresis 24 (2003) 3917.

[55] T. Tsuda, K. Nomura, G. Nakagawa, J. Chromatogr. 248 (1982) 241.

[56] J. Charvatova, Z. Deyl, V. Kasicka, V. Kral, J. Chromatogr. A 990 (2003) 159.

[57] J. Charvatova, V. Kasicka, T. Barth, Z. Deyl, I. Miksik, V. Kral, J. Chromatogr. A 1009 (2003) 73.

[58] J. Charvatova, V. Kasicka, Z. Deyl, V. Kral, J. Chromatogr. A 990 (2003) 111.

[59] N. Guan, Z.R. Zeng, Y.C. Wang, E.Q. Fu, J.K. Cheng, Anal. Chim. Acta 418 (2000) 145.

[60] X.J. Wu, H.X. Liu, H. Liu, S.S. Zhang, P.R. Haddad, Anal. Chim. Acta 478 (2003) 191.

[61] H.B. Li, Y.Y. Chen, Z.R. Zeng, C.H. Xie, X.L. Yang, Anal. Sci. 21 (2005) 717.

[62] Y. Tian, Z.R. Zeng, Y.Y. Chen, C.H. Xie, H.B. Li, X.L. Yang, J. Liq. Chromatogr. Relat. Technol. 28 (2005) 2931.

[63] Y.F. Pai, C.Y. Liu, J. Chromatogr. A 982 (2002) 293.

[64] J. Qiao, L. Qi, H. Ma, J. Sep. Sci. 32 (2009) 3936.

[65] Y. Shen, L. Qi, J. Qin, H. Yan, J. Qiao, H. Zhang, Y. Chen, L. Mao, L. Wan, Talanta 84 (2011) 501.

[66] L. Xu, Y. Sun, Electrophoresis 28 (2007) 1658.

[67] L. Xu, X.Y. Dong, Y. Sun, Electrophoresis 30 (2009) 689.

[68] L. Xu, Y. Sun, J. Chromatogr. A 1183 (2008) 129.

[69] X.W. Zhang, J. Yang, S.F. Liu, X.C. Lin, Z.H. Xie, J. Sep. Sci. 34 (2011) 3383.

[70] C. Nilsson, S. Birnbaum, S. Nilsson, J. Chromatogr. A 1168 (2007) 212.

[71] S.Y. Zhou, J.J. Tan, Q.H. Chen, X.C. Lin, H.X. Lu, Z.H. Xie, J. Chromatogr. A 1217 (2010) 8346.

[72] J. Olsson, L.G. Blomberg, J. Chromatogr. B Analyt. Technol. Biomed. Life Sci. 875 (2008) 329.

[73] J.J. Pesek, M.T. Matyska, J. Chromatogr. A 887 (2000) 31.

[74] M.T. Matyska, J.J. Pesek, A. Katrekar, Anal. Chem. 71 (1999) 5508.

[75] J.J. Pesek, M.T. Matyska, S. Menezes, J. Chromatogr. A 853 (1999) 151.

[76] J.J. Pesek, M.T. Matyska, S.J. Cho, J. Chromatogr. A 845 (1999) 237.

[77] J.L. Chen, Electrophoresis 30 (2009) 3855.

[78] J.L. Chen, J. Chromatogr. A 1216 (2009) 6236.

[79] X. Huang, J. Zhang, C. Horvath, J. Chromatogr. A 858 (1999) 91.

[80] S. Eeltink, F. Svec, J.M.J. Frechet, Electrophoresis 27 (2006) 4249.

[81] T. Huang, J.Q. Mi, X.X. Zhang, J. Sep. Sci. 29 (2006) 277.

[82] A. Malik, Electrophoresis 23 (2002) 3973.

[83] W. Li, D.P. Fries, A. Malik, J. Chromatogr. A 1044 (2004) 23.

[84] X.L. Dong, R.A. Wu, J. Dong, M.H. Wu, Y. Zhu, H.F. Zou, Electrophoresis 30 (2009) 141.

[85] H. Lu, Q. Li, X. Yu, J. Yi, Z. Xie, Electrophoresis 34 (2013) 1895.

[86] J.-L. Chen, H.-J. Syu, Anal. Chim. Acta 718 (2012) 130.

[87] G. Danger, M. Ramonda, H. Cottet, Electrophoresis 28 (2007) 925.

[88] J. Kohr, H. Engelhardt, J. Microcolumn Sep. 3 (1991) 491.

[89] C.A. Bolger, M. Zhu, R. Rodriguez, T. Wehr, J. Liq. Chromatogr. 14 (1991) 895.

[90] J.R. Mazzeo, I.S. Krull, Biotechniques 10 (1991) 638.

[91] M. Strege, A. Lagu, Anal. Chem. 63 (1991) 1233.

[92] S. Hjerten, M. Kiesslingjohansson, J. Chromatogr. 550 (1991) 811.

[93] Z. Liu, H.F. Zou, M.L. Ye, J.Y. Ni, Y.K. Zhang, Electrophoresis 20 (1999) 2891.

[94] Z. Liu, H.F. Zou, J.Y. Ni, Y.K. Zhang, Anal. Chim. Acta 378 (1999) 73.

[95] M.L. Ye, H.F. Zou, Z. Liu, J.Y. Ni, Y.K. Zhang, J. Chromatogr. A 855 (1999) 137.

[96] J. Zhang, W. Zhang, T. Bao, Z. Chen, J. Chromatogr. A 1339 (2014) 192.

[97] X. Jiang, Y. Jiang, G. Shi, T. Zhou, J. Sep. Sci. 37 (2014) 1671.

[98] C. Wang, S. de Rooy, C.-F. Lu, V. Fernand, L. Moore, Jr., P. Berton, I.M. Warner, Electrophoresis 34 (2013) 1197.

[99] Q. Qu, C. Gu, X. Hu, Anal. Chem. 84 (2012) 8880.

[100] R.-P. Liang, C.-M. Liu, X.-Y. Meng, J.-W. Wang, J.-D. Qiu, J. Chromatogr. A 1266 (2012) 95.

[101] G. Guiochon, J. Chromatogr. A 1168 (2007) 101.

[102] K. Cabrera, J. Sep. Sci. 27 (2004) 843.

[103] A. Ghanem, T. Ikegami, J. Sep. Sci. 34 (2011) 1945.

[104] N. Ishizuka, H. Minakuchi, K. Nakanishi, N. Soga, H. Nagayama, K. Hosoya, N. Tanaka, Anal. Chem. 72 (2000) 1275.

[105] E.C. Peters, M. Petro, F. Svec, J.M.J. Frechet, Anal. Chem. 69 (1997) 3646.

[106] E.C. Peters, M. Petro, F. Svec, J.M.J. Frechet, Anal. Chem. 70 (1998) 2296.

[107] I. Gusev, X. Huang, C. Horvath, J. Chromatogr. A 855 (1999) 273.

[108] A.S. Rathore, E. Wen, C. Horvath, Anal. Chem. 71 (1999) 2633.

[109] S. Eeltink, F. Svec, Electrophoresis 28 (2007) 137.

[110] X. Wang, Y. Zheng, C. Zhang, Y. Yang, X. Lin, G. Huang, Z. Xie, J. Chromatogr. A 1239 (2012) 56.

[111] F. Svec, E.C. Peters, D. Sykora, J.M.J. Frechet, J. Chromatogr. A 887 (2000) 3.

[112] H.F. Zou, X.D. Huang, M.L. Ye, Q.Z. Luo, J. Chromatogr. A 954 (2002) 5.

[113] N. Tanaka, H. Kobayashi, N. Ishizuka, H. Minakuchi, K. Nakanishi, K. Hosoya, T. Ikegami, J. Chromatogr. A 965 (2002) 35.

[114] E.F. Hilder, F. Svec, J.M.J. Frechet, Electrophoresis 23 (2002) 3934.

[115] D. Allen, Z. El Rassi, Electrophoresis 24 (2003) 3962.

[116] C. Legido-Quigley, N.D. Marlin, V. Melin, A. Manz, N.W. Smith, Electrophoresis 24 (2003) 917.

[117] S. Eeltink, G.R. Rozing, W.T. Kok, Electrophoresis 24 (2003) 3935.

[118] D.N. Gunasena, Z. El Rassi, Electrophoresis 33 (2012) 251.

[119] J.D. Hayes, A. Malik, Anal. Chem. 72 (2000) 4090.

[120] L.J. Yan, Q.H. Zhang, H. Zhang, L.Y. Zhang, T. Li, Y.Q. Feng, L.H. Zhang, W.B. Zhang, Y.K. Zhang, J. Chromatogr. A 1046 (2004) 255.

[121] H. Colon, X. Zhang, J.K. Murphy, J.G. Rivera, L.A. Colon, Chem. Commun. (2005) 2826.

[122] H. Eghbali, K. Sandra, F. Detobel, F. Lynen, K. Nakanishi, P. Sandra, G. Desmet, J. Chromatogr. A 1218 (2011) 3360.

[123] A. Palm, M.V. Novotny, Anal. Chem. 69 (1997) 4499.

[124] Y. Guo, L.A. Colon, Chromatographia 43 (1996) 477.

[125] A. Banholczer, U. Pyell, J. Chromatogr. A 869 (2000) 363.

[126] K.D. Bartle, P. Myers, J. Chromatogr. A 916 (2001) 3.

[127] A. Dermaux, P. Sandra, M. Ksir, K.F.F. Zarrouck, HRC-J. High Resolut. Chromatogr. 21 (1998) 545.

[128] P. Sandra, A. Dermaux, V. Ferraz, M.M. Dittmann, G. Rozing, J. Microcolumn Sep. 9 (1997) 409.

[129] L. Roed, E. Lundanes, T. Greibrokk, Electrophoresis 20 (1999) 2373.

[130] L. Roed, E. Lundanes, T. Greibrokk, J. Chromatogr. A 890 (2000) 347.

[131] O. Kornysova, E. Machtejevas, V. Kudirkaite, U. Pyell, A. Maruska, J. Biochem. Bioph. Methods 50 (2002) 217.

[132] M. Lammerhofer, F. Svec, J.M.J. Frechet, W. Lindner, J. Chromatogr. A 925 (2001) 265.

[133] P.J. Vickers, N.W. Smith, J. Sep. Sci. 25 (2002) 1284.

[134] H. Huang, Y. Jin, M. Xue, L. Yu, Q. Fu, Y. Ke, C. Chu, X. Liang, Chem. Commun. (2009) 6973.

[135] B.H. Xiong, L.H. Zhang, Y.K. Zhang, H.F. Zou, J.D. Wang, HRC-J. High Resolut. Chromatogr. 23 (2000) 67.

[136] W. Wei, G.A. Luo, C. Yan, Am. Lab. 30 (1998) 20C.

[137] W. Wei, G.A. Luo, G.Y. Hua, C. Yan, J. Chromatogr. A 817 (1998) 65.

[138] N.W. Smith, Z. Jiang, J. Chromatogr. A 1184 (2008) 416.

[139] G. Blaschke, B. Chankvetadze, J. Chromatogr. A 875 (2000) 3.

[140] N.M. Maier, P. Franco, W. Lindner, J. Chromatogr. A 906 (2001) 3.

[141] K. Kalikova, T. Slechtova, J. Vozka, E. Tesarova, Anal. Chim. Acta 821 (2014) 1.

[142] J.M. Plotka, M. Biziuk, C. Morrison, J. Namiesnik, Trac-Trend. Anal. Chem. 56 (2014) 74.

[143] Y. Zhang, D.R. Wu, D.B. Wang-Iverson, A.A. Tymiak, Drug Discovery Today 10 (2005) 571.

[144] S. Mayer, V. Schurig, HRC-J. High Resolut. Chromatogr. 15 (1992) 129.

[145] S. Fanali, P. Catarcini, G. Blaschke, B. Chankvetadze, Electrophoresis 22 (2001) 3131.

[146] D. Wistuba, V. Schurig, J. Chromatogr. A 875 (2000) 255.

[147] C. Wolf, P.L. Spence, W.H. Pirkle, E.M. Derrico, D.M. Cavender, G.P. Rozing, J. Chromatogr. A 782 (1997) 175.

[148] A. Dermaux, F. Lynen, P. Sandra, HRC-J. High Resolut. Chromatogr. 21 (1998) 575.

[149] M. Li, X. Liu, F. Jiang, L. Guo, L. Yang, J. Chromatogr. A 1218 (2011) 3725.

[150] V. Schurig, D. Wistuba, Electrophoresis 20 (1999) 2313.

[151] D. Wistuba, V. Schurig, Lc Gc Eur. 22 (2009) 60.

[152] M. Pursch, L.C. Sander, J. Chromatogr. A 887 (2000) 313.

[153] M. Girod, B. Chankvetadze, G. Blaschke, J. Chromatogr. A 887 (2000) 439.

[154] D. Mangelings, N. Hardies, M. Maftouh, C. Suteu, D.L. Massart, Y.V. Heyden, Electrophoresis 24 (2003) 2567.

[155] J.-J. Fu, J.-J. Qin, Q. Zeng, Y. Huang, H.Z. Jin, W.-D. Zhang, Chemical & Pharmaceutical Bulletin 58 (2010) 1263.

[156] J. Zheng, W. Bragg, J. Hou, N. Lin, S. Chandrasekaran, S.A. Shamsi, J. Chromatogr. A 1216 (2009) 857.

[157] F. Kitagawa, K. Inoue, T. Hasegawa, M. Kamiya, Y. Okamoto, M. Kawase, K. Otsuka, J. Chromatogr. A 1130 (2006) 219.

[158] D. Wang, X. Song, Y. Duan, L. Xu, J. Zhou, H. Duan, Electrophoresis 34 (2013) 1339.

[159] R. Dai, L. Tang, H. Li, Y. Deng, R. Fu, Z. Parveen, J. Appl. Polym. Sci. 106 (2007) 2041.

[160] E.F. Hilder, A.J. Zemann, M. Macka, P.R. Haddad, Electrophoresis 22 (2001) 1273.

[161] M.C. Breadmore, M. Macka, N. Avdalovic, P.R. Haddad, Analyst 125 (2000) 1235.

[162] M.S. Nutku, F.B. Erim, J. Microcolumn Sep. 11 (1999) 541.

[163] E.F. Hilder, M. Macka, P.R. Haddad, Anal. Commun. 36 (1999) 299.

[164] M.C. Breadmore, E.F. Hilder, M. Macka, N. Avdalovic, P.R. Haddad, Electrophoresis 22 (2001) 503.

[165] D.M. Li, H.H. Knobel, V.T. Remcho, J. Chromatogr. B 695 (1997) 169.

[166] M.M. Dittmann, G.P. Rozing, J. Microcolumn Sep. 9 (1997) 399.

[167] X. Wang, H. Lue, X. Lin, Z. Xie, J. Chromatogr. A 1190 (2008) 365.

[168] D. Hoegger, R. Freitag, J. Chromatogr. A 1004 (2003) 195.

[169] K. Zhang, C. Yan, Z.C. Zhang, Q.S. Wang, R.Y. Gao, J. Liq. Chromatogr. Relat. Technol. 26 (2003) 2119.

[170] H.J. Fu, C.H. Xie, H. Xiao, J. Dong, J.W. Hu, H.F. Zou, J. Chromatogr. A 1044 (2004) 237.

[171] F. Ye, Z. Xie, K.-Y. Wong, Electrophoresis 27 (2006) 3373.

[172] F. Ye, S. Wang, S. Zhao, J. Chromatogr. A 1216 (2009) 8845.

[173] J. Lin, J. Lin, X. Lin, Z. Xie, J. Chromatogr. A 1216 (2009) 801.

[174] G. Ding, Z. Da, R. Yuan, J.J. Bao, Electrophoresis 27 (2006) 3363.

[175] R.A. Wu, H.F. Zou, H.J. Fu, W.H. Jin, M.L. Ye, Electrophoresis 23 (2002) 1239.

[176] P.Q. Huang, X.Y. Jin, Y.J. Chen, J.R. Srinivasan, D.M. Lubman, Anal. Chem. 71 (1999) 1786.

[177] K. Mistry, I. Krull, N. Grinberg, Electrophoresis 24 (2003) 1753.

[178] R. Stol, W.T. Kok, H. Poppe, J. Chromatogr. A 914 (2001) 201.

[179] W.T. Kok, J. Chromatogr. A 1044 (2004) 145.

[180] E. Venema, J.C. Kraak, H. Poppe, R. Tijssen, J. Chromatogr. A 837 (1999) 3.

[181] Y. Vander Heyden, S.T. Popovici, P.J. Schoenmakers, J. Chromatogr. A 957 (2002) 127.

Rationale

Capillary electrochromatography has often been described as the future step towards fast separations allowing higher peak capacities and column efficiencies. Although many researchers reported achieving these characteristics (especially in comparison to HPLC); nonetheless, the implementation of CEC as an industrial applicable separation technique is not yet reported after 25 years of research. In much of the earlier packed column CEC literature high efficiencies are obtained on columns packed with non-porous particles, or with porous material but under poorly retentive conditions or by analyzing solutes undergoing electrostatic peak focusing phenomena.

Nowadays, a consensus exists that the effective CEC column performance is in many cases only mildly better or comparable to HPLC, and that the possible advantages of CEC are surpassed by the advances in UHPLC technology. Furthermore, the inherent problems of capillary separation techniques, such as a relatively limited detection sensitivity and challenging hyphenation to mass spectrometry, prevent the development of CEC as a widely applicable technique.

The efficiencies encountered in the separations of neutral and retained molecules are lower than theoretically expected. Generally, this is explained by the limited control of the column technology and design. Packed columns are hampered by the necessity of the frits and extra band broadening is created by the difference in EOF between the packed and empty section of the column. Monolithic columns on the other hand show limited repeatability and reproducibility, while wall effects and poor pore size control also induce band broadening effects. Finally, the radii of CEC open-tubular columns are on the one hand too wide to obtain efficient separations and on the other hand to small to achieve sensitive on-column detection.

Until now, the performance of the separation has been measured as the number of plates/meter of the column or through minimum plate heights. The latter method utilizes the *H* vs. *u* curves to obtain a minimum plate height at a certain mobile phase velocity. Most comparisons between different CEC columns of the same or different formats and between CEC and other separation techniques are obtained by comparing the van Deemter plots of

the respective methods. However, the plate height versus mobile phase velocity plots does not provide a complete and unambiguous picture of the performance and are therefore not suited to provide an unbiased comparison. For example, HPLC and UHPLC are fairly limited in the column length and particle size because of the applicable pressure. However, the length of the CEC column and the particle size is not limited by the applied voltage. Therefore, a comparison between the two techniques should incorporate this fundamental difference. Moreover, to obtain a broader comparison between different formats and particle sizes, a comparison should incorporate not only the minimum plate heights but also the fastest separation time possible to reach a given efficiency.

The author agrees with the statement that column design and technology are not yet fully developed but also believes that other underlying, not yet clarified, phenomena are hampering the performance of CEC. As the developments of current technology (better detection sensitivities, simplified hyphenation to MS and the availability of pressurized buffer vials) allows easier and better separation, a re-evaluation of CEC as highly performant separation technique should be performed.

Therefore, the following chapters describe the performance evaluation of capillaries with different stationary phases (different morphologies and different chemistry). Furthermore, the influence of temperature as a critical parameter for the performance and separation power in CEC will be investigated.

Chapter 4

Kinetic performance evaluation and perspectives of contemporary packed capillary electrochromatography

Capillary electrochromatography (CEC) is in essence a highly efficient and fast separation technique but practical constraints limit the current performance, robustness and routine implementation of the technique. In this chapter the kinetic performance limit (KPL) curve was used to evaluate commercial packed column CEC; this firstly to assess the broader applicability of the kinetic plot approach in electrodriven chromatographic techniques, and secondly to allow a more general unbiased comparison with HPLC performance. Evaluations were performed with a mixture of well retained and electrophoretically neutral phenones, in order to observe only chromatographic processes. Comparison was performed with HPLC, with a column packed with an identical stationary phase to allow measurement of the performance under optimal conditions, and not with µ-LC on the CEC column as extra column peak broadening phenomena would thereby negatively affect the µ-LC performance. This comparison demonstrated that current HPLC performance largely outcompetes what is achievable with contemporary packed column CEC. Interestingly, significantly improved CEC performance could be obtained at lower temperatures (10°C) suggesting a persistent degree of Joule heating phenomena taking place in the contemporary packed column (100 µm) CEC approach. Effective suppression of the latter opens possibilities for increasing the applicable voltage and outperforming HPLC and UHPLC.

Published as De Smet S, Lynen F, Kinetic Performance Evaluation and Perspectives of Contemporary Packed Column Capillary Electrochromatography, Journal of Chromatography A, 1355 (2014, 261-268)

1 Introduction

After two decades of CEC development, industrial implementation of CEC remains largely unreported. Although a limited number of capillary electrodriven techniques effectively broke through (such as nucleotide sequencing tools [1-3]), the acclaimed advantages of CEC should have resulted in a number of genuinely applied methods. The absence thereof can be partially related to inherent problems of capillary separation techniques such as a relatively limited detection sensitivity and challenging hyphenation to mass spectrometry [4-6], or to specific CEC related issues such as the absence of commercial instrumentation allowing gradient analysis, method robustness issues and short column life time. A major issue in CEC is also the fact that the generation of flow is coupled to the properties of the particle and that for that reason selectivity and flow generation cannot be optimized independently. Many of the modern end-capped HPLC packing materials produce only very low EOF velocities. Although solutions could conceivably be envisaged for the above, according to the author, a major hurdle of contemporary CEC is that the effective CEC column performance is in many cases only mildly better or comparable to HPLC, and which is quickly becoming obsolete by the advances in UHPLC technology. This stands to contrast to the ultra-high efficiency CEC results described earlier. However, in much of the earlier packed column CEC literature high efficiencies are obtained on columns packed with non-porous particles, or with porous material but under poorly retentive conditions [7-12] or by analyzing solutes undergoing electrostatic peak focusing phenomena [12-16]. Implementation of an independent tool, allowing the least biased evaluation of CEC column performance seems therefore a necessary development.

In liquid chromatography the comparison of columns in terms of achievable efficiency and speed of analysis, has been much facilitated since the introduction of the kinetic performance limit (KPL) method [17]. As described in Chapter I, the resulting kinetic plot (KP) thereby converts the plate height versus linear velocity curve to a speed versus efficiency curve and incorporates column permeability information, as the maximum efficiency is limited by the highest applicable pressure drop.

In HPLC the plot can be constructed by implementing the values of the efficiency and the pressure drop, measured at different linear mobile phase velocities (u_0) into the next two equations (Eq. IV.1-IV.2) [18]:

$$N = \frac{\Delta P_{max}}{\eta} \left(\frac{K_{v0}}{u_0 H}\right) \quad \text{Eq. IV.1}$$

$$t_0 = \frac{\Delta P_{max}}{\eta} \frac{K_{v0}}{{u_0}^2} \quad \text{Eq. IV.2}$$

where t_0 is the column void time, η is the viscosity, K_{v0} the column permeability and ΔP_{max} represents the maximum pressure the instrument can provide or the column can endure. As the method assumes a constant plate height at the same linear mobile phase velocities, regardless of the column length, one of the prerequisites is the occurrence of an invariable column permeability irrespective of the length of the column. A second prerequisite of the KPL method is the invariable retention factor between compared kinetic plots to preserve an identical retention behavior of the standards. Note that both prerequisites can be detrimentally affected when ultra-high pressures are used, leading to the occurrence of heating, increasing plate heights and decreasing retention. The KPL approach is particularly suitable to compare the performance of columns with broadly differing properties. For example, in this way the maximal achievable performance of open tubular and monolithic formats and of columns packed with various particle sizes and morphologies at various temperatures can be directly compared through a single kinetic plot [19-24]. In pressure driven techniques like LC, the maximum number of plates that can be obtained with a certain mobile phase velocity is determined by the permeability of the column. However, CEC is only limited by the mobility of the electro-osmotic flow (EOF). Thus the practical constraint in CEC is not the pressure drop but the potential drop as demonstrated in Equation IV.3:

$$u_0 = \mu_{EOF} \frac{\Delta V}{L} \quad \text{Eq.IV.3}$$

where μ_{EOF} stands for the electroosmotic flow mobility, V for the applied voltage and L represents the total length of the capillary. Derived from Equation IV.3 the kinetic plot in CEC can be described by the next Equations (Eq. IV.4-IV.5) [25].

$$N = \mu_{EOF} \frac{\Delta V}{H u_o} \qquad \text{Eq. IV.4}$$

$$t_0 = \mu_{EOF} \frac{\Delta V}{{u_o}^2} \qquad \text{Eq. IV.5}$$

In a similar way as in pressure driven techniques, where the KP is obtained by extrapolation to the maximum deliverable system pressure, can the KP in electrodriven techniques be obtained by extrapolating to the maximum voltage. Unmistakable, the most important prerequisite of the KP approach in CEC comprises an invariable electroosmotic flow (EOF), independent of the length and position in the capillary. The dependency of the EOF is represented in Equation IV.6:

$$\mu_{\mathrm{EOF}} = \frac{\varepsilon_0 \varepsilon_\mathrm{r} \zeta}{\eta} \qquad \text{Eq. IV.6}$$

where ε_0 is the vacuum permittivity, ε_r is the dielectric constant of the background electrolyte and ζ is the zeta potential [26]. As described in Chapter I, the zeta potential is related to δ and to the surface charge σ by Equation IV.7 [27,28]:

$$\zeta = \frac{\sigma \delta}{\varepsilon_0 \varepsilon_\mathrm{r}} \qquad \text{Eq. IV.7}$$

To maintain the same electro-osmotic mobility a uniform zeta potential is needed in the capillary. In a packed capillary, where the zeta potential will be defined by the charged particles, a difference in inter-particle porosity occurs at the wall, compared to the middle of the capillary. This non-uniformity of the EOF is worsened with non-homogenously packed columns, whereby typically a lower packing density is observed close to the wall. This wall effect lowers exponentially with the distance to the wall, but creates a mismatch in the zeta

potential and hence leads to a less uniform mobility and mobile-phase velocity. Therefore, to implement kinetic plots, a uniform or as close as possible uniform bed is necessary.

In this chapter the KPL method is applied for the evaluation of the performance of packed columns in CEC with realistically retained solutes which contain both hydrophobic and polar functionalities. Comparison with HPLC is performed and the influence of temperature on the CEC performance is investigated. The approach is used to estimate the potential of CEC.

2 Experimental

2.1 Chemicals, solutions and material

MilliQ Water was prepared in house by water purification instrument from Millipore (Bedford, New Hampshire, USA). Acetic acid was obtained by Fiers (Fiers N.V., Kuurne, Belgium). Acetonitrile of HPLC quality originated from Biosolve (Valkenswaard, Netherlands). Octanophenone, decanophenone, dodecanophenone tris(hydroxymethyl)amino-methane (TRIS) and thiourea were purchased from Sigma-Aldrich (Bornem, Belgium). Stock solutions of thiourea, octanophenone, decanophenone and dodecanophenone were prepared at 8000 µg/mL in water or acetonitrile (ACN, dependent on their solubility and diluted to 50 µg/mL concentrations (in the same solvent) composition as the mobile phase) for all samples.

2.2 Apparatus and chromatography

CEC measurements were performed on a CE 7100 system (Agilent Technologies, Waldbronn, Germany) equipped with an air-cooling system, autosampler, diode array detector and a built-in system to pressurize the vials. All chromatographic analyses in CEC mode were performed on commercially capillary columns (Agilent Technologies) packed with 3 µm Hypersil-C18 particles (250 mm effective length, 335 mm total length, 100 µm i.d.). The temperature was varied between 10 and 45°C by the built-in air cooled thermostat. The mobile phase was filtered with syringe filters (Grace, 0.45 µm PVDF filters). Injection in CEC was performed electro-kinetically by applying 8 kV during 4 seconds. An alignment interface

for standard capillaries of 75 µm ID (and above) with an optical slit of 75 µm was used. HPLC analyses were performed on a 1260 Infinity system (Agilent Technologies) equipped with a variable wavelength detector and a micro flow cell of 1.2 µL. An ODS Hypersil column (150*4.6 mm, 3 µm) was obtained from Thermo-Scientific (Waltham, MA, USA). The injection volume was 1.2 µL.

Both the electrochromatographic runs and HPLC analyses were performed with a mobile phase consisting of a mixture of 25 mM Tris-acetate buffer at pH 8.5 and ACN. Detection was performed at 240 nm and all obtained data was processed using Chemstation B.04.03 software.

3 Results and discussion

The performance of packed column CEC has often been illustrated through the analysis of inert solutes such as polyaromatic hydrocarbons [26,29-31]. The choice of these solutes is meaningful as they are electrically neutral, depict strong hydrophobic interactions in the reversed phase mode and contain strong chromophores. On the other hand, and especially from a diffusion perspective, these test solutes are not necessarily very representative of most analytes suitable for CEC analysis. This is, for example, illustrated by the significantly shallower C-term measured in the van Deemter curves of these solutes both in CEC [31] and in (U)HPLC [32,33] compared to the more polar analogues. This is related to the faster diffusion of purely aromatic solutes, not containing any polar functionalities, in and out of the stationary phase and through an aqueous/organic mobile phase. The mobility and therefore the diffusion coefficients of more polar solutes are typically slowed down by hydrogen bridge formation, dipole-dipole interactions and because they tend to be surrounded by solvation shells in aqueous environments. Due to their charge neutrality and UV absorbance therefore short chain phenones were first selected for construction of the van Deemter curves under well retained conditions (*k* 2-5). However, as highly repeatable solute retention could only be obtained under conditions of high organic content (i.e. 80% acetonitrile/20% TRIS-acetate buffer pH 8.5) in the mobile phase, longer chain phenones such as octanophenone, decanophenone and dodecanophenone were finally selected for the evaluation of the columns via the KPL method while ensuring satisfactory solute retention. The separation of the 3 solutes and of thiourea on a 25 cm bed packed with 3 µm C18 particles is illustrated in Fig. V.1A at 17.5 kV. The corresponding retention factors were

1.4, 2.6 and 5, and the RSD%'s varied from 0.21 to 0.77 and from 0.87 to 1.7, for the intra-day and day to day repeatability, respectively. Although the peak symmetry is improving for increasing retention, this coincided with an increase in the minimal plate heights from 9.21 to 9.57 and 9.85 µm illustrating the bias insufficiently retained solutes can introduce in CEC column evaluation. The van Deemter curves, depicted in Figure IV.1B, were constructed by analysis of the mixture at 10 different voltages between 7.5 and 30 kV. Optimal velocities were measured at 0.7 mm/s.

These reported plate heights (corresponding to reduced plate heights of ≈3) might seem high in the light of earlier reports, but are in line with reported results for the analysis of (neutral) polar solutes in CEC [15,34,35]. A less than optimal packing efficiency, a slower than expected mass transfer and the possible occurrence of Joule heating phenomena are the likely causes of the measured plate heights.

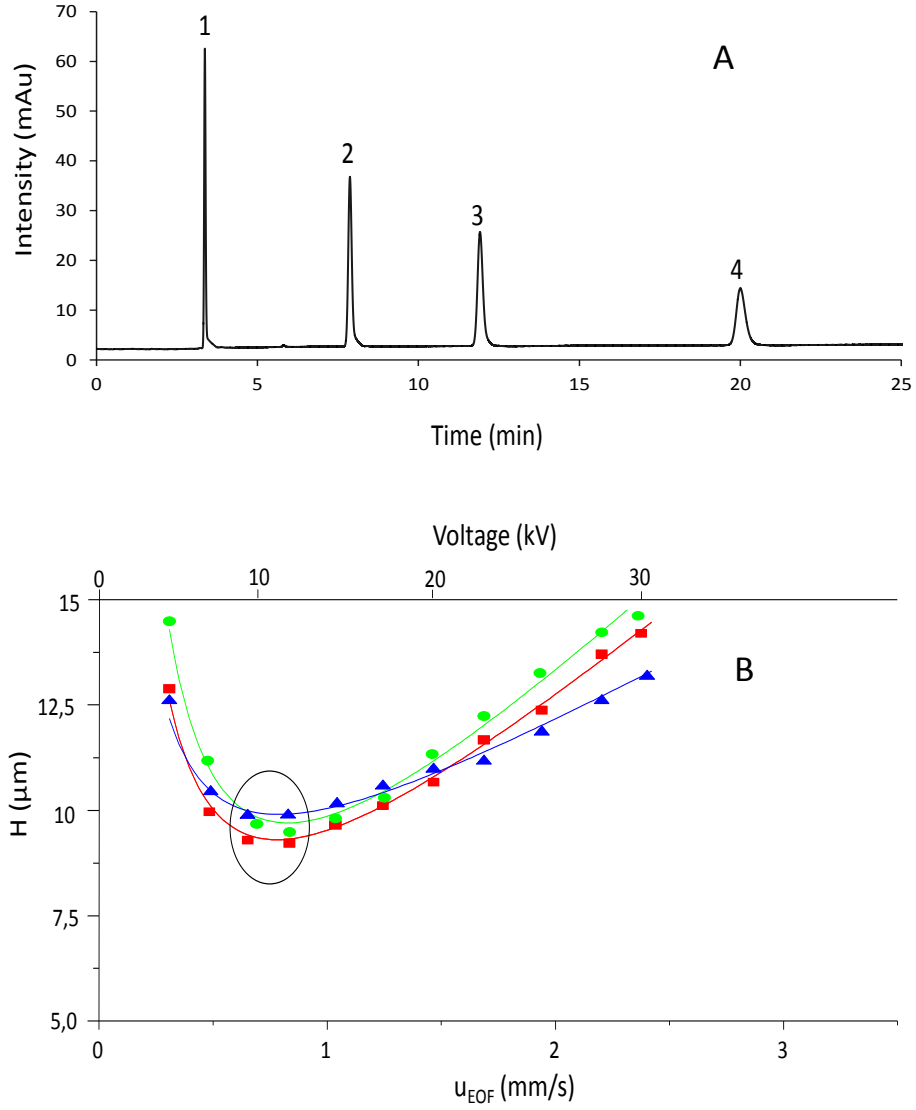

Figure IV.1. Electrochromatogram (1A) and van Deemter curves (1B) in CEC. Sample consisted out of thiourea (1), octanophenone (2-red squares), decanophenone (3-green circles), dodecanophenone (4-blue triangles). Mobile phase composition: 80% ACN/20% 25mM Tris-Acetate pH 8.5.

Nevertheless the corresponding kinetic plots can be constructed from this data, in analogy with HPLC, by extrapolating the results to the maximum applicable voltage by using following equations (Eq. IV.8-IV.10) as described by Fekete at al. [25]:

$$t_{EOF,KPL} = \lambda \cdot t_{EOF,exp} \qquad \text{Eq. IV.8}$$

$$t_{R,KPL} = \lambda \cdot t_{R,exp} \qquad \text{Eq IV.9}$$

$$N_{KPL} = \lambda \cdot N_{exp} \qquad \text{Eq. IV.10}$$

Where λ represents

$$\lambda = \frac{\Delta V_{max}}{\Delta V_{exp}} \qquad \text{Eq IV.11}$$

The plots are represented in Figure IV.2. Every point on these curves illustrates the maximal efficiency and shortest analysis time which can be obtained on any given length of this type of column. The top right section of these plots illustrates the asymptotic region where further elongation of the column, for a given maximum available voltage (i.e. 30 kV) will not further increase the plate count (as one thereby wanders even deeper in the B-term region of the van Deemter curve).

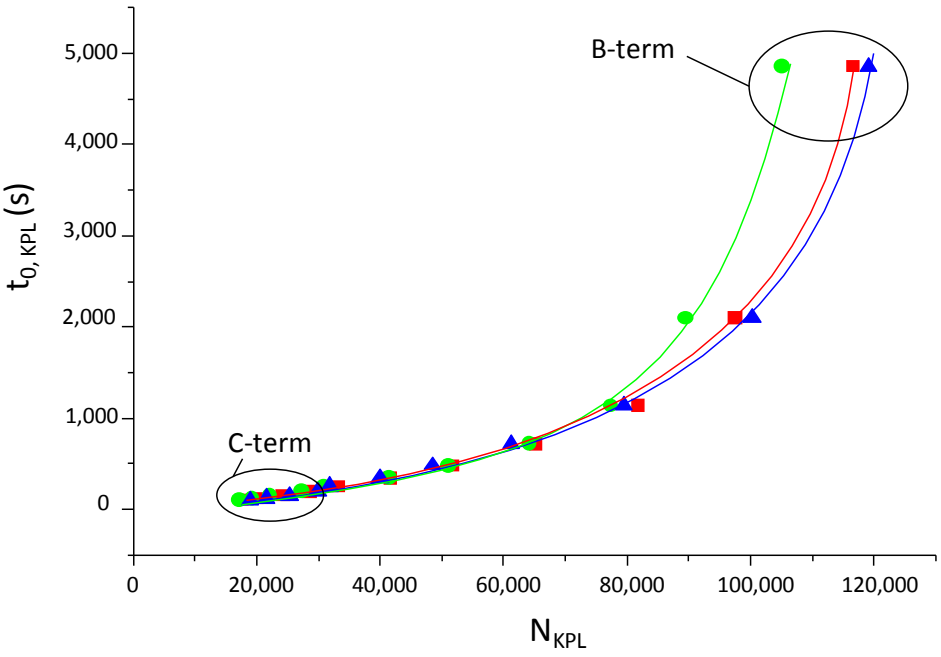

Figure IV.2. Kinetic plots obtained in CEC according to the data represented in Figure IV.1. Sample consisted out of Thiourea (1), octanophenone (2-red squares), decanophenone (3-green circles), dodecanophenone (4-blue triangles).

It allows, for example, to predict that for octanophenone 120,000 plates will be obtained on a comparable column packed with the same particles over length of 1.5 m and that it will require 200 minutes to elute this solute (t_0 = 83 min). The bottom left section of these curves illustrates the C-term regime or what performance is possible with very short columns of this type. For example 5,000 plates can be obtained for octanophenone with a t_0 of 0.43 min (t_R = 1.05 min) on a packed bed of 11 cm.

As in CEC the coupling of packed capillaries is currently not possible and as this would inevitably require the manufacturing of a new column with a different length for every point on the maximum performance curve, the pragmatism of this type kinetic plot can be questioned. However, these curves illustrate well that obtaining very high separation efficiencies or ultrafast analyses in CEC under realistically retained (and therefore separated) conditions, with the goal of outcompeting pressure driven techniques, is not possible with packed column CEC in this current format (3 µm dp and 30 kV available voltage).

The availability of longer packed beds up to 1.5 m would be most welcome, as this would allow operation close to the minimum of the van Deemter curve while operating at 30 kV, and therefore allow more efficient use of the available instrumental capabilities. Although this length would still only deliver 120000 plates, values which are today more easily reachable in HPLC by coupling a limited number of conventional columns at somewhat more elevated temperatures [24,36].

To illustrate how this performance compared to pressure driven techniques identical analyses were performed on commercial 150 x 4.6 mm stainless steel HPLC columns packed with the same Hypersil 3 µm ODS stationary phase. This comparison was deliberately performed with the LC equivalent under optimal conditions (i.e. implying measurements on well-developed columns under conditions were extra-column peak broadening phenomena were minimized) and not with µ-LC of the CEC columns. This as the latter carries no practical value and as extra-column peak broadening phenomena in isocratic µ-LC are almost impossible to suppress, leading to poor LC performance and therefore to experimental bias. Note that both the HPLC and CEC separations were performed with identical mobile phase compositions.

In Figure IV.3A the corresponding HPLC chromatogram at a flow rate of 0.8 mL/min is represented. Comparison with Figure IV.1A and analysis of Table IV.1, reveals significantly higher retention factors in HPLC compared to CEC. This is caused by a lower packing density in the CEC columns [37], leading to an increased phase ratio ($\beta = V_m/V_s$, whereby V_m and V_s correspond to the volume of mobile and stationary phase, respectively) and/or by retention time reductions due to Joule heating effects, affecting the partitioning process [38-40]. In the corresponding van Deemter curves, represented in Fig. V.3B, the minimal plate heights were 7.9, 7.6 and 7.8 µm for octano-, decano- and dodecanophenone, respectively. Shallower C-terms and correspondingly faster optimal velocities compared to the CEC equivalents are thereby also observed. This phenomenon could be related to either Joule-heating phenomena or due to less efficient mass transfer between the two phases caused by the lower packing efficiencies in the CEC columns.

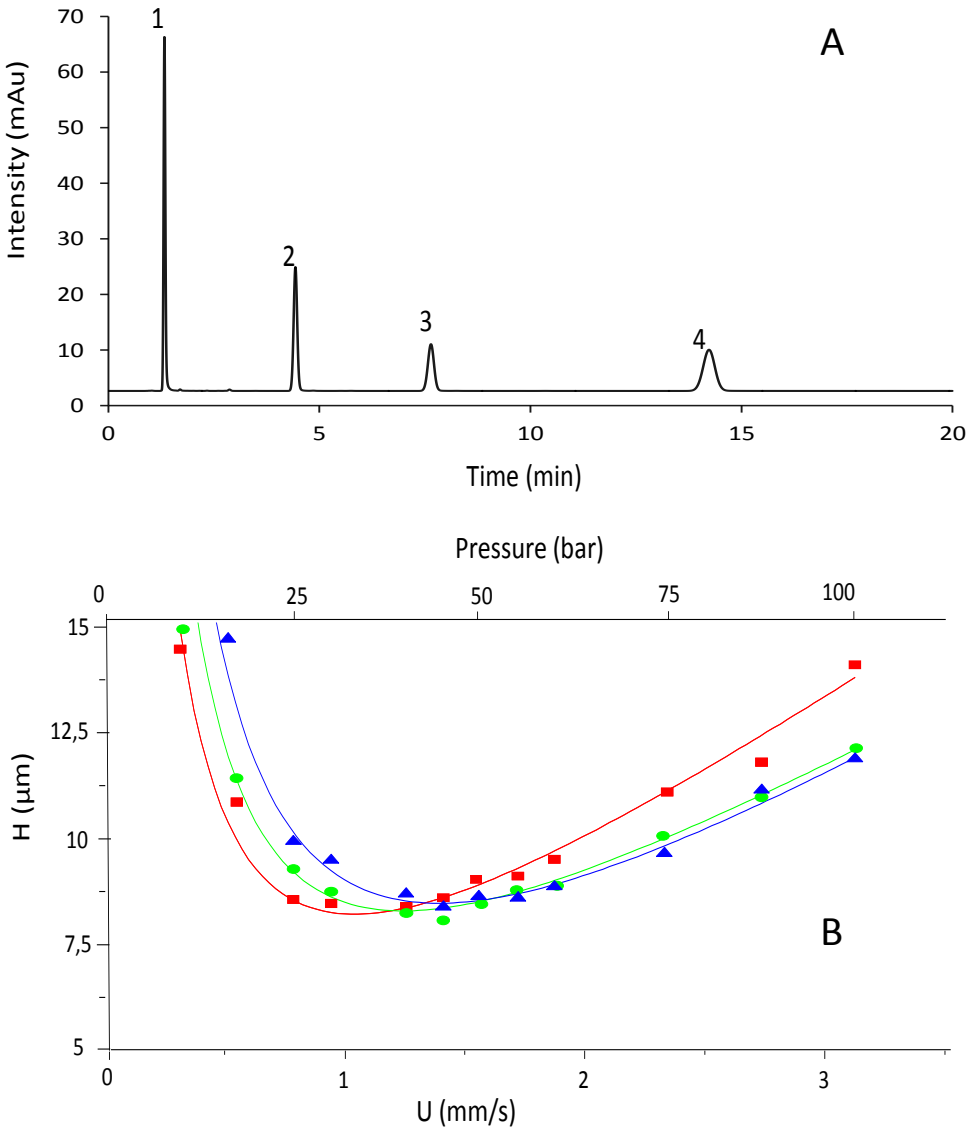

Figure IV.3. Chromatogram (3A) and van Deemter curves (3B) in HPLC. Red squares: octanophenone (2). Green dots: decanophenone (3). Blue triangles: dodecanophenone(4). Mobile-phase composition: 80% ACN/20% 25mM Tris-Acetate pH 8.5.

The corresponding kinetic plots for the HPLC column are constructed in Figure IV.4. For comparison the achievable performance of HPLC is overlaid with the CEC curves. HPLC curves were thereby extrapolated to 400 bar and the CEC curves to 30 kV.

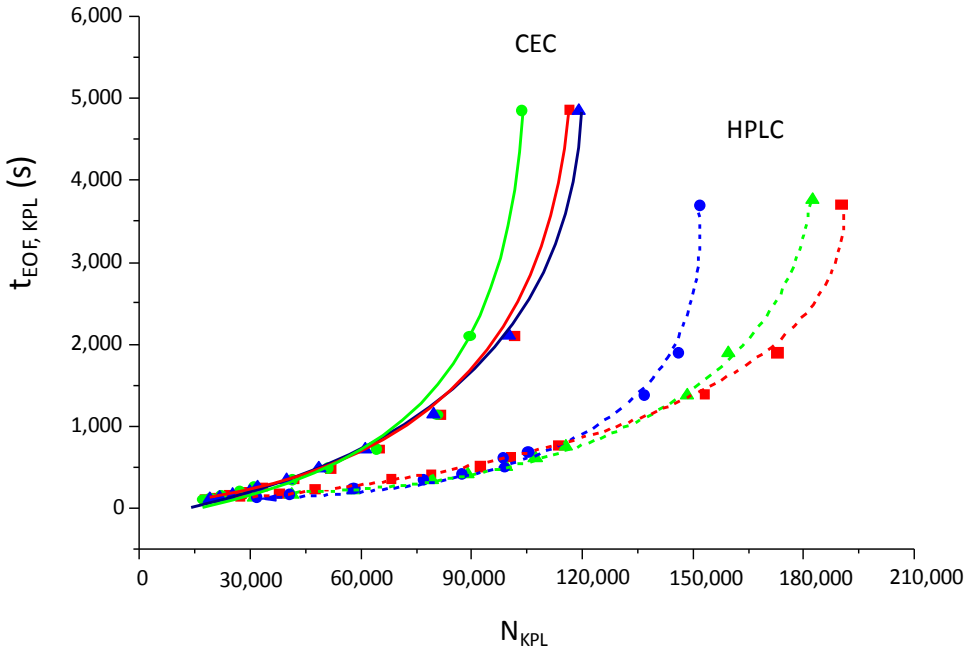

Figure IV.4. Comparison of kinetic plots in CEC and HPLC. The dashed curves represent the HPLC kinetic plots and the full curves the kinetic plots of CEC. Red squares: octanophenone (2). Green dots: decanophenone (3). Blue triangles: dodecanophenone (4). Mobile phase composition: 80% ACN/20% 25mM Tris-Acetate pH 8.5.

These figures illustrate the limitation of this type of packed column CEC compared to current HPLC. For octanophenone, efficiencies cannot reach 120,000 plates in CEC while for HPLC up to 200,000 plates are possible. Even more, the comparison of the elution of the solutes on a vertical line for CEC and HPLC shows that the same efficiency can be obtained in less time with conventional HPLC. However, the maximum plate numbers are only reached at very long analysis times and are therefore not very practical. The plate numbers of the kinetic plot can also be visualized as a function of t_{EOF}/N^2. This kinetic plot for octanophenone, shown in Figure IV.5, visualizes better the differences in the C-region.

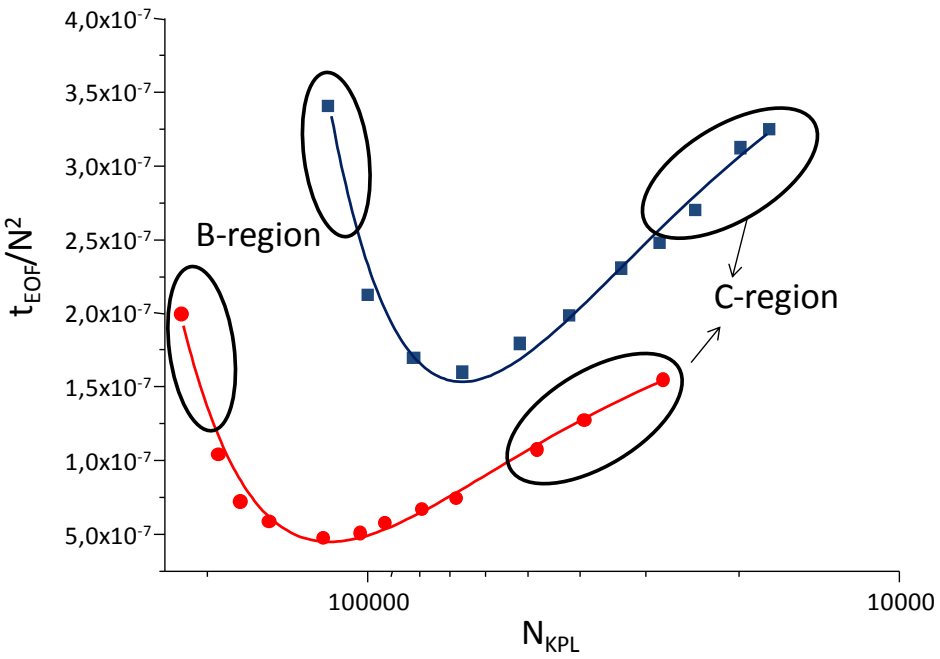

Figure IV.5. Comparison of kinetic plots in CEC and HPLC for octanophenone. The red curve represents the HPLC kinetic plot and the blue curves the kinetic plot of CEC. Mobile phase composition: 80% ACN/20% 25mM Tris-Acetate pH 8.5.

Figure IV.5 demonstrates that HPLC analyses performed on short columns (C-region) are preferential in terms of speed and efficiency as well. As the current developments in UHPLC further exacerbate this situation to the detriment of CEC, more insight in the underlying causes of the less than expected CEC performance is necessary in order to remediate this situation.

Particular attention thereby needs to be paid to the possible development of radial thermal gradients in the used CEC format due to Joule heating phenomena. A faster than expected increase in current as a function of the applied voltage, is typically considered to be indicative of this phenomenon [28]. In Figure IV.6A this is represented for a series of analyses at various temperatures. The measurement under the coolest operational conditions (10°C) resulted in all cases in the lowest generation of current. However, one would expect, upon absence of Joule heating, a linear increase in current versus voltage. The plots illustrate that at even low temperatures some degree of non-linearity is measured and that, when the experiments are performed at increasing temperatures, the degree of deviation is enhanced.

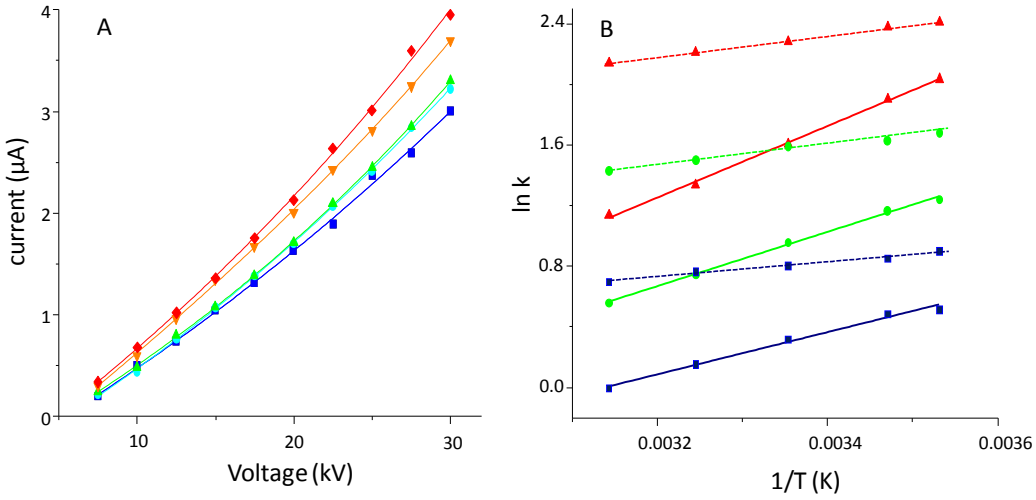

Figure IV.6. Current versus voltage profiles (A) at various temperatures and the van 't Hoff plots (B) of the three phenones as measured in CEC and in HPLC on the same type of stationary phase. The current was measured at 10°C (blue squares), 15°C (cyan dots), 25°C (green up pointed triangles), 35°C analysis (orange down pointed triangles) and 45°C (red diamonds). The van 't Hoff plots of octanophenone, decanophenone and dodecanophenone, were represented by blue squares, green dots and red triangles, respectively. The CEC and HPLC data were represented by full and dotted lines, respectively.

The possible occurrence of detrimental Joule heating is also attested by the unconventional drop in solute retention as a function of temperature. In Table IV.1, Figure IV.6B and in Figure IV.7 the retention data, the corresponding van 't Hoff plots and the chromatograms are respectively represented to illustrate this phenomenon.

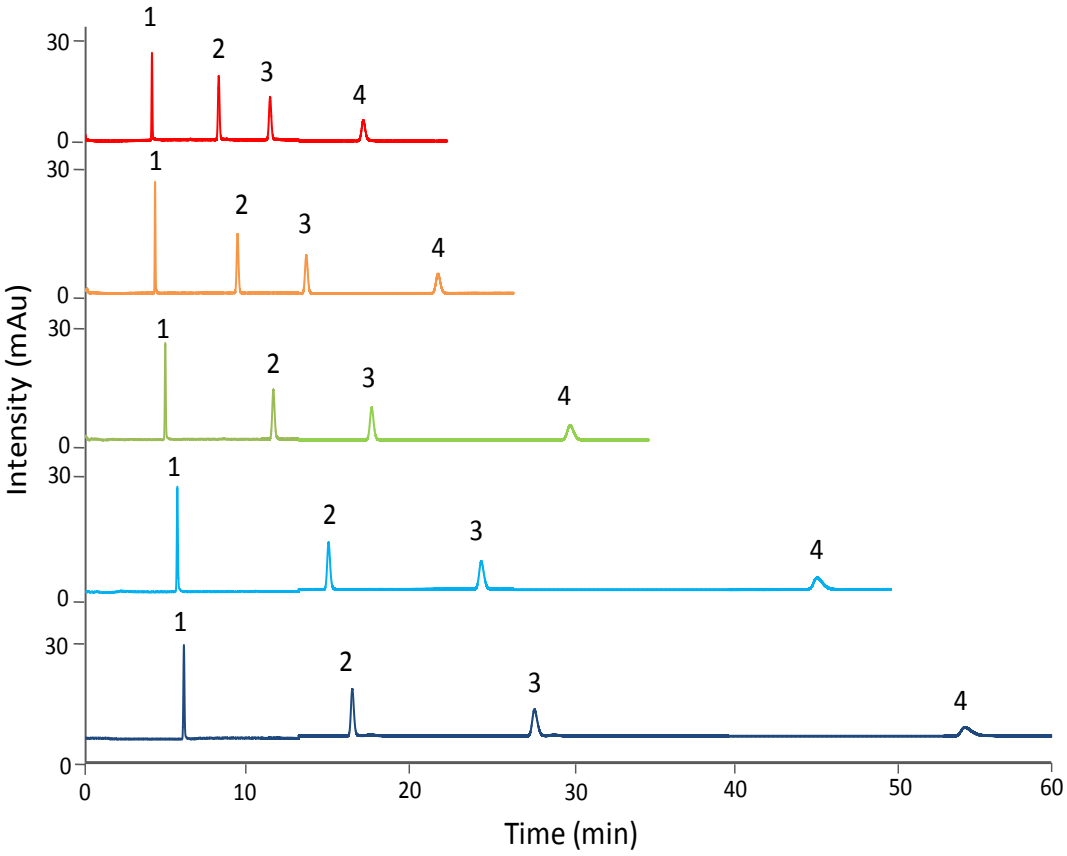

Figure IV.7: CEC electrochromatograms at 10°C; 15°C, 25°c, 35°C and 45°C at 17.5 kV. The separated components are in order of elution thiourea (1), octanophenone (2), decanophenone (3) and dodecanophenone (4).

A reduction in retention factor for dodecaphenone from 7.6 to 3.1 (-60%) is thereby measured when increasing the temperature from 10 to 45°C. For comparison, in HPLC a comparable reduction in retention is typically observed when temperature is raised by at least 60-80°C [41-44]. The comparison of the van 't Hoff plots, depicted in Figure IV.6B, demonstrate the sharp decline in retention in CEC with increasing temperature, compared to HPLC.

Table IV.1. The retention comparison at different temperatures in CEC and HPLC

	k CEC					k HPLC
	10°C	**15°C**	**25°C**	**35°C**	**45°C**	**25°C**
octanophenone	1.67	1.62	1.37	1.16	0.99	2.36
decanophenone	3.45	3.21	2.59	2.11	1.74	4.80
dodecanophenone	7.64	6.68	5.00	3.90	3.11	9.82

As the measured retention in CEC is dropping about twice as fast this strongly indicates the occurrence of significantly higher temperatures in the center of the capillary than the set (air cooled) temperature by the instrument thermostat. These results could indicate interesting possibilities for the application of temperature gradients instead of the, harder to realize, mobile phase compositional gradients, to increase the eluotropic strength in CEC. It also points to possible strategies to allow increased CEC retention (at low temperatures) while still using large fractions of organic modifier, in this way opening up possibilities for more repeatable CEC analyses. However, these temperature phenomena mainly affect the reachable efficiencies in a detrimental way.

In Figure IV.8 the CEC van Deemter curves for octanophenone were constructed from 10°C to 45°C. A 24% improvement in minimal plate height (from 8.29 to 6.31 µm), which is thereby observed between 25 and 10°C, illustrates the benefits of operating CEC on packed columns at reduced temperatures. Interesting is that now, under these cooler conditions, an indeed lower minimal plate height is obtained in CEC (6.31 µm) compared to HPLC (7.8 µm) on the same stationary phase.

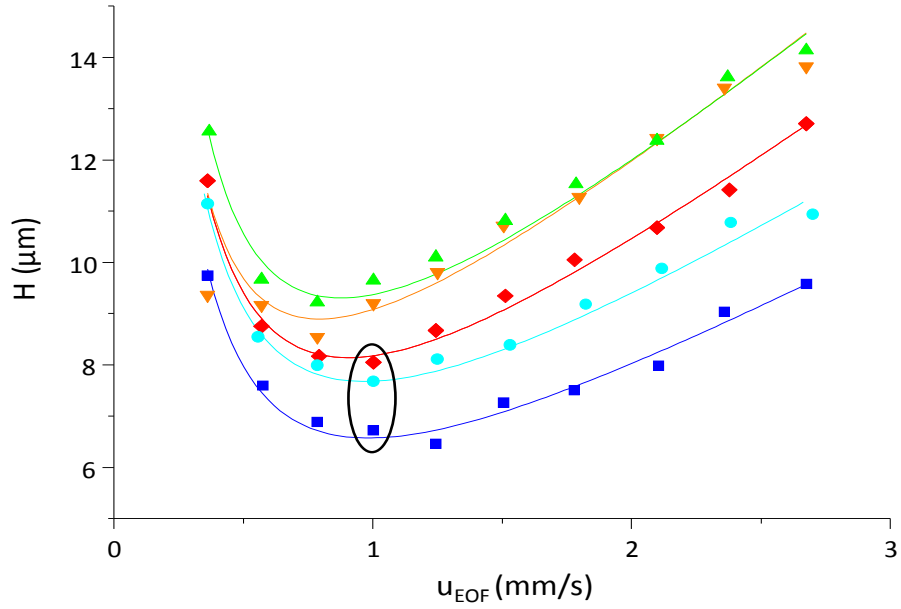

Figure IV.8. The van Deemter curves of octanophenone obtained at different temperatures. Blue square: 10°C. Cyan dots: 15°C. Green up pointed triangles: 25°C. Orange down pointed triangles: 35°C. Red diamonds: 45°C.

Better control of the Joule heating phenomenon at the lower temperatures is probably, also in the light of the above discussion, the cause of the observed results. Comparison with the van Deemter curves at higher temperatures learns that at 35°C and 45°C again lower plate heights (12% reduction) are obtained compared to the 25°C experiments. This observation, however, requires critical assessment as, as discussed above, this coincides with a retention factor reduction from 1.67 to 0.99. The somewhat improved minimum plate height value, at 45°C, is related to an overall faster mass transfer at more elevated temperatures, which leads to a reduced C-term (and particularly to a reduced C_s term or the resistance to mass transfer in the stationary phase). Additionally, also note that the lower retention at higher temperatures further lowers the contribution of the resistance to mass transfer in the stationary phase (as the relative importance of the C_s term lowers to the benefit of the C_m term). Nevertheless, these effects appear to be simultaneously being counterbalanced by increased Joule heating leading to the intermediate value in terms of measured minimum plate height at 45°C compared to 10°C.

Note that the above reasoning that Joule heating phenomena are occurring in these CEC experiments is based on the Ohm's law plots and on the Van 't Hoff curves depicted in Figure IV.6, which both allow strong support of this interpretation. Nevertheless, an alternative interpretation of the shapes of the van Deemter curves obtained in CEC at various temperatures could lead to the conclusion that the Joule heating is a lesser problem in CEC than is concluded here. This rationale involves that the C and B-term values and the optimal velocities should increase in the experiments including Joule heating. As this is not observed in Figure IV.8 one could conclude that other phenomena are at the origin in the observations in Figure IV.6.

On the other hand, one might expect significant peak broadening and van Deemter curve distorting phenomena to take place when Joule heating is occurring in the columns, leading to strong radial temperature profiles. As experimental results show that the best performance in the van Deemter curves and in practice are obtained when using lower temperatures, the Joule heating assumption which is presented here seems the most probable explanation of these phenomena. However, it is clear that further work on the construction of van Deemter curves and kinetic plots in CEC at various temperatures imposes itself to corroborate the results.

It should be noted that in HPLC the optimal velocity is also increasing as a function of temperature (due to the faster mass transfer) but that, by contrast to the above CEC results, the minimal plate height is thereby independent of the temperature when frictional heating is negligible [46] and close to $\approx 2d_p$ for fully porous particles. These results illustrate that in CEC, from a practical perspective, the low temperature experiments are more interesting compared to the high temperature analyses. This can be illustrated through the peak capacity values of 102 and 67 which are measured for the 10 and the 45°C chromatograms, respectively (obtained via Eq. 14 in [45]). This indicates that low temperature CEC allows a significant increase in peak capacity with a 25 cm column under the described conditions.

Transformation of the plate-height curves, collected at the different temperatures for octanophenone, to the electrochromatographic kinetic plots, allows generalization of these observations. The resulting plots, depicted in Figure IV.9A reveal again more plates can be achieved in less time at 10°C for all columns lengths. Nonetheless also these plots do not

allow assessment of the actual separation performance due to the decreasing retention at more elevated temperatures. In Figure IV.9B this drawback is addressed by use of the effective plate number ($N_{eff} = N*(k^2/(1+k)^2)$) which is adequately correcting for the lesser resolution which is reached under conditions of poor retention. Very comparable profiles are observed when replacing the abscissa by peak capacity values. From the resulting kinetic plots, depicted in Figure IV. 9B, it can now be deduced that an analysis at a lower temperature (10°C and 15°C) is always preferable in terms of maximum achievable (effective) efficiency (and peak capacity), while Figure IV.9C demonstrates that analyses at lower temperatures are also preferable in terms of speed of the analysis, compared to the analyses at higher temperatures (25-45°C). Yet, despite the lower plate height, the maximum performance even with low temperature CEC remains lower compared to the HPLC results represented in Figure IV.3-4.

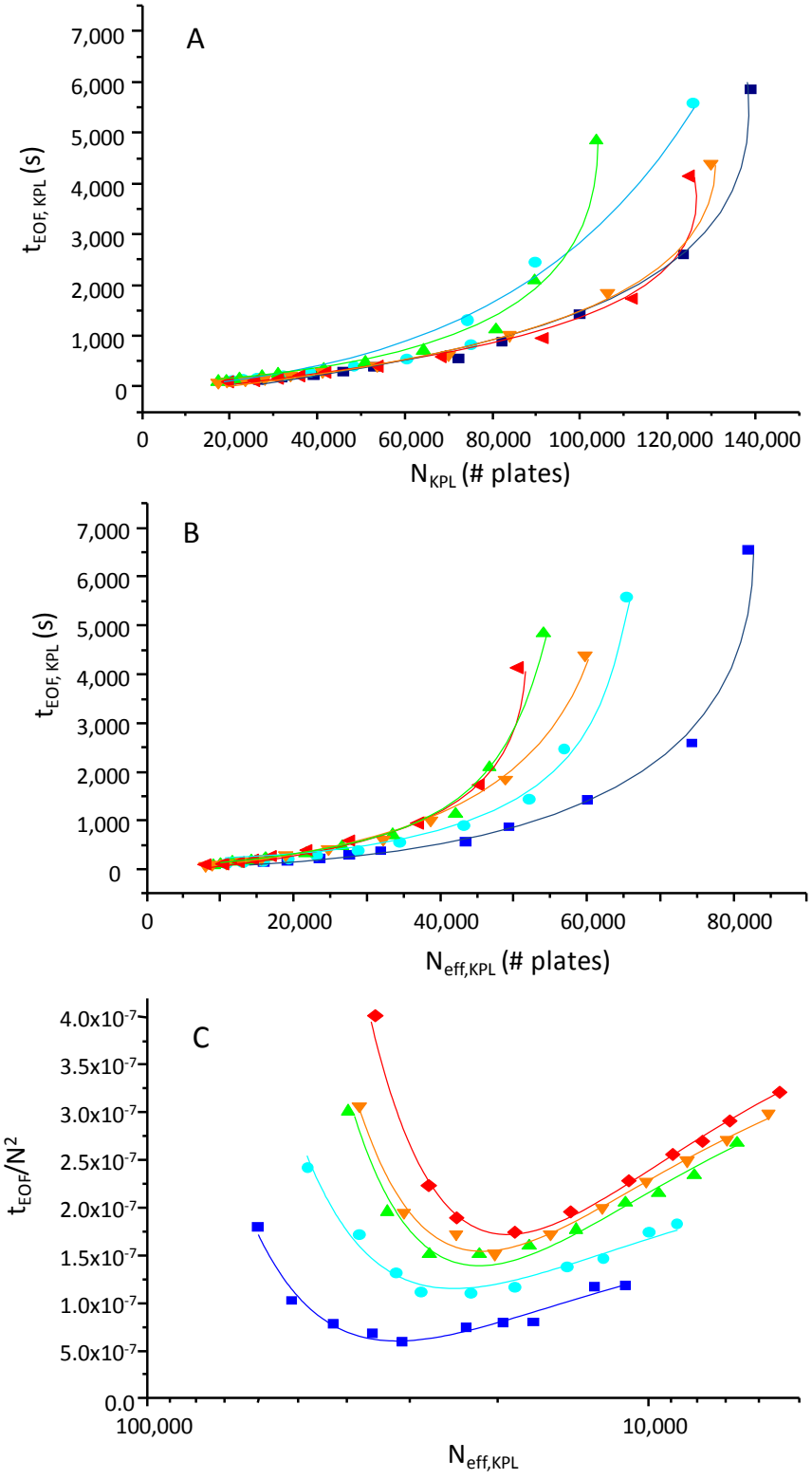

Figure IV.9. The electrochromatographic kinetic plots of octanophenone represented as N_{KPL} (A)or $N_{KPL, eff}$ (B) as a function of $t_{EOF, KPL}$. The effective plates are also represented as a function of t_{EOF}/N^2 (C). In A-C: dark blue square: 10°C, cyan dots, green up pointed triangle: 25°C, orange down pointed triangle: 35°C, and the red diamond: 45°C.

The above results allow extrapolating of the measured CEC performance towards formats where it should truly become an attractive alternative for the pressure driven equivalents. Essentially CEC performance will only become a competitive alternative for HPLC if columns (of comparable length) can be packed with (porous) sub-micron particles. To illustrate this in Figure IV.10, new kinetic plots where constructed for simulated columns, packed with smaller particle sizes (1.8, 1 and 0.5 µm), based on the information from the 10°C van Deemter data in Figure IV.8. The van Deemter data were subsequently extrapolated via the reduced plate heights and reduced linear velocities towards the expected curve profile for the smaller particles. The reduced linear velocity and reduced plate height are particle independent values. Assuming that the particle size distribution, the packing density and the diffusion coefficients are constant, their linear velocities and plate heights can be simulated in a straightforward way.

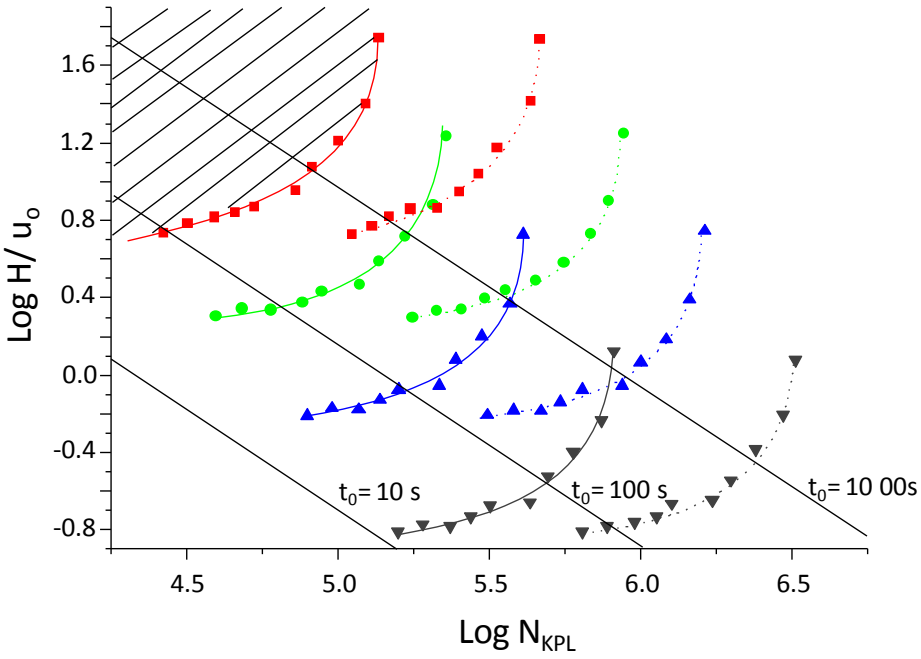

Figure IV.10. The simulated kinetic plots at 30 kV (full line) and 120 kV (spotted line) for a particle diameter of 3 µm (red squares), 1.8 µm (green dots), 1 µm (blue up pointed triangles) and 0.5 µm (grey down pointed triangles). The contemporary CEC region is demarcated by the hatched area.

Note that these extrapolations are only valid if the degree of Joule heating is the same, if the magnitude of the EOF remains constant and if the packing density can be maintained. Both

the former assumptions are defendable, as when using the same mobile phase conditions and the same capillary diameter, no increase in current generation is to be expected. The same is valid for the latter as the magnitude of electro-osmotic flow is not much dependent on the particle size (except when smaller than 50 nm due to double layer overlap). The most challenging issue in this performance and for CEC as a whole is, however, that with conventional slurry packing approaches, satisfactory columns packed with 0.5 µm particles cannot be manufactured as the packing pressures involved would be astronomical. Nevertheless in the light of the many alternative packing approaches which have been described (such as supercritical fluid and electrokinetic packing strategies [46-48]), this thought experiment is worthwhile pursuing if only to assist the future CEC developments. This extrapolation shows, for example, that a maximal (asymptotic) performance of 820000 plates should be obtainable with 0.5 µm particle diameters (i.e. 6 times more than is possible with the current 3 µm format) in 144 min.

An interesting foreseeable evaluation in the field of capillary electrochromatography is the possibility to apply more elevated voltages above the 30 kV safety limit which is used today. As successful CE experiments at 120 kV (and higher) have already been reported the results are hereby extrapolated to this voltage [49-53]. Under the assumption the Joule heating phenomenona can be sufficiently suppressed (e.g. by lowering ionic strength, by using low conductivity buffers or by the use of narrower capillaries), retentive chromatography with column performances up to 3,600,000 plates in 576 min. or to reach a million plates in 21 minutes for retained compounds would be possible.

5 Conclusion

This works introduces the construction of kinetic plots in packed column CEC by considering the maximum voltage as constraining parameter. The methodology was used to investigate the potential of contemporary CEC and the importance of the temperature control in CEC. It is revealed that cooling down to 10°C is beneficial for the efficiency and speed of the analysis. Analyses at low temperature seem to suppress Joule heating phenomena leading to less band broadening and increased retention. High temperatures (up to 45°C) expedite the analyses to the detriment of the effective plate numbers and peak capacity. Comparison of

CEC with HPLC for columns packed with the same stationary phase reveals that electrochromatography in its current format is not yet competitive with the pressure driven analogues. This was mainly ascribed to problems with the efficiency of the packed beds, leading to differences in phase ratio between the HPLC and the CEC columns. However, it was also demonstrated that Joule heating is probably still an occurring problem. The simulation capabilities that the kinetic plots offer illustrate that the future power of CEC resides in the use of sub-micron particles and of ultra-high voltages (120 kV) on packed columns.

6 References

[1] H. Swerdlow, J.Z. Zhang, D.Y. Chen, H.R. Harke, R. Grey, S.L. Wu, N.J. Dovichi, C. Fuller, Anal. Chem. 63 (1991) 2835.

[2] C.P. Fredlake, D.G. Hert, E.R. Mardis, A.E. Barron, Electrophoresis 27 (2006) 3689.

[3] M. Kircher, J. Kelso, Bioessays 32 (2010) 524.

[4] M.C. Breadmore, Electrophoresis 28 (2007) 254.

[5] C.W. Klampfl, J. Chromatogr. A 1044 (2004) 131.

[6] A. von Brocke, G. Nicholson, E. Bayer, Electrophoresis 22 (2001) 1251.

[7] E. Rapp, E. Bayer, J. Chromatogr. A 887 (2000) 367.

[8] F. Moffatt, P.A. Cooper, K.M. Jessop, Anal. Chem. 71 (1999) 1119.

[9] N. Ishizuka, H. Minakuchi, K. Nakanishi, N. Soga, H. Nagayama, K. Hosoya, N. Tanaka, Anal. Chem. 72 (2000) 1275.

[10] R.J. Boughtflower, T. Underwood, C.J. Paterson, Chromatographia 40 (1995) 329.

[11] C. Yan, R. Dadoo, H. Zhao, R.N. Zare, D.J. Rakestraw, Anal. Chem. 67 (1995) 2026.

[12] E. Wen, R. Asiaie, C. Horvath, J. Chromatogr. A 855 (1999) 349.

[13] F. Lynen, A. Buica, A. de Villiers, A. Crouch, P. Sandra, J. Sep. Sci. 28 (2005) 1539.

[14] C. Puangpila, T. Nhujak, Z. El Rassi, Electrophoresis 33 (2012) 1431.

[15] M.G. Cikalo, K.D. Bartle, P. Myers, J. Chromatogr. A 836 (1999) 35.

[16] A. Messina, C. Desiderio, A. De Rossi, F. Bachechi, M. Sinibaldi, Chromatographia 62 (2005) 409.

[17] G. Desmet, D. Clicq, P. Gzil, Anal. Chem. 77 (2005) 4058.

[18] G. Desmet, D. Clicq, D.T.T. Nguyen, D. Guillarme, S. Rudaz, J.L. Veuthey, N. Vervoort, G. Torok, D. Cabooter, P. Gzil, Anal. Chem. 78 (2006) 2150.

[19] K. Broeckhoven, D. Cabooter, F. Lynen, P. Sandra, G. Desmet, J. Chromatogr. A 1217 (2010) 2787.

[20] D. Cabooter, F. Lestremau, A. de Villiers, K. Broeckhoven, F. Lynen, P. Sandra, G. Desmet, J. Chromatogr. A 1216 (2009) 3895.

[21] D. Cabooter, F. Lestremau, F. Lynen, P. Sandra, G. Desmet, J. Chromatogr. A 1212 (2008) 23.

[22] S. Heinisch, G. Desmet, D. Clicq, J.-L. Rocca, J. Chromatogr. A 1203 (2008) 124.

[23] D. Clicq, S. Heinisch, J.L. Rocca, D. Cabooter, P. Gzil, G. Desmet, J. Chromatogr. A 1146 (2007) 193.

[24] F. Lestremau, A. de Villiers, F. Lynen, A. Cooper, R. Szucs, P. Sandra, J. Chromatogr. A 1138 (2007) 120.

[25] V. Fekete, A. Fekete, J. Fekete, A. Liekens, P. Schmitt-Kopplin, G. Desmet, Jpc-J. Planar Chromat. 23 (2010) 440.

[26] K.D. Bartle, P. Myers, J. Chromatogr. A 916 (2001) 3.

[27] A.S. Rathore, C. Horvath, J. Chromatogr. A 781 (1997) 185.

[28] A.S. Rathore, E. Wen, C. Horvath, Anal. Chem. 71 (1999) 2633.

[29] J.H. Knox, J. Chromatogr. A 831 (1999) 3.

[30] K. Jinno, H. Sawada, Trac-Trend. Anal. Chem. 19 (2000) 664.

[31] M.M. Dittmann, G.P. Rozing, J. Chromatogr. A 744 (1996) 63.

[32] A. de Villiers, F. Lynen, P. Sandra, J. Chromatogr. A 1216 (2009) 3431.

[33] A. de Villiers, H. Lauer, R. Szucs, S. Goodall, P. Sandra, J. Chromatogr. A 1113 (2006) 84.

[34] A.-M.K. Weed, J. Dvornik, J.J. Stefancin, A.A. Gyapong, F. Svec, Z. Zajickova, J. Sep. Sci. 36 (2013) 270.

[35] I. Gusev, X. Huang, C. Horvath, J. Chromatogr. A 855 (1999) 273.

[36] F. Lestremau, A. Cooper, R. Szucs, F. David, P. Sandra, J. Chromatogr. A 1109 (2006) 191.

[37] S. Bruns, J.P. Grinias, L.E. Blue, J.W. Jorgenson, U. Tallarek, Anal. Chem. 84 (2012) 4496.

[38] A.S. Rathore, K.J. Reynolds, L.A. Colon, Electrophoresis 23 (2002) 2918.

[39] G.F. Chen, U. Tallarek, A. Seidel-Morgenstern, Y.K. Zhang, J. Chromatogr. A 1044 (2004) 287.

[40] N.M. Djordjevic, F. Fitzpatrick, F. Houdiere, G. Lerch, G. Rozing, J. Chromatogr. A 887 (2000) 245.

[41] J.V. Tran, P. Molander, Y. Greibrokk, E. Lundanes, J. Sep. Sci. 24 (2001) 930.

[42] C.R. Zhu, D.M. Goodall, S.A.C. Wren, Lc Gc N. Am. 23 (2005) 54.

[43] G. Vanhoenacker, A.D.S. Pereira, T. Kotsuka, D. Cabooter, G. Desmet, P. Sandra, J. Chromatogr. A 1217 (2010) 3217.

[44] G. Vanhoenacker, P. Sandra, Anal. Bioanal. Chem. 390 (2008) 245.

[45] S. Pous-Torres, J.J. Baeza-Baeza, J.R. Torres-Lapasio, M.C. Garcia-Alvarez-Coque, J. Chromatogr. A 1205 (2008) 78.

[46] L.A. Colon, T.D. Maloney, A.M. Fermier, J. Chromatogr. A 887 (2000) 43.

[47] T.D. Maloney, L.A. Colon, J. Sep. Sci. 25 (2002) 1215.

[48] M.M. Robson, S. Roulin, S.M. Shariff, M.W. Raynor, K.D. Bartle, A.A. Clifford, P. Meyers, M.R. Euerby, C.M. Johnson, Chromatographia 43 (1996) 313.

[49] K.M. Hutterer, J.W. Jorgenson, Electrophoresis 26 (2005) 2027.

[50] K.M. Hutterer, H. Birrell, P. Camilleri, J.W. Jorgenson, J. Chromatogr. B 745 (2000) 365.

[51] K.M. Hutterer, J.W. Jorgenson, Anal. Chem. 71 (1999) 1293.

[52] J.W. Jorgenson, K. Hutterer, Abstr. Pap. Am. Chem. S. 216 (1998) U200.

[53] W.H. Henley, J.W. Jorgenson, J. Chromatogr. A 1261 (2012) 171.

Chapter 5

Possibilities and limitations of hydrophilic interaction capillary electrochromatography on native silica packed columns

The potential of native silica particles as stationary phases in packed column hydrophilic interaction capillary electrochromatography (HI-CEC) is described in this chapter. Therefore, the procedure to pack capillaries with native silica particles was optimized, with the emphasis on the optimization of the frits. The fundamental evaluation of the columns was performed through analysis of neutral polar test solutes, to allow unbiased study of the chromatographic performance. Capillaries were packed with 5 and 3 µm particles and a reduced plate height of 2 was obtained. The kinetic plot method was utilized to demonstrate the ultimate potential of the packed columns. The influence of the organic modifier content on the EOF velocity and on the solute retention was investigated. The potential of packed column HI-CEC was subsequently investigated with nitrobenzenes, genotoxic solutes and polar polymeric compounds on columns of various dimensions.

In preparation as De Smet S, Lynen F, Possibilities and limitations of hydrophilic interaction capillary electrochromatography on native silica packed columns.

1 Introduction

During the last decades hydrophilic interaction liquid chromatography (HILIC) has emerged as a viable complementary technique to reversed-phase liquid chromatography (RPLC) for the analysis of polar and basic compounds. Possible separation of these solutes in reversed-phase mode can only be achieved with the use of highly or totally aqueous mobile phases, which can lead to stationary phase collapse. Furthermore, in most cases satisfactory separation is still inhibited due to the still insufficient retention. Therefore, separation modes such as normal phase and hydrophilic interaction liquid chromatography are more suitable for the analysis of polar compounds due to their hydrophilic stationary phase. The former is, however, limited by the often too low solubility of these solutes in the organic solvents. The latter is more suited for these analyses due to the aqueous content of HILIC type mobile phases [1-4]. Also, as described in Chapter III, CEC with polar stationary phases and a non-aqueous mobile phase often results in poor efficiencies and poor control of EOF [5,6].

In 1998, Wei et al. investigated the CEC analyses of basic compounds on capillaries packed with bare silica, revealing a complex retention mechanism including phenomena related to the normal-phase, reversed-phase and ion-exchange modes, dependent on the modifier content (and on the pH of the mobile phase). This was later confirmed by Mckeown et al., who investigated the retention behavior of polar compounds on Hypersil materials with different purity [7,8].

In 2001, the term HI-CEC was introduced by Ye et. al who packed capillaries with hydrophilic, strong cation-exchange particles of poly(2-sulfoethyl aspartamide) coated silica (5 µm) and obtained separations with a maximum efficiency of 111,000 plates/m [9]. Neutral molecules were separated by their hydrophilicity in the inversed order as observed in reversed-phase chromatography. However, three different mechanisms contributed to the retention of basic compounds: electrophoresis, hydrophilic interaction and ion-exchange interaction. Therefore, the interpretation and prediction of elution order of e.g. basic compounds becomes more complex. HI-CEC has until now only been reported 30 times and only two contributions describe the use of packed bed capillaries. In 2005, Valette et al. described the application of a packed bed of aminopropyl silica particles (3 µm) where the direction of the

EOF proved to be dependent on the nature of the ions in the electrolyte [10].

Most of the HI-CEC work thus far has been focused on the use of monolithic capillaries and to a lesser extent on open-tubular capillaries. The monolithic format gained popularity due to the easier column preparation process, the possibility of implementing different functional groups on the same polymeric support and more importantly because of the absence of the need to fabricate retaining frits. The applied polar monoliths in electrodriven techniques can be divided in three categories: silica-based [1,2,11-18], polyacrylamide [1,2,4,19,20] and polymethacrylate [1,4,17,21-23] based monoliths. In monolithic columns the EOF velocity and retention(-mechanisms) can easily be altered by changing the incorporated functional groups in the structure. However, the monolithic bed tends to shrink during the polymerization process, which induces wall effects [24,25]. The resulting difference in the EOF velocity and the mass transfer close to the wall, compared to the middle of the monolith, can induce mild to severe band broadening. Furthermore, in monolithic columns the control of the pore size (influenced by the porogen) is challenging, leading to poor column-to-column repeatability, as mentioned in Chapter III.

Furthermore, a fundamental comparison between HI-CEC and HILIC has been lacking. The evaluation and comparison of the performance of HI-CEC is therefore important. Moreover, the evaluation of such columns with neutral polar test solutes will generate a better insight into the hydrophilic interaction mechanism and reveal possible limitations of the technique. As in most reported HI-CEC and HILIC results the retention is fairly limited, it is therefore also interesting to investigate the band broadening processes occurring for more retained components ($2<k<10$).

Note that the sintering of the frits in capillaries packed with native silica particles is easier and should result in more robust silica particles. Consequently, the lifetime of the columns should be extended. In addition, packed beds consisting of native silica particles result in a high presence of free silanol functions on the surface, which enables the generation of a high EOF. This effect will be amplified as the mobile phases for HI-CEC contains a high concentration of ACN, which promotes also the generation of a high EOF (as explained in Chapter I).

Therefore, hydrophilic interaction electrochromatography should in principle be a performant technique and should offer a favorable complementary separation mode next to reversed-phase based electrochromatography.

In this study, capillaries were packed with native silica particles for the application of hydrophilic interaction CEC. The capillaries are evaluated with a neutral polar test mixture under well retained conditions. As a consequence, the separation is purely based on hydrophilic interactions and the performance of CEC capillaries, packed with bare silica particles, can be investigated in an unbiased way. The effect of the ionic strength and organic modifier concentration on the separation parameters (retention, mobile-phase velocity and efficiency) is examined and the possibilities of packed columns HI-CEC are explored with various representative test samples on various column dimensions.

2 Experimental

2.1 Reagents and materials

Fused-silica capillaries (75 µm ID) were purchased from CM Scientific (Silsden, United Kingdom). The native nucleosil particles (5 and 3 µm), produced by Macherey-Nagel (Düren, Germany), were obtained from Filterservice (Eupen, Belgium). Milli-Q water was prepared in house by purification and deionization of tap water in a Milli-Q plus water instrument from Millipore (Bedford, New Hampshire, USA). Acetic acid, acetonitrile, acetone and ammonium acetate of HPLC quality originated from Biosolve (Valkenswaard, Netherlands). The sodium silicate solution and all test compounds used for CEC-UV were purchased from Sigma-Aldrich (Bornem, Belgium). Stock solutions of all compounds were prepared at 10,000 µg/mL in water or ACN, dependent on their solubility, and diluted to 75 µg/mL (in the same solvent composition as the mobile phase) prior to analysis.

2.2 Instrumentation and chromatography

The 7100 CE system (Agilent Technologies, Waldbronn, Germany) used in this work includes an air-cooled thermostat, auto-sampler, diode array detector and a built-in system to pressurize vials. The mobile phase was filtered with syringe filters (Grace, 0.45 µm PVDF filters). Electrokinetic injections were performed by applying a voltage difference of 8 kV during a time span of 4 s.

A stock solution of ammonium acetate buffer was prepared by adding acetic acid to a 25 mM ammonium acetate solution until a pH of 5.5 was obtained. The mobile phase was prepared by adding the required volume of the buffer stock solution to ACN. Consequently, the mobile phase was degassed in an ultrasonic bath for 10 minutes prior to analysis. Analysis temperature was maintained at 25°C. All obtained data was processed with Chemstation B.04.03 software.

New columns were conditioned by increasing the voltage in a stepwise way to 30 kV in a 2 hour time span. Changes in mobile-phase composition were obtained by flushing the column in steps of increasing voltage to 30 kV with assisted pressure (10 bar) on the inlet to initiate the mobile-phase movement. The columns were stored with a mobile-phase composition of ACN/H_2O (1/1, v/v) and the capillary ends were submerged into vials filled with the same solvent composition.

2.3 Packing procedure

The CEC columns were packed by an in-house developed slurry packing techniques [26]. The packing set-up is described in Figure V.1.

A Gilson 307 pump, equipped with a 5SC pump head, was connected to a pressure release valve. The other ports of the valve were connected to the slurry reservoir and to the waste line. The slurry reservoir was fabricated by drilling a small hole in the top frit of an emptied HPLC column (10 cm, 4.6 mm). The capillary column was connected to the slurry reservoir via a Valco union and a graphite/vesper ferrule, which can withstand the pressure while being reusable. The capillary inlet was positioned close to the bottom of the reservoir and the latter was partially submerged (vertically) in an ultrasonic bath to maintain the particles suspended in the slurry for a longer time.

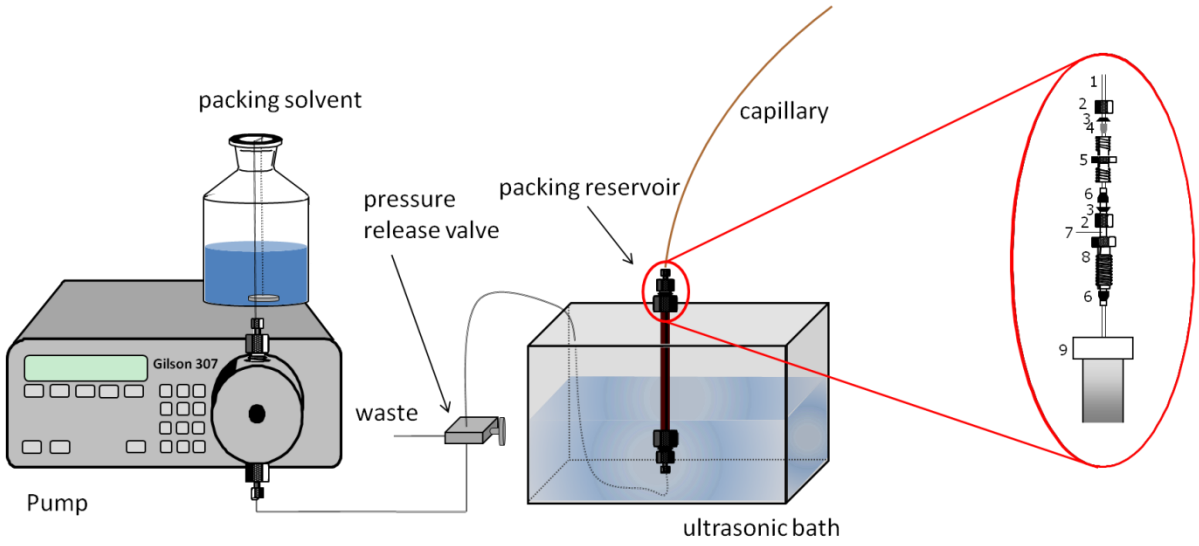

Figure V.1. The used set-up to slurry pack capillaries with on the right a close up of the connection between the column and the capillary. (1: fused-silica capillary, 2: 1/16" Swagelock nut, 3: 1/16" Swagelock back ferrule, 4: vespel ferrule (0.4 mm ID), 5: 1/16 x 1/16 Swagelock union, 6: 1/16" Waters ferrule, 7: 1/16" stainless steel HPLC tubing, 8: 1/16" Waters nut, 9: packing reservoir inlet.

The packing procedure, depicted in Figure V.2, comprised several steps. Prior to packing, the fused-silica capillaries were rinsed for 15 minutes with 1 M NaOH, H_2O and MeOH. Subsequently, the capillaries were dried for 30 minutes under a N_2 flow. 20 mg Nucleosil particles were wetted with 40 µL of 1/1 (v/v) mixture of water/sodium silicate to create a sticky plaster. The inlet end of the column was dipped several times into the mixture such that a small amount was introduced into the capillary. Subsequently, the introduced material was sintered at 300°C with the help of a heating filament. The strength and the permeability of the frit was tested by pumping the packing solvent through the column at 600 bar for 5 minutes. 75 mg of the packing material (5 Nucleosil particles, 120 Å) was suspended in 1 mL of the packing solvent, consisting of acetone and H_2O (30/70, v/v) and sonicated for 15 minutes. Note that a packing and slurry solvent consisting of 90% acetone and 10% water was used for the packing of capillaries with the 3 µm particles. Subsequently, the slurry was introduced into the packing reservoir and the pressure was quickly raised to 600 bar and maintained for 2 hours, while the system was submitted to ultrasonic agitation. The pressure was then slowly released during the course of one hour. Subsequently, the column was flushed during 6 hours at 600 bar with water to which 0.3% sodium silicate solution was added. The outlet frit was sintered with the heating ribbon while the capillary

was still pressurized. Consequently, the pressure was slowly released and the direction of the capillary was inversed. The excess packing material was flushed out the capillary while the capillary was simultaneously conditioned with mobile phase (acetonitrile/buffer) during 2 hours at a pressure of 250 bar. Finally, the packed bed and frits were inspected for fractures or unpacked sections with the help of an optical microscope.

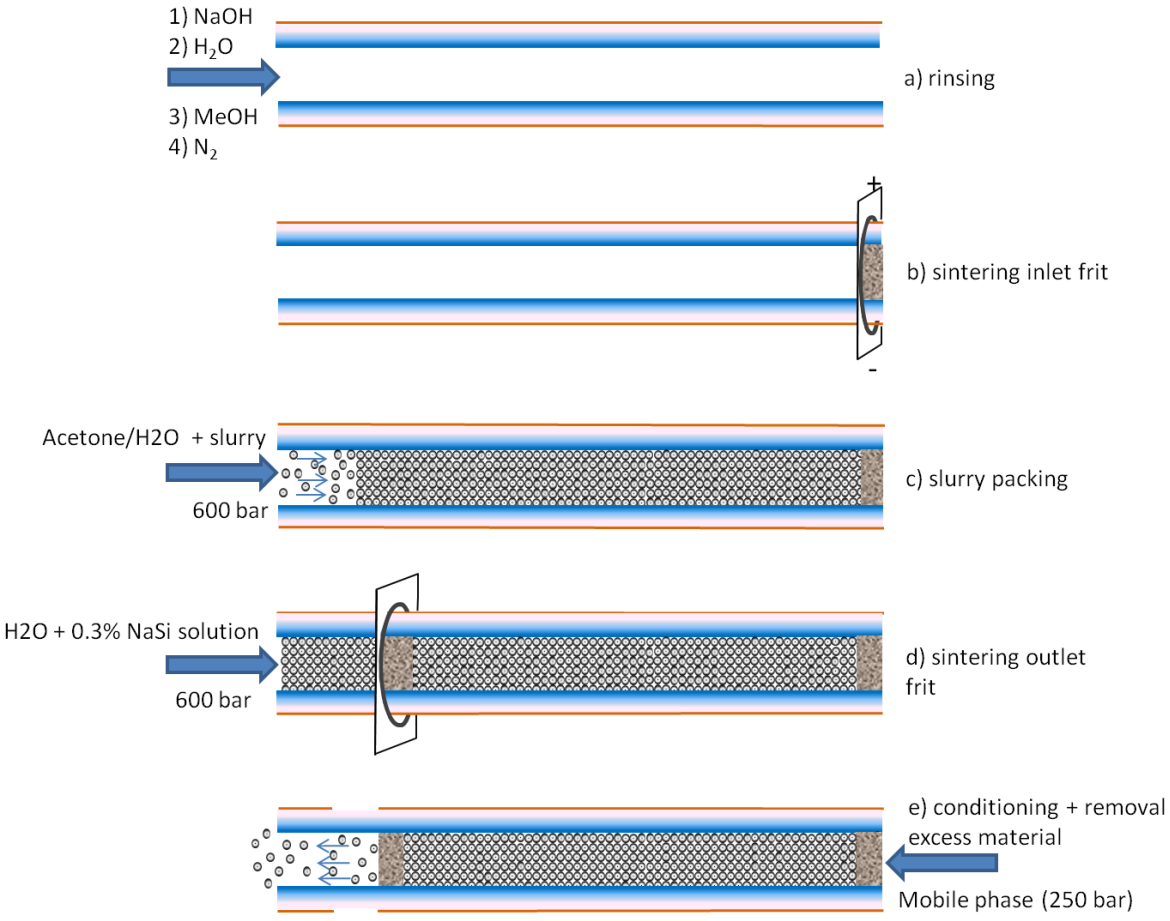

Figure V.2. Schematic representation of the packing procedure.

3 Results and discussion

3.1 Optimization of the packing procedure

As it is known that the composition of the slurry solvent, the packing procedure itself and the frit fabrication have a large influence on the separation performance in CEC, much emphasis has been set on optimization of these aspects in this work. The retaining inlet frit was formed by introducing and heating a mixture of native silica particles and sodium silicate in the capillary. Ideally, the frits should exhibit strong mechanical characteristics, a good permeability and should be as similar to the packing materials as possible to avoid band broadening due to inhomogeneities in the packed bed and because of the different retention mechanism and different EOF generation which can therefore be involved. Therefore, a new inlet retaining frit consisting of the packed material is usually formed during the packing procedure and subsequently the initial frit is removed. However, in this work the original frit functions as the permanent inlet frit as the packing material and the frit material are of the same type, facilitating the column manufacturing process. Therefore, the retention and the EOF are expected not to be altered much by the inlet frit. Note, however, that the surface properties of the thermally treated material might differ somewhat from the untreated material. Nevertheless, it is critical to obtain the formation of a mechanically stable porous frits to allow subsequent packing. Various frit forming procedures have been described in Chapter III. In this work the high pressure and high temperature sintering strategy in water with diluted sodium silicate has been selected for this purpose. In this approach the permeability and mechanical stability can be controlled by altering the sodium silicate concentration. High concentrations increases the strength but causes a decrease in the permeability, while low concentrations improve the permeability but lead to frits which are not always able to withstand high packing pressures. Sintering with the heating filament provides a frit from 0.3-1.5 mm dependent on the sintering time and filament dimensions, as depicted in Figure V.3.

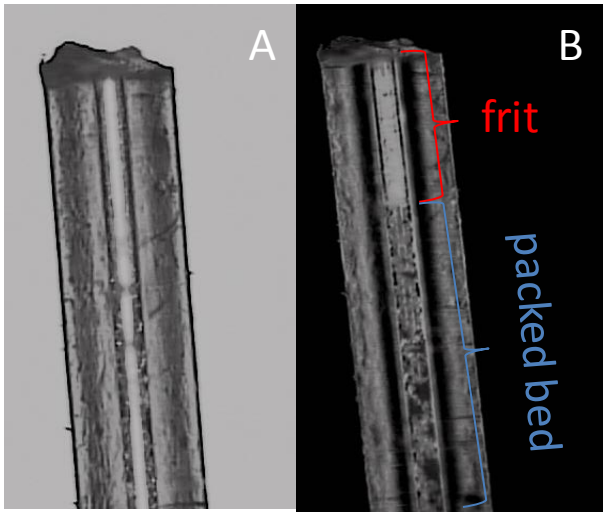

Figure V.3. Photograph of an empty fused-silica capillary (75 µm ID, 375 µm OD) (A) and a packed capillary (B), zoomed in (10X) on the sintered inlet frit (2 mm) by an optical microscope.

The sintering time was altered between 3 and 30 seconds, in order to optimize the frits in terms of thickness, mechanical stability and performance. The evaluation of the frits was performed by comparing the lifetime of the columns (with a 25 cm packed bed of 5 µm particles) and the efficiency of a well retained component, in this case cytosine. As demonstrated in Table V.1, sintering for 3 or 5 seconds resulted in unstable frits, prone to break at high pressures or under influence of the electrical field.

The highest efficiency was obtained with sintering times for both the inlet and outlet frit of 10 seconds, however at the cost of the column lifetime. Frits with good mechanical stability were only obtained when sintering during 15 seconds or longer. Satisfactory column efficiencies (18,800 plates) were thereby obtained, leading to column life times of at least 25 runs. The use of longer sintering times (>20 seconds) resulted in mechanically stronger frits but also in reduced column performance. Inspection of the these frits by optical microscopy revealed multiple cracks in the frits and in the surrounding packing material, leading to band broadening effects.

Table V.1. The performance of the frits as a function of the sintering times

Sintering time (s)	Efficiency cytosine (plates)	Lifetime (runs)
3	/	0
5	/	0
10	18850	5
15	18790	>25
20	17158	>25
25	14189	>25
30	12450	>25

* Analyses were performed on 25 cm packed bed columns (5 µm, 75 µm ID) Separation conditions and column dimensions are further specified in Figure V.4.

During packing, a distinction is usually made between the slurry solvent and the packing solvent. The latter is the solvent in which the particles form a suspension after ultrasonic agitation. Methanol, isopropanol, acetone, water and mixtures thereof were investigated both as slurry and as packing solvents. Pure acetone proved to be the most suitable solvent to keep the native silica particles in a slurry but the packing speed with acetone prooved to be too high; resulting in a inhomogeneous packed beds and poor column performance. Water as slurry and packing solvent resulted in more performant columns but only with a very short packed bed (<10 cm) as the particles in the slurry settled down swiftly in the packing reservoir. An optimum column performance and packed bed length could be obtained with a mixture of acetone and water (65/35, v/v), which was used as slurry and packing solvent. The particles stayed in slurry for over 1.5 hours (without extra agitation) and the packing speed was sufficiently low to obtain a more homogeneous packed bed. The packing was performed as described in the experimental section. Subsequently, the packed capillary was rinsed with low concentrations of sodium silicate (0.4%) added to the water. As a consequence, the sodium content of the water was raised and sintering of the outlet frit was more easily achieved. Subsequent to the sintering of the outlet frit, the UV-window was formed 1 cm away of the outlet frit by thermolytic removal of the polyimide coating.

3.2 Evaluation of the packed columns

The performance of the packed columns in HI-CEC was evaluated through the separation of toluene and four nucleobases: adenine, guanine, thymine and cytosine. The strong hydrophilic interactions of the nucleobases with polar stationary phases are ideal to evaluate the performance, however under very acidic or basic conditions these solutes will become ionized and the observed efficiency will be inevitably influenced by electrofocusing or electrodispersion phenomena. Therefore, the background electrolyte was buffered to a pH of 5.5 to achieve a separation of the neutral bases based only on chromatographic hydrophilic interaction. The analysis in CZE mode under the same conditions, presented in Figure V.4A, resulting in five co-eluting compounds at the EOF time, corroborates the alleged neutrality of these compounds.

A separation of the test mixture on a 25 cm packed bed with 5 µm particles is illustrated in Figure V.4B. The corresponding retention factors were 0.32, 2.1, 2.45, and 2.73 and the RSD %'s for the run-to-run repeatability varied from 0.4 to 1.57% and from 0.87 to 2.4%, for the retention times and the peak areas, respectively. It can be seen that satisfactory retention can be obtained in pure HI-CEC even with relatively large aqueous content in the mobile phase (10%). This illustrates that the applicability range of HI-CEC is probably larger than currently recognized. As the application of smaller particle diameters in CEC is appealing to enhance the efficiency and the performance of the columns, the performance of a 25 cm packed capillary with 3 µm particles was investigated with the same test mixture as is illustrated in Figure V.4C.

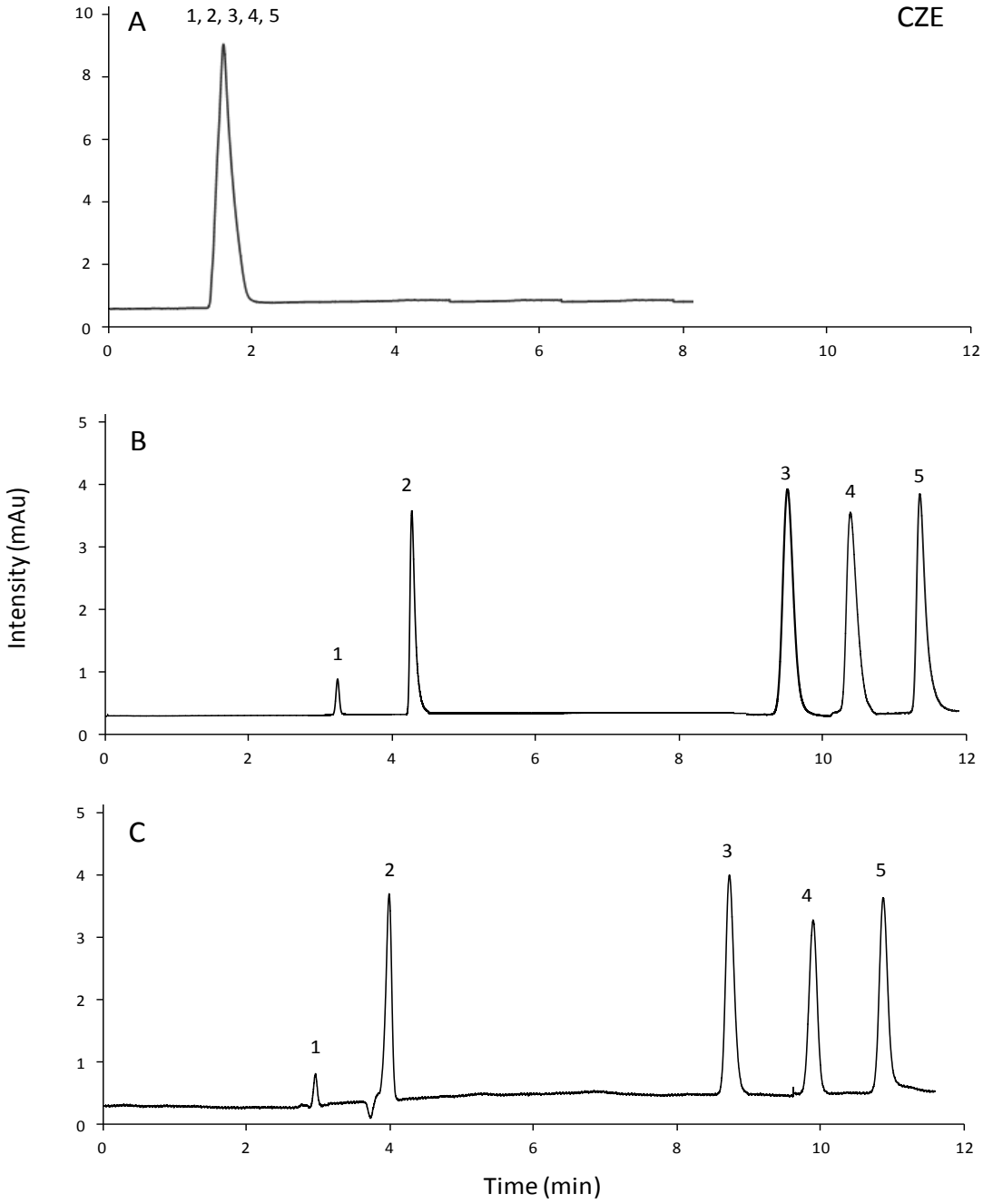

Figure V.4. Electropherogram (A) and electrochromatograms (B-C) of the separation of toluene (1), thymine (2), adenine (3), guanine (4) en cytosine (5) on an empty capillary with an effective length of 25 cm (A) and capillaries (75 µm ID, 25 cm effective length) packed with 5 µm (A) and 3 µm (B) particles. The mobile phase consisted of a 90/10 mixture ACN and ammonium acetate (50 mM, pH 5.5). Injection was done by applying 8 kV for 4 seconds and separation was performed at 30 kV.

A visual comparison between the two chromatograms reveals some discrepancies between the elution times of the solutes. A higher EOF (1.4 mm/s versus 1.15 mm/s) is obtained for the column packed with 3 µm particles. However, the retention of the nucleobases is quite similar on both capillaries. Apparently, the column packed with the 3 µm particles demonstrates slightly lower retention compared to the 5 µm particle packed bed (except for thymine), as illustrated in Table V.2. The difference in EOF velocity and retention can be related to subtle differences in packing density of the columns, but also to inherent differences between the two types of silica in terms of available surface area.

Table V.2. Efficiency and retention of the nucleobases on a 25 cm packed column under the experimental conditions provided in Figure V.4.

Compound	5 µm packed bed		3 µm packed bed	
	N	***k***	***N***	***k***
Toluene	17582	/	20059	/
thymine	16425	0.32	21888	0.35
adenine	15379	2.08	21137	1.95
guanine	17351	2.45	24219	2.38
cytosine	18791	2.73	26972	2.65

The improved column efficiency obtained when using the smaller 3 µm particles can be observed in Figure V.4 and Table V.2. The maximum achievable efficiency of these capillaries in HI-CEC is demonstrated by their corresponding Van Deemter curves, as depicted in Figure V.5A and B. The minimum reachable plate heights for the 5 and 3 µm particle packed capillaries are 9.7 and 6.6 µm, respectively and are both obtained at a mobile-phase velocity of 0.7 mm/s. This corresponds with an efficiency of 25,780 and 37,500 plates, respectively. These plate heights are obtained for cytosine, the most retained solute, while the van Deemter curves of adenine depicts a significantly higher minimum (11 and 9.8 µm). Furthermore, the absolute value of the C-term is almost as high as the value of the B-term. For example, the van Deemter curve of cytosine allows calculation of the A, B, and C terms corresponding to 0.12, 6.4 and 5.7, respectively. As expected a rather low A value is obtained

as the mobile phase in CEC follows a less tortuous path. Note that the peak widths of the nucleobases are decreasing with increasing retentions, indicating that to some extent electromigration could be occurring next to the chromatographic separation. Alternatively, this could also be related to injection phenomena, which are typically affecting the early eluting signal to a longer extend.

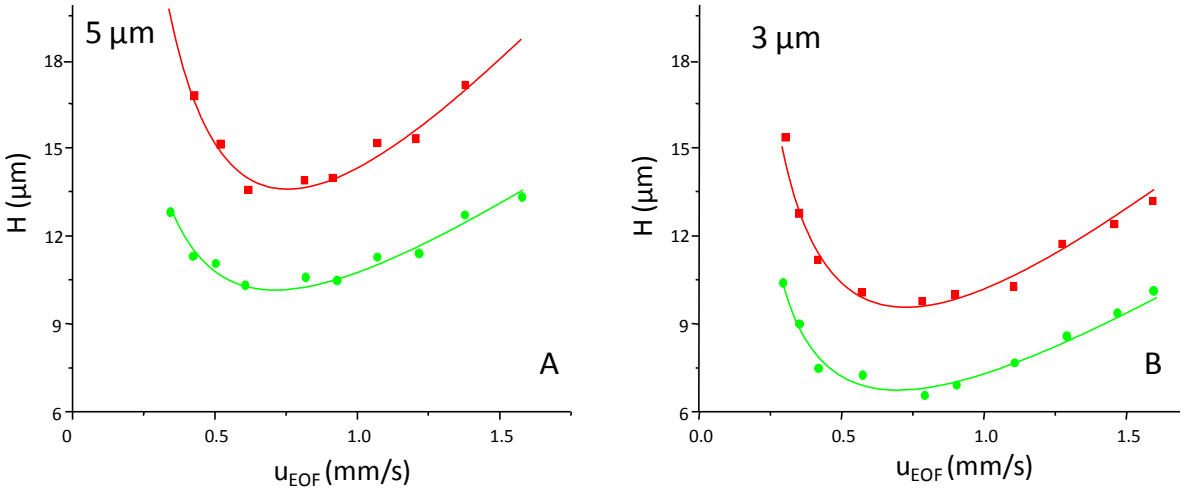

Figure V.5. The H versus u plots for adenine (red squares) and cytosine (green dots) analyzed on a capillary (effective length: 25 cm) packed with 5 µm particles (A) and 3 µm particles (B).

Comparison of the two plate height minima reveals the expected difference in the performance of the two columns. In pressure-driven chromatography, a plate height minimum of twice the particle diameter (*H*= 2*dp) is expected at the optimum flow velocity when using fully porous particles. In CEC lower plate heights are in principle expected according to the conventional rationale. The results observed here and in the work outlined in Chapter IV, dealing with the evaluation of the performance of CEC in the reversed-phase mode with commercial columns, however, increasingly show that the true column performance of packed capillaries, when evaluated with neutral and well retained solutes, is not exceeding what is achievable in HPLC [27]. It is worthwhile stressing that much of the CEC literature is blurring these observations by either presenting results obtained with insufficiently retained or even charged solutes. The reason for the higher than expected plate heights in CEC can be related to a number of issues such as the occurrence of peak broadening injection phenomena, packing density and homogeneity issues and due to the

occurrence of residual Joule heating phenomena. The reduced plate heights of 1.94 and 2.2 for the 5 and 3 µm particle based column, respectively, demonstrate that a somewhat more efficient packing is obtained when 5 µm particles are applied. This is most probably to the more challenging packing of smaller particles as the composition of the packing solvent also needed to be altered to 90% acetone and 10% water to obtain a packed bed of 3 µm particles with sufficient length. This as the length of the capillaries is limited by the generated back pressure during the packing process. The change in composition results in a higher packing speed in the first section of the packed bed (and hence to a less homogeneous bed), while the packing speed lowers quickly as the bed grows. Nevertheless, the capillaries packed with the 3 µm particles are more efficient compared to the 5 µm particles and are therefore more interesting in terms of applications. The higher performance is also illustrated in Figure V.6, where the corresponding kinetic plots are depicted for both capillaries [27]. These curves show that 3 µm particles always surpass the 5 µm particles in terms of maximum achievable plates and in speed of analysis to achieve a certain efficiency.

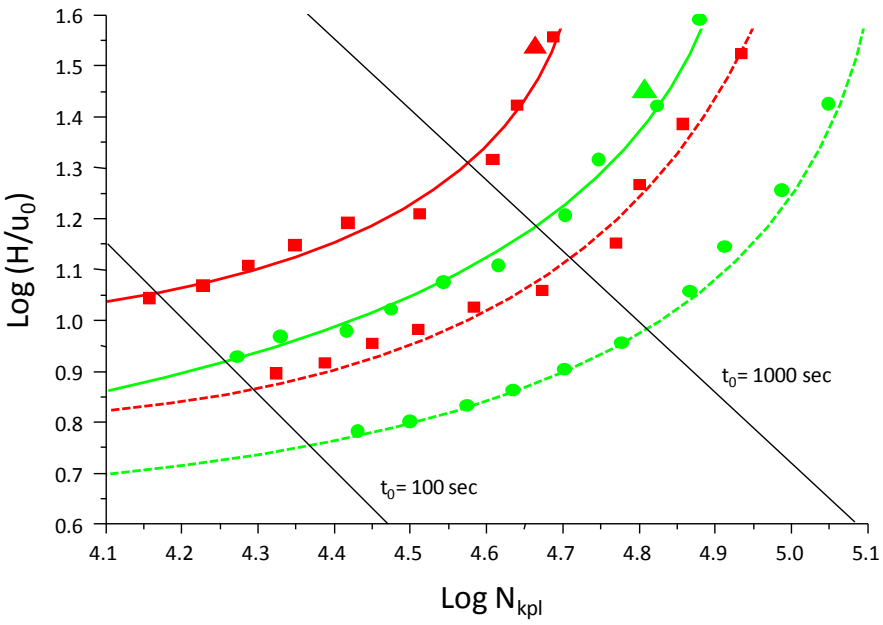

Figure V.6. The kinetic plots obtained for adenine (red squares) and cytosine (green dots) on capillaries packed with 5 µm (full line) and 3 µm particles (dotted line), respectively. The experimental values measured on a 75 cm packed column (5 µm particles) are marked by a red (adenine) and green (cytosine) triangle.

These kinetic plots demonstrate, for example, that a maximum efficiency of 110,000 plates can be reached for cytosine after an analysis of 2.5 hours (on a 1 meter column). The same analysis on a capillary packed with 5 µm particles would only reach an efficiency of 87,000 plates. On the other hand, an efficiency of 10,000 plates can be reached after 3 and 4.2 minutes for a capillary packed with 3 µm and 5 µm particles, respectively. Although, the kinetic plot is merely a simulation, the potential thereof was demonstrated by performing the same analysis on a 75 cm packed bed capillary (containing 5 µm particles). The resulting values are plotted in the kinetic plots and demonstrate that the measured values are close to the expected value and therefore corroborate the utility of the kinetic plots as a measurement of performance. More specifically, efficiencies of 47,100 and 64,700 plates were obtained for adenine and cytosine while theoretical efficiencies of 49,200 and 66,900 plates were expected, respectively.

Note that the use of smaller particles in liquid chromatography enables faster separations (for a given efficiency) but that the maximum achievable efficiency is thereby lower compared to larger particles as the maximum length of columns is then restricted by the backpressure. This effect has been described in Chapter I and is illustrated in Figure I.3, and reveals once more that the independence of the generated flow and the particle diameter in CEC is beneficial.

In CEC, the column is certainly the heart of the chromatographic system as it is responsible for the separation and the generation of the mobile-phase flow (EOF). However, also and especially in CEC the characteristics of the mobile phase influence the EOF velocity. The variation of the EOF versus the acetonitrile content is for example illustrated in Figure V.7A. The EOF mobility was thereby determined from the elution time of toluene, which is not retained in the HI-CEC mode. In these experiments, the total ionic strength in the mobile phase was kept constant (10 mM ammonium acetate), as was the pH, while the acetonitrile content was varied from 20 to 95%. An increase in EOF velocity (varying from 1.1 to 1.8 mm/s) of 60% was thereby observed corresponding with an increase in acetonitrile content from 20 to 95%. Similar results were observed in RP-CEC and in monolithic HI-CEC [8,28,29]. Note that the increase in velocity is linear, which has not always been the case in previous reports as this depends on the applied experimental conditions (ionic strength and pH should remain the same).

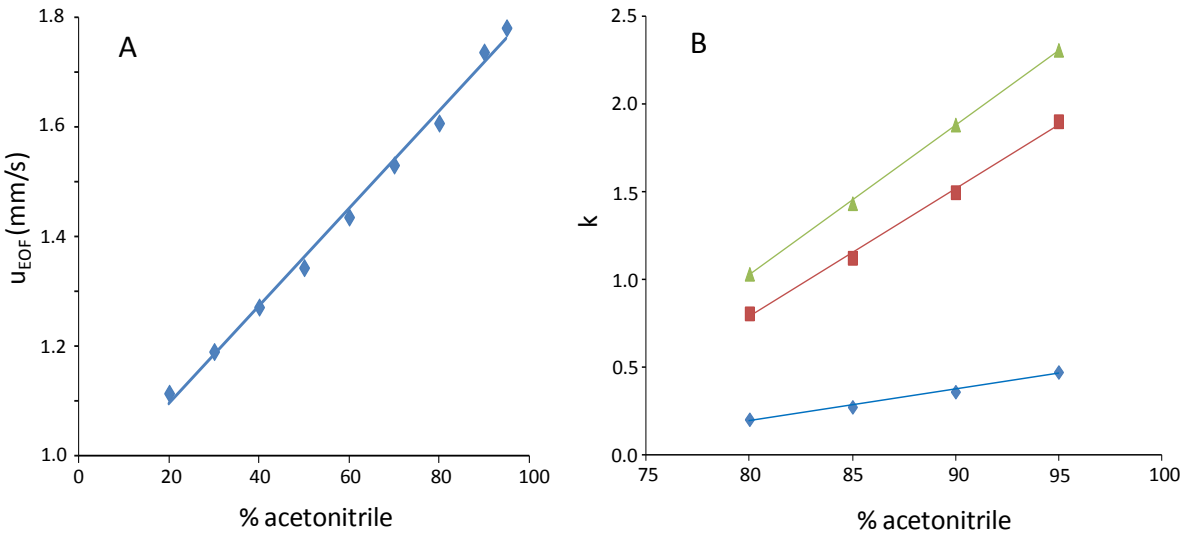

Figure V.7. Effect of the organic modifier content on the EOF velocity (A) and on the retention factor (B) of adenine (red), cytosine (green) and thymine (blue). All other analysis conditions are the same as specified in Figure V.4.

The previous reports on native silica based packed column CEC with organic buffers demonstrated that the retention mechanism was a complex mixture of ion-exchange chromatography, hydrophilic interaction chromatography, electromigration and even some reversed-phase chromatography [7,8]. However, these reports were focused on the separation of basic drugs and therefore their test mixture was not representative for the true performance of HI-CEC with native silica. In order to investigate the retention behavior of the neutral solutes, the acetonitrile-buffer ratio was therefore also varied while maintaining a constant pH and ionic strength. The effect of the organic modifier content in the buffer on the retention of the nucleotide bases is depicted in Figure V.7B.

In contrast to reversed-phase CEC, an increase in acetonitrile content results in a linear increase in retention, confirming the hydrophilic interaction based retention mechanism. For example, the retention factor of cytosine decreases from 2.3 to 1 when the strong eluting solvent content (the aqueous buffer) in the mobile phase was increased from 5 to 20%. At lower percentages of acetonitrile (and hence at higher levels of the strong eluting solvent) overlap and co-elution of the solutes occurred. The results show that the resolution and the retention factor is increasing with a decreasing amount of aqueous buffer in the mobile

phase and therefore it can be concluded that the separation mechanism is based only on the hydrophilic interaction retention mechanisms. The achievable increase in resolution with decreasing levels of aqueous buffers is also demonstrated in Figure V.8, where Triton X-100 is analyzed in the isocratic mode with a mobile phase containing different percentages of aqueous buffer.

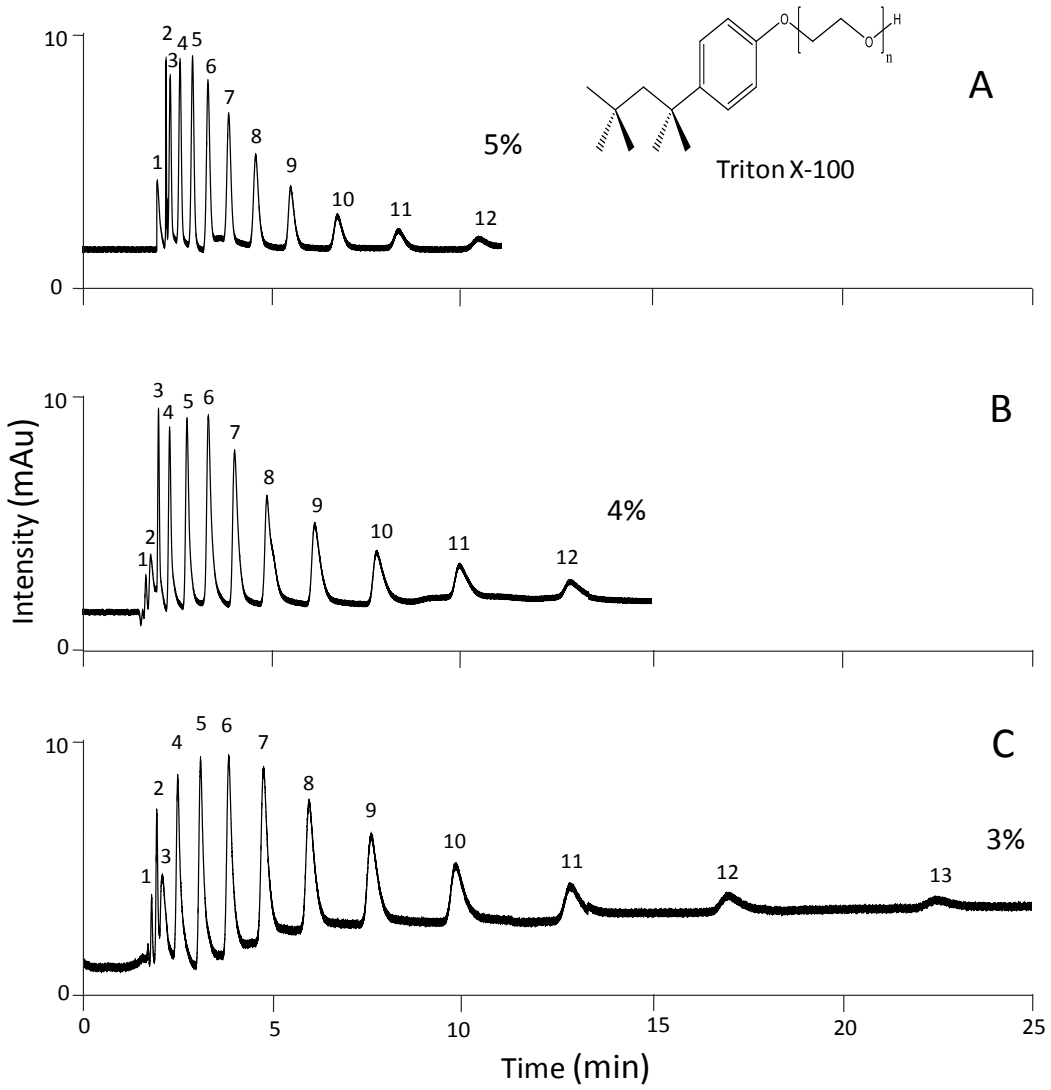

Figure V.8. The separation of Triton-X 100 on a 25 cm particle packed bed with a mobile phase consisting of acetonitrile and 5% (A), 4% (B) and 3% (C) of 100 mM ammonium acetate (pH 5.5) added. Injection was done electrokinetically by applying 5 kV during 8 seconds and the separations were performed at 30 kV.

Triton X-100 is a nonionic detergent composed of hydrophobic 4-phenyl groups coupled to polyethylene oxide functions. The retention in the HI-CEC mode is a consequence of the

interaction between ethylene oxide group and the polar stationary phase. The solute becomes more polar with longer polyethylene oxide groups, explaining why the short chain polymers elute first compared to the larger structures. It can be seen that the retention increases significantly at lower levels of aqueous buffer. This improves to some extent the separation of the less retained solutes. At 10% aqueous buffer all solutes were co-eluting (data not shown).

Figure V.9 also depicts the high retention which can be obtained for polar compounds in packed column HI-CEC. A mixture of toluene and three nitro-derivates is thereby separated. This type of nitroaromatic compounds is interesting to separate in the HI-CEC mode as these molecules are both neutral and polar and therefore allow to investigate the retention behavior and peak broadening only caused by chromatographic processes. Furthermore, the development of a separation method for nitro-derivates and their isomers is appealing as a possible orthogonal methodology to existing HPLC methods for the analysis of explosive residues.

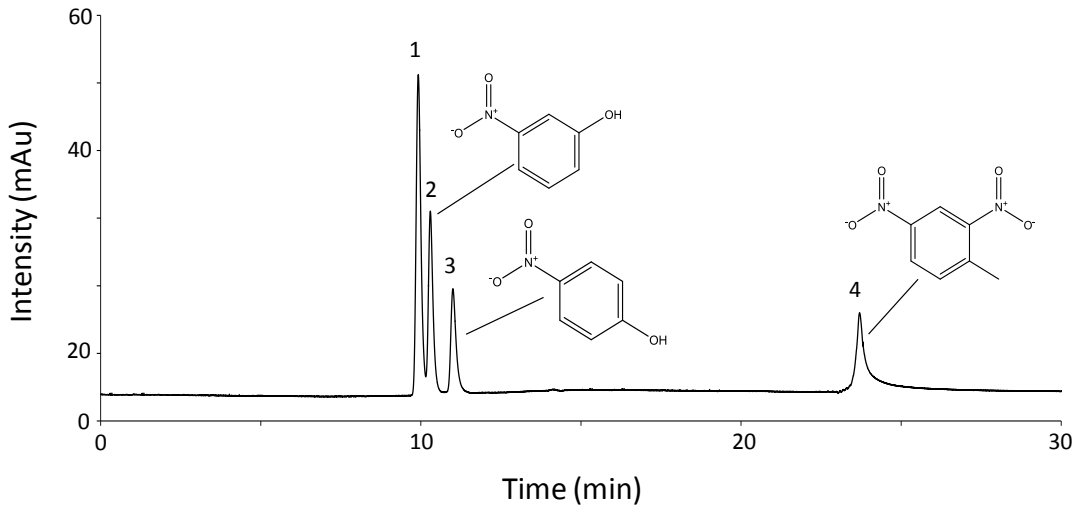

Figure V.9. Separation of toluene (1), 3-nitro-phenol (2), 4-nitro-phenol (3), 2,4 dinitro-toluene on a 25 cm packed bed (5 µm particles) with a mobile phase consisting of 5% 100 mM ammonium acetate (pH 5.5) added to acetonitrile. Injection: 8 kV for 4 seconds. Separation was performed at 30 kV.

As the polar nitro-group of the solute interacts strongly with the stationary phase, this explains the higher retention factor (*k*=2.4) measured for the dinitro-derivate compared to

the mono nitro-substituted derivates (*k*=0.07 and 0.2). This separation demonstrates once again that the separation mechanism is solely based on hydrophilic interaction of the solutes with the stationary phase. The strength of the HI-CEC separation mechanism is demonstrated by the successful baseline separation of the two isomers. Note the occurrence of significant band broadening for the most retained solute. Apparently, dinitro-component interacts in a stronger manner with the stationary phases, resulting in a lower efficiency. This illustrates that the efficiency of more retained components in HI-CEC should be further investigated.

Finally, the importance and possible relevance of HI-CEC was demonstrated by the analysis of a number of representative genotoxic impurities encountered in pharmaceutical drug synthesis. Genotoxic impurities can be introduced into pharmaceutical formulations during the synthesis of an active pharmaceutical ingredient (API), either as a starting material or as a by-product, or they can be formed by degradation of the API or of other components of the formulation. These impurities can damage genetic information in the cells and therefore cause mutations. Consequently, the control, detection and analysis of these impurities in drugs is important in the pharmaceutical industry [30]. The potential of HI-CEC with native silica is illustrated by Figure V.10, which depicts the analysis of a mixture of pharmaceuticals and some typical genotoxic alerting solutes.

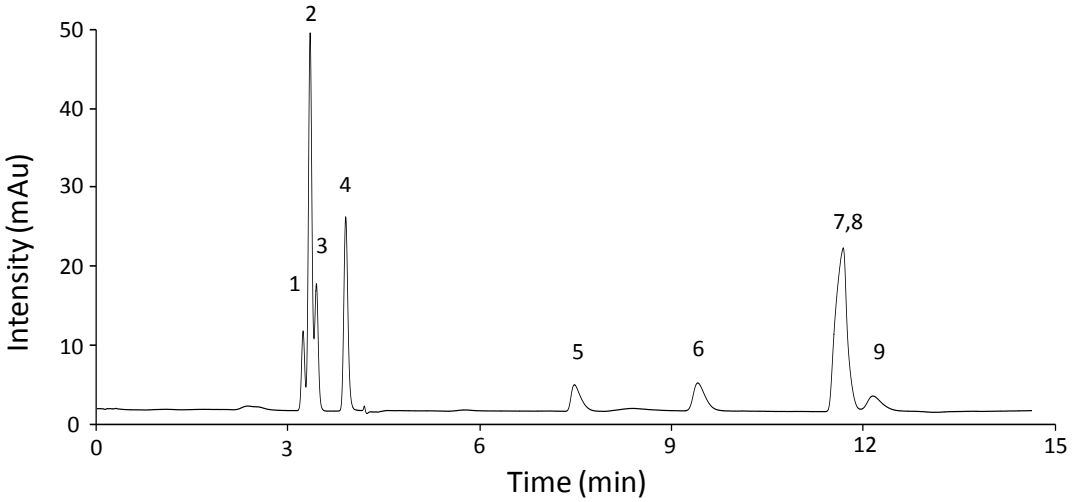

Figure V.10. The analysis of toluene (1), naphtylamine (2), aniline (3), 5-aminoindol (4), 2-amino-pyridine (5), 3-amino-pyridine (6), nortryptiline (7), 5-amino-2-methylpyridine (8),dipenhydramine (9). Mobile-phase composition 50 mM ammonium acetate pH 5.5 with 97.5% ACN. The separation was performed on a 75 µm ID capillary with a 25 cm packed bed (5 µm particles) and with an applied voltage of 30 kV.

Toluene and 7 solutes could be successfully separated in a time span of 12.5 minutes. The poorly retained solutes (1-4) exhibit a satisfactory gaussian peak shape, but were not baseline separated. On the other hand, band broadening effects and some degree of peak tailing can be observed for the more retained components (5-9). Note, however, that solutes 5,6 and 8 are ionized at a pH of 5.5 and therefore injection phenomena related to electrodispersion can introduce band broadening effects, as explained in Chapter II. The limited efficiency of the more retained solutes can be explained by the research completed in Chapter IV, which indicates that Joule heating still occurs in capillaries with 75 µm ID. Therefore, better control of Joule heating and analyses at lower temperature could be beneficial for the column performance. However, this would, inevitably, influence the retention mechanism. The implementation of a gradient run where the water content increases as a function of time would allow an expedited analysis and would decrease the peak width artificially. However, the application of a mobile-phase gradient run is still not possible with the current state-of-the-art CEC instrumentation.

Note also that the retention of the ionized solutes is a result of hydrophilic interaction with the stationary phase and of electrophoresis. All solutes could be separated to some extent, except solute 7 and 8 which were co-eluting under these isocratic conditions. Compared to HPLC literature, the retention factors and elution order of the solutes are changed [31]. For

example, in the HILIC experiment 2-aminopyridine and 3-aminopyridine are co-eluting with a retention factor of 0.66, while in the HI-CEC experiment these solutes are separated with retention factors of 1.27 and 1.87, respectively as shown in Table V.3.

Table V.3. Comparison of the retention of polar pharmaceutical solutes in HILIC and HI-CEC separations

	Compound	*k* HILIC [31]	*k* HI-CEC
1	toluene	0	0
2	naphtylamine	0.07	0.07
3	aniline	0.14	0.13
4	5-aminoindol	0.21	0.25
5	2-aminopyridine	0.66	1.27
6	3-aminopyridine	0.66	1.87
7	nortryptiline	2.41	2.70
8	5-amino-2-methyl-pyridine	1.48	2.70
9	dipenhydramine	2.69	2.82

Furthermore, the retention of 5-amino-2-methyl-pyridine in HI-CEC is remarkably higher with a retention factor 2.70 (compared to 1.48 in HILIC). The different behavior of these pyridine-derivates can be explained by their basic nature. At a pH of 5.5, such a solute will be positively ionized and therefore electrophoresis should expedite its elution time. However, the ionized pyridine derivates are also more polar, resulting in an increased hydrophilic interaction with the stationary phase. Furthermore, the occurrence of an ion-exchange mechanism between the negatively ionized silanol groups and the pyridine groups can also influence the retention behavior.

4 Conclusions

This chapter describes the packing of capillaries with bare silica particles with various diameters and the evaluation of these packed capillaries with a neutral test mixture. It revealed that the packing efficiency of slurry packed capillaries decreases with the particle diameter. The performance of the capillaries was evaluated by developing the corresponding kinetic plots, demonstrating that smaller particle diameters are still preferable, despite of the lower packing efficiency. Furthermore, the influence of the organic modifier content on the retention of the solutes and on the EOF velocity was investigated. It was shown that the retention of neutral polar solutes is caused by only hydrophilic interaction of the solutes with the stationary phase. The promising efficiency and potential of the optimized and characterized capillaries was finally demonstrated by the analyses of a mixture of nitro-derivates and of a mixture of genotoxic impurities.

5 References

[1] C.H. Xie, H.J. Fu, J.W. Hu, H.F. Zou, Electrophoresis 25 (2004) 4095.

[2] X.L. Dong, R.A. Wu, J. Dong, M.H. Wu, Y. Zhu, H.F. Zou, Electrophoresis 30 (2009) 141.

[3] H.J. Fu, W.H. Jin, H. Xiao, H.W. Huang, H.F. Zou, Electrophoresis 24 (2003) 2084.

[4] D.N. Gunasena, Z. El Rassi, Electrophoresis 33 (2012) 251.

[5] A. Maruska, U. Pyell, J. Chromatogr. A 782 (1997) 167.

[6] A. Maruska, U. Pyell, Chromatographia 45 (1997) 229.

[7] A.P. McKeown, M.R. Euerby, H. Lomax, J. Sep. Sci. 25 (2002) 1257.

[8] W. Wei, G.A. Luo, G.Y. Hua, C. Yan, J. Chromatogr. A 817 (1998) 65.

[9] M.L. Ye, H.F. Zou, L. Kong, Z.D. Lei, R.N. Wu, J.Y. Ni, Lc Gc N. Am. 19 (2001) 1076.

[10] J.C. Valette, C. Demesmay, J.L. Rocca, E. Verdon, Chromatographia 62 (2005) 393.

[11] X. Wang, N. Zheng, Y. Huang, J. Wang, X. Lin, Z. Xie, Electrophoresis 34 (2013) 3091.

[12] X. Wang, Y. Zheng, C. Zhang, Y. Yang, X. Lin, G. Huang, Z. Xie, J. Chromatogr. A 1239 (2012) 56.

[13] X. Lin, X. Wang, T. Zhao, Y. Zheng, S. Liu, Z. Xie, J. Chromatogr. A 1260 (2012) 174.

[14] J. Hu, L. Yin, L. Jia, J. Sep. Sci. 34 (2011) 565.

[15] G. Huang, Q. Lian, W. Zeng, Z. Xie, Electrophoresis 29 (2008) 3896.

[16] K. Horie, T. Ikegami, K. Hosoya, N. Saad, O. Fiehn, N. Tanaka, J. Chromatogr. A 1164 (2007) 198.

[17] F. Ye, Z. Xie, K.-Y. Wong, Electrophoresis 27 (2006) 3373.

[18] V. Guryca, Y. Mechref, A.K. Palm, J. Michalek, V. Pacakova, M.V. Novotny, J. Biochem. Bioph. Methods 70 (2007) 3.

[19] M. Jonnada, R. Rathnasekara, Z. El Rassi, Electrophoresis 36 (2015) 76.

[20] D.N. Gunasena, Z. El Rassi, J. Chromatogr. A 1317 (2013) 77.

[21] J. Lin, S. Liu, J. Lin, X. Lin, Z. Xie, J. Chromatogr. A 1218 (2011) 4671.

[22] X. Wang, X. Lin, Z. Xie, J.P. Giesy, J. Chromatogr. A 1216 (2009) 4611.

[23] X. Wang, H. Lue, X. Lin, Z. Xie, J. Chromatogr. A 1190 (2008) 365.

[24] A.M. Siouffi, J. Chromatogr. A 1000 (2003) 801.

[25] M. Motokawa, H. Kobayashi, N. Ishizuka, H. Minakuchi, K. Nakanishi, H. Jinnai, K. Hosoya, T. Ikegami, N. Tanaka, J. Chromatogr. A 961 (2002) 53.

[26] F. Lynen, A. Buica, A. de Villiers, A. Crouch, P. Sandra, J. Sep. Sci. 28 (2005) 1539.

[27] S. De Smet, F. Lynen, J. Chromatogr. A 1355 (2014) 261.

[28] G. Choudhary, C. Horvath, J. Chromatogr. A 781 (1997) 161.

[29] M.M. Dittmann, G.P. Rozing, J. Chromatogr. A 744 (1996) 63.

[30] D. Bartos, S. Gorog, Curr. Pharm. Anal. 4 (2008) 215.

[31] S. Louw, F. Lynen, M. Hanna-Brown, P. Sandra, J. Chromatogr. A 1217 (2010) 514.

Chapter 6

Poly(styrene-divinylbenzene-vinylsulfonic acid) as retentive and electroosmotic flow generating phase in open-tubular CEC

In this work, a new sulfonated polystyrene based porous layer was synthesized on the wall of a capillary by a single step in situ polymerization process. To obtain a capillary suited for electrochromatography, vinylsulfonic acid (VSA) was, next to divinylbenzene (DVB), copolymerized to induce charges for the electroosmotic flow (EOF) generation. The VSA ratio in the monomer mixture and the polymerization time were optimized while the chromatographic characteristics of the obtained open tubular columns were investigated in electrochromatography. To allow unambiguous study of only chromatographic processes, evaluations were performed with a mixture of sufficiently retained and electrophoretically neutral parabens. Comparison of SEM pictures and chromatograms revealed that the polymerization time had a great influence on the polymer layer morphology and on the chromatographic performance. An increase in the VSA ratio, led to an increase in the mobile-phase velocity but simultaneously lowered paraben retention. Minimal plate heights of 10 µm, equivalent to the capillary internal diameter, were obtained. The open-tubular character of this optimized porous layer column allowed successful analyses at elevated temperature, resulting in a maximum efficiency of 85,500 plates for a 75 cm capillary and linear velocities up to 1.4 mm/s. Finally, a thermal gradient was successfully applied, leading to artificial sharpened peaks with a peak capacity of 55 in a 20 minutes time span.

Published as De Smet S, Lynen F, Investigation of poly(styrene-divinylbenzene-vinylsulfonic acid) as retentive and electroosmotic flow generating phase in open-tubular electrochromatography, Journal of Chromatography A, 1404 (2015), 81-88.

1 Introduction

As described previously, a great variety of column types have already been applied in CEC, which can mainly be divided in three formats. Whereas the vast majority of research has been done on the packed bed format, followed closely by the monolithic type, comparatively little research has been performed on the open-tubular format.

The achievable high efficiency in CEC has extensively been demonstrated for packed capillaries [1-4]. However, packed-column CEC is hindered by some significant practical problems such as the fabrication of the frits and by the difficulty to pack micrometer sized particles in the narrow-bore capillaries in a homogeneous way. Moreover, the classical packing materials consist of silica particles which are functionalized. Therefore, it can often be difficult to separate basic compounds due to the presence of silanol groups, needed to generate an adequate EOF.

An alternative to the classical silica particles can be the use of organic polymeric stationary phases. These stationary phases have been extensively investigated in monolithic capillaries. These are prepared by the in-situ polymerization of organic precursors in the presence of a porogen and are covalently linked to the silanized wall. There is no need for retaining frits, narrow columns (20-100 µm) can be prepared and no gaseous bubbles will be formed during analysis (hence there is no need for pressurization during analysis) [5-9].

The organic porous monoliths in CEC are typically based on acrylamide, methacrylate and styrene polymers, whereas research has mostly been focused on methacrylate based monoliths [7,10,11]. However, polystyrene monoliths have been successfully applied for highly efficient separations of biomolecules in HPLC. These monoliths are chemically stable under a wide pH range and the morphology can be adjusted by the copolymerization of other monomers and the selection of the proper porogenic solvent [12-14]. Despite their use in HPLC, the research on the use of polystyrene monoliths (and stationary phases in general) in CEC is still fairly limited. Horvath et al. investigated the potential of bimodal CEC monoliths for the analyses of peptides and proteins [15]. Jin et al. and Xiong et al. applied a one-step polymerization with methacrylic acid as EOF generating comonomer to obtain a negatively-charged polystyrene monolith [16,17]. They obtained efficient separations on a 20 cm column of aromatic compounds and biomolecules with respectively 28,000 and 18,000 plates. However, the efficiency of highly retained small and uncharged organic compounds (*k*

> 1.5) was not investigated. Furthermore, methacrylic acid only allows for an adequate EOF at pH 7 or higher. To achieve generation of EOF at lower pH's Huang et al. changed the charge bearing monomer to the strong acids vinyl sulfonic acid (VSA) and vinyl benzene sulfonic acid (VBSA). Separation of parabens and acidic compounds at a wide pH range (3-8) were obtained and after optimizing the polymerization conditions, a maximum efficiency of 8,800 (VSA) and 16,400 plates (VBSA) for 20 cm columns (effective length) was observed [18,19]. The porosity of the monoliths can be controlled by changing the porogen or the composition of the monomer mixture. Various approaches have been described to characterize the monolith porosity [20].

However, as described in Chapter IV and V, monolithic capillaries are often less efficient compared to packed particle columns and the column to column reproducibility is often poor. The lower encountered efficiencies can be associated with wall effects caused by the shrinkage of the polymer network during the curing step of the monolith. On the other hand, it has been demonstrated that open-tubular chromatography can be a viable and possible alternative for the packed and monolithic format. Unlike the packed and monolithic column types, the performance of open- tubular capillaries is directly linked to the internal diameter of the capillary. Small internal diameters are required to facilitate efficient solute diffusion into the stationary phase [21]. More narrow capillaries provide higher efficiency and a higher concentration of an on-column loaded sample [22]. Last but not least, the Joule heating in open-tubular columns will be non-existent or limited due to the small internal diameters involved (5-20 µm). The latter might allow the effective use of temperature gradients in CEC and could solve the two-decade long problem of gradient analysis in CEC without major modification of the commercial instrumentation. However, the loading capacity and retention of many OT-LC (and CEC) capillaries is limited due to the high phase ratio ($\beta = V_m/V_s$, whereby V_m and V_s correspond to the volume of mobile and stationary phase, respectively). A porous layer of polymer, attached to wall, will increase the surface area and therefore enhance the loadability of the stationary phase. The group of Karger developed a strategy to form a porous open-tubular crosslinked polystyrene layer, attached to the wall [23,24]. The layer was prepared by filling a pretreated capillary (to functionalize the wall) with a mixture of the monomers and ethanol as solvent. The polymerization will thereby

preferentially take place at the non-polar wall instead of in the polar solvent, resulting in the formation of a porous polymer layer at the capillary wall with a vacant center. The proportion of monomer mixture and solvent was critical to achieve a layer at the wall instead of a monolith. The high performance of these capillaries in HPLC was attested by several proteomic analyses resulting in peak capacities of 400 and whole protein analyses . Subsequently, the same group produced an open-tubular HILIC mode capillary by the polymerization of divinylbenzene and vinylbenzylchloride, followed by modification of the polymer wall with ethylenediamine as functional group [26].

Regardless of reported highly efficient analyses of biomolecules obtained by open-tubular polystyrene capillaries in nano-LC, there are very few reports on the use of open-tubular polystyrene based capillaries in CEC (to the best of our knowledge). Huang et al. applied a styrenic stationary phase in 20 µm ID capillaries, modified with quaternary ammonium groups as charge bearing moieties and dodecyl chains as retention sites [27]. Separation of four proteins with a counter-directional electro-osmotic flow (due to the presence of the basic ammonium groups) was obtained in this way. However, the potential of polystyrene based stationary phases is often described through the separations of large biomolecules, while a lower performance is obtained for the separation of small organic molecules. Therefore, an intriguing challenge presents itself in the manufacturing of open-tubular highly performant styrenic capillaries with an acidic EOF generating moiety incorporated. The emphasis in this chapter was set on the preparation of such an open-tubular capillary by a single step polymerization. VSA was added as pH independent EOF generating component to a monomer mixture of styrene and divinylbenzene. To the best of the authors' knowledge, it is the first time that VSA was used as comonomer in a styrene-based open-tubular CEC column. Therefore the fundamental performance of this type of column is evaluated in detail only with small, retained, organic and neutral molecules. This at it allows disconnection of the chromatographic performance from electrophoretic phenomena in an unambiguous way. The influence of changes in the polymerization time, monomer composition and effect of elevated analysis temperatures are evaluated to optimize the synthesis and analytical conditions.

2. Experimental

2.1 Reagents and materials

Fused-silica capillaries (10 µm ID) were purchased from CMscientific (Silsden, United Kingdom). Milli-Q water was prepared in house by purification and deionization of tap water in a Milli-Q plus water instrument from Millipore (Bedford, New Hampshire, USA). Acetic acid, acetonitrile, toluene, dichloromethane, ethanol (EtOH) and ammonium acetate of HPLC quality originated from Biosolve (Valkenswaard, Netherlands). Styrene, divinylbenzene, vinylsulfonic acid, trimethoxy silyl propyl methacrylate, azobisisobutyronitrile (AIBN) and all test compounds were obtained from Sigma-Aldrich (Bornem, Belgium). Stock solutions of all compounds were prepared at 10.000 µg/mL in water or ACN, dependent on their solubility, and diluted to 125 µg/mL (in the same solvent composition as the mobile phase) prior to analysis.

2.2 Preparation of PLOT Column

The capillaries were prepared as described by Yue et al. with the adaptation that vinyl sulfonic acid is added to the polymerization mixture [23]. Fused-silica capillaries with 10 µm I.D. and a length of 1.5 meter were rinsed for 3 hours with 1 M NaOH at 25 bar, washed with water and MeOH and finally dried under N_2 for 1 h to remove residual water and methanol. The 10 µm ID pretreated capillary was filled with a freshly prepared solution of 15% 3-(trimethoxysilyl) propyl methacrylate (v/v) in toluene. The capillary was sealed at both ends and placed in the oven at 120°C for 10 hours. Subsequently the capillary was washed with acetonitrile and dried with nitrogen at 25 bar. Inhibitors present in styrene and divinylbenzene were removed by flushing the liquids through a basic alumina column. The monomer mixture, containing styrene, divinylbenzene and vinyl sulfonic acid, was dissolved in ethanol (40/60 v/v). AIBN (25 mg) was added as initiator to 10 ml of the polymerization mixture. The solution was degassed by ultrasonication for 15 minutes and subsequently introduced in the capillary. Both ends were sealed and the capillary was placed in the oven at 75°C during 15 -120 minutes. The column was rinsed with acetonitrile during 30 minutes to elute un-bounded polymer and subsequently conditioned with the mobile phase at 25 bar during 1 h. A 25 cm part was cut from both capillary ends resulting in a capillary with a total

length of 1 meter. Prior to analysis, the open-tubular poly (styrene-divinylbenzene-vinylsulfonic acid) (PSDVB-VSA) capillaries were cut at desired lengths (33.5 -82.5 cm).

2.3 Chromatographic conditions for CEC

The 7100 CE system (Agilent Technologies, Waldbronn, Germany) used in this work includes an air-cooled thermostat, autosampler, diode array detector and a built-in system to pressurize vials. The mobile phase was filtered with syringe filters (Grace, 0.45 µm PVDF filters). Injections were performed electrokinetically or hydrodynamically. An alignment interface for standard capillaries of 25 µm ID was used. A stock solution of ammonium acetate was prepared by adding acetic acid until a solution with the desired pH was obtained. The mobile phase was prepared by adding the required volume of the stock solution to ACN. Consequently, the mobile phase was degassed in an ultrasonic bath for 10 minutes prior to analysis. Analysis temperatures were always maintained isothermal at 25°C, 40°C or 60°C, respectively. Furthermore, a temperature gradient was applied by increasing the set air temperature. The gradient was kept isothermal for 1 minute at 25°C, subsequently the temperature was raised to 60°C with a 2°C/minute rate, and kept at this temperature during 12.5 minutes. Detection was performed at 214 and 254 nm and all obtained data was processed with the Chemstation B.04.03 software. New columns were conditioned by increasing the voltage in a stepwise way to 30 kV in a 120 minute time span. If not specified otherwise, all shown analyses were obtained at 25°C with a mobile phase consisting of 25 mM ammonium acetate mixed with acetonitrile to a 70/30 ratio and run at an operating voltage of 30 kV. The effective capillary length was 25 cm with a total length of 33.5 cm.

3. Results and Discussion

Ideally, open-tubular columns applied in liquid chromatography should have an internal diameter of 1-2 µm to obtain comparative and even higher efficiencies as in gas chromatography [21]. However, this work was still performed on 10 µm capillaries due to practical considerations (on-column detection, easy clogging during film preparation). The preparation of the polymeric film was reminiscent of PLOT column based work by the group of Karger with some important adaptations [23]. To obtain sufficient EOF in CEC, an ionizable moiety should be present in the stationary phase. Therefore, a charge bearing monomer

should be copolymerized in the polystyrene-divinylbenzene polymer. As the altered polymerization conditions of this novel approach inevitably influence the morphology and the physical characteristics of the porous polymer layer, these aspects needed to be investigated and optimized. The initial polymerization mixture consisted of a monomer mixture of styrene, divinylbenzene and vinyl sulfonic acid (S/DVB/VSA 1/1/1 v/v) dissolved in ethanol (40/60 v/v). As the initially employed long polymerization times of 16 hours and more resulted in clogged capillaries, this was reduced by more than one order of magnitude to allow the generation of open-tubular capillaries. The polymerization process of the porous layer on the inner lining of the capillary was assessed by scanning electron microscopy (Figure VI.1A-C) and the corresponding electrochromatographic performance was investigated by the separation of thiourea (as EOF marker) and four parabens, as depicted in Figure VI.2. The choice of parabens as representative test mixture relies on their electrophoretic neutrality at all applied pH's (3-8) to allow unambiguous occurrence of only chromatographic processes (and not electrophoresis) in all experiments. The small solutes were also selected (and not bio-macromolecules) as they partition between the two phases and are thereby effectively absorbed in the polymeric matrix. The latter allows more fundamental chromatographic insight but also leads to peak broadening due to the slower mass transfer and suboptimal performance at room temperature, as was observed in packed column HPLC before [28].

During polymerization the polymer forms spherical shapes, covering the entire wall. The hydrophilic solvent (EtOH) in the center of the capillary tube forces the polymerization to start at the hydrophobically derivatized wall, as the polystyrene polymer is also hydrophobic from nature. As polymerization starts at several points in the capillary next to each other, this results after a time in the formation of a thin porous layer of polymer. Note that this process is analogous to the OTLC column manufactured by Karger et al. with the exception that the VSA was thereby absent [23].

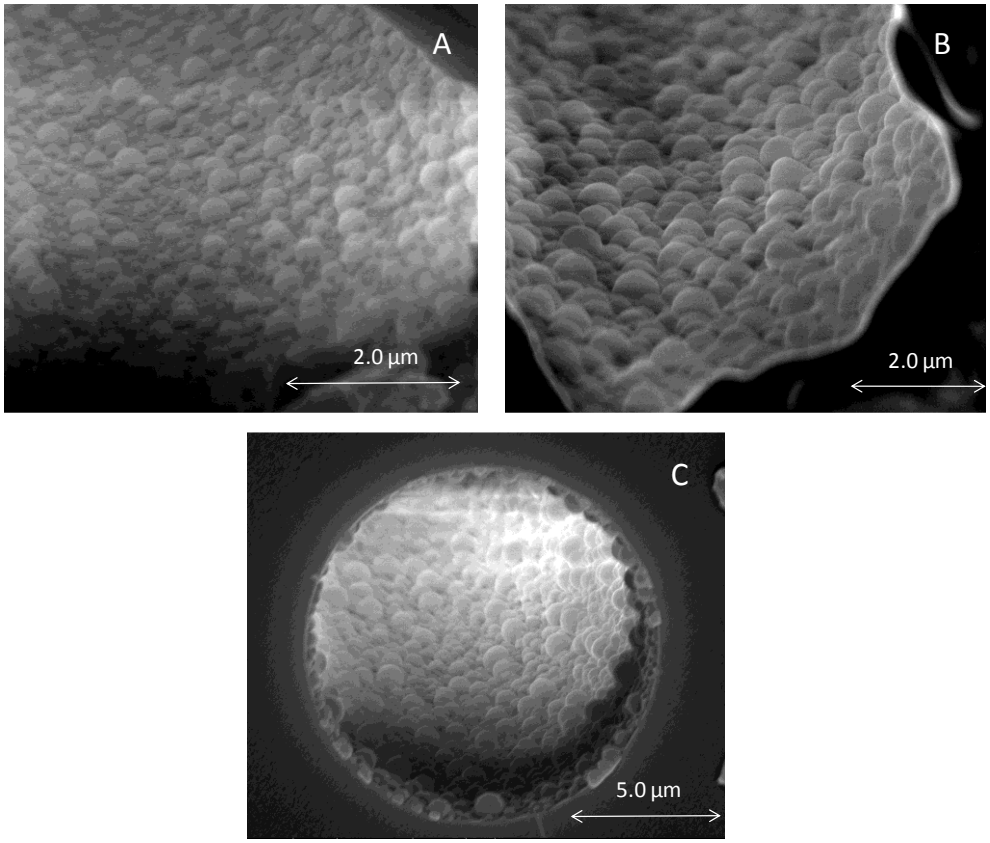

Figure VI.1. SEM micrographs of polystyrene based open-tubular layers in 10 µm capillaries after a polymerization time of 15 (Figure 1A), 30 (Figure 1B) and 60 (Figure 1C) minutes.

However, after 15 minutes (Figure VI.1A), the growth of the spherical polymer globes is not yet sufficient to cover the entire wall with a relatively uniform layer. In this early stage, the polymer particulates have radii ranging from 40 to 250 nm. The absence of uniformity and the broad size distribution are also reflected in the analysis of thiourea and the parabens on the resulting column (Figure VI.2A). Although the compounds are distinctively separated, the peak shape is poor and the efficiency is neglectable due to the extensive tailing of the retained components. This can be explained by the discontinuous stationary phase and the broad size distribution of the spherical shapes on the wall. After 30 minutes, the globular polymer nodules increase in thickness and are linked together, covering the entire wall, as illustrated in Figure VI.1B. The polymer particulates have now grown to a thickness between 400 and 600 nm. Each nodule is surrounded and bordered by other polymer globes and hence, a wall covering layer of porous polymer is formed. The higher uniformity of the stationary phase layer is reflected in the chromatograms in Figure VI.2B. Improved peak shapes and increased retention are thereby observed. For example, the retention factor of

butylparaben of the 15 minutes and the 30 minutes polymerized capillary increased from 1.23 to 1.78, respectively. However, more retained compounds ($k \geqslant 2$) are tailing somewhat, resulting in a maximum efficiency of 4,000 plates for butylparaben. On the other hand, a longer polymerization time (1 hour and more) resulted in a thicker layer of maximum 950 nm, but with a broad size distribution (smallest polymer globes are 300 nm), as some polymer globes are limited in their growth by sterical hindrance (Figure VI.1C). Therefore, there is slightly more retention at the long polymerization time but the broader size distribution lowers somewhat the efficiency compared to the optimum polymerization time of 30 minutes and in addition more peak tailing is thereby observed (Figure VI.2C).

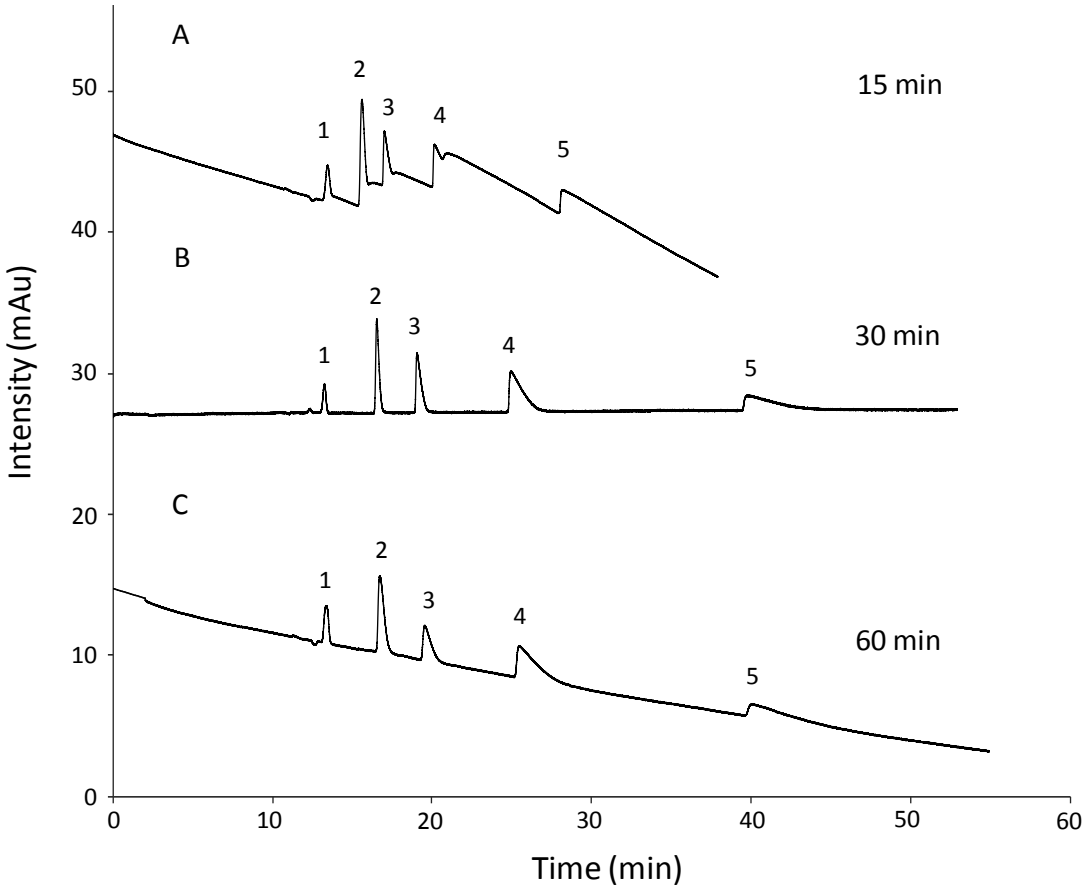

Figure VI.2. Effect of the polymerization time on the chromatographic characteristics. The monomer mixture contained styrene/divinylbenzene/ vinyl sulfonic acid (1/1/1 v/v) in a 40/60 v/v ratio to the solvent (ethanol). The total effective length of the capillary was 50 cm, all other analysis parameters were the same as described in the experimental section. A separation of thiourea (1), methyl- (2), ethyl- (3), propyl- (4) and butylparaben (5) was obtained.

It can be concluded that the presence of vinyl sulfonic acid in the polymer did not alter the reversed phase separation mechanism and that also a thin film can be produced by this modified polymerization protocol. The presence of VSA in this work is of high importance as this copolymer is responsible for the generation of the EOF.

The presence of a higher amount of VSA groups in the polymer should generate a higher EOF and expedite the analyses. Therefore, the influence of the VSA concentration in the monomer composition on the chromatographic properties was evaluated. Consequently, a series of four open-tubular capillaries were prepared in which the ratio of S/DVB/VSA was altered in the range of 1/1/0.5 to 1/1/2 while the ratio between the monomer mixture and the solvent (40/60) was maintained. Clearly, the presence of increasing amounts of VSA as comonomer decreased the hydrophobicity of the crosslinked polystyrene layer while coinciding also with lower retention factors of the parabens (Table VI.1).

Table VI.1. The influence of the VSA ratio on the efficiency and retention factor. The monomer ratios are expressed as the relative v/v amounts of styrene, divinylbenzene and sulfonic acid, respectively.

	Efficiency *N* (plates)			Retention factor (*k* or k_{app})		
S/DVB/VSA	1/1/0.5	1/1/1	1/1/2	1/1/0.5	1/1/1	1/1/2
methylparaben	24118	26922	27415	0.25	0.22	0.18
ethylparaben	20018	22169	24879	0.40	0.35	0.31
propylparaben	5106	5776	7823	0.80	0.73	0.68
butylparaben	3483	4053	4976	2.00	1.78	1.43

For example, the retention factor of butylparaben decreases from 2 to 1.43 for the capillaries treated with S/DVB/VSA ratios of 1/1/0.5 and 1/1/2, respectively. In addition, the EOF velocity increases from 0.70 mm/s to 1.09 mm/s, respectively, as depicted in Figure VI.3.

Furthermore, a favorable effect on efficiency and peak shape of the parabens can be noticed if higher VSA ratios are applied in the monomer mixture. For example, the efficiency of methylparaben increases from 24118 to 27415 when comparing the capillary with the lowest and the highest applied VSA ratio in the monomer mixture, respectively, while the retention factor (*k*) for the same compound decreases from 0.25 to 0.18, as depicted in Table VI.1. These effects can be partially explained by the lower retention factor of the compounds but also by the different morphology of the porous polymer layer. A maximum increase of the VSA ratio by a factor 4 resulted in only a 80% percent increase of the mobile-phase velocity, suggesting that the amount of copolymerized VSA groups was not directly proportionate with the increase in the VSA ratio. Due to the possibilities to perform faster and more efficient analyses, the optimized monomer mixture with a S/DVB/VSA ratio of 1/1/2 was used for further research.

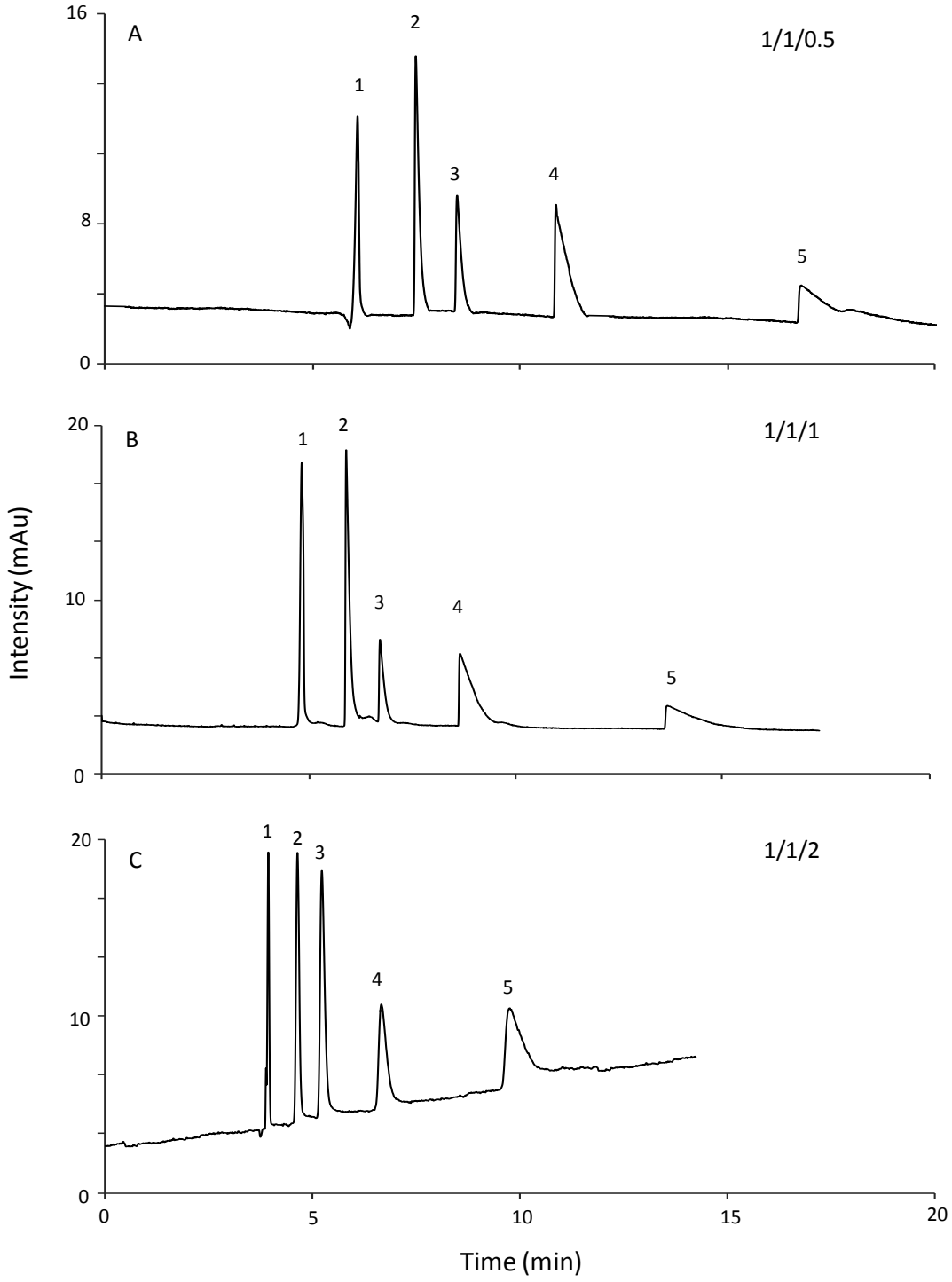

Figure VI.3. The effect of the VSA ratio in the monomer mixture on the chromatographic characteristics. Three different ratios of S/DVB/VSA were tested: 1/1/0.5 (A), 1/1/1 (B) and 1/1/2 (C). Analysis parameters were the same as described in the experimental section. The type of compounds, the elution order and the column dimensions remained the same as in Figure VI.2.

Upon further increasing VSA ratios (larger than 2.5) the polymerization started at every point across the capillary, resulting in a clogged capillary or in the best case a monolithic capillary rather than an open-tubular capillary. The lower hydrophobicity of this new polymer causes a change in the polymerization mechanism, as the polymerization now occurs across the whole capillary, instead of only at the hydrophobic wall. As a consequence the format then changes from open-tubular to monolithic and the solvent, ethanol, serves in this case as a porogen. As the goal of this work was to optimize open-tubular conditions, the monolithic format was not further optimized and the chromatographic characteristics of the latter were not evaluated.

The lowering of the retention and the increase of the mobile-phase velocity with increased VSA ratios in the monomer mixture demonstrates that the VSA monomer is tightly embedded in the porous polymer layer. Furthermore, the FT-IR spectrum of the polymer (polymerized in bulk) showed bands at 1069 and 1093, which were not present in the FT-IR spectra of a PS-DVB polymer. These bands are corresponding with the presence of sulfonic acid. In addition, Figure VI.4 demonstrates that a sufficiently high and a stable EOF was generated at both low and high pH conditions suggesting that the EOF is generated by a strong acid, such as vinyl sulfonic acid, which is deprotonated even at low pH conditions.

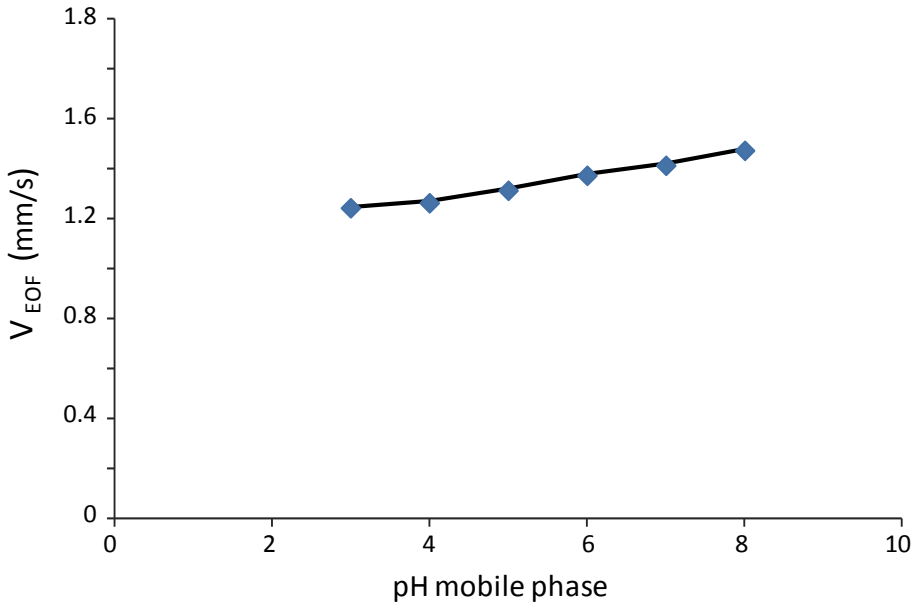

Figure VI.4. The effect of the pH of the buffer on the mobile-phase velocity.

The residual small dependency of the EOF on the pH which is observed, can be related to the influence of the higher ionic strength at the lower pH's, as a consequence of the addition of increasingly larger amounts of acid, which is known to lower the EOF. Alternatively, as the influence of residual silanol groups on the capillary wall cannot be excluded, this could also explain this phenomenon.

The EOF generation of the optimized capillary was sufficiently high to perform analyses up to well into the C-term of the van Deemter curve, while an analysis of a capillary with PS/DVB/VSA ratio of 1/1/1 was only possible in the B-term, even with the used relatively short columns (25 cm) and applying the highest voltages (30 kV). The van Deemter curves, illustrated in Figure VI.5, were constructed by analyses of the test mixture at 10 different voltages ranging between 7.5 and 30 kV.

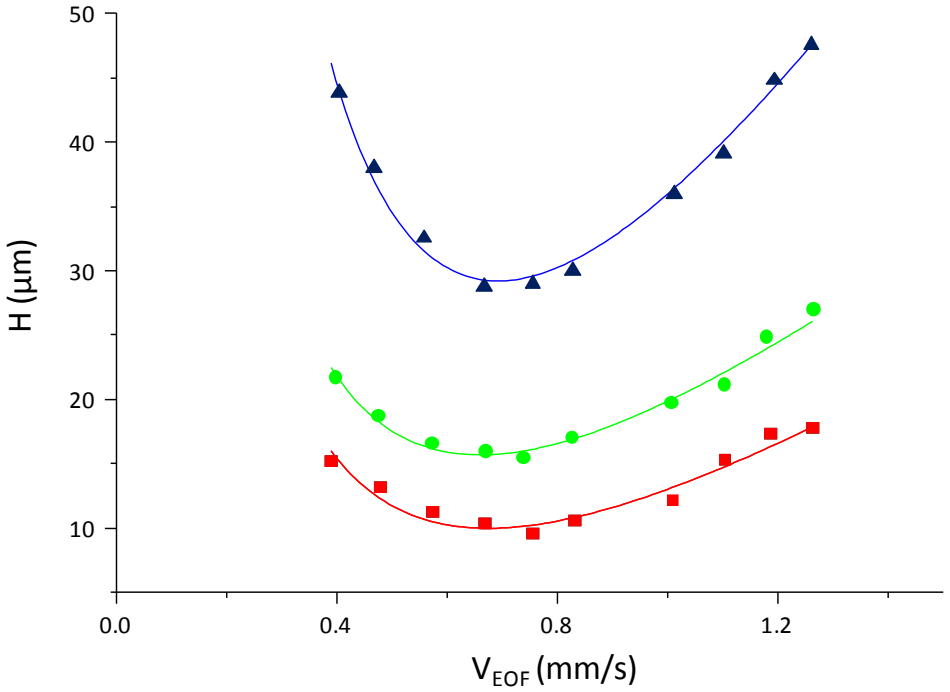

Figure VI.5. Constructed van Deemter curves of methylparaben (squares), ethylparaben (circles), propylparaben (triangles). All data points were calculated from the separation of the parabens on a S/DVB/VSA (1/1/2) open-tubular capillary with the same analysis parameters as described in the experimental section.

Optimal velocities were measured at 0.7 mm/s with a minimal plate height of 9.8 µm for the poorly retained methylparaben which corresponds with the minimal theoretical plate height

for open-tubular columns of 10 µm ID ($N = L/H = L/d_c$). However, the van Deemter curves of ethylparaben en propylparaben reveal a detrimental effect of retention on the minimum plate heights coinciding with minimums of 14.9 and 28 µm, respectively. These reported plate heights and their accordingly steep increase in the slope of the C-term (corresponding with increasingly slower mass transfers) can be explained by the morphology of the porous polystyrene layer. It should be noted that this is fairly consistent with the systematically poor results obtained with poly(styrene-divinylbenzene) based packed columns when analyzing small molecules in HPLC. It appears that also here the diffusion of the small molecules in PS-DVB/VSA material is too slow at room temperature [28]. The material should therefore also further be evaluated for the analysis of large molecules, who will, as is the case with PS-DVB, not migrate into the material and therefore offer improved results. Furthermore, the open-tubular character of the capillary induces slow mass transfer kinetics from the mobile phase to the stationary phase, due to the slow diffusion coefficients of solutes in liquids (compared to the diffusion in gases).

To assess the maximum performance of the open tubular columns, the kinetic plots were constructed in the same manner as described in Chapter IV.

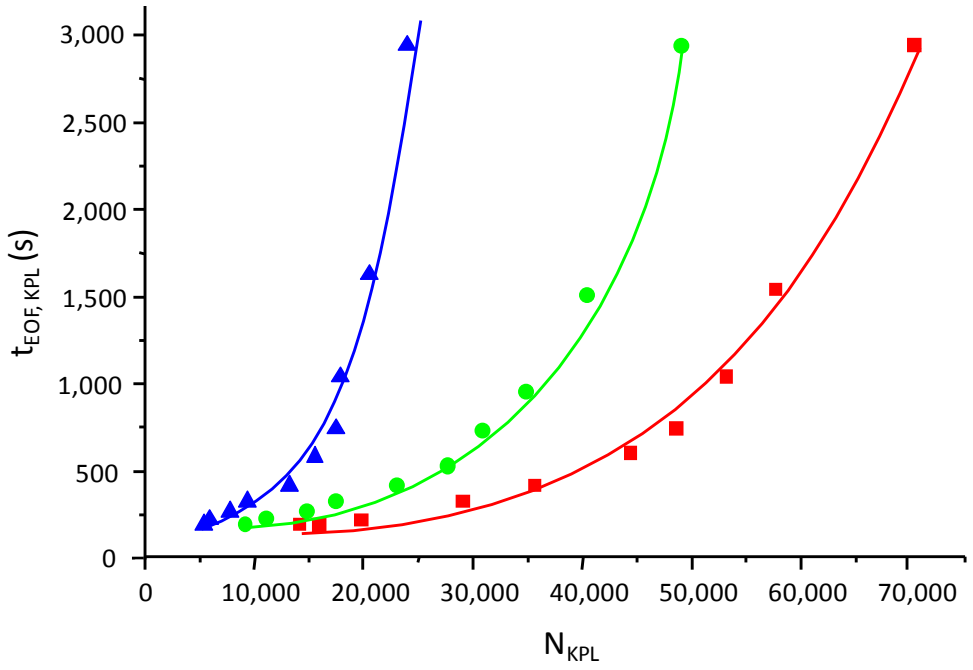

Figure VI.6. Constructed kinetic plots of methylparaben (red squares), ethylparaben (green circles), propylparaben (blue triangles).

The kinetic plots in Figure VI.6 demonstrate again the limited performance of the well retained solutes. A maximum efficiency of 17,000 plates is obtained for an EOF time of 50 minutes. Less retained solutes such as methylparaben, can obtain a maximum performance of 70,000 plates in the same time. These maximum efficiencies are lower compared to those obtained in Chapter IV for packed capillaries, where a maximum of 120,000 plates was obtained (for an EOF time of 85 minutes). These results indicate that the slow mass transfer still limits the performance of open tubular CEC with 10 µm capillary (if the stationary phase is polystyrene based). Smaller inner radii will improve retention and mass transfer velocity and hence, result in more performant columns.

To examine the repeatability, the same analyses were performed on the same column in consecutive days. The RSD% of the retention time varied from 0.52 to 0.93% for the day to day repeatability. More imperatively, the repeatability of the manufacturing process was also investigated by analyzing the same test mixture on 3 columns, prepared in the same manner but on different days. Figure VI.7 illustrates the analysis of the test mixture on the three columns. The RSD of the retention times was thereby varying between 1.57 to 2.75%.

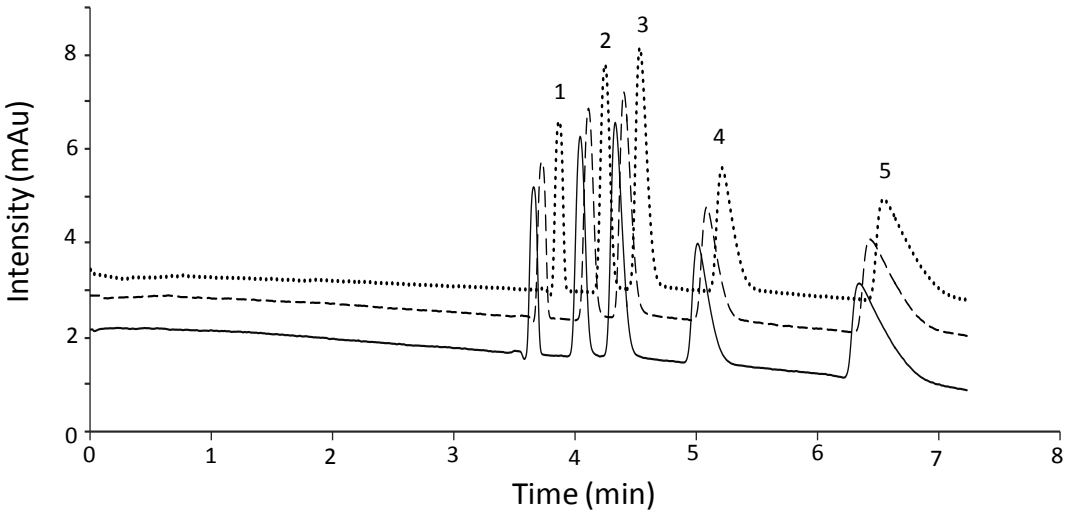

Figure VI.7. Overlay of three separations, run with the same conditions but on three different capillaries, prepared at three different days. The mobile phase was composed of ammonium acetate (25 mM, pH 5.5) and acetonitrile (60/40). All other analysis parameters were the same as described in the experimental section. The compounds and the elution order remained thereby the same as in Figure VI.2.

As mentioned before, the internal diameter of open-tubular capillaries should in principle be further restricted due to the limited diffusion kinetics of the solutes in liquid media (compared to gaseous mobile phases). However, the sensitivity of open-tubular columns in CEC will be limited for on-column UV-detectors, compared to packed or monolithic columns (with broader ID's of 20 to 100 µm). On the other hand, very narrow capillaries dissipate Joule heating more effectively and should improve column efficiency and signal to noise ratios. The used narrow open-tubular capillaries are therefore more suited to perform electrodriven analyses even at higher temperatures. In order to investigate this, isothermal analyses were performed at 25°C, 40°C and 60°C. Note that these set temperatures were corresponding to the temperatures of the environment in the vicinity of the capillary, as the actual temperature in the capillary center cannot be measured during analysis. Figure VI.8A-C illustrates that a higher set temperature coincides with a higher mobile-phase velocity, due to the lower viscosity of the mobile phase. An increase in the temperature from 25°C to 60°C corresponded with an increase in mobile-phase velocity from 0.95 mm/s to 1.37 mm/s (+40%). Additionally, a drop in retention as a function of temperature could also be noted. A reduction in retention factor for butylparaben from 1.0 to 0.67 (-33%) coincided with a rise in temperature of 35°C. As this drop in retention is comparable or even lower compared to the drop in retention in HPLC at elevated temperatures, this individually proves that no problematic Joule-heating phenomena is taking place in the capillary during these analyses [29,30].

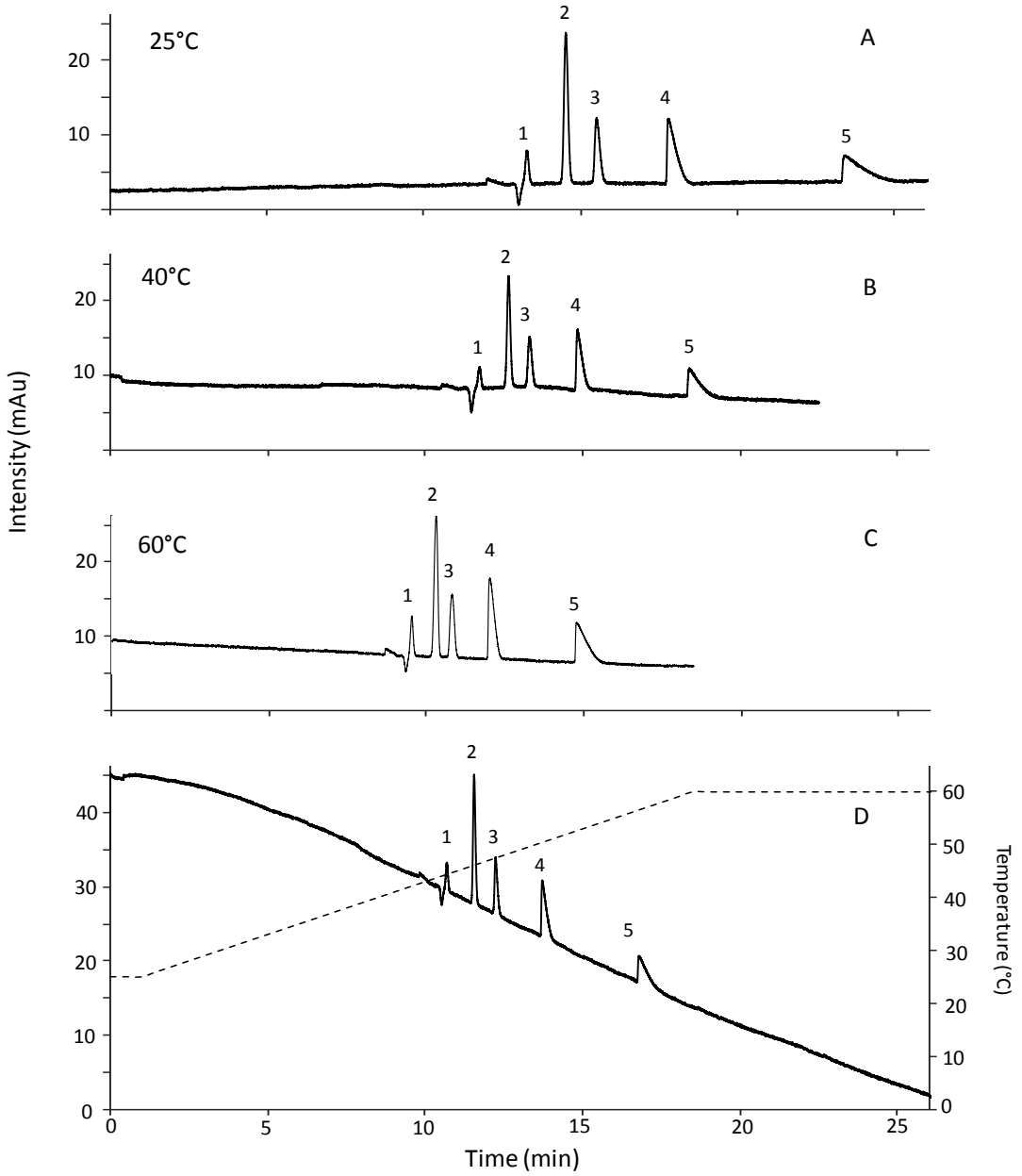

Figure VI.8. The influence of set air temperature on the chromatographic characteristics. Three isothermal runs at 25°C (A) 40°C (B) and 60°C (C) and a temperature programmed run (D) were depicted. The mobile phase was composed of ammonium acetate (25 mM, pH 5.5) and acetonitrile (60/40). The effective capillary length was 75 cm. All other analysis parameters were the same as described in the experimental section. The compounds and the elution order remained the same as in Figure VI.2.

However, the effect of the elevated temperatures on the efficiency is more ambiguous. Table VI.2 reveals a beneficial effect on the efficiency of the four parabens at higher set temperatures (40°C), but simultaneously the efficiency decreases at further elevated temperatures (60°C). These observations are directly related to the shifting shape and position of the van Deemter curves at different temperatures.

Table VI.2. The efficiency and retention factors of the parabens, analyzed at different set temperatures and thermal gradients.

Compound	Efficiency N (plates)			Retention factor (k or k_{app})			
	25°C	40°C	60°C	25°C	40°C	60°C	Grad
methylparaben	73245	85577	64505	0.16	0.13	0.09	0.14
ethylparaben	53622	65066	46848	0.33	0.26	0.18	0.22
propylparaben	24364	39724	26816	0.5	0.39	0.28	0.30
butylparaben	8790	17586	14897	1.0	0.83	0.67	0.69

More importantly these results indicate interesting possibilities for the application of temperature gradients instead of the, harder to realize, mobile-phase compositional gradients, to increase the eluotropic strength in CEC. Note that the measured set temperature in the cassette is the actual temperature of the air surrounding the capillary and that therefore this is not necessarily the actual temperature at the capillary center. The author assumes that there will be a small time delay before the set temperature is reached in the capillary center. The optimal temperature gradient ranged between 25°C and 60°C, with a gradient rate of 2°C/minute. Figure VI.8D, illustrates a significant drop in the apparent retention factors of the retained components. A comparison between the (apparent) retention factor of the gradient analysis on the one hand and the isothermal run at 25°C and 40°C on the other hand, reveals a drop in retention factor for butylparaben of 30 and 17 percent, respectively. Hence, the gradient expedites the analysis. Nevertheless, the

retention of butylparaben at 60°C (isothermal) was still lower compared to the gradient. The gradient runs also induced a peak focusing effect, resulting in sharper peak shapes and less tailing. In order to quantify this effect, the average peak capacity of the isothermal runs and of the gradient run was measured as described in literature [31-33]. A peak capacity of 55 was obtained for the gradient run (with a time interval of 20 minutes), while the peak capacities of the isothermal runs at 25, 40 and 60°C were 50, 54 and 38, respectively. Hence, the gradient run is the more favorable choice due to the reduced analysis time and the improved peak shape while obtaining slightly higher peak capacities. Clearly, the influence of temperature in open-tubular CEC needs further investigation. Note, that the velocity of the mobile-phase will change during such a temperature based gradient run, in contrary to pressure driven techniques or mobile-phase gradients. This change undoubtedly further effects the overall efficiency of the analyses.

A simulation of the *H* vs. *u* curves at different temperatures can be used to investigate the possible effect of elevated temperatures on the plate height behavior as a function of the linear velocity. This simulation is based on the A-C parameters of the Knox equation, acquired from the experimental measured curve of methylparaben at 25°C. According to Chen and Horvath, the A-C parameters of the Knox equation are constant and only the viscosity of the solvent, η, and the diffusion coefficient of the solute in the solvent, D_m, are dependent on the temperature [34,35].

Therefore, a *H* versus u curve can be constructed by rewriting the Knox-equation in terms of the plate height (*H*) and the linear velocity u_{EOF}:

$$H = d_p \left[A \left(\frac{d_c u_o}{D_m}\right)^{1/3} + B \left(\frac{D_m}{u_{o d_c}}\right) + C \left(\frac{d_c u_o}{D_m}\right) \right] \qquad \text{Eq. VI.1}$$

Whereby the diffusion coefficients of methylparaben in a 30/70 mixture of acetonitrile/water can be calculated by implementing the Wilke-Chang equations [34,36-38]:

$$D_m = 7.4\ x\ 10^{-8}\ \frac{T\sqrt{\alpha_{sv}M_{sv}}}{\eta_{sv}V_{b,a}^{0.6}} \qquad \text{Eq. VI.2}$$

and

$$D_{m,T} = D_{m,298}\ \frac{\eta_{298}}{\eta_T}\ \frac{T}{298} \qquad \text{Eq. VI.3}$$

where T represents the absolute temperature, V_b is the molar volume at the normal boiling point, M is the molar mass and α stands for the association coefficient. The subscripts sv and a represent the solvent and the solute, respectively.

The viscosity at different temperatures and different can be assessed by the equation developed by Chen and Horvath [34,35]:

$$\eta(\alpha,T) = exp\left[\alpha\left(-3.476 + \frac{726}{T}\right) + (1-\alpha)\left(-5.414 + \frac{1566}{T}\right) + \alpha(1-\alpha)(-1.762 + \frac{929}{T})\right] \qquad \text{Eq. VI.4}$$

where α is the volume fraction of acetonitrile. By calculating the D_m, η and the A-C terms (from the experimental curve measured at 25°C), the H vs. u curves were simulated for four different temperatures, as illustrated in Figure VI.9.

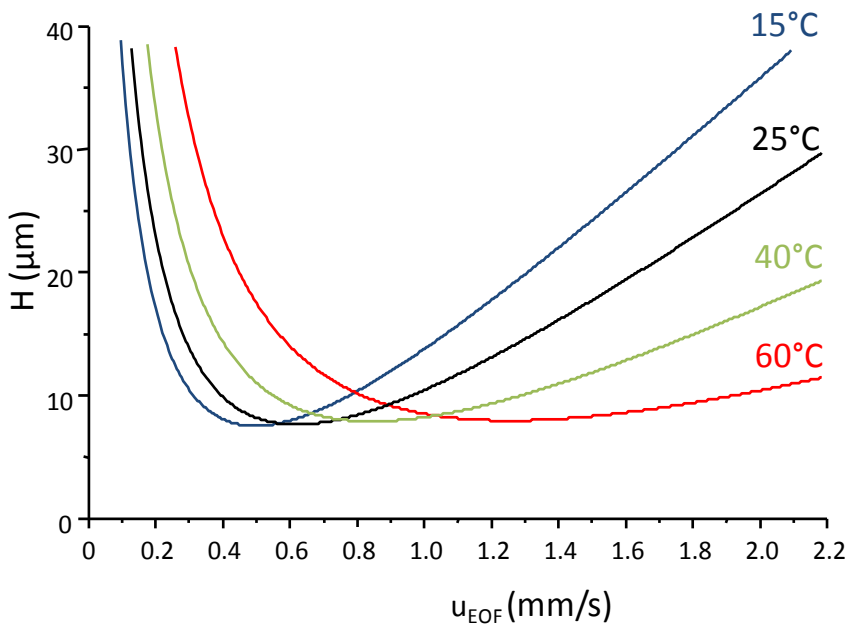

Figure VI.9. Simulated plate-height curves for 10 µm ID capillaries at four different temperatures. The plots were calculated by implementing the A-C parameters from the methylparaben H vs. u curve at 25°C (Figure VI.5) in Eq.VI.1. Diffusion coefficients for methylparaben in 30/70 acetonitrile/water were calculated according to Wilke-Chang and Eq. VI. 2-4.

Figure VI.9 demonstrates that a change in temperature has a significant influence on the plate height curves. The minima in the plate heights are shifted to higher mobile velocities and the C term of the curves are less steep with increasing temperature. For example, at 15°C a minimum plate height is obtained at 0.45 mm/s while at 60°C a minimum is obtained at 1.1 mm/s. At higher temperatures, on the other hand, the *B*-term will also shift to higher mobile velocities and consequently the plate heights will increase if too low mobile velocities are used (in the *B*-term area). Note that the minimum plate height is not affected by an increase in temperature. However, it should be stressed that this is only true for fast sorption systems.

This new *H* vs. u curves allows to produce the corresponding kinetic plots. Two significant effects of temperature are hereby visible, as presented in Figure VI.10.

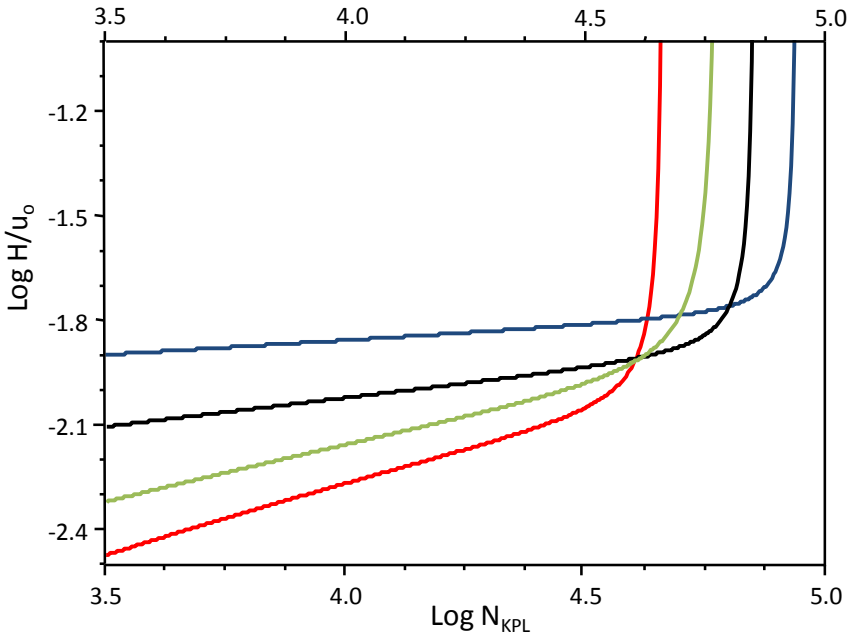

Figure VI.10. Simulation of kinetic plots for 10 µm ID capillaries at different temperatures (blue: 15°C, black: 25°C, green: 45°C, red: 60°C). Based on the obtained van Deemter curves represented in Figure VI.9.

Figure VI.10 illustrates that the KP curves obtained for the higher temperatures are shifted to lower log H/u_o values. Hence, the elevated temperatures allows an expedited analysis for a given column (and stationary phase) and a maximum voltage, while the efficiency of the analysis is not affected. On the other hand, the highest obtainable efficiency will be reached at the lowest temperature. For instance, at 15°C an efficiency of 95,000 plates will be obtained for a 1 meter capillary (and same stationary phase as described in this chapter), while only 45,000 plates will be reached at 60°C. In this case, the B-term is predominant. However, in this region analyses will become very long and are less favorable to apply.

4 Conclusion

The work in this chapter illustrates the development and application of an open-tubular capillary with a porous polymer layer of poly(styrene-divinylbenzene-vinylsulfonic acid) in capillary electrochromatography. The vinylsulfonic acid generates a stable and sufficiently highly EOF over a wide pH range. The polymer layer was optimized in terms of polymerization time and monomer composition to obtain an optimum peak shape and EOF

generation. This work revealed that as high as possible VSA ratios (S/DVB/VSA 1/1/2) are beneficial for the analysis time, efficiency and peak shape of the retained compounds. Furthermore, a polymerization time of 30 minutes, resulting in a layer thickness of 400-600 nm seemed to be the optimum to achieve efficient separations on 10 µm ID capillaries. These optimized preparation conditions led to an optimum plate height of 10 µm. However, the plate heights increase steeply with retention. Therefore, the beneficial effect of performing analyses at elevated temperature were studied. Isothermal analyses at high temperature (40°C) were favorable in terms of efficiency and peak shape but the application of a temperature gradient expedited the analysis time significantly, while preserving the peak capacity.

5. References

[1] S. Ludtke, T. Adam, K.K. Unger, J. Chromatogr. A 786 (1997) 229.

[2] T. Adam, S. Ludtke, K.K. Unger, Chromatographia 49 (1999) S49.

[3] R. Dadoo, R.N. Zare, C. Yan, D.S. Anex, Anal. Chem. 70 (1998) 4787.

[4] C. Yan, R. Dadoo, H. Zhao, R.N. Zare, D.J. Rakestraw, Anal. Chem. 67 (1995) 2026.

[5] D. Allen, Z. El Rassi, Electrophoresis 24 (2003) 3962.

[6] A. Ghanem, T. Ikegami, J. Sep. Sci. 34 (2011) 1945.

[7] C. Legido-Quigley, N.D. Marlin, V. Melin, A. Manz, N.W. Smith, Electrophoresis 24 (2003) 917.

[8] R.a. Wu, L. Hu, F. Wang, M. Ye, H. Zou, J. Chromatogr. A 1184 (2008) 369.

[9] E.F. Hilder, F. Svec, J.M.J. Frechet, Electrophoresis 23 (2002) 3934.

[10] M. Bedair, Z. El Rassi, Electrophoresis 25 (2004) 4110.

[11] H.F. Zou, X.D. Huang, M.L. Ye, Q.Z. Luo, J. Chromatogr. A 954 (2002) 5.

[12] Z. Kucerova, M. Szumski, B. Buszewski, P. Jandera, J. Sep. Sci. 30 (2007) 3018.

[13] Y.P. Zhang, W. Li, X.J. Wang, L.B. Qu, G.L. Zhao, Y.X. Zhang, Anal. Bioanal. Chem. 394 (2009) 617.

[14] T. Hirano, S. Kitagawa, H. Ohtani, T. Kinoshita, Y. Ishigaki, N. Shibata, S. Nii, Anal. Bioanal. Chem.

405 (2013) 8319.

[15] I. Gusev, X. Huang, C. Horvath, J. Chromatogr. A 855 (1999) 273.

[16] W.H. Jin, H.J. Fu, X.D. Huang, H. Xiao, H.F. Zou, Electrophoresis 24 (2003) 3172.

[17] B.H. Xiong, L.H. Zhang, Y.K. Zhang, H.F. Zou, J.D. Wang, HRC-J. High Resolut. Chromatogr. 23 (2000) 67.

[18] H.-Y. Huang, Y.-C. Liu, Y.-J. Cheng, J. Chromatogr. A 1190 (2008) 263.

[19] H.Y. Huang, H.Y. Lin, S.P. Lin, Electrophoresis 27 (2006) 4674.

[20] C. Stassen, G. Desmet, K. Broeckhoven, L. Van Lokeren, S. Eeltink, J. Chromatogr. A 1325 (2014) 115.

[21] J.W. Jorgenson, E.J. Guthrie, J. Chromatogr. 255 (1983) 335.

[22] E. Guihen, J.D. Glennon, J. Chromatogr. A 1044 (2004) 67.

[23] G.H. Yue, Q.Z. Luo, J. Zhang, S.L. Wu, B.L. Karger, Anal. Chem. 79 (2007) 938.

[24] Q. Luo, G. Yue, G.A. Valaskovic, Y. Gu, S.L. Wu, B.L. Karger, Anal. Chem. 79 (2007) 6174.

[25] M. Rogeberg, S.R. Wilson, T. Greibrokk, E. Lundanes, J. Chromatogr. A 1217 (2010) 2782.

[26] Q.Z. Luo, T. Rejtar, S.L. Wu, B.L. Karger, J. Chromatogr. A 1216 (2009) 1223.

[27] X. Huang, J. Zhang, C. Horvath, J. Chromatogr. A 858 (1999) 91.

[28] G. Vanhoenacker, A.D.S. Pereira, T. Kotsuka, D. Cabooter, G. Desmet, P. Sandra, J. Chromatogr. A 1217 (2010) 3217.

[29] S. De Smet, F. Lynen, J. Chromatogr. A 1355 (2014) 261.

[30] S. Heinisch, J.-L. Rocca, J. Chromatogr. A 1216 (2009) 642.

[31] J.W. Dolan, L.R. Snyder, N.M. Djordjevic, D.W. Hill, T.J. Waeghe, J. Chromatogr. A 857 (1999) 1.

[32] S.J. Marin, B.A. Jones, W.D. Felix, J. Clark, J. Chromatogr. A 1030 (2004) 255.

[33] S. Pous-Torres, J.J. Baeza-Baeza, J.R. Torres-Lapasio, M.C. Garcia-Alvarez-Coque, J. Chromatogr. A 1205 (2008) 78.

[34] F. Lestremau, A. de Villiers, F. Lynen, A. Cooper, R. Szucs, P. Sandra, J. Chromatogr. A 1138 (2007) 120.

[35] H. Chen, C. Horvath, J. Chromatogr. A 705 (1995) 3.

[36] J.W. Li, P.W. Carr, Anal. Chem. 69 (1997) 2550.

[37] K. Miyabe, R. Isogai, Anal. Sci. 29 (2013) 467.

[38] K. Miyabe, R. Isogai, J. Chromatogr. A 1218 (2011) 6639.

Chapter 7

Investigation into the potential of wall-coated ordered mesoporous layers as retaining phase in open-tubular electrochromatography

The coating of the stationary phase on the inner layer of narrow bore capillaries could be a straightforward way to manufacture CEC capillaries. In this chapter the coating of an ordered mesoporous material, namely SBA-16, functionalized with C18 chains, was therefore evaluated as novel stationary phase in CEC. The coating performance was characterized and optimized by the separation of a test mixture containing neutral solutes. The neutrality of the used test solutes ensures that any observed separation is induced only through chromatographic behavior. An SBA-16 layer of 600 nm in an 50 µm ID capillary was obtained as most the promising capillary. A maximum efficiency of 31,000 plates was thereby obtained. The SBA-16 layer generated an EOF velocity of 0.42 mm/s under these conditions. The dependency of the retention and of the EOF velocity with the modifier content was investigated. A reduction in EOF velocity with higher modifier content was thereby observed.

The research described in this chapter is the result of the collaboration between the Separation Science Group (SSG, UGENT) and the Center of Ordered Materials, Organometallics & Catalysis (COMOC, UGENT). COMOC was responsible for the development, characterization and optimization of the sol, while SSG was responsible for production and the analytical evaluation of the coated capillaries.

1 Introduction

As mentioned in Chapter III, the efficiency of open-tubular chromatography is directly linked to the internal diameter of the column. Moreover, the internal diameter should ideally be reduced to 2-5 µm to ensure sufficiently fast mass transfer kinetics between the stationary and liquid phase [1]. However this has a detrimental effect on the sample loading capacity of the column. As a consequence, the already limited sensitivity of CEC with UV-detection is thereby further hampered by the small optical pathway. Furthermore, the retention in much of the published OT-LC and OT-CEC work is too limited due to the detrimental phase ratios which are used to allow for sufficient column efficiency.

These problems can to some extent be overcome by enhancing the surface area of the coated wall significantly. In Chapter VI a polystyrene based polymer layer was applied as a novel stationary phase in CEC. However, the longer retained solutes (k>2) displayed relatively low efficiencies and peak tailing due to the slow mass transfer kinetics in the polystyrene layer and due to the slow mass transfer through the mobile phase in 10 µm capillaries. Silica materials on the other hand, often demonstrate their superior (faster) mass transfer kinetics compared to organic polymeric layers. Therefore, the presence of a thin layer of silica with a porous structure should be beneficial to enhance the efficiency in CEC.

Some contributions describing the use of an ordered mesoporous[1] structure have been reported in liquid chromatography [2-6]. Contrary to conventional silica synthesis, these highly-ordered mesoporous silica particles are synthesized by the polycondensation of tetraethyl-ortho-silicate in a template formed by micelles structures. The latter form an ordered supramolecular structure. After the polycondensation, these micelles are removed by a calcination step. The particles tested in various LC-modes were all of MCM-41 based silica type where cetyl-trimethylammonium-bromide (CTAB) was used as template forming micel. Spherical particles with a narrow size distribution were thereby obtained, but with a small mesopore size (2-6 nm). It would be particularly interesting to apply highly-ordered mesoporous stationary phases depicting large pore sizes and especially a particularly high surface area in open-tubular CEC. The rationale is thereby that the occurrence of a thin layer

[1]Note that micropores are smaller than 2 nm, while mesopores have pore sizes between 2 and 50 nm and macropores have pore sizes larger than 50 nm.

of ordered mesoporous material should allow for comparable or higher retention factors compared to the use of un-ordered silica, leading to the possible use of thinner coatings in OT-CEC while preserving retention and sample capacity.

Tian et al. synthesized and packed a capillary with large-pore meso-porous SBA-15 silica particles [7]. They obtained particles with a diameter of 400 nm and pore sizes of 12 nm. The capillary was tested by the separation of aromatic compounds and a minimum plate height of 2 µm was obtained. However, the aromatics were only slightly retained (k < 0.5), indicating that band broadening effects were partially suppressed by the poor retention.

To further enhance the pore size, pluronic F127[2] can also be used as template forming micelle. The resulting ordered mesopores silica structure is called SBA-16 and the synthesis should result in mesopores around 25 nm (250 Å). The synthesis, coating, characterization and chromatographic evaluation of the SBA-16 open-tubular layer is described in this chapter. The illustration of the ordered silica in Figure VII.I reveals the cubic 3D structure of the SBA-16 material.

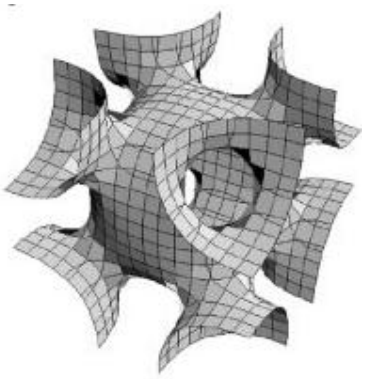

Figure VII.1. The Im3m structure of SBA-16.

[2] Pluronic F127 or Poloxamer 407: a hydrophilic triblock copolymer produced by BASF and generally used as an non-ionic surfactant.

2. Experimental

2.1. Chemicals, solution and material

Fused-silica capillaries (50 µm ID) were purchased from CM Scientific (Silsden, United Kingdom). MilliQ Water was prepared in house by a water purification instrument from Millipore (Bedford, New Hampshire, USA). Acetic acid was obtained by Fiers (Fiers N.V., Kuurne, Belgium). Acetonitrile of HPLC quality originated from Biosolve (Valkenswaard, Netherlands). All test-solutes, pluronic F127, ethanol, HCL, TEOS, and 2-(4-morpholino)ethanesulfonic acid (MES) were purchased from Sigma-Aldrich (Bornem, Belgium). Stock solutions of test solutes were prepared at 8,000 µg/mL in water or ACN, dependent on their solubility and diluted to their final concentrations (in the same solvent composition as the mobile phase) for all samples.

2.2 Synthesis and coating procedure

The synthesis, characterization and optimization of the coating sol has been described before by Ide et al. [8]. To prepare the sol, Pluronic F127 (0.007 mol) was first dissolved in a mixture of ethanol (9 mol) and HCl (0.00005 mol) and subsequently stirred during 2 hours at room temperature. Simultaneously, a solution of TEOS (1 mol), ethanol (19 mol), HCl (0.00025 mol) and H_2O (2.8 mol) was stirred for 1 hour and subsequently refluxed at 80°C during 1 hour. In the final step, the two solutions were mixed together and refluxed for 2 hours at 80°C.

The final solution was left to cool down until room temperature was reached. Subsequently, the capillaries were dynamically coated with the sol. Therefore, the sol and the capillary were introduced in a pressure bomb, which could withstand pressures up to 300 bar. Hereby, the pressure is homogeneously applied by N_2 gas, resulting in the introduction of the sol into the capillary inlet, which is positioned just above the bottom of the pressure bomb, as illustrated in Figure VII.2

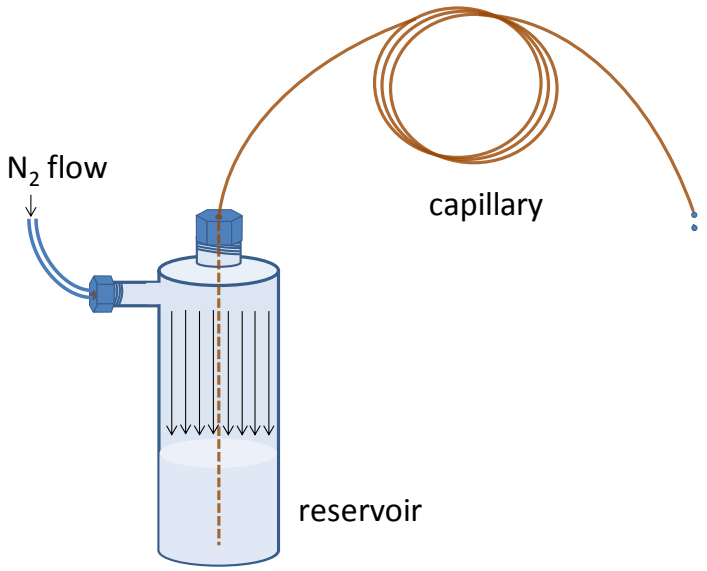

Figure VII.2. Dynamic coating set-up.

After the coating, the columns were dried under a N_2 flow for 12 hours and stabilized in an oven at 120°C for another 12 hours. Subsequently, the columns were calcined in a GC-oven with a N_2 flow at 350°C in order to remove the template forming micelles. The calcination step was deliberately kept at 350°C as higher temperatures would break down the protective polyimide layer covering the capillaries.

After the calcination step, the mesoporous SBA-16 has been formed. In the final step, the stationary phase is functionalized with C18 groups. Octadecyl dimethylchlorosilane was therefore dissolved in toluene and the solution was flushed through the column overnight at room temperature. Subsequently, the columns were rinsed with ACN and conditioned with mobile phase. Prior to analysis, the capillaries were cut such as to obtain total lengths of 60 cm.

2.3 Instrumentation and chromatographic conditions

CEC measurements were performed on two different systems. Analyses on columns CB1 and CC1 were measured with a P/ACE system MDQ (Beckman Coulter, California, USA) equipped with UV-detection and a liquid cooling system, while all other analyses were performed on a CE 7100 system (Agilent Technologies, Waldbronn, Germany) equipped with an air-cooling system, autosampler, diode array detector and a built-in system to pressurize vials.

All runs were performed in an isothermal way at 25°C. The background electrolyte consisted of a mixture of MES (50 mM, pH 6) and ACN. The ratio of organic modifier ranged from 50 to 20% as described further in the results sections. Stock solutions of the test solutes were prepared at 8,000 µg/ml and dissolved in acetonitrile or water, according to their solubility. Runs were performed at 30 kV and samples were injected electrokinetically by applying 5 kV during 1-3 seconds. All analyses were run on capillaries with a total length of 60 cm.

3 Results and discussion

The aim of this work was the successful coating of an SBA-16 based stationary phase, on the inner wall of a capillary to allow testing of its potential in OT-CEC. Therefore, capillaries with an ID of 50 µm were coated as these broader radii, compared to normal 2-10 µm ID of OT-columns, allowed a more facile way to introduce the viscous sol. Furthermore, the sensitivity and loadability of the column will improve with larger radii as the stationary phase volume and the optical pathway are directly related to the ID. Hence, CE-UV detection is possible and will be less hampered by sensitivity problems in this proof-of-concept research.

As mentioned above, the characterization and optimization of the sol and dip coating on silicon substrate were described previously [8]. Brunauer–Emmett–Teller (BET) measurements revealed that the SBA-16 material had a total surface area of 523 m^2/g and a total pore volume of 0.35 cm^3/g. However, it has to be mentioned that the characteristics and the stability of the sol were highly dependent on the temperature and moisture content of the synthesis environment. It was noticed that the polycondensation of the sol was initiated at high humidity and warm days, hampering greatly the repeatability of the sol synthesis.

To investigate the characteristics of this type of coating as stationary phase in OT-CEC, all analyses were also performed on a normal uncoated blank fused-silica capillary, which was directly functionalized with C18 groups. The coated capillaries were distinctive in length, coating time and applied coating pressure, as described in Table VII.1. Note that the lengths in Table VII.1 are representing the coating length of the capillary.

Table VII.1: Column dimensions of and coating conditions applied in the various manufactured capillaries

Code	Total column length during synthesis (cm)	ID (µm)	Coating time (min)	coating pressure (bar)
CB1	60	50	/	/
CB2	200	50	/	/
CC1	60	50	5	8
CC2	200	50	2880	100

All columns were coated with ODS. CB corresponds with capillaries which were not treated with the SBA-16 layer but only derivatized with C18 groups. The capillaries treated with the SBA-16 layer and with C18 groups are indicated as coated capillaries (CC).

The deposited SBA-16 layer was further characterized by SEM pictures and chromatographic analyses. Initially, a capillary of 60 cm was coated during 5 min (CC1). The comparison of the SEM pictures between CC1 and an uncoated capillary (CB1) revealed the rougher surface of CC1, indicating a small deposit of material. However, the thickness of the layer was limited and too small to characterize reliably and was not homogenously spread over the surface, as visualized in Figure VII.3.

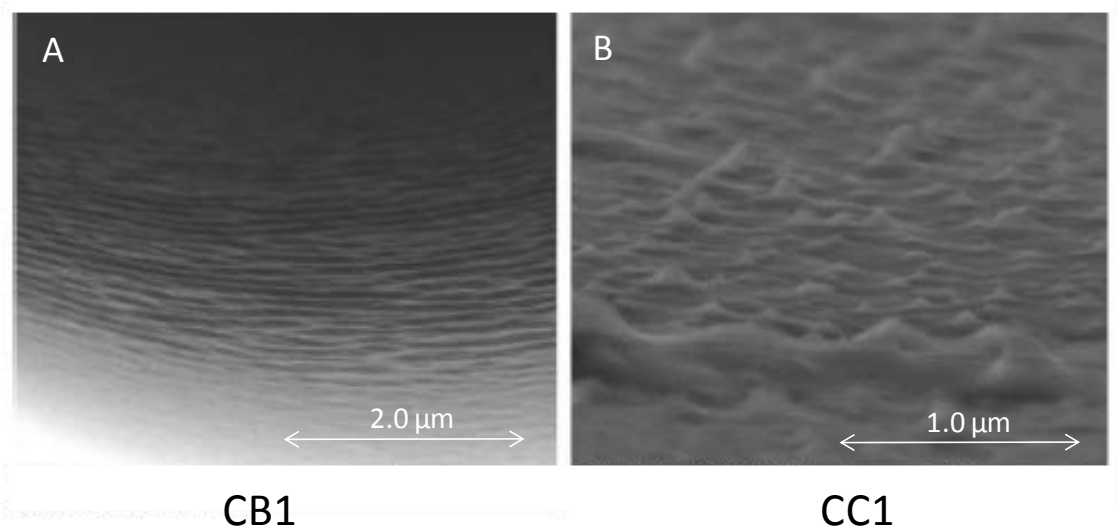

Figure VII.3. SEM micrographs from capillaries CB1 and CC1.

The separation performance was subsequently evaluated in a first stage through analyses of thiourea and four parabens on both capillaries. The choice of parabens as test compounds (as already explained in Chapter VI) relies on the electroneutrality of these solutes in a wide pH-range. Therefore, any observed separation will be the result of a partitioning process between the SBA-16 layer and the mobile phase. Hence, in this way the chromatographic properties of the layer can be evaluated. Figure VII.4 depicts the separation of the parabens on columns CB1 (A) and CC1 (B).

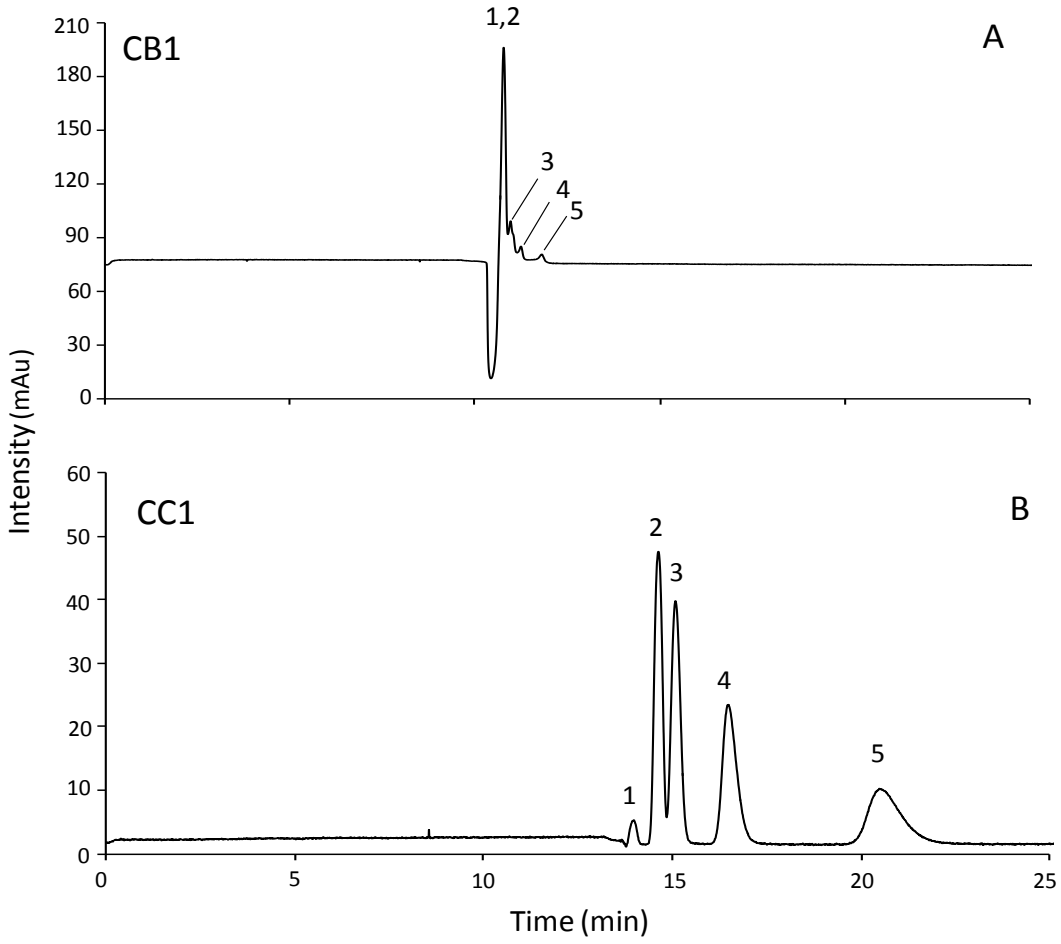

Figure VII.4. The separation of thiourea (150 and 20 µg/mL in A and B, respectively) (1), methylparaben (2), ethylparaben (3), propylparaben (4) and butylparaben on an SBA-16 untreated (A) and treated (B) capillary, respectively. All parabens were present in the sample of a concentration of 75 µg/mL. A mobile-phase composition of 20/80 ACN/MES (pH 6, 50 mM) was utilized at a voltage of 30 kV. Injection was performed by applying 5 kV during 1 s while UV detection was obtained at 254 nm. Capillary dimensions: 60 cm total length; 50 cm effective length; 50 µm ID.

Despite the limited thickness of the deposit of SBA-16 on the inner wall of the capillary, the difference in chromatographic properties between the coated capillary, CC1, and the uncoated capillary, CB1 is clearly visible. On the uncoated capillary, all solutes were eluting in a time span of 1 minute, indicating none or little retention. On the coated capillary, retention significantly increased and the four parabens could be separated and individually identified. For example, a retention factor of 0.5 was obtained for butylparaben. However, methyl- and ethylparaben were not baseline separated and were only slightly retained with retention factors of 0.05 and 0.075, respectively. Another significant difference between the uncoated and the coated column is the lower EOF velocity, determined by the elution time of thiourea. While CB1 displays a mobile-phase velocity of 0.71 mm/s, the EOF velocity of CC1 is at 0.60 mm/s significant lower. This discrepancy can be related to differences in coating efficiencies during the functionalization of the free silanol groups with ODS.

To improve the retention, a thicker SBA-16 layer should be deposited, especially as the SBA-16 layer was not homogeneously coated. To improve the thickness of the layer and to enhance the homogeneity, a new capillary was coated for a longer time (48 hours) and with a higher sol velocity. Therefore, the applied pressure was increased to 100 bar, which is an 8 fold increase. However, the capillary coating length was also altered to 200 cm and therefore the backpressure was increased by a factor of 3.3. As result, the increase in pressure leads to a 2.6-fold increase in sol velocity.

The SEM pictures of the column obtained in this way (CC2) reveal a clear smooth coating, with a thickness of 600 nm, as visualized in Figure VII.5.

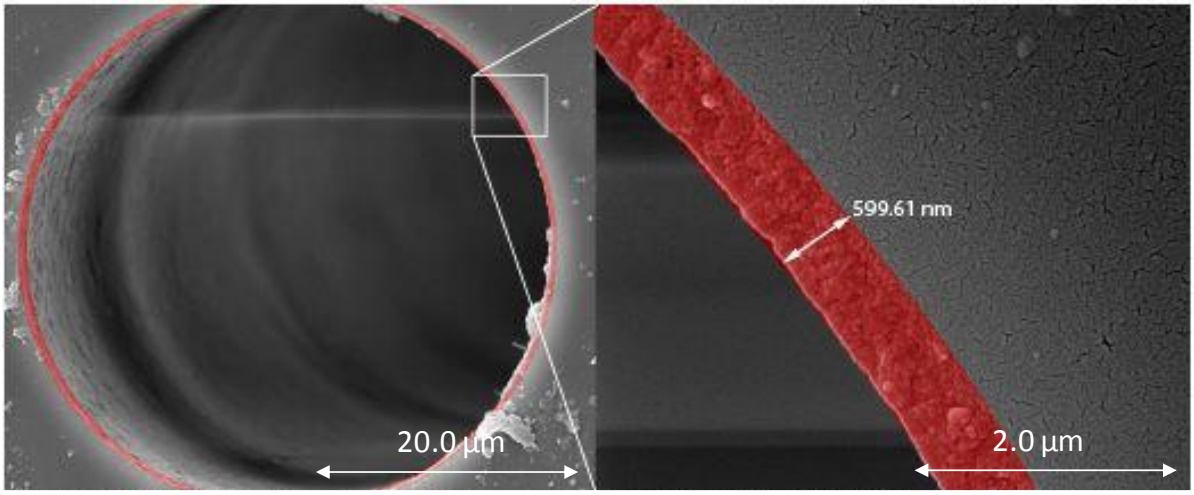

Figure VII.5. SEM micrographs of CC2. The red band indicates the 600 nm thick layer of SBA-16.

The thicker layer is a result of the increased coating time (by a factor of 576). As result, the TEOS groups have enough time to polycondensate over the whole capillary wall, and layer after layer can be formed. The effect of the thickness of the ordered mesoporous layer on the chromatographic separation of parabens is depicted in Figure VII.6.

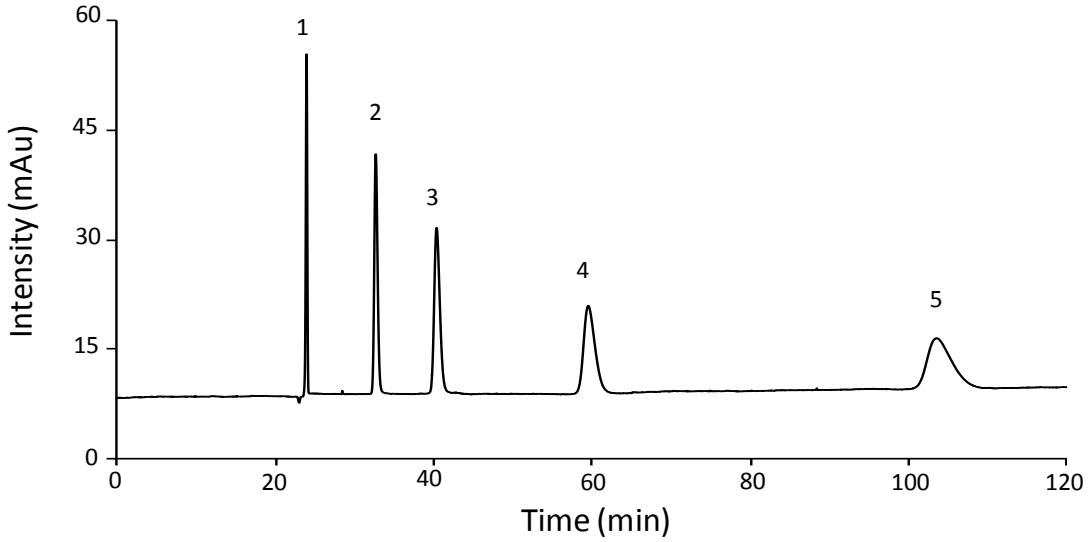

Figure VII.6. Separation of thiourea and the four parabens on CC2. Test mixture consisted of 75 µg/mL of each solute. All other analysis conditions are the same as described in Figure VII.4. Capillary dimensions: 60 cm total length; 52.5 cm effective length; 50 µm ID.

The retention and resolution of the parabens clearly increases when a thicker coated layer is present. The retention factor of butylparaben increases from 0.5 to 3.3 for CC1 and CC2, respectively. Moreover, methylparaben and ethylparaben which were not baseline separated on the CC1 capillary, depict now a resolution of 5.89. Furthermore, the mobile-phase velocity is further reduced to 0.42 mm/s, which is a decrease of 37% and 25% compared to EOF velocity of CB1 and CC1. The obtained results of CC2 are consistent with those of CC1 and demonstrate the larger induced retention of the formed ordered mesoporous layer. However, the evaluation of the efficiency of the parabens is more ambiguous as plate heights between 19.2 µm (methylparaben) and 99.8 µm (butylparaben) reveal in Table VII.2.

Table VII.2. Chromatographic characteristics of the analysis of four parabens on CC2 shown in Figure VII.6.

Compound	t_r (min)	k	N	H (µm)	R_s
thiourea	23.9	/	/	/	/
methylparaben	32.7	0.37	31093	19.2	/
ethylparaben	40.3	0.69	16284	36.8	5.89
propylparaben	59.6	1.5	8976	66.8	7.44
butylparaben	102.75	3.3	6012	99.8	8.11

The minimum (theoretical) plate heights obtained in open-tubular chromatography should ideally be equivalent to the capillary diameter ($H=d_c$). In the case of methyl- and ethylparaben the obtained plate heights are significantly lower than 50 µm. However, as mentioned before, only well retained components are representative for the band broadening effects occurring in the capillary and therefore, the plate heights of propyl- and butylparaben are more realistically describing the performance of the column. The low efficiency and high plate heights of butylparaben can easily be explained by the large radius of the capillary (50 µm) which hampers the effective and fast transfer of the solutes through the mobile phase to the stationary phase due to the low diffusion coefficients of solutes in a

liquid mobile phase [1]. A reduction of the ID of the capillary should therefore significantly improve the efficiency. Furthermore, the plate height is a function of the mobile-phase velocity and the minimum plate height should therefore also be obtained through a van Deemter curve analysis. Finally, the evaluation of the ultimate performance of the column should be done through analyzing the kinetic plots, as described before. This part of the study could, however, not be performed due to the time constraints of the project. Note that a straightforward comparison between the obtained efficiencies on CC1 and CC2 is hindered by the differences in analysis instrumentation. Consequently, different total capillary lengths are used, while the effective length remained the same.

The capillary (CC2) was also investigated for the separation of a homologue series of phenones, which was chosen to demonstrate the potential of the C18 functionalized SBA-16 layer as retentive stationary phase in the reversed phase CEC mode. Figure VII.7A and B depicts the obtained electrochromatograms in this way with an acetonitrile content in the mobile phase of 40 and 50%, respectively.

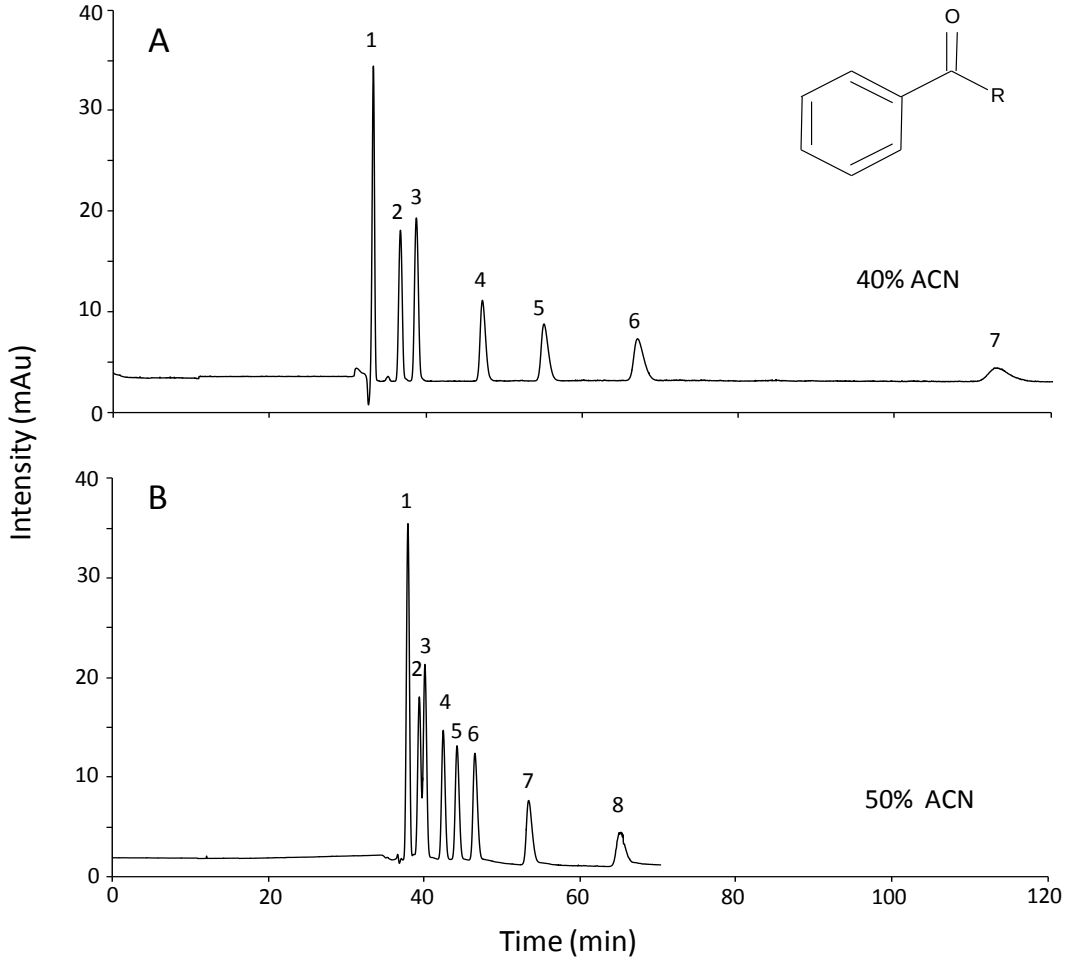

Figure VII.7. Electrochromatograms of the separation of thiourea (1), propiophenone (2), butyrophenone (3), hexanophenone (4), heptanophenone(5), octanophenone (6), decanophenone (7) and dodecanophenone (8) on CC2. Mobiles conditions: MES buffer (pH 6, 50 mM) with 40% ACN (A) and 50% ACN (B). Test mixture consisted of 125 µg/mL of each solute. Capillary dimensions: 60 cm total length; 52.5 cm effective length; 50 µm ID.

At 40% acetonitrile all solutes are baseline separated. The most retained (and detected) solute, decanophenone depicted a retention factor of 2.4 with a corresponding efficiency of 8029 plates. Note that dodecanophenone was not detected in the 40% ACN chromatogram due to the limited detection window of the method. At 50% acetonitrile the retention was lowered with a factor of 5, indicating the strong dependency of the retention on the modifier content. The reversed phase behavior of the coated columns was further confirmed as the retention of decanophenone lowered from 2.4 to 0.4 with increasing organic content.

Furthermore, the dependency of the EOF with the modifier content is quite interesting. For the CC2 capillary, the EOF velocity reduced from 0.42 mm/s at 20 % ACN to 0.26 mm/s at 50 % ACN in a linear way, as depicted in Figure VII.8.

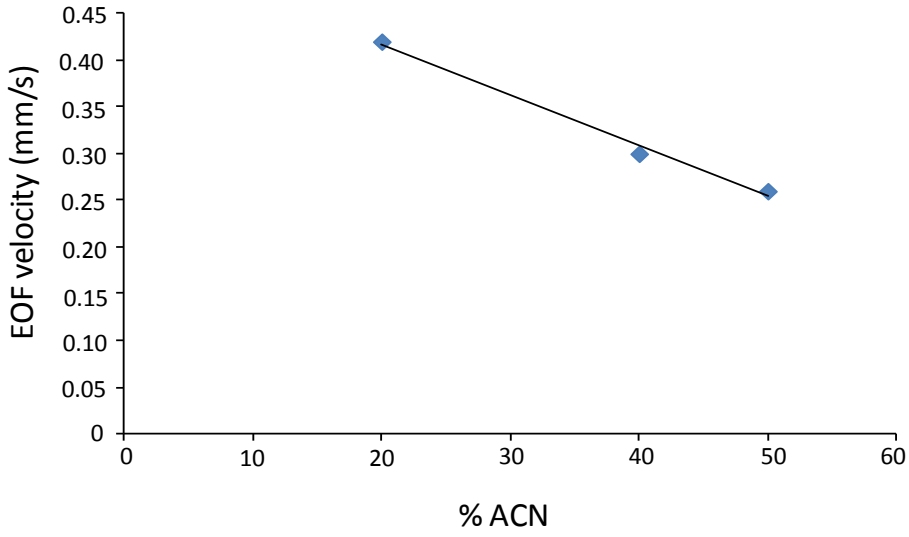

Figure VII.8. The influence of the modifier content on the EOF velocity.

These observations are, however, inversed to the observations in CEC literature and Chapter VI, where increases of EOF velocity are described with increasing modifier content. Therefore, additional measurements should be performed with mobile phases containing different acetonitrile fractions and whereby the same total ionic strengths are used.

4 Conclusion and future prospects

In this chapter, the coating of SBA-16 as stationary phase for CEC analyses was investigated. The mesoporous layer was characterized by SEM micrographs and a layer of 600 nm was obtained after two days of coating. Derivatization of the mesoporous layer with C18 chains allowed the separation of a series of four parabens and eight phenones at different mobile phase conditions. The ordered mesoporous layer demonstrated a significantly improved retention of these solutes, even on broad columns in OT-CEC. However, only low efficiencies and high plate heights were obtained due to the limited mass transfer.

Overall, this chapter describes the proof of concept of the mesoporous layer as a promising retentive stationary phase. However, this type of supporting materials for stationary phases should be further developed and optimized for capillaries with narrower ID (10 µm and beyond) to achieve highly efficient separations. Furthermore, these capillaries should be further characterized in terms of the EOF dependency on ionic strength, pH and modifier content of the mobile phase. Moreover, the poor repeatability of the coating should also be further investigated and improved.

5 References

[1] J.W. Jorgenson, E.J. Guthrie, J. Chromatogr. 255 (1983) 335.

[2] M. Grun, A.A. Kurganov, S. Schacht, F. Schuth, K.K. Unger, J. Chromatogr. A 740 (1996) 1.

[3] T. Shindo, H. Kudo, S. Kitabayashi, S. Ozawa, Microporous Mesoporous Mater. 63 (2003) 97.

[4] A. Kurganov, K. Unger, T. Issaeva, J. Chromatogr. A 753 (1996) 177.

[5] T. Martin, A. Galarneau, F. Di Renzo, D. Brunel, F. Fajula, S. Heinisch, G. Cretier, J.L. Rocca, Chem. Mater. 16 (2004) 1725.

[6] C. Thoelen, K. Van de Walle, I.F.J. Vankelecom, P.A. Jacobs, Chem. Commun. (1999) 1841.

[7] R.J. Tian, J.M. Sun, H. Zhang, M.L. Ye, C.H. Xie, J. Dong, J.W. Hu, D. Ma, X.H. Bao, H.F. Zou, Electrophoresis 27 (2006) 742.

[8] M. Ide, Ordered Mesoporous Silica Materials in Liquid Chromatography: Synthesis and Application, UGent, 2012, 143-160

Chapter 8

Summary, general conclusions and future prospects

Capillary electrochromatography has often been described as an efficient separation technique, which should exceed HPLC in terms of speed and efficiency. In this technique, which can be considered as a hybrid between high-performance liquid chromatography (LC) and capillary electrophoresis (CE), the mobile phase transport through a capillary packed with stationary phase particles is achieved by electroosmotic flow (EOF), while separation occurs by electrophoresis superimposed on the partitioning of the solutes between the mobile and stationary phase.

Initially, very fast CEC separations offering very high efficiencies, when compared to HPLC and micro-LC, were reported. However, many of these results were obtained with poorly retained or with ionized solutes. Therefore, band broadening effects caused by chromatographic behavior (and especially due to mass transfer effects) cannot sincerely be assessed due to the limited interaction time with the stationary phase and/or due the interference of electrofocusing effects if the solute is ionized. Nowadays, CEC is still not implemented in routine analyses and this seems to be at least partially hampered by the insufficient resolution obtained for analyses of well-retained neutral molecules. Most recent research has been focused on the design of numerous stationary phases in each format (packed, open tubular and monolithic capillaries). However, the performance of all these formats and stationary phases should be weighted by an independent tool to evaluate packing strategies and to expose the bottlenecks of contemporary CEC in a better way.

In the framework of this thesis, kinetic plots for CEC were implemented for the first time to allow the least biased evaluation of the performance of capillary electrochromatography as it is today. The kinetic plot approach does not only allow the comparison of the performance of different columns but can also be applied to evaluate the influence of different chromatographic parameters on the performance.

This thesis can be divided in two major parts. The first part, which comprises Chapter I-III, describes the theoretical background and a thorough literature study of contemporary CEC. The second part, which includes Chapter IV to VIII, described the practical work performed in the framework of this thesis.

Chapter I describes the fundamental theory of capillary electrochromatography**.** Emphasis was thereby set on the generation of the electroosmotic flow in electrodriven techniques, as fundamental understanding of this proces is required to understand the dynamics of separations in CEC. Therefore, the influence of the double layer is explained and the role of several parameters, such as pH, temperature and mobile phase composition is thoroughly addresses. The different available methods to evaluate the performance in chromatographic separation systems, such as the van Deemter theory and the kinetic plot method are thereby described in detail.

Chapter II summarizes the current state-of-the-art of the instruments applied in CEC. The hyphenation of different detectors and the consequences of miniaturizing column formats in terms of sensitivity and efficiencies are thereby described. Furthermore, the sample introduction process into the capillary is described as this differs greatly from HPLC. Finally, the importance of temperature control is explained and the rationale for the limitations in the applicable voltage is described.

A thorough literature survey of the different column formats applied in CEC is provided in **Chapter III**. This includes a survey onthe contemporary column manufacturing of packed and open-tubular columns. Furthermore, the different separation modes, thus far reported and described in CEC literature, are outlined in this Chapter. It can be concluded that almost each separation method encountered in HPLC can also be translated to CEC. However, due to the dual separation mechanism of CEC, electrophoresis and partitioning, the separation method in CEC is often a result of the interplay of several separation modes.

The kinetic plot method for CEC was developed and implemented in **Chapter IV**. In comparison to HPLC, CEC is not limited by applicable pressure but the mobile phase velocity is dependent on the applicable potential difference. Consequently, in analogy to kinetic plots in HPLC, data points of H vs. u curve were converted to a time versus N curve by implementing the maximum voltage as a limiting factor. Therefore, efficiencies and

corresponding EOF times (and column lengths) were multiplied a max factor λ. To assess the performance of current CEC, these kinetic plots were constructed for the analysis of well-retained neutral solutes on commercially available capillaries. Subsequently, a comparison between the kinetic plots constructed for CEC and HPLC was performed to evaluate CEC as a separation technique. This comparison revealed that commercially available HPLC columns still outperformed packed CEC in efficiency and analysis speed. Investigation of the current behavior at different voltages revealed that this lower performance could be related to Joule heating effects. The effect of Joule heating on the performance was further investigated by the analysis of a test mixture at different set temperatures. The possible presence of Joule heating was further confirmed by the steep increase in retention measured at the set temperatures (when less Joule heating is occurring). Therefore, the maximum performance of the commercial capillaries was also evaluated at several temperatures, whereby maximum performance was obtained at the lower temperatures. Finally, the kinetic plots for capillaries packed with smaller diameter particles and analyzed at ultra high voltages were constructed to assess the potential of packed CEC in the future.

Most analyses in CEC are performed in the reversed phase mode. However the separation of polar and basic molecules is difficult to achieve on non polar stationary phases. Hydrophilic interaction chromatography with polar stationary phases is more suited to analyze these solutes. In CEC, little research has been done in the exploitation of the hydrophilic interaction mode and most of this research has been focused on the use of monoliths. In **Chapter V** therefore, capillaries were packed with bare silica particles of various sizes and their performance was assessed in various ways. The corresponding van Deemter curves and kinetic plots demonstrated that the packing efficiency was higher with the larger particles but that the overall column efficiency and the ultimate performance of capillaries packed with smaller particles was still better. Furthermore, the mobile phase velocity and the retention behavior of the solutes was investigated as a function of the organic modifier content. The obtained data demonstrated that the retention mechanism was solely based on hydrophilic interaction and that acetonitrile had a significant effect on the mobile phase velocity. In addition, the potential of hydrophilic interaction capillary electrochromatography as separation mode for polar compounds was demonstrated by the separation of several

mixtures including a Triton-X 100 mixture, nitro-aromatic solutes and a mixture of possible genotoxic compounds.

Besides Joule heating, the performance of packed capillaries is often limited due to necessity of frits, which incorporates an inhomogeneity into the packed bed and therefore causes extra band broadening while making the columns fragile. Therefore in **Chapter VI**, an open-tubular capillary was coated with a novel stationary phase: poly(styrene-divinylbenzene-vinyl sulfonic acid). Hereby the styrene-divinylbenzene groups acted as a non polar retaining stationary phase, while the incorporation of the vinyl sulfonic acid groups assured the generation of a sufficiently EOF. A study was performed to optimize the polymerization time and the monomer composition in order to obtain the most performant column. In this way it could be demonstrated that a high amount of vinyl sulfonic acid was beneficial for the efficiency. However, the retention also decreased with increasing amounts of vinyl sulfonic acid in the monomer mixture. The performance of the open-tubular capillaries was further evaluated through the kinetic plot method. The novel open-tubular capillaries were also characterized by a study of the EOF behavior at different pH's and at various temperatures. It was thereby established that high temperatures expedite the analyses significantly as the mobile-phase velocity is increased and as the retention of the solutes decreases with increasing temperatures. Furthermore, the possibility of the use of temperature gradients in open-tubular CEC was successfully investigated, without the presence of problematic Joule heating phenomena.

In **Chapter VII** columns were coated with an ordered mesoporous silica layer, consisting of the SBA-16 material. First, the coating conditions were optimized through the evaluation of SEM micrographs and the corresponding electrochromatograms of neutral test solutes. In this way a thick layer of SBA-16 was successfully deployed as a homogeneous coating on the inner wall of a capillary. Several test mixtures were successfully separated and the influence of modifier content on retention and EOF velocity was investigated. However, the overall efficiency of these columns was limited because of their relatively large internal radii. Further investigation of the coating applied on smaller ID capillaries is necessary in this form of open-tubular CEC.

Overall, in this thesis the performance of contemporary packed capillaries was assessed in an unbiased way and compared to the performance of in-house developed open-tubular capillaries. The kinetic plot in CEC was successfully applied to investigate and demonstrate the underlying problems of current CEC. More particularly, the Joule heating effects in packed capillary CEC should be further suppressed to obtain higher efficiencies. Moreover, it was demonstrated that CEC would only surpass HPLC if ultra-high voltages are applied on CEC capillaries allowing lower plate heights. Open-tubular capillaries on the other hand appear easier to fabricate but are still less efficient compared to packed CEC. This is due to their still too large internal diameters which limits the speed of mass transfer of the solutes.

The research described in this thesis allows to conclude that improvements in packed CEC can still be obtained by the use of smaller particles for packed capillaries and through the application of capillaries with smaller internal diameters in open-tubular approaches. One of the main bottlenecks of CEC, i.e. the need for a mobile phase gradient, could be partially resolved by the introduction of temperature gradients in open-tubular columns. However, the application of temperature gradients in CEC implicates the necessity of an effective Joule heat dissipation mechanism. Therefore, the future of CEC could reside in further improvement of the open-tubular capillaries.

However, implementation of CEC as a routine analysis technique would require that CEC capillaries can be produced in a more reproducible manner. It became apparent during the course of this thesis that the production of (packed and open-tubular) CEC capillaries, is still a craft, rather than a science. Capillaries fabricated with the same procedure by different persons or at different laboratories will often differ in chromatographic properties. Moreover, the efficiencies obtained with the classic stationary phase morphologies (i.e. open-tubular, monolithic and packed capillaries) are often comparable or worse as current HPLC columns. The developed kinetic plot method for CEC demonstrated furthermore that the limitation in maximum applicable voltage is more constraining the length of the column compared to the maximum applicable pressure in HPLC. Therefore, the only option to achieve higher efficiencies resides in the application of smaller particles or of capillaries with smaller internal diameters. However, both approaches complicate the production procedure of the capillaries to a great extent and new production processes should be developed.

More recently, microchips have been introduced as a new format in liquid chromatography and in CEC. These so-called pillar array columns are produced by etching and imprinting techniques (such as photolithography) in a very repeatable manner. Therefore, it could be interesting to investigate the applicability of the most performant microchips in the CEC mode for comparison with the above described approaches in future work.

Samenvatting, conclusies en toekomstperspectieven

Capillaire elektrochromatografie (CEC) wordt beschouwd als een hybride van hoge performantie vloeistofchromatografie (HPLC) en capillaire elektroforese (CE). Hierbij beweegt de mobiele fase zich door het capillair onder invloed van een elektrisch veld en worden de componenten gescheiden door een combinatie van een elektroforetisch en een chromatografisch proces. CEC wordt beschouwd als een hoog-efficiënte scheidingstechniek met hoge piekcapaciteiten in vergelijking met HPLC.

De eerste gerapporteerde CEC analyses bewezen de superioriteit van deze scheidingstechniek op vlak van efficiëntie en analysesnelheid. Echter werd het merendeel van deze analyses uitgevoerd met licht geretenteerde of geladen componenten. Hierdoor is de interactie van de stationaire fase met de componenten gelimiteerd en kunnen de chromatografische processen die bandverbreding veroorzaken niet of onvoldoende geëvalueerd worden. Bovendien wordt de efficiëntie van geladen componenten niet alleen bepaald door de chromatografische scheiding maar ook door elektrofocusering. Daardoor werd er historisch een vertekend beeld weergegeven van de performantie van CEC. Analyses van neutrale en meer geretenteerde componenten toonden aan dat er veelal een lagere efficiëntie behaald werd dan verwacht. De oorzaak wordt hierbij meestal toegeschreven aan de onvoltooide optimalisatie en ontwikkeling van geschikte strategieën om CEC capillairen te produceren. Daarom heeft het CEC onderzoek zich de afgelopen jaren toegespitst op de ontwikkeling van verschillende stationaire fases in al zijn vormen (gepakte, open-tubulaire en monolithische capillairen). Tot op heden is er echter nog altijd geen onafhankelijke methode om de performantie van deze stationaire fases te evalueren en te vergelijken.

Daarom werden in het kader van deze thesis, kinetische plots voor CEC geïmplementeerd om de performantie van CEC zo neutraal mogelijk te kunnen evalueren. Hierdoor kunnen de pijnpunten en 'bottlenecks' van CEC beter geïdentificeerd en geëvalueerd worden. Bovendien laat de kinetische plot methode ook toe om de invloed van verschillende chromatografische parameters op de performantie beter te meten.

Deze thesis kan onderverdeeld worden in twee grote luiken. Een eerste deel, bestaande uit hoofstukken I-III, omvat de theoretische achtergrond van CEC, gecombineerd met een grondige literatuurstudie. Het tweede luik, bestaande uit hoofdstukken IV-VII, beschrijft het praktisch werk dat werd uitgevoerd in het kader van deze doctoraatstudie.

De fundamentele theorie van capillaire elektrochromatografie werd behandeld in **Hoofdstuk I.** Aangezien CEC een hybride techniek is, werd daarvoor eerst de achterliggende theorie van capillaire elektroforese en vloeistofchromatografie besproken. Hierbij werd er dieper ingegaan op de dubbellaag theorie, de zeta-potentiaal en op de invloed van de verschillende parameters op de elektroosmose. Het begrijpen van de elektroosmotische flow (EOF) in al zijn facetten laat toe om het achterliggende dynamisme van de scheidingen in CEC te begrijpen. Vervolgens werd er dieper ingegaan op de theoretische principes van de chromatografische scheiding. Hierbij werd er aandacht besteed aan de verschillende gangbare methodes om de efficiëntie en performantie van scheidingssystemen te evalueren. Ten slotte wordt in dit hoofdstuk de theoretische achtergrond CEC beschreven, aangezien scheiding, opwekking van EOF en bandverbreding in CEC verwant zijn aan de processen die plaats vinden in CE en HPLC maar daar niet volledig mee overeenstemmen.

In **Hoofdstuk II** werden de CEC instrumentatie en de recentste ontwikkelingen op het vlak van instrumentatie beschreven. Hierbij werd er specifiek aandacht besteed aan de koppeling van de verschillende detectoren met de instrumentatie en aan de invloed van de geminiaturiseerde kolomformaten op de detectiegevoeligheid. Daarnaast werd er ook aandacht besteed aan de verscheidene manieren die toelaten om de graad van *Joule heating* effecten onder controle te houden. Ten slotte werd er dieper ingegaan op de maximale spanningsverschillen die kunnen aangelegd worden met commerciële en experimentele instrumenten.

Een uitgebreide literatuurstudie beschrijft in **hoofdstuk III** de verschillende stationaire fases en de verschillende scheidingsmethodes die al werden toegepast in CEC. Hierbij worden de voor- en nadelen van de verschillende stationaire fases types uitvoerig beschreven. Vervolgens worden de applicaties en de verschillende methodes besproken. Daarbij wordt er extra aandacht besteed aan de kenmerkende eigenschappen van CEC, veroorzaakt door de dualiteit (retentie en elektroforese) van het scheidingsmechanisme.

Na hoofdstuk III wordt in een **rationale** de beperkingen van CEC, die beschreven werden in de voorgaande hoofdstukken, samengevat en besproken. Hierbij worden er doelstellingen en hypotheses geformuleerd die in het praktische gedeelte van deze thesis onderzocht worden. Er kon geconcludeerd worden dat een vergelijking tussen HPLC enerzijds en CEC anderzijds heel moeilijk is, zonder de ontwikkeling van een methode die een neutrale vergelijking mogelijk maakt. Pas na de ontwikkeling hier van, kunnen de verschillende scheidingsmethodes en stationaire fases met elkaar vergeleken worden en kan er dieper ingegaan worden op de achterliggende problemen die de performantie van hedendaagse CEC belemmeren.

In het praktische gedeelte, werd de kinetische plot (KP) methode voor CEC ontwikkeld en toegepast op verschillende kolomformaten. De ontwikkeling van de kinetische plot methode in CEC werd beschreven in **hoofdstuk IV.** CEC is, in tegenstelling tot HPLC, niet gelimiteerd door de maximale druk (geleverd door de pomp), maar door het aangelegde potentiaalverschil. Daarom kan een kinetische plot gesimuleerd worden door te extrapoleren naar het instrumenteel hoogst mogelijk aangelegde potentiaalverschil. Hierbij werd er, analoog aan de kinetische plots voor HPLC, een H (plaathoogte) vs. u (mobiele fasesnelheid) plot geconverteerd naar een tijd versus N curve. De ontwikkeling van de kinetische plot in CEC laat ondermeer toe om de performantie van hedendaagse commerciële CEC kolommen te vergelijken met HPLC. Hiervoor werden er analyses uitgevoerd, zowel in de CEC als in de HPLC mode, met goed geretenteerde en neutrale moleculen. De corresponderende kinetische plots werden vervolgens ontwikkeld en vergeleken. Er kon geconcludeerd worden dat efficiëntere en snellere analyses behaald werden met de commerciële HPLC aanpak dan met commerciële CEC kolommen. HPLC is dus vandaag superieur in termen van chromatografische performantie. Verder onderzoek toonde eveneens aan dat de stroomontwikkeling in CEC niet lineair verliep met een toename in het aangelegd voltage, wijzende op de mogelijke aanwezigheid van *Joule heating* effecten. Het effect van dit fenomeen op de performantie werd verder onderzocht door het uitvoeren van analyses bij verschillende temperaturen. Dit resulteerde in het bekomen van maximale performanties bij de laagste temperaturen. Om de mogelijke toekomst van CEC met gepakte capillairen te voorspellen werd er tenslotte een simulatie uitgevoerd die de performantie

beschrijft van CEC capillairen gepakt met sub-µm partikels en die geanalyseerd werden bij ultrahoge voltages.

De meeste analyses in CEC worden uitgevoerd met de omkeer-fase (RP) scheidingsmode. De scheiding (en vooral retentie) van polaire en basische componenten is echter moeilijk te verwezenlijken op de daarbij gehanteerde hydrofobe fases. Hydrofiele interactie vloeistofchromatografie (HILIC) met polaire stationaire fases is daartoe meer geschikt. Tot op heden is er in CEC maar weinig onderzoek uitgevoerd naar de HILIC methode en het meeste onderzoek op dit gebied heeft zich tot nu toe toegespitst op het gebruikt van polaire monolithische kolommen. Daarom werd er in **hoofdstuk V** onderzoek uitgevoerd naar capillairen gepakt met niet-gemodificeerde silica partikels, aangezien dit de meest voor de hand liggende en meest robuuste polaire stationaire fase is. In dit hoofdstuk werd er dan ook verder ingegaan op de pakkingstrategie en op de invloed van de partikelgrootte op de performantie van de kolom. Hiervoor werd er een vergelijking gemaakt tussen de ontwikkelde van Deemter curven en de kinetische plots. Er werd aangetoond dat er een significant verschil was tussen de pakkingefficiëntie van de kolom gepakt met 5 µm partikels vergeleken met een kolom gepakt met 3 µm partikels. De uiteindelijke efficiëntie en performantie van analyses, uitgevoerd op de gepakte capillairen, was echter beter met capillairen gepakt met de 3 µm partikels. Daarnaast werd er ook een onderzoek uitgevoerd naar de invloed van de mobiele fase samenstelling op de retentie van de hydrofiele componenten en op de snelheid van de EOF. De verkregen data toonde aan dat het retentiemechanisme gebaseerd was op zuivere hydrofiele interactie en dat de concentratie aan acetonitrile een significant effect had op de snelheid van de mobiele fase. Bovendien werd de kracht van hydrofiele interactie CEC nader aangetoond door de scheiding van verschillende mengsels van polaire componenten.

In vorige hoofdstukken werd al eerder aangetoond dat *Joule heating* effecten de performantie van gepakte capillairen limiteren. Daarnaast worden er gedurende het pakkingsproces ook niet homogene delen (*frits*) in de pakking geïntroduceerd. Deze *frits* begrenzen aan beide zijden het gepakt bed en functioneren als filter die het gepakt bed immobiliseren maar permeabel zijn voor de mobiele fase. Doordat de *frits* een niet-homogeen deel vormen, veroorzaken ze bandverbreding tijdens de scheiding. Daarom werd er in **hoofdstuk VI** een open-tubulair (OT) capillair aangemaakt, bestaande uit een

polymeerlaag van poly(styreen-divinylbenzeen-vinylsulfonzuur). Hierbij wordt de polymeerlaag immers chemisch gebonden aan de capillairwand en is er geen nood aan *frits* om de stationaire fase te immobiliseren. De gepolymeriseerde styreen-divinylbenzeen groepen vormen de apolaire basis voor de retentieve stationaire fase en de aanwezigheid van de vinylsulfonzuur (VSA) groepen verzekert de generatie van een EOF. De eerste stap van het onderzoek beschrijft de optimalisatie van het productieproces. Ondermeer de polymerisatietijd en de monomeer compositie werden daarbij zodanig geoptimaliseerd dat de meeste performante stationaire fase bekomen werd. Een betere efficiëntie werd ook bekomen bij hogere concentraties van VSA in het monomeermengsel. Dit resulteerde echter in een meer polaire stationaire fase wat vervolgens een effect had op de retentie van de hydrofobe componenten in het testmengsel. De performantie van de capillairen werd verder onderzocht met behulp van de kinetische plot methode. Hierdoor werd duidelijk dat OT-CEC met deze capillairen interessant kan zijn voor de analyse van zwak geretenteerde componenten. De performantie van sterk geretenteerde componenten echter is gelimiteerd door de grotere bandverbreding die daarbij optreedt. Dit fenomeen kan waarschijnlijk verklaard worden door de trage diffusie van de componenten in de mobiele fase naar de stationaire fase en door de lage massa transfer die typisch is voor polystyreen gebaseerde stationaire fases. Om de diffusiesnelheid te verhogen werden er vervolgens analyses uitgevoerd bij hogere temperaturen. Hierdoor werden de analysetijden gevoelig verkort en daalde de retentie met stijgende temperaturen. Bovendien werd de mogelijkheid onderzocht om een temperatuursgradiënt in CEC te gebruiken als alternatief voor de mobiele fase gradiënt (die niet of moeilijker te verwezenlijken is in CEC). De geoptimaliseerde gradiënt (tussen 20 en 60°C) versnelde de analyse gevoelig gecombineerd met een vergelijkbare piekcapaciteit als een isothermische analyse bij 25°C.

Hoofdstuk VI toonde aan dat OT-CEC met stationaire fases gebaseerd op polystyreen minder geschikt lijken om performante analyses te bekomen van sterk geretenteerde organische moleculen. Daarom werd er in **hoofdstuk VII** een geordende laag van een type mesoporeus silica, SBA-16 genaamd, gecoat op de wand van het capillair. Hierbij werden eerst de coatingcondities geoptimaliseerd en geëvalueerd aan de hand van SEM beelden en aan de hand van CEC analyses van neutrale testcomponenten. Een coating van enkele honderden nanometers kon homogeen afgezet worden op de binnenwand van een capillair.

Verschillende testmengsels konden gescheiden worden en de invloed van het acetonitrile gehalte in de mobiele fase op de retentie en op de EOF-snelheid werd onderzocht met deze nieuwe stationaire fase. Deze studie werd echter uitgevoerd op capillairen met relatief brede interne diameters (50 µm ID) en daarom zijn de gemeten performantie en efficiënties van deze capillairen eerder beperkt. Verder onderzoek naar de ontwikkeling van SBA-16 coatings op capillairen met kleinere interne diameters is dan ook nodig. Hierbij moet ook aandacht besteed worden aan de reproduceerbaarheid van de sol productie en de coating procedure.

Het doel van deze thesis was de evaluatie en vergelijking van de performantie van hedendaagse CEC in al zijn facetten. Daarom werd de kinetische plot methode voor CEC ontwikkeld en toegepast om de onderliggende problemen van hedendaagse CEC aan te duiden en verder te onderzoeken. Uit deze thesis werd enerzijds duidelijk dat Joule opwarmingeffecten beter onderdrukt moeten worden in CEC met gepakte capillairen. Dit zou leiden tot hogere efficiëntie en performantie gecombineerd met de mogelijkheid om analyses uit te voeren bij hogere voltages. Anderzijds zijn open-tubulaire capillairen gemakkelijker te produceren maar minder performant in vergelijking met gepakte capillairen. Omdat de opwarmingseffecten daarbij echter beter onderdrukt kunnen worden laat dit toe om te analyses bij hogere temperaturen uit te voeren en om een temperatuursgradiënt in te stellen.

Dit doctoraatsonderzoek toont aan dat de performantie van CEC beperkt wordt door verscheidene factoren zoals de kolommorfologie, beperkte controle van opwarmingseffecten en de gelimiteerd voltages. Daarom zou er verder onderzoek verricht moeten worden naar efficiëntere temperatuurscontrole en naar het gebruik van temperatuurgradiënten in CEC om de techniek meer toepasbaar te maken.

Om CEC met gepakte capillairen competitief te maken met HPLC, moeten er grotere potentiaalverschillen aangelegd worden in combinatie met capillairen gepakt met kleinere partikels. Daarvoor dienen er nieuwe pakkingsstrategieën ontwikkeld te worden en zal de CEC-instrumentatie meer complex worden. Bovendien blijft reproduceerbaarheid van het productieproces voor zowel gepakte, monolithische als open-tubulaire CEC capillairen beperkt.

Daarom dient er verder onderzoek gedaan worden naar de ontwikkeling van mogelijke alternatieven voor de klassieke kolommorfologieën. *Microchips*, bijvoorbeeld, kunnen meer reproduceerbaar aangemaakt worden door gebruik van een lithografisch of *etching* proces. Recent onderzoek heeft bovendien aangetoond dat *micro pillar array* kolommen een hogere efficiëntie kunnen vertonen (door hun minieme A-term) vergeleken met standaard HPLC-kolommen. Het zou daarom interessant zijn om de meest performante microchips ook uit te testen in CEC.

Dankwoord

Na vijf jaren lever ik met trots dit doctoraat af. Deze jaren worden terecht beschreven als de mooiste tijd van iemands leven. De vrijheid die je geniet in je onderzoek, de flexibele werkomgeving, de internationale context, de talloze vriendschappen die je eraan overhoudt, het "eureka" gevoel na een wetenschappelijke doorbraak...zijn maar enkele voordelen die de meeste doctoraatstudenten ervaren. Er wordt echter vergeten dat een doctoraat ook het resultaat is van zwoegen en zweten, van vele frustraties en van lange werkdagen (en nachten). Bovenal is een doctoraat niet het resultaat van één individu, maar eerder een samenspel van velen waarbij de doctoraatstudent de 1ste viool bespeelt. Daarom wil ik ook alle vrienden, familie en collega's bedanken die bijgedragen hebben tot deze thesis.

In het bijzonder wil ik mijn promotor *prof. Frédéric Lynen* bedanken voor zijn ongebreidelde steun, inspiratie en motivatie. Als ik mijn doctoraat vergelijk met een muziekstuk, dan was *Frédéric* de dirigent die me, soms met lichte aandrang, de weg wees in het wetenschappelijk onderzoek. Daarnaast wil ik zeker ook *prof. em. Pat Sandra* bedanken. Hij introduceerde mij (en velen anderen) in de wereld van de scheidingswetenschappen en stond met raad en daad bij tijdens mijn masterthesis en de beginjaren van mijn doctoraatstudie.

Daarnaast wil ik het Instituut voor de Aanmoediging van Innovatie door Wetenschap en Technologie in Vlaanderen (IWT) bedanken voor de financiële steun die dit doctoraat mede mogelijk maakte.

Uiteraard moet ik ook *Marc* bedanken voor de technische bijstand tijdens mijn masterjaar en de goede raad en levenswijsheden die hij mij toevertrouwde. Daarnaast wil ik zeker ook Pieter bedanken voor zijn input, de hulp met de TOF-MS en zijn IT-kennis. Bij uitbreiding wil ik Olivier bedanken voor alle SEM metingen.

De leuke tijd die ik beleefde tijdens mijn doctoraat was uiteraard grotendeels te danken aan mijn fijne collega's van de SSG groep. Mike, Jente, Tim, Bram, Thomas, Maarten, Kai, Bes, Sander, Piotr, Kevin, Polet, Nick, Barbara, Pieter-Jan, Olivier: dank u voor al de leuke

etentjes, aperitieven en digestieven, voor de leuke dagen en avonden. Ik hoop dat er nog veel leuke momenten mogen volgen.

Uiteraard wil ik ook al mijn andere vrienden bedanken. Chemie-, Chemica-, fiets- en rugbyvrienden: er zijn er velen die een woordje van dank verdienen maar teveel om allemaal op te sommen. Ik wil hierbij toch in het bijzonder de "tussenshotjes" vrienden bedanken. De momenten in Barcelona, Mallorca en Lagos (maar evengoed de Gentse zesdaagse) zullen me altijd bijblijven. Dit hoeft uiteraard niet het einde zijn van onze vermaarde avonturen.

Daarnaast wil ik ook mijn gehele familie bedanken voor de onvoorwaardelijke steun die ik altijd heb genoten. Mama, papa, bedankt voor al die mooie jeugdjaren. Jullie hebben mij onvoorwaardelijk gesteund, gemotiveerd en ingetoomd wanneer nodig. Als ik terugkijk naar mijn zorgeloze jeugd op de boerderij, samen met Marieke, besef ik maar al te goed dat jullie de fundering hebben gelegd voor dit doctoraat. Bedankt voor alles.

A mis suegros y mi cuñado, gracias por recibirme con los brazos abiertos en vuestra familia . Por todas las cosas tan ricas de comer que hay siempre en vuestra despensa. Y sobretodo por enseñarme como se disfruta de la buena vida en España.

The last person I have to thank is by far the most important one during my PhD studies. Probably I say it not enough (or not at all) but Elena, thank you for your listening ear and your support. I know that the dream of an extended stay in Belgium was not including a grumpy, stressed PhD student. However, we are now four years together and you still stand by my side. I am looking forward to our future together.

Address: Landjuweelstraat 37,
9050 Ledeberg, Belgium
Telephone: +32 498 66 10 54
Email: sepdesmet@gmail.com
Date of birth: November 07, 1987
Place of birth: Geraardsbergen
Nationality: Belgian

SEPPE DE SMET

EDUCATION

Oct 2010-currently	**PhD in Chemistry**, Ghent University, Belgium *Improving the performance of contemporary packed and open-tubular CEC.* Promotor: Prof. dr. F. Lynen Funding: IWT grant
2005-2010	**Master in Chemistry**, Ghent University, Belgium, Master thesis: *Development of an online HPLC-MS method to detect antioxidants in organic products* Promotor: Prof. dr. P. Sandra
1999-2005	Sciences-mathematic, Koninklijk Atheneum Geraardsbergen, Belgium

DISTINCTIONS

2010	Laureate UDIAS Student Award

A1 PUBLICATIONS

- Kalili KM, De Smet S, van Hoeylandt T, Lynen F, de Villiers A, Comprehensive two-dimensional liquid chromatography coupled to the ABTS radical scavenging assay: a powerful method for the analysis of phenolic antioxidants., Analytical Bioanalytical Chemistry, 406 (2014) 4233-4242
- De Smet S, Lynen F, Kinetic Performance Evaluation and Perspectives of Contemporary Packed Column Capillary Electrochromatography, Journal of Chromatography A 1355 (2014), 261-268

- De Smet S, Rambla Alegre M., Miserez B., Lynen F., Sandra P., Optimization of a Radical Scavenging Assay Coupled On-line to Liquid Chromatography for Elucidation of Antioxidants in Complex Samples, Journal of Separation Sciences 38 (2015), 724-731
- Karacelik AA, Kücük M, Iskefiyeli M, Aydemir S, De Smet S, Miserez B, Sandra P, Antioxidant components of Viburnum opulus L. determined by on-line HPLC-UV-ABTS radical scavenging and LC-UV-ESI-MS methods, Food Chemistry 175 (2015), 116-114
- De Smet S, Lynen F, Investigation of poly(styrene-divinylbenzene-vinylsulfonic acid) as retentive and electroosmotic flow generating phase in open-tubular electrochromatography, Journal of Chromatography A 1404 (2015), 81-88
- De Smet S, Lynen F, Possibilities and limitations of hydrophilic interaction capillary electro-chromatography on native silica packed columns (in preparation)

POSTER PRESENTATIONS

- De Smet S, Rambla Alegre M, Miserez B, Lynen F, Sandra P, Determination of antioxidants in food using HPLC hyphenated to an optimized ABTS-radical scavenging assay, Poster presented at the 11th Chemistry Conference for Young Chemists (ChemCYS), Blankenberge, Maart 2012
- Matthias Ide, De Smet S, Lynen F, Sandra P, Increasing retention through ordered mesoporosity: re-enabeling WCOT capillary electrochromatography, Poster presented at the 36th International Symposium in Capillary chromatography, Riva Del Garda, May 2012
- De Smet S, Lynen F, Kinetic Performance evaluation and perspectives of packed column capillary electrochromatography, Poster presented at the 39th International Symposium on High-Performance Liquid-Phase Separations and Related Techniques, Amsterdam, June 2013
- De Smet S, Lynen F, Hydrophilic interaction electrochromatography applied in packed and open tubular capillaries, Poster presented at the 39th International Symposium on High-Performance Liquid-Phase Separations and Related Techniques, Amsterdam, June 2013

- De Smet S, Lynen F, Hydrophilic interaction electrochromatography applied in packed capillaries, Poster presented at the 38th International Symposium on Capillary Chromatography, Riva Del Garda, May 2014

ORAL PRESENTATIONS

- De Smet S, Lynen F, Kinetic performance evaluation and perspectives of packed column capillary electrochromatography, Oral Presentation at the 12th Chemistry Conference for Young Chemists, Blankenberge, February 2014
- De Smet S, Lynen F, Temperature as a tool to improve efficiency and peak capacity in packed column and open tubular capillary electrochromatography, Oral Presentation at the 22nd International Symposium on Electro- and Liquid Phase Separation Techniques, Helsinki (Finland), August 2015